NASA-CR-192689

NASA/USRA

University Advanced Design Program

Proceedings of the 4th Annual Summer Conference

(NASA-CR-192689) NASA/USRA UNIVERSITY ADVANCED DESIGN PROGRAM FOURTH ANNUAL SUMMER CONFERENCE (USRA) 166 p

N93-71976
--THRU--
N93-72009
Unclas

Z9/01 0153300

NATIONAL AERONAUTICS & SPACE ADMINISTRATION
UNIVERSITIES SPACE RESEARCH ASSOCIATION

Kennedy Space Center

June 13-17, 1988

Steve Hartman

NASA/USRA
UNIVERSITY ADVANCED DESIGN PROGRAM

PROCEEDINGS OF THE
4TH ANNUAL SUMMER CONFERENCE

HOWARD JOHNSON PLAZA-HOTEL
COCOA BEACH, FLORIDA
JUNE 13-17, 1988

Cosponsor: American Institute of Aeronautics and Astronautics

NASA/USRA UNIVERSITY ADVANCED DESIGN PROGRAM
FOURTH ANNUAL SUMMER CONFERENCE
Cosponsor: American Institute of Aeronautics and Astronautics

The NASA/University Advanced Design Program is operated by the Universities Space Research Association (USRA) under grants from NASA Headquarters (NGT 21-002-080 and NGT 80001). Inquiries regarding the program may be directed to the Program Manager:

John Alred, Ph.D.
Universities Space Research Association
17225 El Camino Real, Suite 450
Houston, Texas 77058
(713) 480-5939

FOREWORD

The Program

The NASA/USRA University Advanced Design Program is a unique program that brings together NASA engineers, students, and faculty from United States engineering schools by integrating current and future NASA space/aeronautics engineering design projects into the university curriculum. The Program was conceived in the fall of 1984 as a pilot project to foster engineering design education in the universities and to supplement NASA's in-house efforts in advanced planning for space and aeronautics design. Nine universities and five NASA centers participated in the first year of the pilot project. Close cooperation between the NASA centers and the universities, the careful selection of design topics, and the enthusiasm of the students has resulted in a very successful program that now includes thirty-four universities and eight NASA centers.

The study topics cover a broad range of potential space and aeronautics projects which could be undertaken during a 20–30-year period beginning with the Space Station Initial Operating Configuration scheduled for the mid 1990's. Both manned and unmanned endeavors are embraced, and the systems approach to the design problem is emphasized. The student teams pursue the chosen problem during their senior year in a one or two semester capstone design course and submit a comprehensive written report at the conclusion of the project. Finally, student representatives from each of the universities summarize their work in oral presentations at the annual Summer Conference, held at one of the NASA centers and attended by the university faculty, NASA and USRA personnel, and aerospace industry representatives.

The Proceedings Volume

As the Advanced Design Program has grown in size, it has also matured in terms of the quality of the student projects. Distribution of the comprehensive final reports is very limited, so the results of the studies have reached only a small audience,

principally those who attend the Summer Conference. In order to broaden the distribution, the decision was made to publish a Proceedings volume which summarizes the project results and roughly parallels the Conference presentations. The present volume is the first in this series and represents the student work accomplished during the 1987-1988 academic year and reported at the 4th Annual Summer Conference held at the Kennedy Space Center, June 13-17, 1988.

ACKNOWLEDGMENTS

This publication was made possible through the efforts of a great many people. First of all, we are grateful to the students, the university faculty, and their teaching assistants for the excellent technical work. Second, we are indebted to those individuals from NASA Headquarters and from the NASA centers who conceived the program in the beginning, have provided valuable guidance throughout, and, through their keen interest in the student projects, are in large part responsible for the boundless enthusiasm of the students. Finally, we thank the staff at the USRA Advanced Design Program Office for the preparation of the manuscripts and the staff of the Publications Services Office of the Lunar and Planetary Institute for their excellent work in the preparation of the final Proceedings volume.

TABLE OF CONTENTS

AERONAUTICS PROJECTS

SPACE PROJECTS

Aeronautics Projects

N/R

HYPERSONIC DRONE VEHICLE DESIGN: A MULTIDISCIPLINARY EXPERIENCE

UNIVERSITY OF CALIFORNIA, LOS ANGELES

UCLA's Advanced Aeronautic Design group focussed their efforts on design problems of an unmanned hypersonic vehicle. It is felt that a scaled hypersonic drone is necessary to bridge the gap between present theory on hypersonics and the future reality of the National Aerospace Plane (NASP) for two reasons: (1) to fulfill a need for experimental data in the hypersonic regime, and (2) to provide a testbed for the scramjet engine which is to be the primary mode of propulsion for the NASP.

The group concentrated on three areas of great concern to NASP design: *propulsion, thermal management,* and *flight systems.* Problem solving in these areas was directed toward design of the drone with the idea that the same design techniques could be applied to the NASP.

A 70° swept double-delta wing configuration, developed in the 70's at NASA Langley, was chosen as the aerodynamic and geometric model for the drone. This vehicle would be air launched from a B-1 at Mach 0.8 and 48,000 feet, rocket boosted by two internal engines to Mach 10 and 100,000 feet, and allowed to cruise under power of the scramjet engine until burnout. It would then return to base for an unpowered landing. Preliminary energy calculations based on flight requirements give the drone a gross launch weight of 134,000 pounds and an overall length of 85 feet.

PROPULSION GROUP

The efforts of the propulsion group have been directed towards developing tools to analyze the effects of aircraft geometry and freestream conditions on scramjet performance. Specifically, the group has been concerned with the shock structure, boundary-layer growth and inlet geometry of a Mach-10 drone research vehicle, and the impact of these parameters on the efficiency and thrust of the scramjets.

The tools used to analyze the flowfield have primarily consisted of pre-existing computer software. Six programs (STUB, INLET, CPIPE, SEAGULL, SCRAM, EDDYBL) were used to evaluate different components of the drone's underbody and scramjet engines (see Fig. 1). SCRAM is a one-dimensional program for the estimation of scramjet performance of a hypersonic vehicle. SCRAM begins with the geometry of the vehicle and calculates gross estimates of thrust, efficiency, and other engine parameters. It is used by our group as a check for the more detailed analysis. STUB allows an analysis of the detached shock structure off the nose of the vehicle, which SEAGULL is unable to analyze due to the region of subsonic flow behind the detached shock. SEAGULL calculates inviscid conical shock structures and freestream conditions for axisymmetric geometries. SEAGULL is used to calculate the shock structures over the drone forebody and the expansion waves in the exhaust plume of the nozzle. EDDYBL is a two-dimensional/axisymmetric, compressible, turbulent boundary-layer program. Using the freestream conditions from SEAGULL, EDDYBL is used to calculate the boundary-layer growth along the vehicle. INLET uses an inviscid analysis to design hypersonic engine inlets. For given inlet conditions and desired combustor entrance conditions, INLET calculates the cowl geometry required. Data from SEAGULL and EDDYBL will be used to generate inlet conditions for use with INLET, and EDDYBL will be used to calculate the boundary-layer growth in the inlet. Finally, CPIPE is a one-dimensional code for the analysis of scramjet combustor performance. CPIPE will use the output conditions from INLET to calculate the combustor efficiencies. An overall momentum balance on the engine gives the actual thrust of the scramjet engine configuration. The use of these codes allows a detailed analysis of scramjet engine performance from nose to tail of the vehicle. A more detailed description of work on the scramjet performance analysis is given in the following sections.

SCRAM

SCRAM is a one-dimensional airframe-integrated scramjet simulation program. It is currently being used by NASA on the National Aerospace Plane (NASP) project as a first iteration on scramjet performance calculations. It is available to the Advanced Aeronautics Design (AAD) students on IBM PC computers and has been run using the hypersonic cruise vehicle (HCV) geometry as inputs.

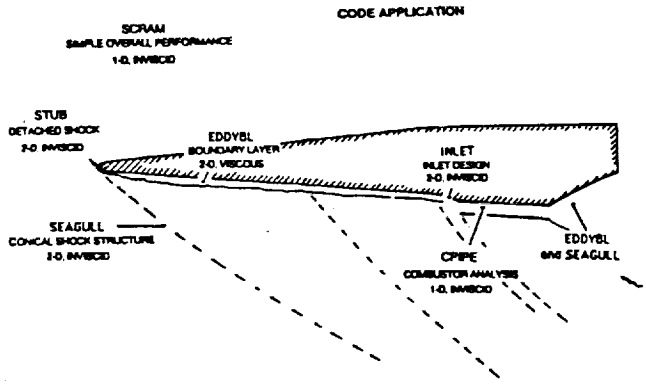

Fig. 1. Code Application

The inputs to SCRAM include freestream conditions, scramjet geometry, and other parameters necessary for calculating the flowfield, such as kinetic energy efficiency, which approximates momentum losses due to shocks, and temperatures along the surfaces. SCRAM calculates the flowfield characteristics for five stages of the scramjet: freestream, forebody, inlet, combustor, and nozzle. It outputs the flow conditions at the end of each stage, as well as boundary-layer thicknesses. It then calculates the engine-cycle performance parameters and outputs them in an overall summary.

SCRAM is used in two ways for the hypersonic drone concept. First, it is used to help determine the sizing of the engine. By developing a scaled drone instead of a full-sized, piloted hypersonic vehicle, there is a concern that the scramjet engine will not be large enough to produce sufficient thrust. Since SCRAM generates values that are optimistic for the engine performance, it offers a means of evaluating relative worth of designs prior to a more detailed analysis using the other programs.

SCRAM was also used to check the other programs used by the propulsion group, such as INLET, CPIPE, and SEAGULL. Flow conditions at each stage generated by SCRAM can be used as inputs into the other codes so that output values can be compared. Thus, SCRAM offers a quick and simple means of verifying the other programs being used for the project.

STUB

The detached shock structure generated by a supersonic blunt body is described by a computer program using the time-dependent technique outlined by Anderson[1]. Inputs to the program include upstream properties and body shape. Flowfield properties and the shock structure are then computed.

As listed by Anderson, the governing differential equations for steady supersonic flowfields and steady subsonic flowfields are hyperbolic and elliptic, respectively. Anderson points out that the fact that the nature of the governing equations changes from elliptic to hyperbolic across the sonic line causes severe mathematical and numerical difficulties. However, the *unsteady* equations of motion described by Anderson[2] are hyperbolic with respect to time, regardless of whether the flow is supersonic or subsonic. Therefore, the time-dependent technique is utilized as a means of determining the detached shock structure generated by a supersonic blunt body.

The flow is assumed to be adiabatic, inviscid, and rotational. Body forces are neglected. The procedure used in the program is described below.

First, the shock shape and location relative to the body are assumed. The flowfield is then covered with grid points, and values for density, velocity components, and other flow properties are arbitrarily assumed. These guesses are denoted as the "initial" values of these properties at time equal to zero.

The finite-difference method is then applied to the spatial derivatives in the nondimensionalized conservation equations (conservation of mass, of x and y momentum, and of energy) presented by Anderson. MacCormack's predictor-corrector technique is used for the finite-difference calculation of the time derivatives in the conservation equations.

Time steps are introduced, and new values of flowfield properties and shock shape are computed with advancing time until the flow properties converge to a so-called steady-state value. The shock structure is altered accordingly at each step so that upstream values will correspond to the computed steady-state values downstream of the shock (as calculated using shock relations immediately behind the shock). These final "steady-state" values in fact become the solutions for the correct shock structure and downstream flowfield properties.

This program was used to evaluate the flowfield near the nose of the vehicle, thus providing inputs for EDDYBL to calculate the boundary-layer growth along the forebody of the vehicle.

SEAGULL

SEAGULL is a code designed for the analysis of a two-dimensional or axisymmetric supersonic inviscid flow of an ideal gas. For the purposes of the Propulsion Design group, SEAGULL was used to model the external compression along the forebody of a scramjet engine. SEAGULL provides only an inviscid solution for the forebody flowfield and shock structure, and thus a boundary-layer code, EDDYBL, was used with SEAGULL to iteratively solve for a viscous flowfield solution.

SEAGULL was run for a sample geometry of one 5°-compression ramp. The results of this run are shown in Figs. 2 and 3. All values shown are at the surface of the vehicle (since SEAGULL is a two-dimensional code, it produces variation in flowfield properties in both the axial and radial directions). The end flowfield properties calculated using SEAGULL (and EDDYBL) were used as inputs for the program INLET.

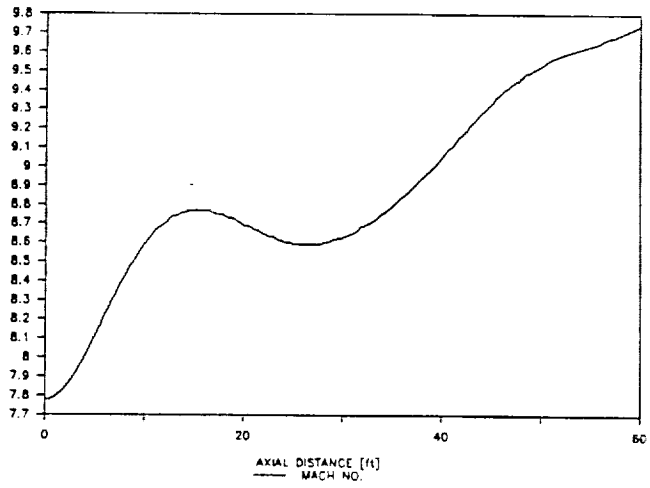

Fig. 2. Axial Distance [ft] vs. Mach No.

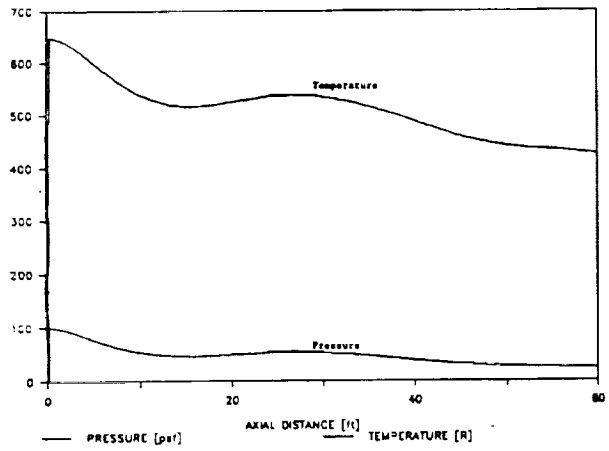

Fig. 3. Axial Distance [ft] — Pressure [psf] vs. Temperature [R]

EDDYBL

EDDYBL is a fully compressible, two-dimensional or axisymmetric computer program for the calculation of boundary-layer properties. The program accounts for mass flux as the body surface, heat flux, pressure and temperature gradients, and both transverse and longitudinal body curvature. The program does not, however, account for the effects of shock/boundary-layer interaction or separated flow.

For the purposes of the propulsion design group, EDDYBL will be used in conjunction with the programs SEAGULL and INLET, which perform inviscid analyses on the forebody and inlet of the scramjet, respectively. Provided with upstream conditions and geometry from these programs, EDDYBL outputs the boundary-layer characteristics of the flow field. The boundary-layer thickness was then used to redefine the geometry, thus creating a new inviscid input geometry for the programs SEAGULL and INLET. This alters the shock structure calculated for the forebody or inlet, respectively, and thus alters the upstream conditions used for EDDYBL. This iterative procedure was used until the flowfield properties converged on a viscous solution.

EDDYBL was helpful in determining the overall performance of a given scramjet configuration by calculating the boundary-layer growth at the inlet entrance (or cowl lip), and thus determining the effective mass flow entering the engine. Further calculations of boundary layer growth within the inlet helped determine the effective contraction ratio of the inlet, which in turn was important in determining the combustion efficiency. Overall, using EDDYBL in conjunction with the inviscid codes SEAGULL and INLET will provide a more realistic evaluation of the performance of a given scramjet configuration.

The resulting boundary-layer thickness for the first sixty feet of the drone are shown in Figs. 4 and 5. Transition to turbulence was shown to occur at a Reynolds number of about 35,000,000, which compares favorably with experimental results of hypersonic flow oven cones.[3] The boundary-layer thickness was found to be unacceptably thick entering the inlet, however, thus indicating the need for boundary-layer diversion or suction.

INLET

INLET is the main code to aid in designing the internal cowl and centerbody geometries of the scramjet. It is a two-dimensional inviscid code that uses the method of characteristics to determine the internal shock structure of the inlet. Given the conditions at the entrance to the inlet and the desired combustor entrance conditions, INLET calculates the cowl geometry required. Although the distinction between the forebody and inlet can be nebulous, the propulsion group has decided to use SEAGULL mainly for external compression and INLET for internal compression. Thus the main benefit of using INLET is that it determines the cowl geometry. However, it is necessary to have the desired combustor entrance

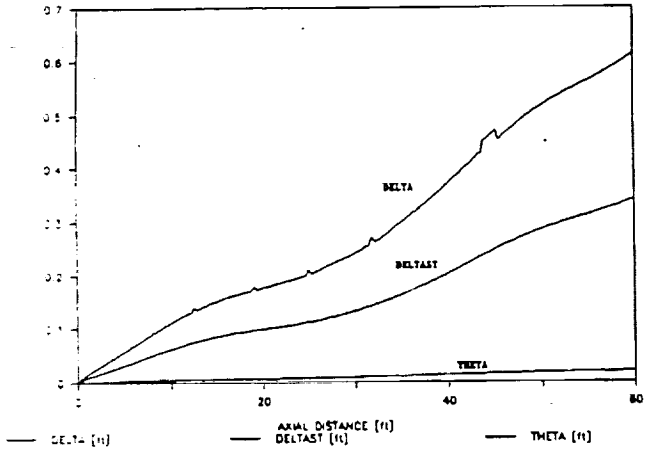

Fig. 4. Axial Distance [ft] — Delta [ft] vs. Deltast [ft] vs. Theta [ft]

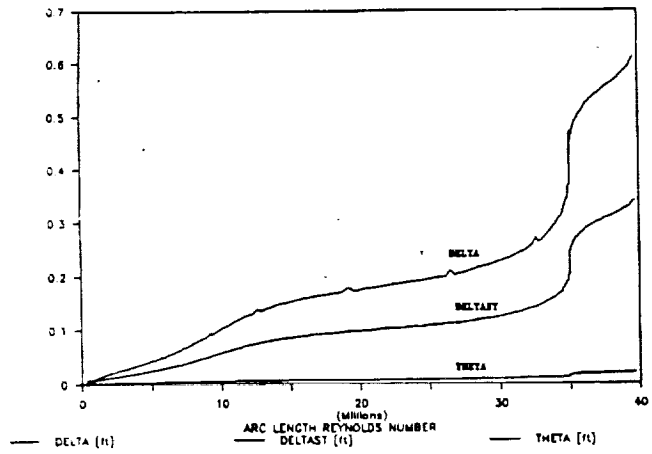

Fig. 5. Arc Length Reynolds Number — Delta [ft] vs. Deltast [ft] vs. Theta [ft]

requirements, as well as the upstream entrance conditions (acquired from SEAGULL). It was therefore necessary to iteratively use INLET and CPIPE (combustor code) to determine (1) what combustor entrance requirements are optimal for a Mach-10 flight condition, and (2) whether INLET can provide a reasonable cowl geometry for those requirements.

CPIPE

CPIPE is a one-dimensional real gas analysis of the combustion of hydrogen in air in a supersonic channel. Given the initial upstream conditions and geometry definition, CPIPE outputs the downstream one-dimensional flow properties.

CPIPE was used to model the combustor region of the scramjet engine. CPIPE is a relatively simple analysis of the combustor as it uses only one-dimensional conservation equations to calculate the downstream conditions. However, more complicated analyses of the supersonic combustor are rare and tend to concentrate on the flow structure in specific areas of the combustor (i.e., directly behind a flameholding structure or fuel-injection area). In addition, CPIPE has several useful features such as (1) possibilities for several fuel-injection points at a variety of angles, (2) estimates of ignition and flameholding likelihood, and (3) estimates of heat flux, given temperature distribution. Thus, CPIPE served the purpose of scramjet performance analysis without being unnecessarily complex.

Since CPIPE is one dimensional it will be necessary to average the flowfield values obtained from INLET in order to input the appropriate values in CPIPE.

CPIPE was validated using actual wind tunnel test data run at NASA Langley Research Center. Temperature and pressure distributions for various combustor designs that were tested in Langley's supersonic combustor test facility, were also used to validate CPIPE[4].

THERMAL MANAGEMENT GROUP

The phenomenon of aerodynamic heating was first experienced in reentry vehicles where heating rates on the order of tens of Btu/ft^2 were encountered for relatively short periods of time. In spite of high heating rates, the short time interval that the vehicles were in the critical regime allowed the problem to be managed with passive systems, such as ablative surfaces or heat sink structures.

Air breathing vehicles, while generally experiencing less intense heating rates, tend to be in the critical regimes for much longer periods of time. The aircraft skin does not possess sufficient thermal capacity to act as a heat sink. In addition, requirements for reusability and turnaround time rule out ablative surfaces.

With these considerations, the aim of the thermal management group was to design and compare active cooling systems that met the requirements of the hypersonic drone and its flight envelope. The design procedure involved the determination of a flight condition to be studied; justification of the use of an active regeneration cooling system; and, finally the optimization of the design of such a system.

First, to obtain useful data from flight tests, a suitable flight profile needed to be established. Given a range of Mach numbers (5-12) for scramjet operation and a rough estimation of the fuel tank size (8 feet in diameter, 40 feet in length), the task was to find a flight condition where active cooling was needed (due to material temperature limitations) while maximizing the flight time available for data collection and experimentation.

The group developed a code called Hypersonic Equilibrium Temperature and Heat Flux (HETAQ) to help develop a database of flight conditions. HETAQ varied Mach numbers from 5 to 12, altitudes from 70,000 feet to 115,000 feet, and nose radii from 1 to 6 inches. Lees' Approximate Method was used for determining heating rates, and an energy balance of the convective heat transfer with the radiative heat transfer produced the skin equilibrium temperature. A simple routine incorporating the thrust equation was used to determine the total flight time available, given the geometry of the proposed fuel tank, Mach number, and altitude. The code calculated time to thermal equilibrium for aluminum and titanium noses at each given flight condition. This was necessary to prove that the time required for the craft to reach thermal equilibrium would be less than the cruise flight time.

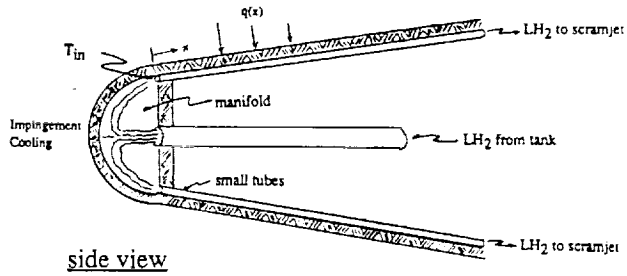

side view

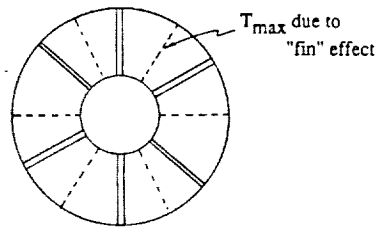

end view

* Maximum skin temperature is midway between coolant tubes

* Tubes welded to skin chosen to simplify fabrication

Fig. 6. Combined Impingement and Actively Cooled Panel Concept for the Drone Nose

Once the database was developed from the HETAQ code, the group selected a flight condition suitable for the entire design team. The propulsion group wanted the highest speed at which the heating rates could be handled. However, traveling faster meant shorter flight times (lower I_{sp}). Based on HETAQ data, anything faster than Mach 9 or 10 would use too much fuel and create undesirable heating rates. Therefore, the speed was set at Mach 10, and the altitude set at 100,000 feet. In addition, the nose radius was set at one inch, since a small nose radius produces a higher equilibrium temperature (the temperature that would arise without cooling), which we wanted in order to justify the use of an active cooling system. Indeed, the final calculated equilibrium temperature was 4000° R, high enough to require an active cooling system.

In summary, with a flight profile of Mach 10 at 100,000 feet, and with a nose radius of one inch, results from HETAQ determined that the stagnation point and points aft required cooling.

The next step then was to write a program to analyze a combination impingement-cooling and regenerative-cooling system. ACSES, or Actively Cooled Structure Evaluation System, is a FORTRAN code that models the system for a given flight condition and system variables. The purpose of ACSES is to allow the investigator to vary such parameters as tube diameter, coolant mass flow rate, and tube spacing. It enables study of the effects of these parameters on maximum skin temperature, total heat load, and coolant pressure drop. The code first analyzes the impingement cooling manifold at the nose, determines the coolant temperature exiting the manifold, and then calculates maximum wall temperatures cooled by tubes extending aft of the nose.

A method commonly used to cool the leading edge of a gas turbine airfoil involves the impingement of jets of a coolant against the leading edge's inside surface. Impingement cooling can also be applied to the nose of the hypersonic drone research vehicle. Livingood[5] presents Nusselt number correlations determined experimentally for jet impingement upon a concave, semi-hemispherical surface. Since the nose of the hypersonic test vehicle was modelled as a semi-hemisphere, a subroutine program was written in FORTRAN to utilize the Nusselt number correlations in determining the final fluid bulk temperature exiting the semi-hemisphere.

The geometrical parameters of the manifold, coolant properties, and fluid temperatures entering the manifold were inputted into the program. The output was TBOUT, the fluid bulk temperature exiting the manifold and entering the regenerative cooling system. The calculations was an iterative one: using film temperatures based on initial guess for TBOUT, coolant properties were determined; these properties were put into Livingood's correlation for average Nusselt number to find the average heat transfer coefficient; calculating the total heat transfer due to aerodynamic heating, the heat transfer coefficient was used to determine TBOUT; this value was compared with the initial guess, and the procedure repeated until values converged. Thus, the output of this subroutine returned a value for TBOUT, an input value used for analysis of the tube system.

Next, the tube system was analyzed using the fin concept and divided into sections resembling thin-walled circular shells. The temperature at the midpoint between two tubes could not exceed the maximum allowable wall temperature. In the code, a provision was provided to branch each tube (at a specified distance) into two additional tubes to further increase the heat transfer and reduce the midline temperature of the skin.

The first coolant studied was liquid hydrogen. The other coolants considered, Therminol 60 and aqueous glycol (30%), required the addition of a heat exchanger. A heat exchanger design code, provided by a member of the UCLA faculty, was used in conjunction with ACSES to design systems with these coolants. Graphs were generated detailing the relation of the number of tubes to skin maximum temperature at each station for a constant mass flow rate.

These techniques and tools developed by the thermal management group would allow the analysis and preliminary design of the active cooling system of a hypersonic research vehicle.

FLIGHT SYSTEMS GROUP

The flight systems group has been involved in conceptual sensor design to meet the needs of the thermal management and propulsion groups. Devices were designed to measure the following important parameters: outer skin friction of the aircraft, shock-wave structure, engine temperatures, flow velocity, flow constituent concentration, and pressure. Factors that made the design challenging were extremely high temperatures, pressures, flow velocities, numerous shock waves, and turbulence—all associated with the operation of the vehicle at hypersonic speeds.

Device design used concepts from such diverse fields as quantum mechanics, solid state physics, fiber optics, and fluid dynamics.

Flush Air Data System

This system is designed to measure angle of attack, velocity, and angle of slideslip of the aircraft. The technique used is similar to that of the Space Shuttle. The system consists of four sets of small pressure orifices imbedded around the nose, aligned along its vertical and horizontal diameters.

Platinum Resistance Thermometer

This sensor utilizes the characteristic of platinum to change its resistance with temperature. A platinum resistor is placed in the middle of a balanced bridge circuit. The rest of the circuit is made relatively temperature insensitive. Measurements taken with this sensor have proven to be accurate to within 4%. Because the only part of the circuit that needs to be exposed to the temperature to be measured is the platinum, the limits of the sensor are that of the platinum itself. This is sufficient for the needs of the hypersonic vehicle.

Interferometric Pressure Sensor

This sensor uses a continuous-wave, low-power laser in a Michelson interferometer to measure displacement distances accurately, and then deduce the pressure. A quartz film is placed flush with the wall where the pressure is to be measured. Below it is a substrate film that is transparent to the laser being used. One of the reflecting aluminum slabs of the interferometer is placed in the quartz, and one in the substrate. The pressure will change the height of the aluminum in the quartz film, where the Michelson interferometer then measures.

MOSFET Hydrogen Senducer

This sensor measures the hydrogen concentration in the combustor using a tiny semiconductor device called a MOSFET. The normal gate is replaced with a palladium surface that is sensitive to hydrogen. When placed in contact with the combustor flow, the hydrogen reacts with the palladium, and this is measured by the MOSFET. This allows realtime measurement with a proven accuracy of within 4%. Placement of the sensor is flush with the combustor walll so that no part interferes with the combustor flow. The sensor is capable of withstanding temperatures of the surrounding combustor walls.

Fiber Optic Pressure Sensor

An elastic drum is attached flush with the combustor wall, allowing the pressure to enter inside. An optical fiber is wrapped around the drum, and the drum will vibrate and bend in response to the pressure. A laser beam of known intensity is injected into the optical fiber. Intensity loss due to the pressure-induced curvature of the drum can be measured giving an accurate pressure measurement.

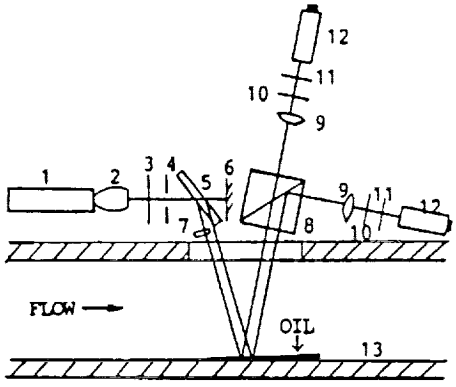

1 HE-NE LASER
2 TELESCOPE
3 NEUTRAL DENSITY FILTER
4 IRIS DIAPHRAGM
5 INTERFEROMETER FLAT
6 STOP
7 HALF-WAVE RETARDATION PLATE
8 POLARIZATION BEAM SPLITTER
9 FOCUSING LENS
10 POLARIZER
11 FILTER
12 SILICON PHOTODIODE
13 MODEL SURFACE

Fig. 7. Schematic of Dual-Laser-Beam Skin Friction Interferometer

Coherent Anti-Stokes Spectroscopy (CARS)

This device uses lasers to measure temperature, pressure, flow velocity and flow constituents in the combustor. The laser light is passed through a quartz window into the combustor where it produces emission spectra of molecules. The spacing of these intensity vs. frequency curves is a function of temperature and pressure. A shift in spectrum frequency is a function of velocity. Since each type of molecule has its own distinct spectrum, the intensity of this spectrum is a function of how many molecules of this type is flowing through the combustor. Therefore, analyzing the spectrum allows one to derive these four parameters.

Dual-Laser Skin Friction Interferometer

The skin friction sensor uses a non-intrusive, double-laser beam oil viscosity balance technique. Two out-of-phase laser beams reflected from an oil film gives alternate constructive and destructive interferences and the number of fringes and thus the rate of change of the oil film over a given time span can be precisely computed in terms of the known laser wavelength. The skin friction is related to the rate of change of thickness of the flowing oil film. The oil film used is silicon oil because of its wide range of viscosity, its relative insensitivity to temperature, low surface tension, and its very low vapor pressure. Its advantages include accuracy, simplicity, low cost, non-intrusiveness, and it can be used in turbulent flow.

Multiple Shock-Wave Sensor

This optical sensor is intended to measure shock waves that are at oblique angles to the combustor walls. Pulsed laser beams are emitted into the combustor through quartz windows. When a beam hits a shock wave, part of it will be reflected back. The rest will continue until it hits another shock wave, or the opposite combustor wall, so the detector will receive a number of intensity pulses with time. From the time delay of the reflected wave, the distance to the shock wave can be computed. This arrangement permits detection of several shock waves inside the combustor, as long as there are oblique shock waves.

Sapphire Diaphragm Sensor

This device measures pressure and temperature with a sapphire diaphragm placed flush with the aircraft's surface. First, pressure is measured by passing linearly polarized light through the diameter of the diaphragm. Due to the photoelastic effect, a fraction of the light becomes elliptically polarized as pressure is applied to the diaphragm; the attenuation of

linearly polarized light is thus a function of pressure. Temperature measurement simply makes use of the black body radiation emitted by the sapphire as it is heated up.

Fiber Optic Vortex Flowmeter

An optical fiber is placed across the diameter of the pipe carrying hydrogen for the coolant system. At one end of the fiber is a light-emitting diode. As the light travels down the fiber, there is a frequency shift which is a linear function of the mean flow speed of hydrogen in the pipe. The detectable frequency change can be changed with the choice of fiber material, the tension in the fiber, and by changing the frequency of the light-emitting diode. This device has been tested with only a slight deviation from linearity of the frequency shift with a 5% accuracy.

REFERENCES

1. Anderson, Jr, J.D. (1984) *Fundamentals of Aerodynamics*, McGraw-Hill, New York.
2. Anderson, Jr, J.D. *Modern Compressible Flow*, McGraw-Hill Book Company, New York, 1982.
3. Potter J.L., Whittield J.D. "Boundary-Layer Transition Under Hypersonic Conditions," Agardograph 97, NATO Advisory Group for Aeronautical Research and Development, May 1965.
4. McClinton C.R., Torrence M.G., Gooderum P.B., and Young I.R. Nonreactive Mixing Study of a Scramjet Swept-Strut Fuel Injector. *NASA TN D-8069,* December 1975.
5. Livingood J. and Gauntner J. Heat-Transfer Characteristics of a Single Circular Jet Impinging on a Concave Semihemispherical Surface. *NASA TM X-2859.* August, 1973.

AIR TRANSPORTATION SYSTEMS FOR THE CALIFORNIA CORRIDOR OF 2010

CALIFORNIA POLYTECHNIC STATE UNIVERSITY, SAN LUIS OBISPO

INTRODUCTION

In 1986 NASA and USRA identified Cal Poly as one of seven "Centers of Aircraft Design Education," and accepted a proposal from Cal Poly to conduct a three-year study of the potential for Lighter-Than-Air (LTA), Vertical Take-Off And Landing (VTOL), and Short Take-Off And Landing (STOL) aircraft concepts for air transportation within the California corridor. The project emphasizes configurations that are both innovative and unconventional in design for use in the 2010 time period.

The topic of LTA/VTOL/STOL aircraft was selected because it is consistent with the mission of the NASA Ames Research Center and is a broad topic that succeeding classes at Cal Poly can continue to iterate and refine to produce meaningful results for NASA.

The students have been encouraged to be innovative in order to identify key technology areas that can be developed into future research programs. The aircraft/air transportation systems currently being developed are described below.

VTOL concepts. These include warm-cycle rotary-wing aircraft and joined-wing, variable-diameter tilt rotor.

STOL concepts. These include blown flap flying wing aircraft; upper surface blown cantilever wing aircraft; and upper surface blown delta wing aircraft.

Air Transportation Systems. These incorporate a VTOL aircraft which serves as a "taxi" to and from a continuously moving platform: helipsoid airship/twin turboprop, quad lift fan cantilever wing aircraft; modified deltoid airship/advancing blade concept helicopter; and magnetic levitation train/joined wing, variable diameter tilt rotor.

Air transportation needs in the California corridor include commuter air service, executive air transport, emergency medical service, public service, offshore oil support, and freight/package service.

Along with studying the technical issues normally involved in any aircraft design problem, the topics of safety, noise, public acceptance, and economic viability in commercial operations are also addressed.

STOLIT

Due to record levels of population and travel in the California corridor, time, space, and cost will make ground transportation almost impossible by the year 2010. An Upper Surface Blown Short Take-Off and Landing aircraft was designed to both connect metropolitan areas and alleviate high density traffic. The aircraft was configured through technology surveys, trade studies and an iterative design process based on efficiency, noise, safety, passenger services, and time savings.

In the design of the STOLIT (Short Take Off and Landing Intrastate Transport) aircraft data pertaining to stability and control, propulsion, performance, economics, etc., were calculated and defined (Fig. 1). For stability and control the c.g. was calculated to be at 38 feet behind the nose of the aircraft and the static margin is approximately 40% of the cord. For directional stability a directional coefficient, C_n = 0.098, was calculated and the rudder power was found to be large enough to overcome one-engine-out conditions. The propulsion forces were calculated to be: T_{total} = 4,735 lbs at sealevel, with a T_{req} of 3,250 at 25,000 feet. The takeoff gross weight (TOGW) was calculated to be 30,748 lbs.

Direct operating cost (DOC) values were calculated for two mission profiles, intermetro and commuter. For the intermetro route a DOC of approximately .875 cents per ton mile was calculated for 700 n.m. and the commuter route had a DOC of approximately .82 cents per ton mile for 20 n.m.

Special features introduced in the STOLIT aircraft are: Air Cushion Landing System (ACLS), Upper Surface Blowing, Computer Pilot, and Improved Passenger Processing and Services. Including all these different technologies, the aircraft will be able to operate in a more flexible market.

The STOLIT aircraft is feasible now. The major components of the aircraft, the USB wing and ACLS, have already been

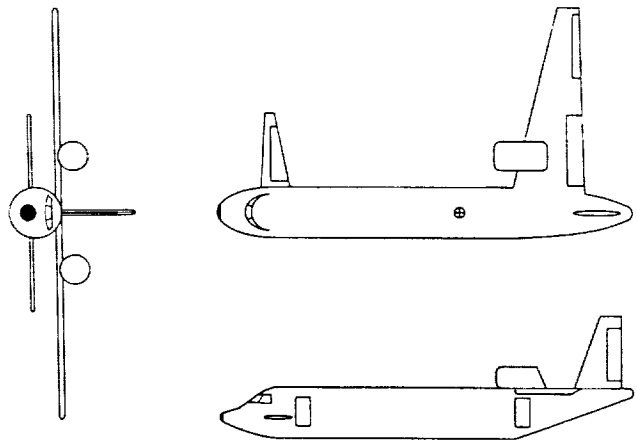

Wing Loading = 82 lbs/ft²
V_{cruise} = 290.2 Kts
Schedual Range = 700 Nm
Span = 54.8 Ft
Total Length = 70.0 Ft
Gross Takeoff Weight = 30,749 lbs

Fig. 1. Upper-surface blown STOL aircraft

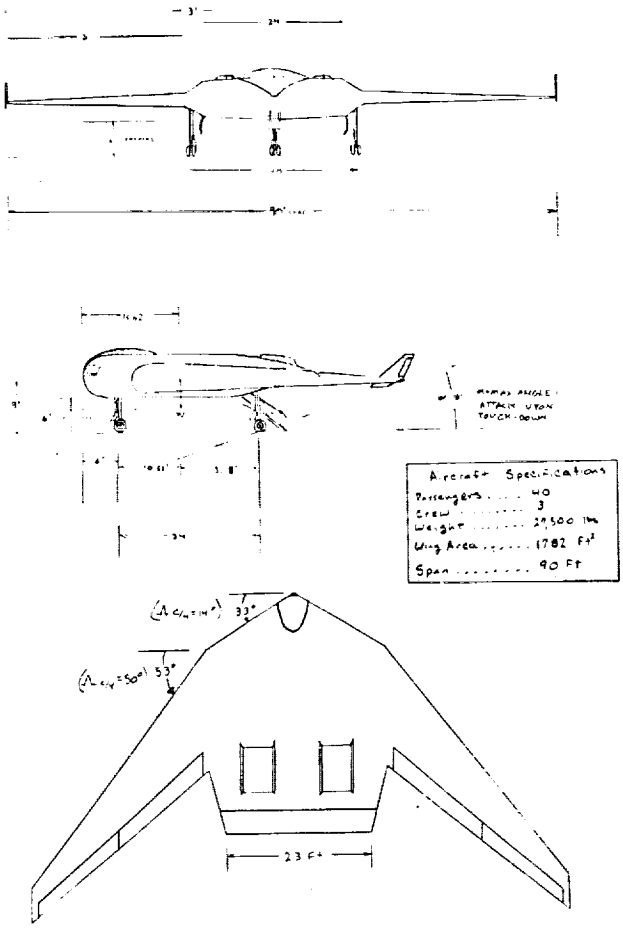

Fig. 2. STOL Flying-Wing aircraft

proven workable. Assumptions were made about materials advances for the skin and airframe which would optimize the design, but the aircraft could almost be built now and certainly in 20 years. The STOLIT is a viable solution for the problems of California corridor commuting. The 40-passenger payload fulfills the requirements proposed by the corridor study as well as requirements for speed, altitude and field length. This aircraft could open up commuter traffic to small communities thus linking people living in remote areas to major centers of business.

Recommendations for further study include refinement of the ACLS and computer pilot, development of higher efficiency engines and use of composites in airframe and skin production.

STOL FLYING WING

California's expanding economy and growing population have placed tremendous demands on the current transportation systems. By the year 2010, these demands are expected to surpass the limits of the existing systems. For this reason, new systems have to be designed incorporating the latest technologies and procedures. One proposed system utilizes STOL aircraft for shuttling commuters throughout California. The STOL Flying Wing has been designed for this purpose (Fig.2).

The advantages of aerodynamic efficiency and structural simplicity, inherent for an all-wing aircraft, are unsurpassed. The large interior cabin with theater-type seating offers passengers the most comfortable environment available. Safety was given priority throughout the design. Features such as an advanced cockpit to eliminate pilot error, and the ability to jettison the outer wing sections to maintain control after a midair collision and eliminate fuel explosions, will reduce airplane catastrophes. Other special features of the design include the use of the engines for control, self-contained passenger loading and unloading, and over-the-wing mounted engines. Weight, cost, and drag were optimized.

The aircraft designed marks a major step away from the traditional pattern followed by passenger aircraft to date. By the year 2010, the conventional cantilever wing aircraft will be too costly to operate. Aircraft like the STOL Flying Wing will be required for their efficiency and passenger preference.

THE 3USB-40 - A FUTURISTIC STOL AIRCRAFT

To satisfy the requirements of Cal Poly's senior design series, a futuristic, three-surface STOL transport, dubbed 3USB-40, was designed to satisfy the proposed air task; several aircraft configurations were compared including dual-fuselage aircraft, all of which would use upper surface blowing (USB) as a high lift mechanism (Fig. 3). Each configuration was rated using several different criteria and given a total score representing its capability to satisfy the design objective. With these criteria defined, the comparison was completed and the cantilever wing was chosen to be the basic configuration of the 3USB-40.

Since USB lift depends solely on high energy engine exhaust moving over the wings, it was found that one-engine-inoperative (OEI) requirements could not be satisfied with only two engines. This is due to an uncontrollable roll rate when one engine is out caused by an extreme imbalance in lift on the wings. At this point, four turbofans were chosen and the weight estimations were begun along with the design of the interior and cockpit. It will be possible to configure the interior of the 3USB-40 as a 21-passenger business jet, a 40-passenger commercial transport, a cargo transport, or any combination of the above.

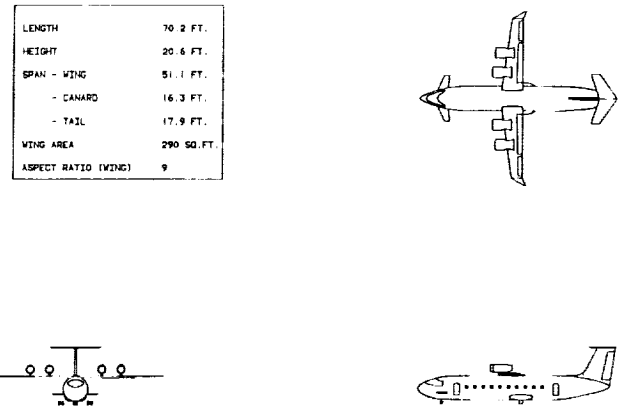

Fig. 3. Three-view drawing, 3USB-40

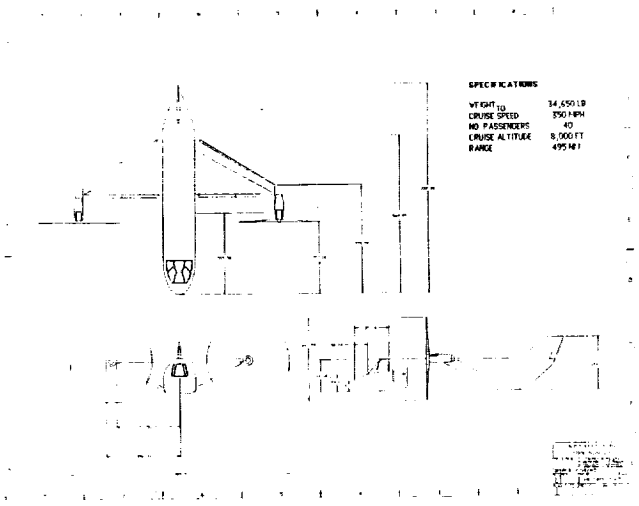

Fig. 4. The Rail and Plane Integrated Design (RAPID) system

It was projected that in the year 2010, the air traffic control system will be automated, so a computer controlled fly-by-light system with a single human backup will be used. The pilot will have enough hands-on flying to keep him/her from boredom, but the bulk of the inflight information will be monitored and processed by computer.

Stability and control iterations were performed, showing a slightly unstable aircraft. Active flight controls were selected to correct this problem as opposed to larger, heavier control surfaces. With the design and components chosen, the 3USB-40 will have a gross weight of 26,767 lbs and a takeoff distance of around 1800 ft on a 95°F day. This is well within safety limits for operation out of a 2500 ft airfield.

It is felt that the 3USB-40 should be a prime candidate for use as a short haul transport in the California corridor in 2010. Research is recommended, however, in the stability and control of aircraft utilizing USB, especially in the takeoff and approach configurations. Continued improvements in propulsive efficiency and artificial intelligence capabilities are also encouraged, both of which should be greatly improved by the year 2010. With these advances made, it is evident that the 3USB-40 could be built and begin servicing the smaller airports in California with very little or no change to the airports themselves. This will be a very important consideration in the future when a new, efficient, state-of-the-art transportation system is being developed.

RAPID

The RAPID (Rail and Plane Integrated Design) system utilizes a magnetic levitation train with an interfacing variable-diameter tilt-rotator aircraft which is designed to meet the increased transportation needs resulting from the projected population increase of 30% by the year 2010 (Fig. 4).

In designing the aircraft, various parameters of weight and balance, stability and control, performance, and cost efficiency were investigated. The weight and balance analysis found a takeoff weight of 34,650 lbs, an empty weight of 31,185 lbs, and a c.g. location of 25.8 ft from the nose and 6.36 ft above the floor. The static longitudinal stability for the airplane in flap-up, gliding flight with propellers windmilling was found to be −0.034, and for gliding flight with fixed controls and no propeller it was found to be −0.1599. Both of these are considered statically stable. The stick-fixed neutral point for gliding flight is 0.2996%, and for windmilling is 0.174% of the mean aerodynamic chord. The performance calculations yielded a maximum rate of climb of 6000 ft/min, a cruise speed of 304 knots at an altitude of 8000 ft, and a maximum range of 495 n.m. The direct operating cost analysis yielded a cost savings of approximately 50% for the RAPID system over strictly aircraft transport.

The use of a removable passenger compartment, which allows for a rapid turnaround time, is one of the main features that gives our aircraft an advantage over other conventional designs (Fig. 5). The tilt rotor gives the flexibility to take off and land vertically in congested metropolitan areas such as on building rooftops, parking lots, etc. The use of a joined-wing configuration gives the aircraft added fuel storage, significant

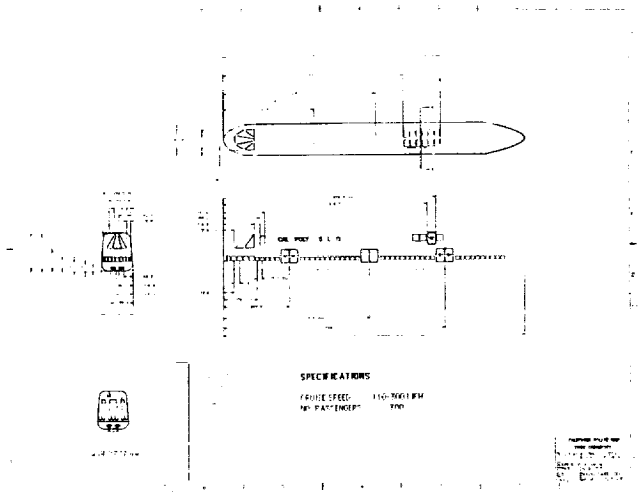

Fig. 5. Removable passenger compartment of the RAPID system

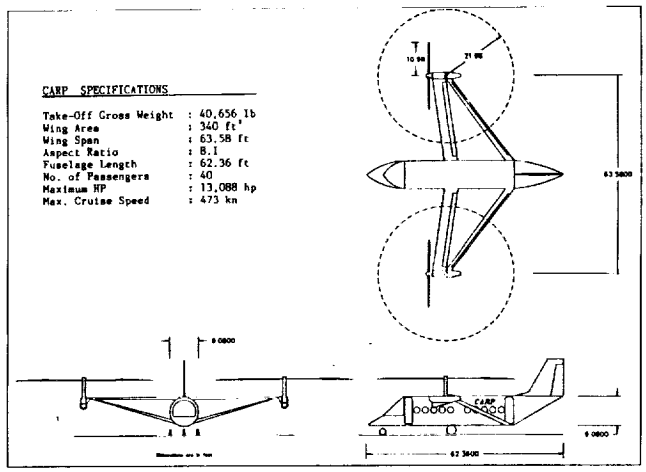

Fig. 6. Variable-diameter tilt rotor aircraft

weight savings, and structural strength. The maglev train allows the use of electric power which is not only more abundant than fossil fuels, but also has less impact on the environment.

The RAPID system is considered a feasible and cost effective solution to the transportation needs in the California Corridor in the year 2010.

CARP

A tradeoff study was done among various VTOL configurations: pure helicopter, compound helicopter, variable compound, stowed rotor, tilt rotor, variable-diameter tilt rotor, and folding tilt rotor (Fig. 6). These were compared on the basis of six requirements: speed, complexity, hover efficiency, noise, empty weight, and productivity factor. A variable-diameter tilt rotor was found to be best suited for the design requirements as set by the California Corridor Study. The chosen design uses a joined wing (thinner airfoil), has both VTOL and STOL capabilities, low disk loading (13 psf), high L/D for cruise, high productivity factor, low noise in cruise, and low tip speed with the TRAC rotor. Problem areas include engines overpowered in cruise due to OEI requirements; transmission and drive system complexity; requires dual control systems, one for cruise and one for hover.

Stability and control: neutral point is 105% mean aerodynamic chord (MAC) in glide and it moves about 7% MAC with full power. The c.g. will never be 42% MAC ahead of neutral point; elevators are satisfactorily sized. The static margin range is -0.06 to -0.42. Two Allison T406 engines will supply 13,088 hp maximum; TOGW = 40,656 lbs; Empty weight = 30,861 lbs. Forward c.g. is 24.41 ft. Aft c.g. is 25.96 ft for a total fuselage length of 62.36 ft. Therefore, the c.g. travel is 1.52 ft. VTOL performance at sea level can climb 7000 fpm; at 6000 ft altitude can climb 5000 fpm. Airplane mode performance: at 15,000 ft, 200 kts, can climb 3235 fpm. Service ceiling is 23,300 ft, (OEI service ceiling: 18,200 ft.). Special features of design: variable diameter rotor, joined wing, tilt pylons, cabin layout has 4 passenger-access doors for quicker turnaround

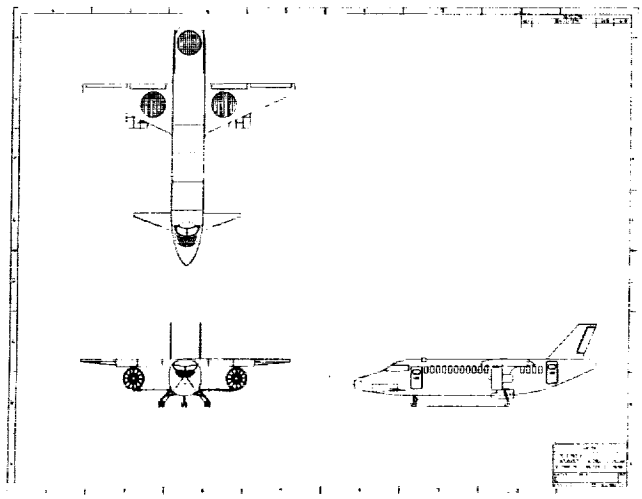

Fig. 7. Commercial VTOL transport

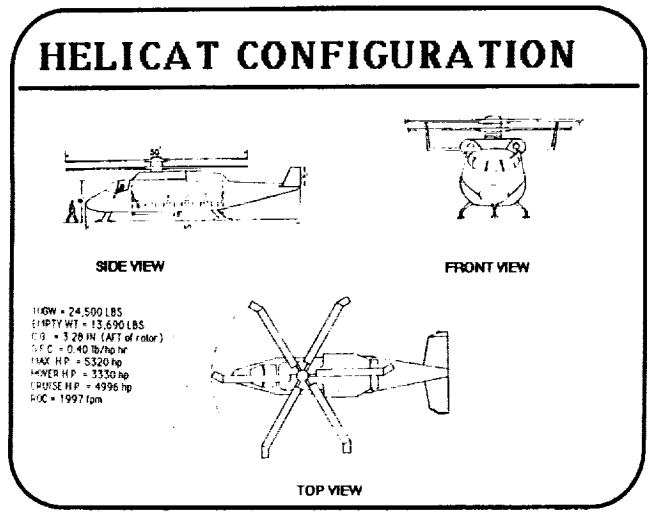

Fig. 8. Advanced Blade Concept Helicat

time, crew is composed of 2 pilots and no flight attendants.

Preliminary design of CARP has progressed quite well. It is strongly recommended that the variable-diameter tilt rotor concept be looked at more closely in VTOL rotorcraft design, for it is a viable concept with few disadvantages. A variable-diameter rotor system seems to be the natural choice for the tilt rotor aircraft, since it combines the vertical takeoff and landing performance of the tandem rotor helicopter with the cruise performance of the turboprop airplane. Areas for further study include cycling engines or cutting one engine back in cruise to alleviate overpowered engines in cruise; savings in weight due to use of composites; finding the actual variable-diameter retraction; placement of rotor relative to the fuselage and their effects on cabin noise levels; aerodynamic and interference effects of the joined wing; special stability considerations for the joined wing and tilt rotor combination.

VTOL

This report is the result of three quarters of senior design work towards the completion of a commercial VTOL (Vertical Take-Off and Landing) transport which will dock and unload/load passengers with a moving airship (LTA-partially lighter than air) to suit the needs of the California Corridor in the year 2010 (Fig. 7). Its goal is to establish the need for the designed aircraft, then by considering its mission profile an analysis of the type of aircraft to fit this mission profile will be presented.

The VTOL presented is a combination Lift Fan for VTOL capability, and two turbofans for cruise flight. Incorporated in the design is a twin vertical tail in conjunction with a canard, and tip sails to reduce its induced drag.

Maximum T.O. Weight: 31,160 lbs.
Number of Crew:
—Flight Observation: 1 Auto pilot, 1 Captain for Flight
—Cabin: 1 Cabin Attendant
Number of Passengers: 39
Design Cruise Speed: 400 knots, M = .70
Critical Mach Drag Rise: M = .74

Range: 400 n.m.
Fuel Weight: 3350 lbs
Absolute Ceiling: 19,820 ft
Service Ceiling: 19,500 ft

Dimensions:

Wing Span: 60 ft
Length: 65 ft
Height (to fuselage top): 13 ft

Wing Area:

Wing Area: 571 sq ft
Root Chord: 14 ft
Tip Chord: 2.8 ft
Wing Sweep: 9°

HELICAT

The commuter congestion in the metropolitan areas, particularly Los Angeles, has been a serious problem over the past years. A system has been proposed, as a rapid transit system, that will help alleviate the Los Angeles Metropolitan traffic congestion for the year 2010.

The configuration chosen for this system was an Advanced Blade Concept (ABC) helicopter (Fig. 8). This configuration was selected based on the needs of the transportation system. Such aspects include high lift capability, low noise (for public acceptance), and that no runway would be required for landing or takeoff.

The weight and balance of the ABC are as follows: takeoff gross weight is 24,500 pounds, the empty weight (with module) is 13,690 pounds, center-of-gravity location is 3.28 inches in front of the rotor, the center of gravity travel is 32 inches ahead and 26 inches behind the main rotor.

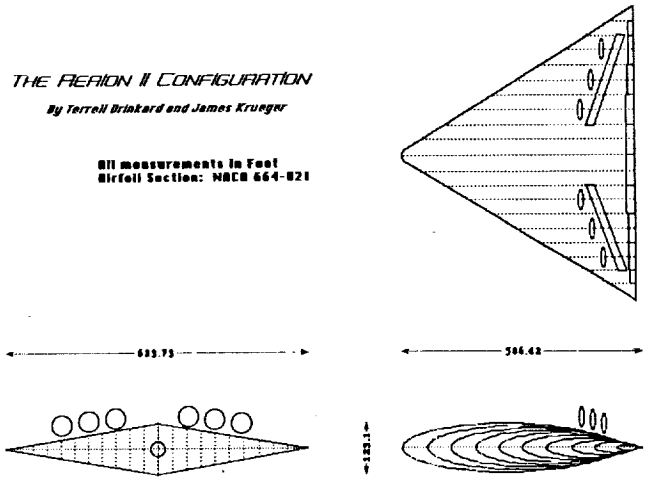

Fig. 9. Three-view drawing

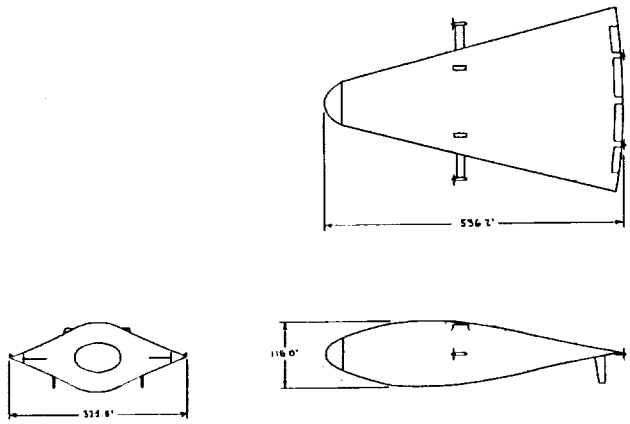

Fig. 10. General Arrangement of the Los Angeles Commuter Air Transit System

The ABC's powerplant design was based on a Pratt and Whitney 125A. The maximum power was rated at 5320 hp for the ABC. It had a specific fuel consumption of 0.40 lb/hp hr.

The stability characteristics of the ABC are as follows: (for trim condition) the thrust required on the rotor is 27,124 pounds, the pitching angle of the rotor is 10.14°, and the flapping angle of the rotor is a -9.63°; the size of the horizontal and vertical stabilizer is found to be 130 ft^2 and 15 ft^2 (for each stabilizer, since there are two vertical tails) respectively.

The performance parameters calculated are as follows: the horsepower for hover is 3330 hp, the horsepower for cruise (204 ft/sec), is 4996 hp, the rate of climb is 1997 ft/min, and the rate of descent is 1878.8 ft/min.

Since the ABC has already proven to be a successful aircraft today, the feasibility of using this aircraft for this system by the year 2010 is quite good. Alternatives in energy sources, such as fusion, solar energy, and microwave power should be investigated. Fly-by-wire and fly-by-light should also be researched.

LTAC

By the year 2010, commuter demands will be forcing the state of California to bring about new, more efficient means of transportation. For that reason, we have come up with what we believe to be an innovative and viable aircraft to meet this foreseen demand. It is basically a cross between a lighter-than-air airship and a passenger aircraft, which we have designated, the Lighter Than Air Craft (LTAC-Fig. 9). In this report the design for the California Corridor LTAC is presented along with the performance specifications, characteristics, design philosophy and methodology. It was analyzed for flight performance, geometry, and direct operating cost using classical performance equations with adapted empirical direct-operating-cost equations. The design was inspired by the basic configuration developed by the Aereon Corporation during the late 1960's. Although the Aereon configuration never went into commercial use, we believe, based on a cost analysis, that the

LTAC put forth in this report would fare quite well in the competitive transportation market. Moreover, it shows promise as a safe, stable, and controllable passenger transport.

LTA

Highway congestion in metropolitan areas is beyond design limits and is not expected to decrease. Various mass transit transportation can be implemented to help relieve some of the expected congestion. This feasiblity study evaluates the advantages of a Lighter-Than-Air (LTA) mass transit system to serve this purpose projected for the year 2010 (Fig. 10).

The mass transit system uses permanently airborne LTA's cruising between 1500 and 2000 feet AGL with compound helicopters interfacing with the LTAs to drop off and pick up passengers traveling in booth compartments. The modular concept provides the advantages of rapid turn around time for the VTOL aircraft that interface with the LTA without hastening passengers or eliminating customer convenience.

Optimization of a dynamic lift configuration of the LTA was accomplished employing the Comprehensive Airship Sizing and Performance Computer Program (CASCOMP). Stability and control calculations were performed and system initiation and operating costs were estimated.

A STUDY ON THE PLANFORM EFFECTS OF HIGH-SPEED VEHICLES

CALIFORNIA STATE POLYTECHNIC UNIVERSITY, POMONA

A study is presented on the planform effects of transport aircraft in the Mach 3 to 6 range. A request for proposal containing a baseline mission profile was common to four aircraft designs. These aircraft were designed to perform the same mission in order to obtain conclusions regarding the performance of the aircraft. The four configurations include the blended-wing-body concept, joined-wing concept, oblique-wing concept and the caret (waverider) concept. This paper presents the top-level performance trends common to the four configurations during high-speed flight. No conclusions are presented on the best planform as all the designs have positive and negative aspects. However, both the positive and negative features of the designs are identified.

DESIGN SPECIFICATIONS

A request for proposal was developed using the available studies done by McDonnell Douglas and Boeing on the high-speed civil transport. The request for proposal is for a complete aircraft design that meets the following criteria.

1. The aircraft must have an overall range of 6500 nautical miles.
2. The design Mach number shall be between 3 and 6.
3. The aircraft must be able to accommodate 250 passengers.
4. The aircraft must be able to operate from existing airports.

Other considerations and goals were established by the design groups. The turnaround-time goal was 1 hour, the noise of the aircraft had a 1-psf overpressure goal while depletion of the ozone layer was to be kept to a minimum. Given this request for proposal, a mission profile was then developed.

The initial design process began with the selection of the mission profile. The mission profile was constrained to meet all the requirements set forth in the request for proposal and be compatible with the Federal Aviation Regulations requirements. The mission profile selected for the four configurations is shown in Fig. 1. It is a generic ferry mission with both climb and descent counted in the total range. The loiter, takeoff and, landing legs of the mission are not included in the overall mission range.

CONFIGURATIONS

The four configurations for the study were the blended-wing-body, the joined-wing, the oblique-wing and the caret (waverider) configuration. Each of the designs has both strong and weak points. The purpose of this study was to study the effects of the four configurations to give aircraft designers a better feel for how these planforms perform at hypersonic speeds.

The blended-wing-body is shown in Fig. 2. It has an aspect ratio of 1.25 with a wing loading of 106 lbs/ft^2. One of the advantages of the blended-wing-body is that it is a proven design. Other aircraft such as the SR-71 and the Concorde utilize blended features. In this design the interference drag is reduced and the fuselage can be used for lift. Another advantage is that the blended configuration contains more volume than other designs. This is important because fuel can be stored in the wings away from the passengers, increasing safety. However, the drag is higher than some of the other configurations and it does not have good low-speed performance.

The joined-wing configuration is shown in Fig. 3. It has a takeoff wing loading of 131 lbs/ft^2 at an aspect ratio of 3.5. The advantage of the joined-wing design is that it is a structurally sound design. The front wing is swept back to meet the rear wing to form a truss. The inherent stability of

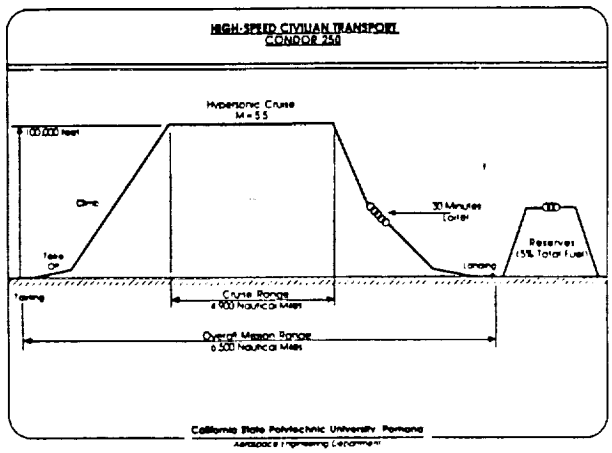

Fig. 1. Mission Profile

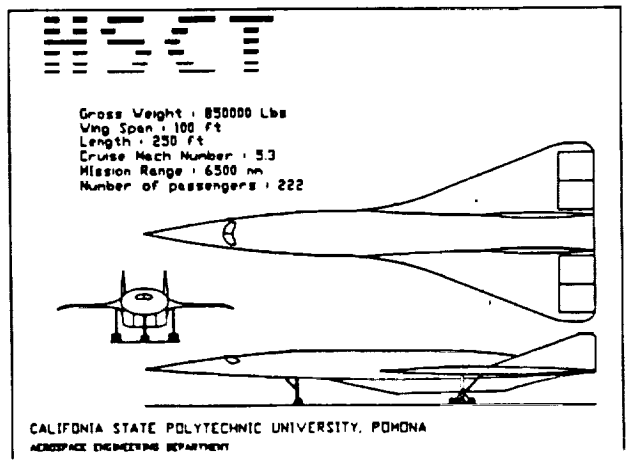

Fig. 2. Blended-Wing-Body

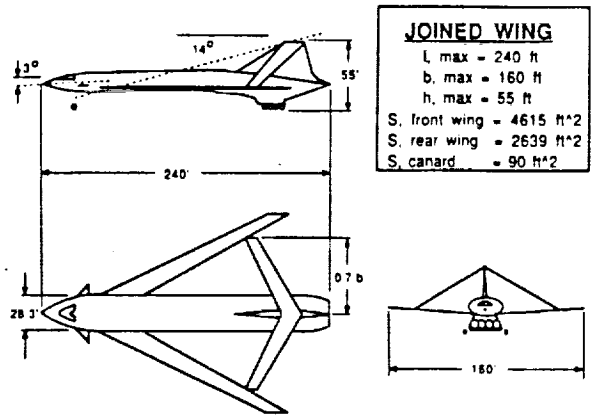

Fig. 3. The Joined-Wing Configuration

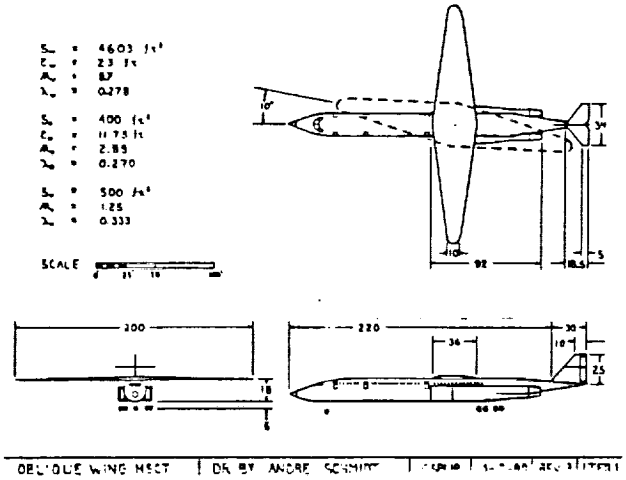

Fig. 4. The Oblique-Wing Configuration

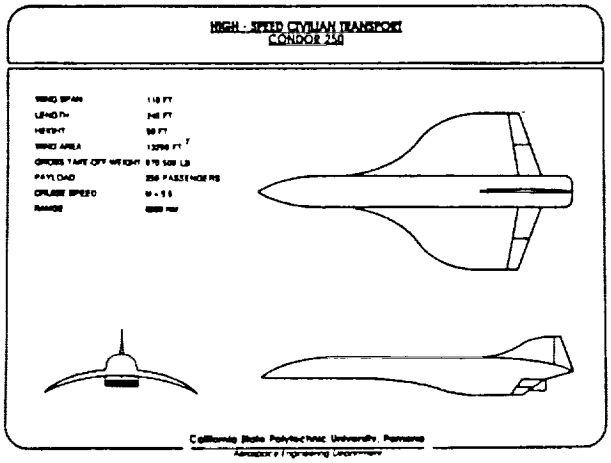

Fig. 5. High-Speed Civilian Transport: Condor 250 (Caret Design)

the truss design allows the wings to be thinner than those on other aircraft. Because of the two lifting surfaces and the thin wings, drag can be reduced while lift can be increased. It should be noted that the joined-wing configuration had to utilize a retractable canard in order to achieve a better roll at takeoff. One of the disadvantages of the joined-wing design is that it has a smaller usable volume than other configurations. Therefore, all of the fuel for the flight must be carried in the fuselage decreasing safety. Another disadvantage is that the joined-wing does not have as good a compression surface for the inlet as the blended configuration.

The oblique-wing configuration is shown in Fig. 4. It has an aspect ratio of 8.7 with a wing loading of 125 lbs/ft^2 pounds per square foot. The major advantage for the oblique-wing is its low-speed performance. The overhead wing will rotate at higher speeds to keep the wing within the Mach cone. This will give the oblique wing moderately good performance at high speeds. The major disadvantage of the oblique design is the rotating wing. First, the aircraft will be unstable as the wing is being rotated. Second, the aircraft will have to carry heavy mechanical devices to rotate the wing. Finally, with this configuration, it will be more difficult to control the heat load on the structure. Other disadvantages are the smaller volume for fuel and the lack of a good compression surface for the inlets.

The caret design is shown in Fig. 5. It has a takeoff wing loading of 70 lbs/ft^2 with a wing area of 13,290 ft^2. The caret is a very good high-speed design with the configuration designed to "ride" the shock wave. The entire bottom of the aircraft acts as a lifting surface and as a compression surface for the inlets. Another advantage is that there is more usable volume (compared to the other three configurations) in this configuration. The major advantage for the design is its low-speed performance.

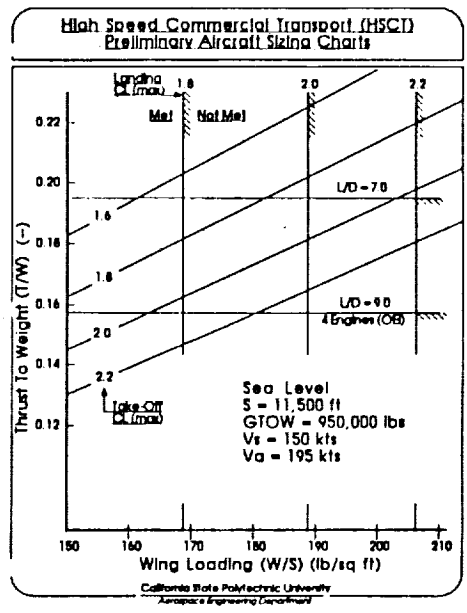

Fig. 6. High Speed Commercial Transport (HSCT): Preliminary Aircraft Sizing Charts

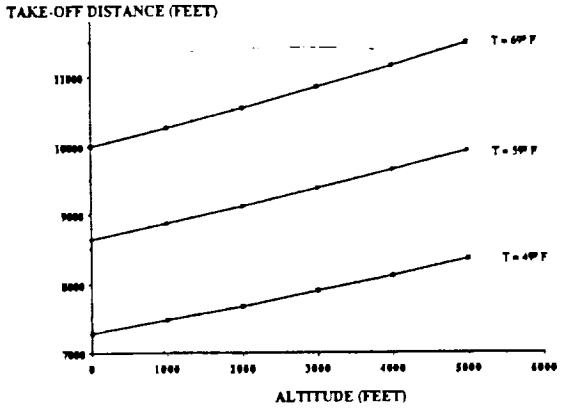

Fig. 7. Take-Off Distances To Climb To 50 Ft.

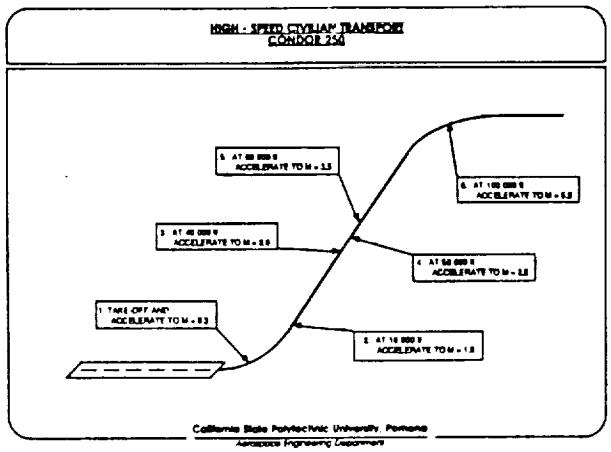

Fig. 8. High-Speed Civilian Transport: Condor 250 (Climb Path)

PERFORMANCE

The four configurations were designed with the generic sizing chart shown in Fig. 6. The sizing chart allowed the determination of the preliminary wing loading and thrust-to-weight ratio for the aircraft to be made. From this chart and an initial weight estimate, the initial planform area and thrust required can be found[1]. The chart allows takeoff, landing, and cruise conditions to be examined on one chart.

The takeoff distance is proportional to the wing loading and inversely proportional to the aircraft thrust-to-weight ratio. A takeoff field distance was chosen to be 11,500 feet so that the aircraft will be able to operate from existing airfields. A simplified method for takeoff and landing performance was found[2]. The synergistic effects of altitude and atmosphere can be included in this analysis by incorporating the effects due to density change. A chart of takeoff distance as a function of altitude for hot, standard, and cold day operations is shown in Fig. 7. .

The climb performance utilizes a minimum time to climb with a dynamic pressure constraint. Minimum time to climb was chosen as the objective flight path because of the noise considerations at takeoff. The climb path is shown in Fig. 8 and uses a maximum dynamic pressure limit of 1000 lbs/ft^2.

The cruise leg of the mission will be at the optimum altitude and Mach number for each of the aircraft. As shown in Fig. 9, the required thrust vs. altitude gives a minimum thrust required at altitudes between 80,000 and 90,000 feet. However, each of the configurations may deviate from this optimum altitude. The reason is that this region is most susceptible to ozone depletion. Therefore, if aircraft are to fly in this region, more time must be spent analyzing pollution effects.

The requirements set forth in the FAR Part 25 state that civilian transport aircraft must use a landing field length proportional to the square of the approach velocity. The joined-wing configuration, for example, has an approach speed

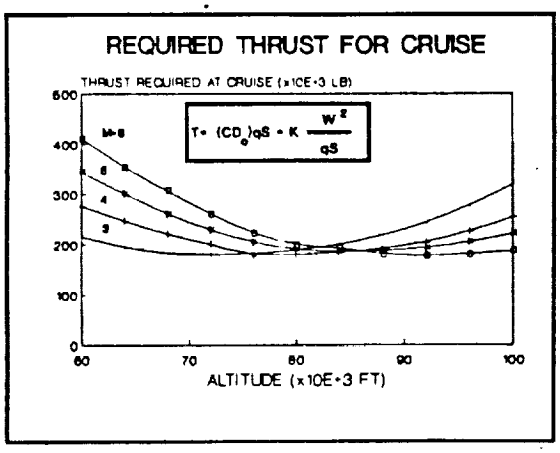

Fig. 9. Required Thrust For Cruise

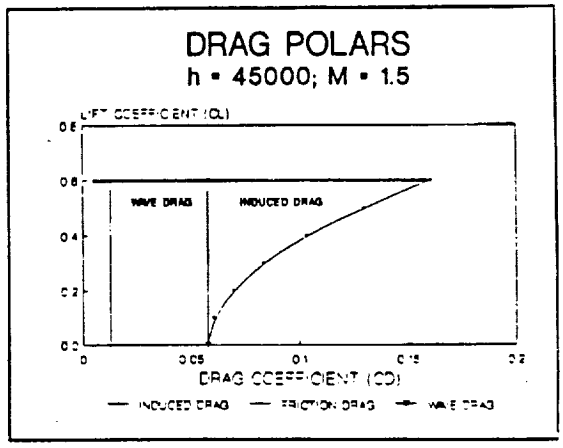

Fig. 10. Drag Polars: h = 45000; M = 1.5

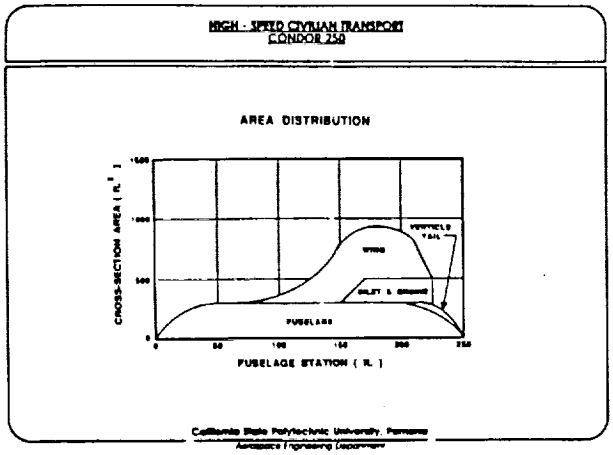

Fig. 11. High-Speed Civilian Transport: Condor 250 (Area Distribution)

of 195 knots with a stall speed of 150 knots. With this approach velocity, and assuming 50% fuel, the aircraft will be able to land within the landing field length.

AERODYNAMICS

The aerodynamics of the four configurations were evaluated using several methods. In the subsonic region, slender body theory was used. In the supersonic range, linearized theory was used, while for speeds above Mach 5, corrected Newtonian impact theory was employed[3,4,5]. A breakdown of the drag at supersonic speeds is shown in Fig. 10. As can be seen, one of the major contributors to drag is wave drag. However, area ruling can be used to reduce wave drag as can be seen in Fig. 11. In order to reduce wave drag at supersonic speeds, the area distribution of the aircraft should have a Gaussian or somewhat parabolic shape. The area distribution is close to being Gaussian but there still is a large amount of area towards the rear of the aircraft. However, this is desirable at hypersonic speeds because the plume of the engines eliminates most of the base drag.

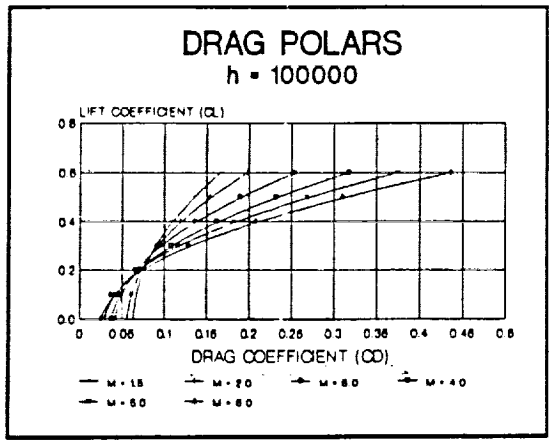

Fig. 12. Drag Polars: h = 100000

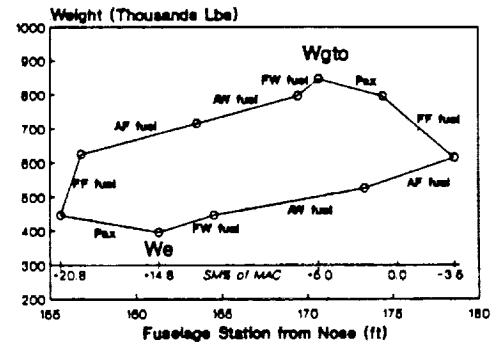

Fig. 13. Center of Gravity Travel

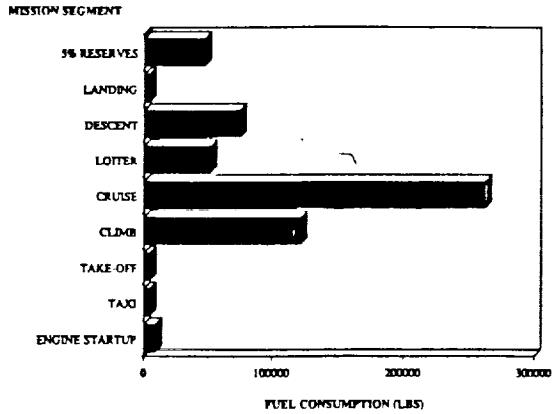

Fig. 14. Mission Fuel Breakdown

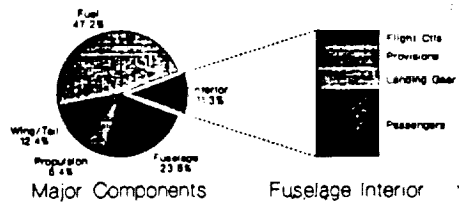

Fig. 15. Weight Distribution

The cruise drag polar for the joined wing configuration is shown in Fig. 12. The zero-lift drag coefficient at cruise is about 0.04 with a lift-to-drag ratio at cruise close to 3.

The center-of-gravity travel for the blended-wing-body is shown in Fig. 13. The center-of-gravity for maximum gross takeoff weight is about 5% of the mean aerodynamic chord (MAC) forward of the mean aerodynamic center giving favorable static stability derivatives. The center-of-gravity travel of the aircraft during normal cruise moves about 8 feet forward with fuel distribution methods being used during transition from subsonic to supersonic speeds. Other weight distribution combinations, including maximum fore and aft, are also shown giving the entire center-of-gravity envelope.

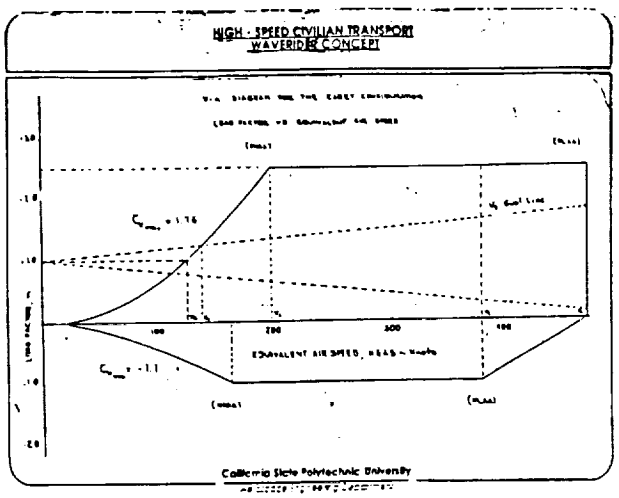

Fig. 16. High-Speed Civilian Transport: Waverider Concept

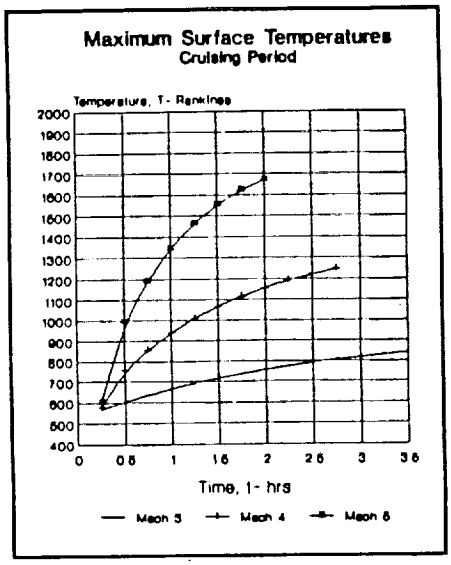

Fig. 17. Maximum Surface Temperatures: Cruising Period

WEIGHTS

The total weight of the aircraft is the sum of the empty weight, fixed weight, and fuel weight. The initial weight of the fuel can be found by finding the fuel fraction for each leg in the mission[2]. A breakdown of the fuel weight is shown in Fig. 14. As can be seen, the cruise portion of the mission uses the most fuel. Therefore, in order to minimize fuel requirements, the cruise leg should be flown at an optimum Mach number and altitude.

The fixed weight is comprised of the crew, passengers, equipment, luggage and inflight refreshments. The weight for each passenger was assumed to be 175 pounds with 40 pounds of baggage each. With these assumptions, the fixed weight of the aircraft is estimated to be 60,000 pounds.

The empty weight of the aircraft was found by summing the component weights of each element, using the General Dynamics method of weight estimation for transport aircraft. A breakdown of the weight distribution for the blended-wing-body configuration is shown in Fig. 15. It can be seen that the fuel comprises the major portion of the weight.

STRUCTURES/HEAT TRANSFER

The maximum loads that the aircraft will encounter are shown on the V-N diagram for the caret design in Fig. 16. The maximum positive load factor for this aircraft is about 2.5; maximum negative load factor is close to -1.0. From this diagram, it can be seen that the gust lines lie within the envelope, required by FAR.

The aircraft will encounter both aerodynamic loads and thermal stresses. The maximum heating rates will occur at the stagnation points of the aircraft such as the nose and the leading edge of the wing[6]. As shown in Fig. 17, the maximum stagnation temperature for Mach 4 is slightly over 1200°R. As the Mach number increases to Mach 5, the stagnation temperature approaches 1700°R. From this data, the materials to be used for the configurations can be determined. If the cruise Mach number is 4 or less the aircraft can be made of a titanium-alloy skin with an aluminum substructure. The titanium will be used as a heat sink and no active cooling will be required. If the Mach number is over 4, the leading edges must be either actively cooled or made of a more heat-resistive material such as carbon-carbon composites.

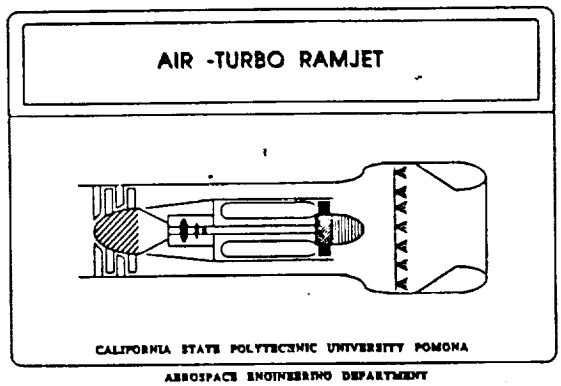

Fig. 18. Air-Turbo-Ramjet

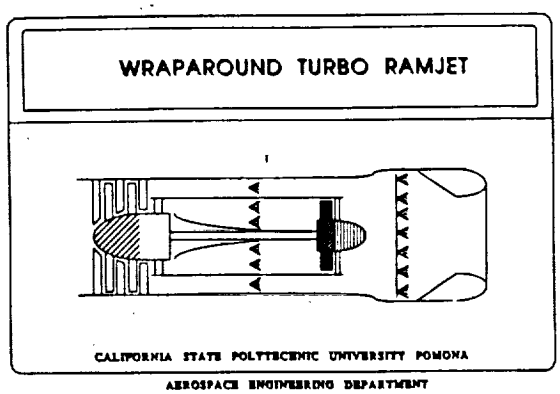

Fig. 19. Wraparound Turbo Ramjet

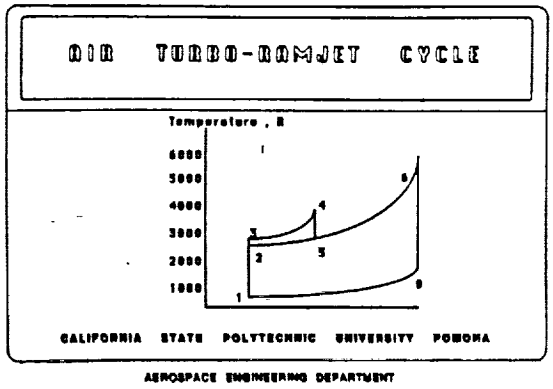

Fig. 20. Air-Turbo-Ramjet Cycle

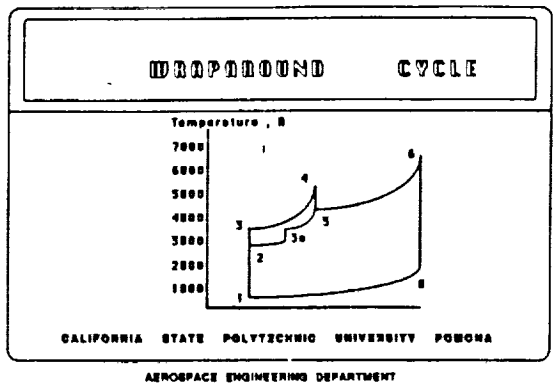

Fig. 21. Wraparound Cycle

PROPULSION

For propulsion of the aircraft, two engine designs were considered. The first was the air-turbo-ramjet as shown in Fig. 18. Aerojet an General Electric supplied generic data on the performance of their air-turbo-ramjet design. The second design was the wrap-around turbojet and is shown in Fig. 19.

A preliminary, idealized-performance-cycle analysis was developed to attain a gross thrust for the engine. The cycles for the two engines are shown in Figs. 20 and 21. The idealized analysis gave a static sea level thrust of about 53,000 pounds at a specific fuel consumption of 2.4 for the air-turbo-ramjet. The wrap-around turbojet provides a slightly lower static sea level thrust of 49,700 pounds but at a specific fuel consumption of 1.6. Because of the savings of fuel, the wrap-around turbojet was the choice for the four configurations.

The installed engine with the inlet is shown in Fig. 22. The inlet is a two-dimensional, variable-ramp, four-shock inlet. The shock system will have three oblique shocks with one normal shock at cruise conditions. The pressure recovery will be maximized by varying the ramp so that the normal component of the Mach number is constant throughout the shocks. This method was developed by Oswatitsch[7].

ENVIRONMENTAL EFFECTS

Noise

FAR 91.55 states that no civil aircraft capable of supersonic flight may operate from a United States airport nor may it operate supersonically in U.S. airspace. Landing waivers have been granted to the Concorde to allow it to land at a few U.S. airports. Current high-speed civil transport studies have been made by McDonnell Douglas and Boeing aircraft companies. Their studies assume subsonic flight over land and as little overland travel as possible. The goal for the designs contained herein was a ground over-pressure of less than 1 lb/ft^2. However, the data for the four configurations were up to 1.5 lbs/ft^2.

Several methods for predicting noise were investigated but the methods from Carlson were chosen[8]. Carlson's method was the most planform sensitive. Cross-sectional area, span distributions, length, weight, planform area and flight path were required for input. The results indicate that below 60,000 feet, lift effects are the major contributor to overpressure. Above 60,000 feet, the volume effects are the most dominant term. This information will be used to help designers refine their configurations.

Air Pollution

The fuel chosen for the four configurations is methane. Methane is considered to be an alkaline or parafin. It constitutes 50 to 90% of natural gas. Combustion of methane in air produces carbon monoxide, hydrocarbons, nitric oxides, sulfur (impurities) oxides and particulates. These products might deplete the ozone layer if a fleet of aircraft should fly in the 80,000- to 90,000-foot region. Unfortunately, this is the region where the minimum thrust required is found for the aircraft. It will then be required by the designers to perform tradeoff studies to determine if the aircraft should be flown above this optimum altitude in order to preserve the ozone layer.

Cost

As subsonic travel loses its ability to maintain the pace and needs of today's traveler, the future businessman will turn to even faster and efficient means of transportation. The cost of

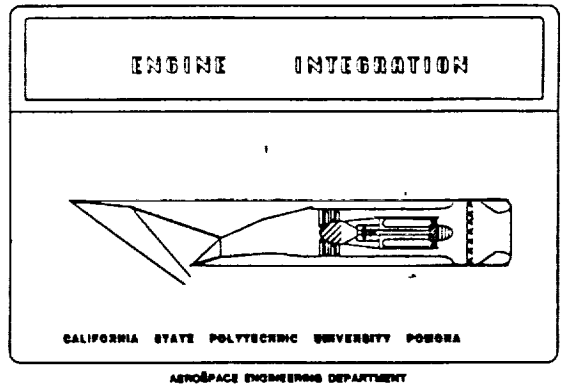

Fig. 22. Engine Integration

the four configurations was estimated using the methods from the Rand Corporation[9]. The estimates were based on 1988 dollars, assuming a 7% increase per year (for inflation) in engineering, manufacturing, tooling and material costs. The cost includes 1 prototype and 3 flight test aircraft. Also included in the cost is the development and production of the aircraft assuming a maximum of 5 aircraft being built per month. With these assumptions, the total flyaway cost estimate is close to $200 million. Since the Boeing 747 sells at $133 million, the high-speed civil transport might pose a viable alternative. However, the operating cost of the aircraft will be substantially more due to the high cost of methane. It is suspected that the high-speed civil transport will not become more realistic until a cheaper, more powerful fuel can be developed.

CONCLUSIONS

1. Each of the aircraft designs has positive and negative aspects. For this reason, no broad conclusions are made regarding the planform. Better conclusions can be found when each of the four configurations are run through a design program with optimization of different parameters. From this, specific conclusions on the best planform for a given optimization function can be drawn.

2. Further studies will be done on the environmental effects of the aircraft. These should include a more accurate cost model, noise profiles, and air pollution control techniques.

3. Energy management techniques should be investigated in order to reduce the amount of fuel needed. This study will help cost and air pollution reductions.

REFERENCES

1. Roskam, J. *Airplane Design: Part 1, Preliminary Sizing of Airplanes*, Roskam Aviation and Engineering Corp., Kansas, 1985.
2. Nicolai, L. *Fundamentals of Aircraft Design*, Mets Inc, California, 1984.
3. Hoak, D.E., et al. *USAF Datcom*, Air Force Flight Dynamics Laboratory, WPAFB, Ohio, 1970.
4. McCormick, B. *Aerodynamics, Aeronautics and Flight Mechanics*, John Wiley & Sons Inc., 1979.
5. Truitt, R. *Hypersonic Aerodynamics*, Ronald Press Co., New York, 1959.
6. Truitt, R. *Fundamentals of Aerodynamic Heating*, Ronald Press Co., New York, 1960.
7. Seddon, J. and Goldsmith, E. *Intake Aerodynamics*, American Institute of Aeronautics and Astronautics Inc., New York, 1985.
8. Carlson, H. Simplified Sonic-Boom Prediction, *NASA TP 1122*, 1978.
9. Levenson, G., et al. *Cost Estimating Relationships for Aircraft Airframes*, The Rand Co., California, 1972.

A PRELIMINARY COMPONENT ANALYSIS OF A MACH-7 HYPERSONIC VEHICLE

CASE WESTERN RESERVE UNIVERSITY

HYDROGEN-FUELED AIRCRAFT (GROUP 1)

A preliminary study of a hypersonic cruise vehicle used a comparison of fuel and cooling requirements for a Mach range of 5-10 to pick operating conditions. The vehicle will cruise at Mach 7 at 100,000 ft which would allow a distance of 8000 nautical miles to be covered in approximately 2 hours.

Aerodynamic heating in the slow-down phase of flight from cruise speed to loiter speed is a significant variable which effects the choice of Mach number. Mach 7 was chosen because a further increase in speed yielded small decreases in time savings and a large increase in aerodynamic heating.

An altitude of 30,400 meters should not produce a significant sonic disturbance on the ground. The initial altitude estimate will be re-evaluated in future studies. A range of 8000 nautical miles is roughly the distance to Japan from the United States with a small margin of safety. Two hours was chosen to allow a one-day business trip to replace the current four-day trip.

BEAM-POWERED AIRCRAFT (GROUP 2)

The purpose of this project is to design a hypersonic transport to attain the range of 6000 nautical miles in approximately 2 hours using beam power. This will be accomplished by taking off at a conventional airport with turbojets, and once over the ocean, where sonic booms would be less of a problem, using beam power from a satellite to power the scramjets, accelerating to Mach 6 at an altitude of approximately 117,000 feet. Our mission objectives are to transport 200 people with assorted payload. We will also determine the feasibility of using this type of transport for equipment and/or business purposes. This would enable us to lower the ticket price for a passenger, while raising the price of cargo that might be needed immediately.

The planned capacity of this transport is approximately 200 seats with available area for luggage and possibly other payloads. The weight of the plane is 462,000 pounds and will be divided into the following areas:

Payload = 42,000 lbs.
Passenger Weight = 36,000 lbs.
Fuel (liquid hydrogen) = 100,000 lbs.
Empty Body Weight = 50,000 lbs.
Landing Gear = 20,100 lbs.
Optics for Laser = 15,000 lbs.

The skin of the aircraft is to be constructed of an aluminum honey-comb covered with a silica-based insulation material and Rene 41 heat shields. The configuration is held together with inconel shoulder bolts. The liquid hydrogen fuel is to be circulated through the scramjet housing for cooling purposes. This will bring it to a high enough temperature so that it can be combusted.

An ANSYS (a computer finite-element analysis) presentation of the airframe skin did not include any supporting members, but the structural members and subsequent analysis can be added if a later simulation is to be done.

Different body configurations were considered by utilizing windtunnel test data obtained from NASA technical reports. From this, a feasible body design was chosen. The tangent-cone method was used to approximate pressure distributions on the top and bottom of the chosen body design. Lift, drag, and stability information could then be calculated and analyzed.

The propulsion system consisted of 5 turbojets providing thrust up to Mach 3 and 3 laser-powered scramjets which increased the speed to Mach 6. Both of these systems use liquid hydrogen for fuel. The majority of the design was sizing the scramjets and stepping through the compression of the airflow from the nose of the plane to the combustion chamber.

SUMMARY OF THE HYDROGEN FUELED AIRCRAFT

Introduction

As research continues in the development of an aircraft capable of travelling at hypersonic flight velocities, both the propulsion and thermal management systems stand out as areas requiring innovative technological breakthroughs. For propulsion, the difficulty involves efficiently compressing and combusting hydrogen in a supersonic stream, i.e., developing a viable scramjet. With thermal management, the challenge lies in development of materials and active cooling systems capable of handling the enormous heat fluxes associated with hypersonic flight.

This paper focuses on these problems and presents component designs for both an active cooling system and an all-external-compression scramjet. These systems are mated to a Mach-6 passenger cruise aircraft whose aerodynamic configuration was derived from an optimization of NASA windtunnel test results. The following outlines the development of the configuration and then focuses in on the design of the two component systems.

Overall, the craft's statistics are:

Total Weight:	295,000 kg
Total Length:	91 m
Wing Span:	34 m
Height:	18 m
Power:	4 Turbojets, 200 kN each
	Scramjets, 900 kN at cruise
Payload:	200 passengers
	21 tons cargo
Fuel:	105,000 kg H_2

Aerodynamics

The objective of the aerodynamics group is to develop a feasible aerodynamic configuration for a hypersonic transport. This is done by studying the NASA windtunnel test results for a large number of assorted body designs. One particular design is chosen as a baseline and then modifications are made based on the conclusions derived from the studies. Next, the tangent-cone method is utilized to calculate pressure distributions on the top and bottom surfaces of the aircraft. From the pressure distribution, lift and drag information is calculated and analyzed.

A number of configurations are investigated. Ideas that are studied include using : (1) a forward-delta wing, a blended wing-body, or a distinct wing-body ("clipped delta"); (2) using a high-profile or low-profile nose with or without canards; (3) tip fins or a vertical tail; (4) vertical position of the wing on the body; (5) engine position; and (6) wing cross-sectional geometry.

Once the body design is chosen, an analysis to obtain pertinent aerodynamic characteristics is performed by constructing a model based on geometries of the final configuration. For supersonic analysis, a technique known as the tangent-cone method is employed. This involves modeling the aircraft as a system of truncated cones, and then, by using hypersonic flow tables, one is able to obtain the pressure distribution over the given surfaces. Integrating this distribution over the prescribed areas provides estimates of lift and drag due to the pressure, but of course, does not account for skin friction and other effects that are not pressure-related.

Calculations of stability are made and the change-in-moment coefficient relative to the change-in-angle-of-attack is analyzed. This parameter remained positive rendering the plane statically and dynamically stable. Conventionally the $dC_n/d\partial$ is to be negative for stability, but the way the moment is defined is opposite to what is conventional so the results are consistent.

Propulsion

The objective of the propulsion team was to design a conceptual scramjet engine system inherently coupled with the airframe. This emphasis on integration comes from the need to efficiently compress, mix, and combust hydrogen without excessive engine length and weight.

The takeoff-and-acceleration to Mach 3.5 portion of the mission is powered by four hydrogen-fueled turbojets each producing 300 kN of thrust. They were sized using 120% of the required takeoff thrust (approximately 1 MN). From Mach 3.5 to cruise at Mach 6, a hydrogen-fueled, all-external-compression scramjet powers the aircraft. The two engine systems are placed on the undersurface of the airframe in an over/under configuration. The turbojets are located above the scramjets and access the airflow through bay doors that close during scramjet operation.

The remaining discussion focuses on the design of a fully integrated scramjet propulsion system. The calculations were simplified by designing solely around conditions at cruise, Mach 6. This enabled the group to work through an iterative optimization under fixed flight conditions.

The first phase was to design the compression surface. The step-by-step design process is as follows: (1) Choose an initial compression ramp angle such that the total pressure loss across the initial oblique shock equals 0.99 and then place the inlet in a position such that the oblique shock intersects the cowl lip; (2) Contour an isentropic compression ramp with Mach lines focused at the cowl lip that turns (compresses) the flow to sufficient combustion pressures; (3) Analyze the shock structure at the focal point (the cowl lip) to determine whether the design has exceeded the theoretical compression limit of the ramp. The expansion-surface geometry was determined using the same technique without the shock structure constraints.

The next phase determines heat addition required in the combustor. By using Rayleigh line heat addition analysis, the amount of heat that could be added to the flow by hydrogen combustion, given the desired combustor-exit Mach number and inlet Mach number, was determined. By comparison with required flight power level, an iterative process was developed that matched mass flow of fuel to the power level required and to Rayleigh line heat addition limitations.

The final phase was to size the effective intake, By computing the mass flow of air required for a stoichiometric burn with the hydrogen, it was possible to calculate the area ratios required at both the beginning of the compression surface and at the engine inlet. By computing the net thrust produced by the propulsion system, and then reiterating all of the previous design phases to match this to the thrust required at cruise, the final dimensions and mass flows associated with this scramjet design were obtained.

Thermal Management

When cruising at hypersonic velocities, the enormous heat fluxes associated with aerodynamic heating become a significant design factor. It has been calculated that during cruise, the influx of heat approaches 70 MW. While 33 MW of this can be naturally radiated off into space from the upper surface of the aircraft, the difficulty lies in dissipating the remaining 37 MW. The following focuses on the design of a system of heat exchangers that will be incorporated into an active cooling system aboard the aircraft. This heat exchanger system utilizes the hydrogen fuel as the heat sink and uses ethylene glycol as the primary coolant and is capable of absorbing up to 45 MW.

To eliminate problems in pumping hydrogen through large areas of the vehicle, a secondary cooling system, utilizing ethylene glycol as the coolant, and the liquid hydrogen fuel as a heat sink is used. The ethylene glycol is nonvolatile and has a large heat capacity. Pumping it throughout the vehicle is not difficult and is not as risky as the hydrogen would be if pumped through the body.

Because of the complications of two-phase flow, the heat exchanger system is separated into three stages: (1) liquid hydrogen, (2) hydrogen phase change, and (3) gaseous hydrogen. The design concentrates on the heat exchange units for stages one and three, leaving stage two as a black box.

The heat exchange unit for the liquid phase is a crossflow heat exchanger because a crossflow provides the most effective

heat transfer. Since the amount of heat that needs to be removed and the flow rate are specified, the temperature change of the hydrogen can be computed. The hydrogen needs to be heated from its storage tank temperature to the temperature at which the phase change will occur, 28 K. The heat exchange unit for this stage is designed with liquid hydrogen flowing within the tubes and ethylene glycol passing over the tube bundle. It is easier to maintain the hydrogen as a liquid by passing it through the tubes. Dimensions of the heat exchanger are $1.0 \times 0.42 \times 0.42$ m. The tube bundle is nine tubes high by ten tubes wide. A material with a low thermal conductivity is needed because it produces a high thermal resistance. This high thermal resistance reduces the heat flux and therefore prevents freezing of the ethylene glycol on the surface of the tubes.

In stage two the heat of vaporization of the hydrogen determines the rate of heat exchange. The change in temperature of the ethylene glycol is caused by the change in enthalpy during the vaporization process of the hydrogen. Multiphase flows are complicated and the problems involved in computing the heat capacity of such a heat exchanger are idealized.

Stage three is where the desired temperatures of both the ethylene glycol and hydrogen are reached. The variance of the specific heat of hydrogen over the large temperature range for this stage make it necessary to break the calculations into four sections, assuming a constant specific heat over each section.

Because the hydrogen is now in the gaseous phase, ethylene glycol is chosen to flow inside the tubes, with the gaseous hydrogen now passing over the tube bundles. The height and width of the hear exchanger units are kept constant throughout stage three. The depth changes for each of the four sections depend on the necessary number of tubes because freezing is not as great a problem in this stage.

With the flow rate of the hydrogen at 18.5 kg/sec (less than the 48 kg/sec needed for propulsion at cruise), the heat exchanger can be run while the aircraft is slowing down. This provides a method of cooling the body down before a landing.

Conclusions

As stated at the outset of this paper, the propulsion and thermal management systems associated with a hypersonic aircraft present a unique set of design challenges. The models presented in this paper attempt to overcome these difficulties by fully interfacing all the different component systems. For example, the airframe of the vehicle serves as both a lifting surface and a compression surface for the propulsion system. Also, the liquid hydrogen provides a heat sink for the active cooling system while performing its primary purpose of powering the aircraft. The key to hypersonic flight lies in this type of system integration.

All three areas of this model require refinement. A viscosity model needs to be included in the aerodynamics code in order to provide a more accurate prediction of the overall drag force. With propulsion, the mixing stage of the engine cycle needs to be modeled before a complete scramjet design can be completed. And, finally, a more intricate model of the piping layout, including flow rates and pipe diameters, is needed to complete the thermal management system.

PRELIMINARY DESIGN OF TWO TRANSPACIFIC HIGH-SPEED CIVIL TRANSPORT

THE UNIVERSITY OF KANSAS

Two high-speed civil transport (HSCT) design concepts are presented. Both transports are designed for a 5500-n.m. range with 300 passengers. The first design concept is a Mach-2.5, joined-wing, single-fuselage transport. The second design concept is a Mach-4.0, twin-fuselage, variable-sweep wing transport. The use of conventional hydrocarbon fuels is emphasized to reduce the amount of change required in current airport facilities. Advanced aluminums are used in the designs when possible to reduce material and production costs over more exotic materials. Methods to reduce airport noise, community noise, and fly-over noise are incorporated into the designs. In addition, requirements set forth by the Federal Aviation Regulations (FARs) have been addressed.

LIST OF SYMBOLS

Symbol	Description	Units
b	Wing Span	ft
c,MGC	Mean Geometric Chord	ft
C_l	Lift Coefficient	—
C_D	Drag Coefficient	—
δ_{lef}	Leading Edge Flap Deflection	deg
δ_{tef}	Trailing Edge Flap Deflection	deg
L/D	Lift-to-Drag Ratio	—
S	Wing Area	ft^2
T	Thrust	lbf
W	Weight	lb
LCN	Load Classification Number	
T-O	Take-off	
L	Landing	
FOD	Foreign Object Damage	

REQUIREMENTS

The design requirements set forth for both airplanes are presented in Table 1. These design requirements have been developed to provide an economically viable, second-generation, supersonic transport. The mission profile for the airplanes is defined in Fig. 1. A brief description of each mission leg is included. The design mission represents a typical Los Angeles-to-Tokyo flight.

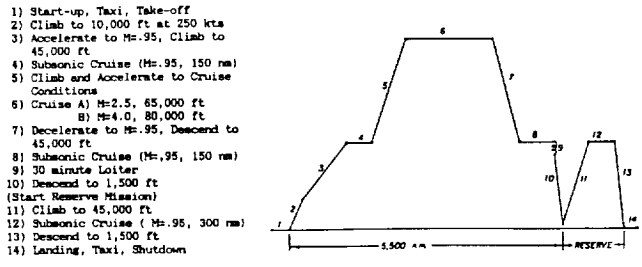

Fig. 1. Mission Profile For A transpacific Supersonic Transport

Table 1. Design Requirements For A Transpacific Supersonic Transport

Payload:	300 passengers at 175 lbs. and 40 lbs. of baggage each.
Crew:	2 pilots and 10 flight attendants at 175 lbs. and 30 lbs. of baggage each.
Range:	Design range of 5,500 n.m., followed by a 30 min. loiter
Cruise:	A) Mach 2.5 at 65,000 ft. B) Mach 4.0 at 80,000 Outbound and inbound subsonic cruise legs at Mach 0.95, 45,000 ft.
Take-off and Landing:	FAR 25 fieldlength of 12,000 ft. Standard day, $W_L = 0.85\ W_{TO}$
Fuel:	A) JP-4 B) JP-7 (Thermally Stable Jet Fuel)
Materials:	A) Advanced aluminum where applicable B) Titanium
Thermal Protection:	As required, rely on passive systems when feasible, use active systems only when necessary
Certification Base:	FAR 25, FAR 36 (noise requirements)

MACH-2.5 TRANSPORT

Configuration Description

The first HSCT design concept is a Mach-2.5, joined-wing, single-fuselage transport, which was developed using the methods of Dr. Jan Roskam[1]. A three-view of this configuration is shown in Fig. 2. Table 2 contains basic information about the airplane. High-temperature aluminum is used in the primary structure to keep production costs low. The joined-wing is incorporated into the Mach-2.5 transport to reduce the wing structural weight, and to improve low-speed trimmed lift capabilities.

A four-post main gear is used to meet Load Classification Numbers (LCN) requirements for current international runways. The four variable-cycle engines are located in pairs under the wings. The nose of the airplane is dropped 12.5° during approach to improve pilot visibility.

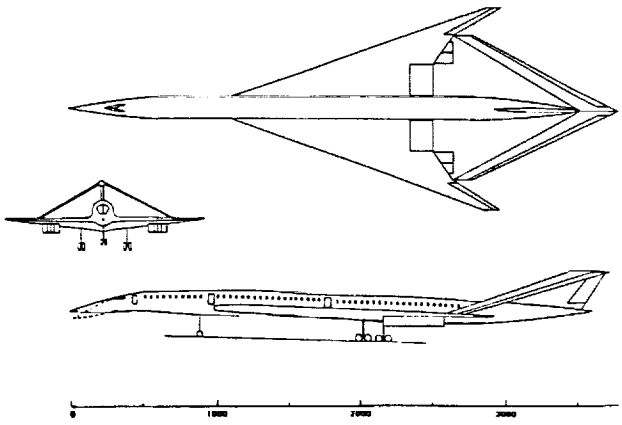

Fig. 2. Mach-2.5 Transport Threeview

Table 2. Mach 2.5 Transport Characteristic Data

	Front Wing	Rear Wing	Vertical Tail
Area (ft^2)	7226	1400	730
MGC (ft)	76	16.5	39
Span (ft)	118	86	20
Aspect Ratio	1.9	5.3	.55
L.E. Sweep	70°	-70°	70°

	Fuselage	Overall
Length (ft)	300	308
Max Height (ft)	15.5	42
Max Width (ft)	14.0	118

Weight	
T.O. Weight	618,000 lbs
Empty Weight	278,000 lbs
Fuel Weight	262,750 lbs
Payload Weight	64,500 lbs
T.O. Thrust	247,200 lbs
Wing Loading	85 lb/ft^2
Thrust/Weight	0.40 lb/lb

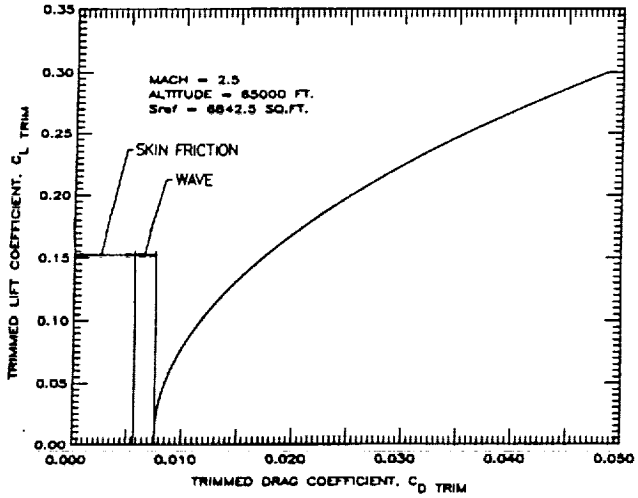

Fig. 3. Mach-2.5 Transport Cruise Drag Polar

Aerodynamics and Stability

The aerodynamic analysis of the airplane was completed with the BDAP program series[2]. The cruise drag polar is presented in Fig. 3. For trimmed flight, a maximum lift-to-drag ratio (L/D) of 8.9 is possible for this airplane. In cruise, the airplane is marginally stable. A combination of fuel management (center of gravity, or c.g. movement) and elevator deflections are used to trim the airplane in cruise.

For low speed flight (take-off and approach), the associated drag polar is presented in Fig. 4. The maximum trimmable lift coefficients are:

Clean:	$C_{L,max} = 1.15$		
T-O:	$C_{L,max} = 130$	$\delta_{tef} = 10°$	$\delta_{tef} = 10°$
Landing:	$C_{L,max} = 1.40$	$\delta_{tef} = 10°$	$\delta_{tef} = 30°$

In subsonic flight, the airplane is unstable and will require stability augmentation. Directionally, the airplane is stable due to the large vertical tail. The rudder has been sized to trim in the event the most outboard engine fails.

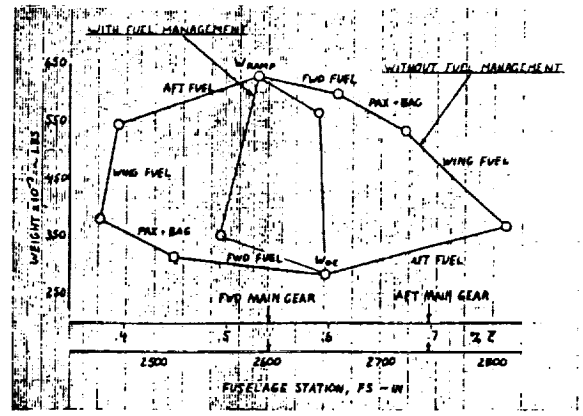

Fig. 4. Mach-2.5 Transport CG Excursion Diagram

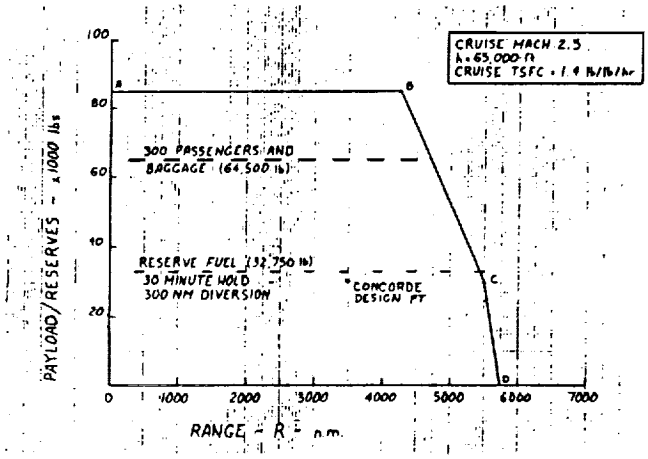

Fig. 5. Mach-2.5 Transport Payload-Range Diagram

Propulsion System Design and Integration

The propulsion system uses four Pratt and Whitney variable-cycle VSCE-516 engines. These engines were chosen for their good performance in both subsonic and supersonic flight regimes, and their reduced noise during takeoff. The engine characteristics are shown in Table 3.

Table 3 - Mach 2.5 Transport Propulsion System Data

Fan Pressure Ratio	3.1:1.0
Bypass Ratio	1.3
Compressor Pressure Ratio	16.0
Primary Burner Exit Temp.	3260°R
Secondary Burner Exit Temp.	2960°R
Scaled Airflow: At Sea Level	755 lbm/sec
At Cruise	519 lbm/sec
Thrust: At Sea Level Static	61300 lbf
At Cruise	15836 lbf
Specific Fuel Consumption	
At Sea Level Static	1.23 lbm/lbf/hr
At Cruise	1.44 lbm/lbf/hr
Engine: Bare Weight	8835 lb
Overall Length	18.2 ft
Max Diameter	6.0 ft
Nacelle: Overall Length	40.0 ft

Weight and Balance

The basic weights for the airplane are presented in Table 4. The c.g. excursion diagram for the airplane, with and without fuel management, is shown in Fig. 4.

Table 4. Mach-2.5 Transport Weights

Structure	187,264 lbs
Powerplant	46,870 lbs
Fixed Equipment	43,870 lbs
Empty Weight	278,004 lbs
Operating Weight Empty	283,414 lbs
Payload Weight	64,500 lbs
Fuel Weight	279,331 lbs
Ramp Weight	627,246 lbs
Take-off Weight	618,000 lbs

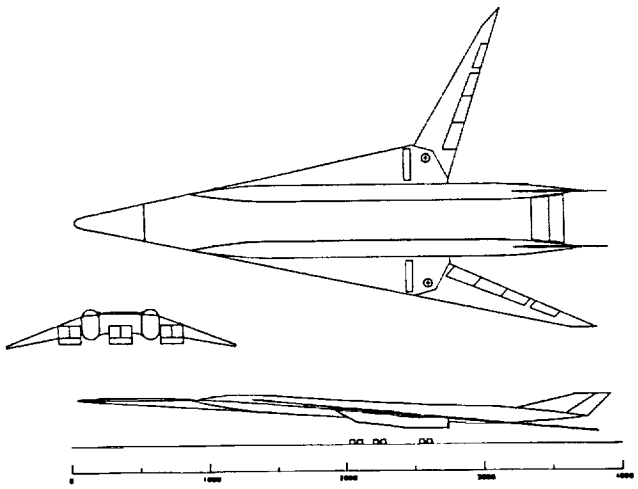

Fig. 6. Mach-4.0 Transport Threeview

Performance

The airplane was originally sized for the 5,500-nautical-mile mission assuming a cruise Thrust-Specific Fuel Consumption (TSFC) = 1.1 and an L/D = 12. These were optimistic assumptions, and the airplane does not have a 5,500-nautical-mile range. As shown in the payload-range diagram of Fig. 5, the range with the design payload is 4,700-nautical-miles. The airplane met all other requirements, including cruise speed, FAR 25 climb gradients, and takeoff and landing distances.

Economic Analysis

The procurement cost of the airplane was estimated to be $271 million per airplane[3,4,5]. Assuming a 14-year depreciation cycle, the direct and indirect operating costs were estimated to be $158,870 per flight and $13,310 per flight, respectively. The one-way ticket prices were determined for a variety of passenger load factors, and airplane finance rates, as shown in Table 5.

Table 5. Break Even, One Way Ticket Prices

Airplane Finance Rate*	Load Factor 50%	70%	90%
6%	$1,440	$1,029	$800
8%	$1,477	$1,055	$821
10%	$1,516	$1,083	$842
12%	$1,557	$1,112	$863

*Assumed fixed annual interest rate

Conclusions and Recommendations

The configuration solved many problems associated with conventional supersonic transports, primarily, poor low-speed performance. The airplane had a high trimmed-approach lift coefficient, and a relatively short field length. However the increased wetted area of the rear wing increased the skin-friction drag, thus reducing the L/D ratio. Coupled with high TSFC, the airplane did not meet its desired mission range.

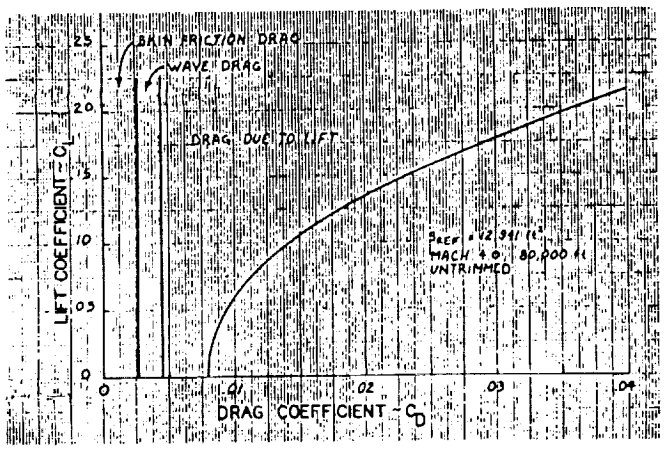

Fig. 7. Mach-4.0 Transport Cruise Drag Polar

For future work, the aerodynamics should be refined to increase the trimmed, cruise L/D ratio. Special attention should be given to the interaction of the main and rear wings. Improvements in engine performance should also be investigated.

MACH-4.0 TRANSPORT

Configuration Description

The second HSCT design concept is a twin-fuselage, variable-sweep wing transport, which was developed using the methods of Dr. Jan Roskam[1]. A threeview of the airplane is shown in Fig. 6. Some basic information about the airplane is presented in Table 6. The twin fuselage concept is used to produce high fineness ratio fuselages and to lower drag. The fuselages are blended into the wing structure. The variable-sweep wing is incorporated into the design to improve low-speed performance, reduce the required fieldlength, and improve takeoff and climbout rates. The "platypus" nose of the airplane is designed to help reduce sonic-boom overpressures. Six turbojet engines are located under the wing, in three pods of two engines each. An unusual "six-poster" landing gear has been designed for the configuration, which will be discussed in detail in the section entitled Special Features Design.

Table 6. Mach 4.0 Transport Characteristic Data

	Wing		Vertical
	Cruise	Approach	Tails
Area	12,941 ft^2	12,941 ft^2	2 x 257 ft^2
Span	138 ft	263 ft	10.7 ft
Aspect Ratio	1.47	5.34	0.44
L.E. Sweep	78°	30°	67°
Thickness Ratio	0.02	0.02	0.03

	Fuselage	Overall
Length (ft)	246	316
Max Height (ft)	10.3	35
Max Width (ft)	10.3	263

Weight	
T.O. Weight	1,155,800 lbs
Empty Weight	531,460 lbs
Fuel Weight	660,000 lbs
Payload Weight	64,500 lbs
T.O. Thrust	520,000 lbs
Wing Loading	89 lb/ft^2
Thrust/Weight	0.45 lb/lb

Aerodynamics and Stability

As with the Mach-2.5 airplane, the aerodynamic analysis was completed with the BDAP program series. Above transonic Mach numbers, the wing is kept in the fully swept (78°) position. The wing/fuselage camber has been designed to optimize the cruise L/D ratio. The airplane drag polar is shown in Fig. 7. The maximum cruise L/D ratio is 7.0. In the cruise

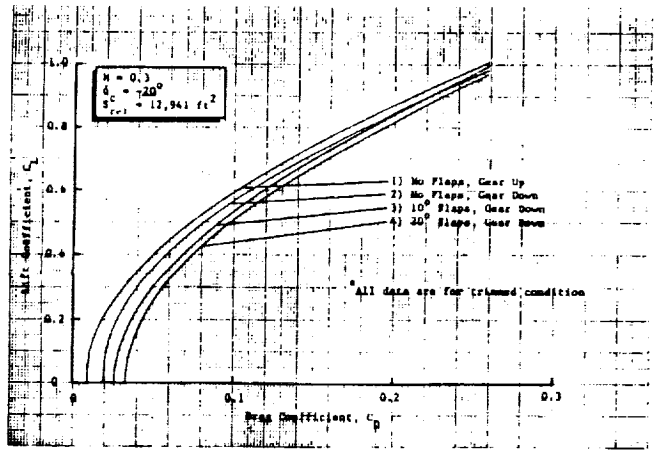

Fig. 8. Mach-4.0 Transport Low Speed Drag Polar

portion of the flight profile the airplane is marginally stable. A fuel management system is used to keep the airplane c.g. travel to a minimum, and a large canard is used to trim and control the airplane. The elevator is not used during cruise, because it reduces the cruise L/D ratio significantly.

Below transonic Mach numbers the wing moves forward. In the takeoff and approach conditions, the wing is swept fully forward (30°). In the approach condition, the airplane is unstable. To help trim the aircraft, the canard is kept in the full up (-20°) position to provide a positive pitching moment. The low-speed drag polar for the airplane is presented in Fig. 8. The flaps on the outboard wing are deflected 20° for takeoff and landing. A double hinged elevator is used to rotate the airplane and to provide longitudinal control. A combination of outboard ailerons and inboard spoilers are used for roll control.

Propulsion System Design and Performance

The propulsion system for the Mach-4.0 airplane consists of six turbojet engines. The turbojet engine was selected since it is capable of operating during all flight regimes of the

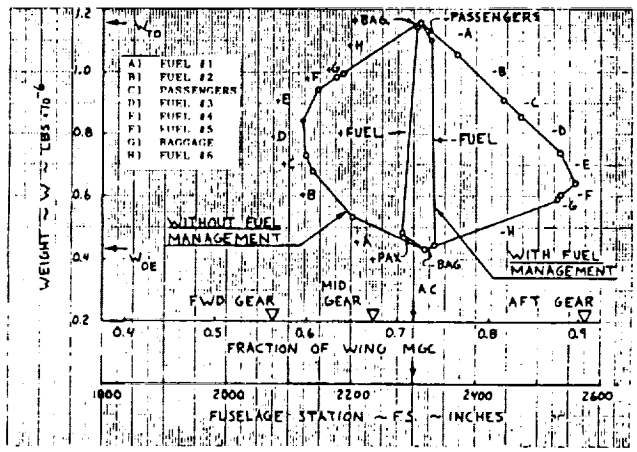

Fig. 9. Mach-4.0 Transport CG Excursion Diagram (Wings Aft)

airplane (Mach 0 to Mach 4). The engine used in this design is a scaled version of the ASTM4-01 engine[6]. The engine characteristics are shown in Table 7.

Table 7. Mach 4.0 Transport Propulsion System Data

Compressor Pressure Ratio	
At Sea Level	14.6
At Cruise	3.0
Turbine Inlet Temp	3500°R
Mass Flow:	
At Sea Level	686 lbm/sec
At Cruise	380 lbm/sec
Thrust:	
At Sea Level Static	86,640 lbf
At Cruise	19,000 lbf
Specific Fuel Consumption	
At Sea Level Static	1.06 lbm/lbf/hr
At Cruise	1.69 lbm/lbf/hr
Engine: Installed Weight	17,684 lbf
Overall Length	12.7 ft
Max Diameter	6.6 ft
Nacelle: Overall Length	68.4 ft

Weight and Balance

The basic weights for the airplane are presented in Table 8. The c.g. excursion diagrams for the airplane with the wing swept aft and the wing swept forward are shown in Figs. 9 and 10, respectively.

Table 8. Mach 4.0 Transport Weights

Structure	326,054 lbs
Powerplant	114,657 lbs
Fixed Equipment	65,846 lbs
Empty Weight	531,462 lbs
Operating Weight Empty	539,422 lbs
Payload Weight	64,500 lbs
Fuel Weight	660,009 lbs
Take-off Weight	1,155,813 lbs

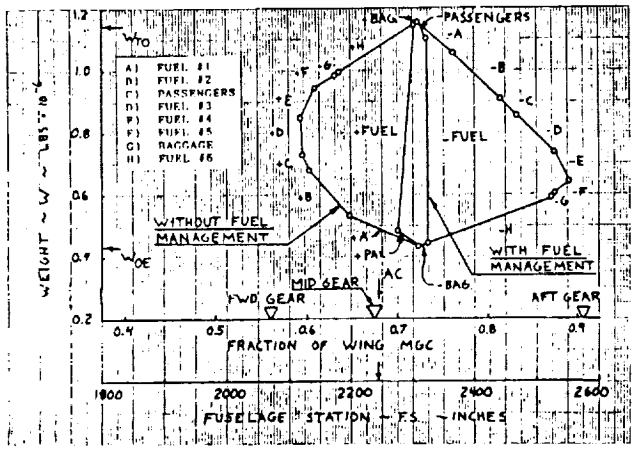

Fig. 10. Mach-4.0 Transport CG Excursion Diagram (Wings Forward)

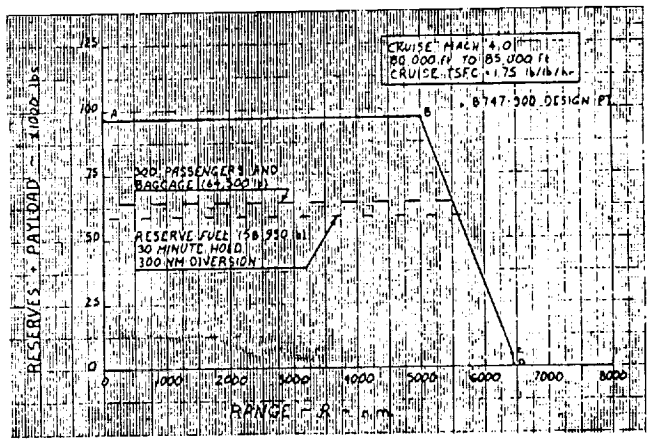

Fig. 11. Mach-4.0 Transport Payload-Range Diagram

Performance

Due to the large thrust-to-weight ratio of the airplane (sized for cruise speed) all FAR climb requirements have been exceeded. To reduce engine noise during takeoff, the engines will be throttled back to the necessary thrust levels. The payload-range diagram is presented in Fig. 11. The airplane meets the design range requirement and compares well with the Boeing 747-300.

Special Features Design

Several special features have been incorporated into the design of the Mach-4.0 transport. The first of these is an unusual landing gear configuration. The gear consists of six main gear struts, with no nose gear. This was done to eliminate nosegear foreign object damage (FOD) problems. Eliminating the nosegear allowed the designers to place two engines on the centerline of the airplane, and move the wing-mounted engines inboard of the wing pivot.

The second special feature is the "platypus" nose, which is used to reduce sonic boom overpressures. The platypus area improves the effective area distribution[8], thus reducing the magnitude of the boom overpressures. In addition, the platypus nose is moveable (canard) for longitudinal control and pitch-trim.

The skin temperatures of the airplane have been estimated and are shown in Fig. 12. The fuel is used as the heat sink to help cool the passenger sections. A titanium multi-wall structure is used in addition to the cooling system to minimize the heat load on the fuel.

Economic Analysis

The procurement cost of the airplane has been estimated to be $638 million[3,4,5]. Assuming a 14-year depreciation cycle, the direct and indirect operating costs have been estimated to be $803,660 and $14,750 per flight respectively. As shown in Table 9, several fixed-interest rates and passenger-load factors were investigated when computing the breakeven ticket prices.

The skin temperatures of the airplane have been estimated, and are shown in Figure 12. The fuel is used as the heat sink to help cool the passenger sections. A titanium multi-wall structure is used in addition to the cooling system to minimize the heat load on the fuel.

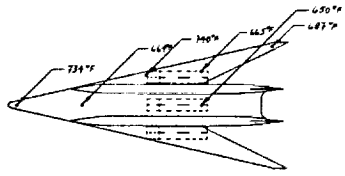

Fig. 12. Skin Temperature Distribution

Table 9. Mach 4.0 Break Even, One Way Ticket Prices

Airplane Finance Rate*	Load Factor 50%	70%	90%
6%	$5,984	$4,274	$3,325
8%	$6,050	$4,322	$3,361
10%	$6,120	$4,372	$3,400
12%	$6,194	$4,424	$3,441

*Assumed fixed annual interest rate

Conclusions and Recommendations

Many unusual features have been incorporated into the Mach-4.0 transport to provide a feasible design concept. Although the high wing sweep is required for Mach-4.0 cruise, the variable-sweep outboard wing section provides good low-speed performance. The landing gear/engine integration alleviates nose gear FOD concerns. The final configuration met all design goals and appears to be a good choice for further consideration.

For future work, several items should be investigated further. The mechanisms involved with the variable-sweep wing and the six-post main gear should be investigated in detail. High-speed windtunnel testing and computer simulation should be initiated to verify the cruise performance, and estimate stability derivatives for a more detailed stability and control analysis.

REFERENCES

1. Roskam J. *Airplane Design: Parts I - VI,* Roskam Aviation and Engineering Corporation, Ottawa, Kansas; 1987.
2. Carlson H.W., Walkley K.B. Numerical Methods and a Computer Program for Subsonic and Supersonic Aerodynamic Design and Analysis of Wings With Attainable Thrust Considerations, *NASA CR-3808,* 1984.
3. Nocolai L.M. *Fundamentals of Aircraft Design,* METS Inc, San Jose, California, 1975.
4. Morris M., et al. Application of Parametric Weight and Cost Estimating Relationships to Future Transport Aircraft, *SAWE Paper* #1292, May 1979.
5. Boren H.E., Jr. A Computer Model For Estimating Development and Procurement Costs of Aircraft (DAPCA-III), *USAF Project RAND,* Mar. 1976.
6. NASA Langley Research Center, Propulsion Data for ASTM4-01, Systems Analysis Branch, VA, July 21, 1987.
7. Hines R.W. Variable Stream Control Engine for Supersonic Propulsion. *J. of Aircraft, Vol. 15, No. 6,* June 1978.
8. Carlson H.W. Simplified Sonic-Boom Prediction, *NASA TP-1122,* 1978.

HIGH-SPEED TRANSPACIFIC PASSENGER FLIGHT

OHIO STATE UNIVERSITY

The design task of high-speed passenger flight across the Pacific Ocean was addressed by four design teams of eight students each. Two teams examined hypersonic flight (Mach >5) and two teams studied supersonic flight (Mach = 3). The specific task of the aircraft was to transport at least 250 passengers 6500 nautical miles while operating from airport runways of 15,000 feet. Four design concepts evolved; the supersonic designs—one a variable-sweep oblique wing and the other a cranked-arrow wing—use conventional turbine engines and liquid hydrocarbon fuels. The two hypersonic configurations, one with a variable-sweep wing and the other with a fixed, swept-wing planform, employ methane fueled, variable-cycle turbojet/ramjet propulsion systems. Both supersonic aircraft weigh less than 700,000 lbs at takeoff, while the variable-geometry hypersonic airplane is the heaviest at 1,100,000 lbs and weighs 170,000 lbs more than the fixed-wing hypersonic design. All the conceptual designs are shown to perform the transport mission, although development and operating cost estimates favor the supersonic designs over the hypersonic configurations.

1. THE AIRCRAFT CONCEPTS

1.1 Aircraft Specifications

The design task was to develop a conceptual design of a commercial passenger aircraft to operate around the Pacific rim. These specifications were kept to a minimum to allow the students to use their initiative to a maximum. The aircraft requirements are presented in Table 1.

The students were to define the configuration, produce an interior view, predict the vehicle mission performance, and estimate its development and operating costs and its impact on the environment.

Table 1. Aircraft Requirements

Range	6500 nautical miles
Payload	250 + passengers
Takeoff and Landing	15000 feet
Cruise	Mach > 3

1.2 Description of the Aircraft

All of the aircraft presented have very different characteristics (wing shape, propulsion system, weight, etc.) which are driven by both the speed range considered and the designers' preferences. Because of the heavy dependence on fuel in sizing these aircraft, the Mach-5 aircraft are larger and heavier that the Mach-3 aircraft. Also, the heating problem is much greater at Mach 5, so the hypersonic planes require more highly-swept wings and/or active cooling systems. The configurations are shown in Figs. 1 and 2, with the parameters summarized in Table 2 and described below.

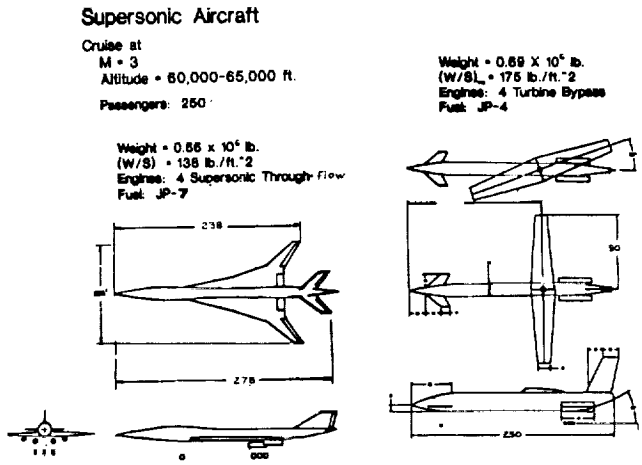

Fig. 1. Supersonic Aircraft

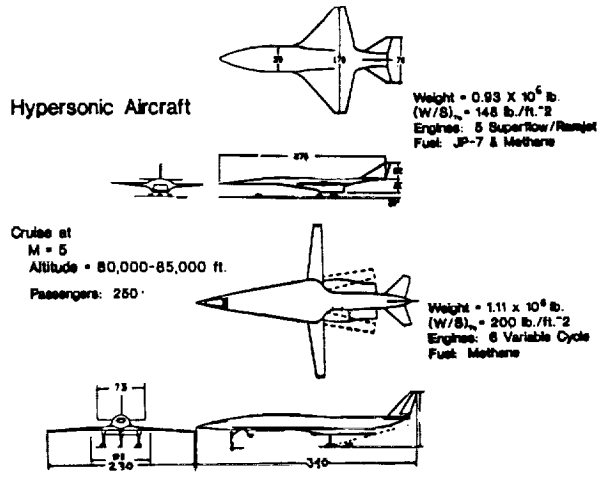

Fig. 2. Hypersonic Aircraft

Table 2. Aircraft Parameters

	Oblique	Cranked Arrow	Variable Planform	Fixed
Cruise Mach	3	3	5	5
Weight	690,000	660,000	1,100,000	930,000
Wing Area (ft^2)	3940	4800	5500	6300
Engine Type	turb.bypass	super-flow	variable cycle	super/ram
No. Engines	4	4	6	5
Fuel Type	JP-4	JP-7	methane	JP-7,methane

The two supersonic aircraft shown in Fig. 1 obviously employ very different methodology in solving this problem. The cranked-arrow wing design uses a fairly conventional modified delta-wing to allow for better subsonic performance while not compromising supersonic aerodynamics. The subsonic two-dimensional section generates a takeoff C_l of 1.4 while still maintaining a cruise $(L/D)_{max}$ of 6.7. The airplane is powered by four advanced-technology, supersonic thru-flow fan engines currently under study at NASA-Lewis Research Center. The oblique wing design uses a different approach to solve the low-speed lifting problem. The wing sweeps both forward and aft at supersonic speeds for efficient cruise while sweeping perpendicular to the fuselage for take-off and landing to generate a subsonic L/D max of 19.2. Propulsion is handled by four turbine-bypass engines. Overall length for both planes is between 250 and 280 ft.

The hypersonic aircraft also employ different methods to generate lift. The variable-planform wing uses a pivoted wing similar to the B-1 wing. The high sweep angle required to maintain a subsonic leading edge at Mach 5 makes this wing an efficient choice to minimize wing area. This design uses the variable cycle engines (VCE) developed by General Electric. The fixed wing design has a moderately swept planform which is designed with a supersonic leading edge. This group examined the thermal problem in detail, or at least as much detail as 20 weeks would allow. An over/under superflow/ramjet system powers this design. These aircraft differ more in weight than the supersonic aircraft, reflecting the degree of optimism expressed in the engine development.

2. AIRCRAFT COMPARISONS

2.1 Approach

Comparisons of the characteristics of the four designs are made, based on the calculations of the design teams. These calculations were made from standard materials supplemented by several computer programs written by the students, obtained from NASA and the Air Force and from prior engineering courses. Table 3 lists the computational methodologies used.

In the following comparisons, the aircraft are designated by their planforms. The oblique wing and cranked arrow titles represent the supersonic designs; the variable-planform and fixed wing designate the hypersonic aircraft.

Table 3. Computational Methods Used in Advanced Design

OSU In-House Programs	*NASA Programs*
Airfoil Design and Analysis	Weights
Vortex Lattice	NASA/Navy Engine
Dynamic Longitudinal & Lateral Stability	Harris Supersonic Wave Drag
Ideal Ramjet Performance	
Air Force Programs	*Student Developed Programs*
Digital DATCOM (Stability Derivatives)	Shock/Expansion
	Method of Characteristics
	Ascent Performance Optimization
	Balanced Field Take-off
	Linear Drag Synthesis

2.2 Aerodynamics

The basic reference for the course is *Fundamentals of Aircraft Design* by L. M. Nicolai. This text contains many methods for aerodynamic computation ranging from linearized theory to semi-empirical methods. Some groups looked into more advanced methods such as the method of characteristics to compute difficult flow regions (e.g., external nozzle flows). Different computer methods were available to generate the lift, drag, and stability characteristics of the aircraft. Digital DATCOM, a vortex lattice code, SUBAERF for subsonic analysis, and the Harris wave drag code for supersonic area ruling were used. Important aerodynamic performance predicted by these methods for the aircraft is presented in Fig. 3.

The supersonic aircraft both employ swept leading edges to optimize L/D at supersonic speeds, but the planforms are very different. The oblique wing design employs a single-spar wing which rotates on a fuselage-mounted pin. This design seeks to optimize low-speed characteristics by maximizing wing span. Drawbacks to this configuration are lack of data on this type of wing, and complicated stability as the wing transitions from unswept to oblique positions. The other supersonic design uses a more conventional delta-wing design. The cranked arrow design provides good subsonic performance while providing an efficient supersonic configuration. This design has the advantage of allowing a simplified structural and aerody-

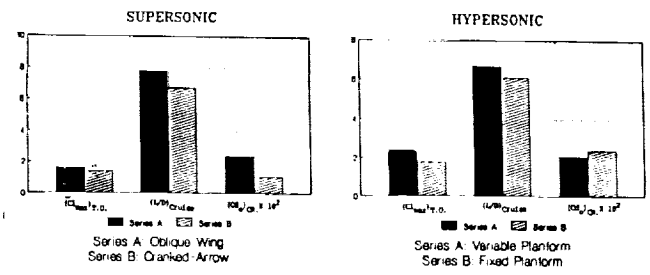

Fig. 3. Aerodynamic Performance

namic analysis. While not offering as much low-speed performance advantage as the oblique wing, the cranked arrow wing provides a more conventional solution.

2.3 Propulsion

This class of aircraft, more than any other class, is dependent on an efficient, powerful, and highly integrated propulsion system. Unfortunately, the airbreathing engine systems of today do not provide an economical solution to the transPacific problem. Advanced engine systems currently under development must fill these needs but accurate data for design is difficult to obtain, making engine selection a demanding task. The Mach-3 aircraft again have a simpler choice than the hypersonic aircraft as the energy of the inlet gases is low enough to allow a single engine with conventional fuels. Good performance in the cruise regime while delivering high transonic thrust is still critical, however. The hypersonic aircraft face a more complicated problem. High enthalpy, pressure, and flow speed require the hypersonic propulsion system to change radically in order to perform at Mach-5 and start from zero velocity. Each group sought its own solution to this problem supported by data from General Electric and NASA, and theory from Hill & Peterson and other texts.

The propulsion systems for the supersonic aircraft shown in Fig. 4 are both based on turbine technology with advanced efficiency-gaining systems. The oblique wing design incorporates a turbine-bypass engine which improves overall fuel efficiency by bypassing air past the the combustor to achieve the most optimal mass-flow rate. This engine system achieves a cruise specific fuel consumption (s.f.c.) of 1.8 lb fuel/lb thrust/hr. The cranked arrow design employs conventional turbine technology in the engine core, but uses a supersonic fan to accelerate the supersonic flow. This configuration reduces drag similar to subsonic turbofan engines; by avoiding deceleration losses. The s.f.c. is given as 1.4 lb fuel/lb thrust/hr. Both engines systems rely on conventional JP fuels. These systems incorporate well-known turbine technology with advanced air-processing techniques.

Operating over a greater Mach range, hypersonic aircraft must use the more complicated systems shown in Fig. 5 to generate thrust. The variable-planform design uses the variable-cycle engine currently under development at General Electric. Performance projections were provided by G.E. which lent credibility to the propulsion values for this group. The cruise s.f.c. for this engine is 2.102 lb fuel/lb thrust/hr. The fixed wing aircraft uses an over/under superflow/ramjet configuration. This configuration has a variable-geometry inlet that diverts air to one engine or the other at different Mach numbers. At takeoff, through the low-speed regime, and up to Mach 3, the superflow engine is used, fueled by JP-7. At Mach 3 the engine system transfers power to the ramjets, which provide thrust to Mach 5. The s.f.c. of the ramjet system is 1.85 lb fuel/lb thrust/hr at cruise. Both of these engine systems are far from operational and have difficulties with heating, combustion, and engine weight. Though there are many difficulties with these propulsion systems, research is currently underway to solve these problems.

2.4 Weights

Weight estimation for all aircraft was provided by the WAATS weight analysis code. This program uses empirical methods to estimate the weight of each component in the aircraft, then generates a composite weight for each system and an overall gross weight. Specific weight information was input when available from reports or engine data to improve the accuracy of the estimation. Both Mach-3 aircraft weighed between 650,000 and 700,000 lbs. This weight was driven by the transPacific range which required a large amount of fuel. As presented in Fig. 6, the fuel fraction of the Mach-3 aircraft ranged from 48% to 61% of the gross weight. The hypersonic aircraft, largely due to their higher s.f.c. values, approximated 1,000,000 lbs in gross weight, with a fuel fraction of 62%. The significant weight increase over the supersonic aircraft and a corresponding large volume requirement makes the Mach-5 transport a more costly flight vehicle than the Mach-3 aircraft. However, as the performance section will show, this cost was balanced by a lower mission time.

2.5 Performance

Many performance methods were used to evaluate the trajectories of the aircraft. As a first approximation the Breguet range equation was used to estimate the fuel fraction required to cross the given 6500-nautical-mile range. To optimize climb

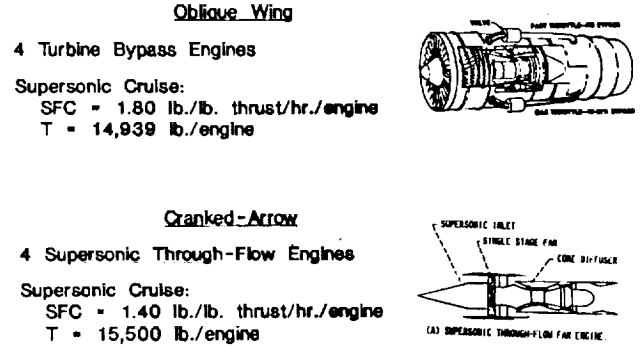

Fig. 4. Supersonic Engines

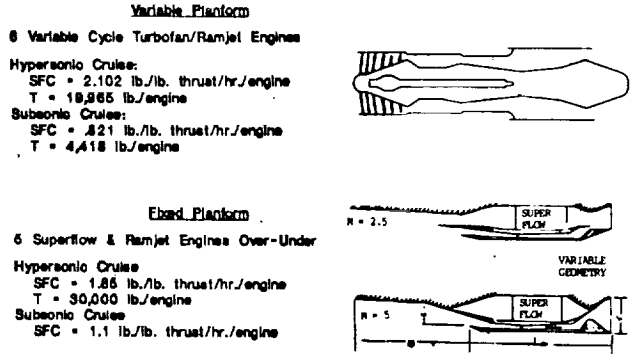

Fig. 5. Hypersonic Propulsion Systems

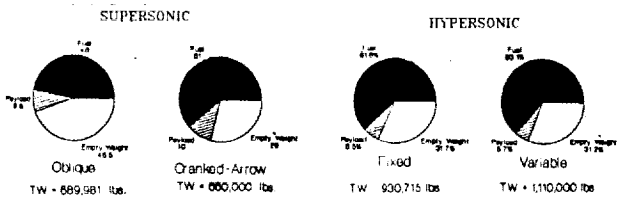

Fig. 6. Weight Breakdown

performance, for example, the students in the cranked arrow wing group developed their own computer code based on the energy-state method (Fig. 7). The constant excess specific power contours are plotted on the altitude vs. Mach diagram to indicate the most advantageous climb. Following the path of greatest excess specific power generates the minimum fuel climb. This trajectory saved more than 40,000 lbs of fuel, compared with a climb trajectory based on near-constant dynamic pressure.

Nicolai's design text provides methods to calculate takeoff and landing characteristics to demonstrate conventional airport capability. All four designs satisfy the 6500-nautical-mile range requirement including the FAA loiter requirement and the 15,000-ft maximum runway requirement.

2.6 Environmental Considerations

The high speeds and altitudes achieved by these aircraft create special environmental problems not faced by conventional transports. Most obviously, speeds above Mach 1 generate sonic booms which can be disruptive to the general public. An analysis of sonic overpressure indicates that overland travel seems unlikely for large transports above Mach 2. Therefore, the target markets for the supersonic/hypersonic transports are transoceanic, generally connecting the North American continent with Asia or Europe. Also, the high altitudes raise concerns of ozone depletion in the cruise range. Though it is impossible to rule out nitrogen-oxygen compound effects as trivial, current studies indicate that propulsion systems using hydrocarbon fuels will not significantly damage the atmosphere. Takeoff and landing engine noise is also a major environmental concern. The new FAA noise regulations present a difficult limit on engine noise. These regulations limit engine manufacturers severely in the maximum thrust expected for the larger engines. Each group weighed these environmental problems in designing their aircraft.

2.7 Economic Analysis

In order to compare these advanced aircraft systems to conventional long-distance transport, a cost estimation was performed. The method used was the empirical costing method in Nicolai's design text. Dollar values were scaled to 1987 dollars using the inflation of the dollar from 1970. Development costs for 250 aircraft built over a 10-year span are presented in Fig. 8, with ticket prices shown in Fig. 9. The Mach-3 aircraft compared very well with conventional

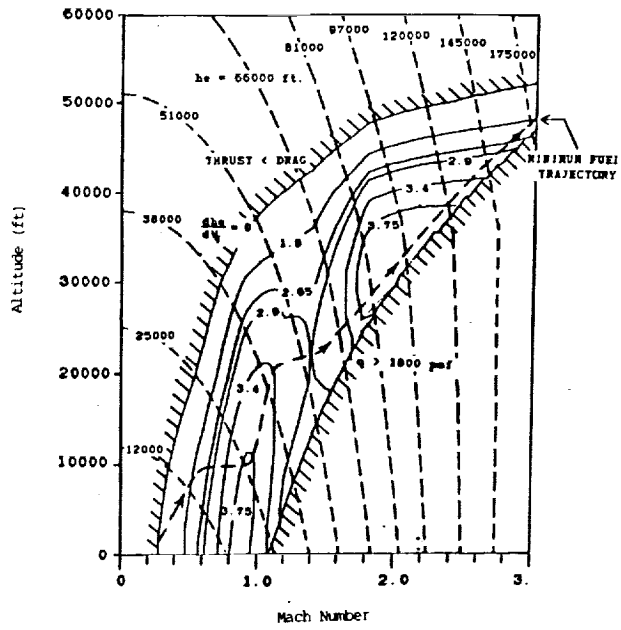

Fig. 7. Contours of Constant $f_s = dh_c / dW_f$

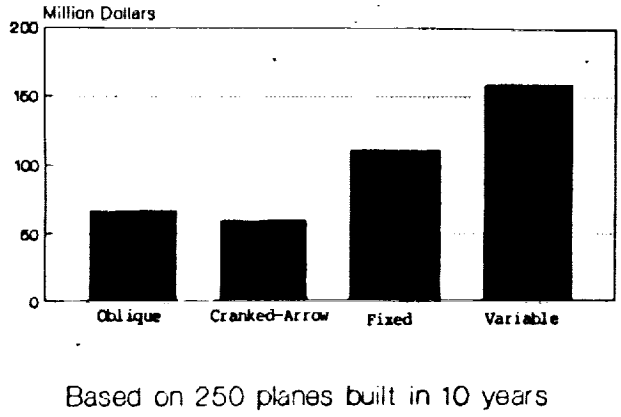

Fig. 8. Cost per Plane (Based on 1987 Dollars)

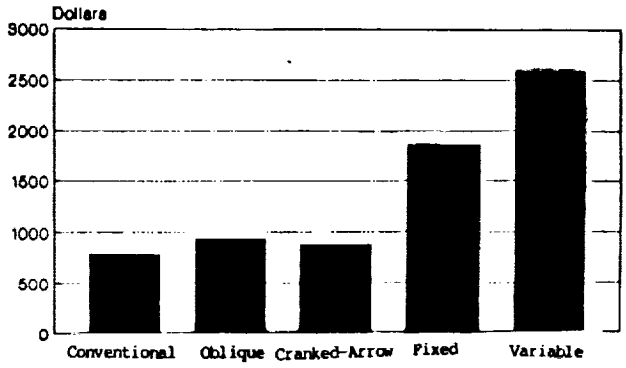

Fig. 9. Ticket Price (Based on 1987 Dollars)

transports, showing only a 10% to 15% increase in ticket price. Compared to the 8- to 12-hour travel-time savings, this makes the Mach-3 transport look very marketable. The Mach-5 transports showed a more marked ticket price increase, 100% to 150%, with only a moderate 1- to 2-hour decrease in travel time from the Mach-3 aircraft. Such cost increases make the hypersonic system much less lucrative than the Mach-3 system. Aircraft costs and profit schedule follow the trends that the ticket price indicates. The aircraft ticket price is highly dependent on fuel price. This makes projecting the ticket costs into the 1990s difficult. Many reports on air travel indicate that passenger travel in the 1990s, especially in the Pacific basin, will increase dramatically in the next decade; making supersonic air travel a viable option.

AIRCRAFT INTEGRATED DESIGN AND ANALYSIS: A CLASSROOM EXPERIENCE

PURDUE UNIVERSITY

AAE 451 is the capstone course required of all senior undergraduates in the School of Aeronautics and Astronautics at Purdue University. During the past year the first steps of a long evolutionary process were taken to change the content and expectations of this course. These changes are the result of the availability of advanced computational capabilities and sophisticated electronic media availability at Purdue. This presentation will describe both the long range objectives and this year's experience using the High Speed Commercial Transport (HSCT) design, the AIAA Long Duration Aircraft design and a Remotely Piloted Vehicle (RPV) design proposal as project objectives. The central goal of these efforts was to provide a user-friendly, computer-software-based, environment to supplement traditional design course methodology. The Purdue University Computer Center (PUCC), the Engineering Computer Network (ECN), and stand-alone PC's were used for this development. This year's accomplishments centered primarily on aerodynamics software obtained from the NASA Langley Research Center and its integration into the classroom. Word processor capability for oral and written work and computer graphics were also blended into the course. A total of 10 HSCT designs were generated, ranging from twin-fuselage and forward-swept wing aircraft, to the more traditional delta and double-delta wing aircraft. Four Long Duration Aircraft designs were submitted, together with one RPV design tailored for photographic surveillance.

Supporting these activities were three video satellite lectures beamed from NASA/Langley to Purdue. These lectures covered diverse areas such as an overview of HSCT design, supersonic-aircraft stability and control, and optimization of aircraft performance. Plans for next year's effort will be reviewed, including dedicated computer workstation utilization, remote satellite lectures, and university/industrial cooperative efforts.

ORGANIZATION OF CLASSWORK AND SCHEDULE

The semester is 15 weeks long with an additional week for final exams. Final reports are due the first day of the last week of class. Oral presentations are given during the last week of class after the written reports have been submitted. These presentations are limited to one hour for each group with about 30 minutes allotted after the presentation for questions from the audience. All faculty members are invited to these presentations.

Formal lectures are presented during the first five weeks of class. These lectures focus both on philosophical issues that have not been emphasized in the classes before this time and on the subject of aircraft performance.

Because no formal course in Aircraft Performance exists in the present curriculum it was very important to discuss performance, propulsion, and other associated aerodynamic terminologies.

Students were assigned written work that outlined the history of their assigned area and its relation to their particular project. In this paper they were asked to discuss issues that they were likely to face during the course of their semester's work and to review possible compromises and conflicts. This forced the students to commit to paper, at an early stage of the design, their thoughts and ideas.

Oral presentations by the students began about six weeks into the semester. The class met Tuesday mornings from 8:30 to 11:20 a.m. and on Tuesday and Thursdays from 2:30 to 3:20 p.m. During the Tuesday morning session each group had one member present an overview, complete with viewgraphs, of a certain area of their project.

These overviews began with weight estimation using historical, statistical data. In addition, tradeoffs between wing loading, and thrust-to-weight ratio for takeoff and cruise were examined, together with the interaction between wing loading, field length, and aerodynamic characteristics for landing and takeoff. The aerodynamics specialist presented an initial planform design and discussed reasons for choosing that design.

Stability and control followed in order of presentation. This group was responsible for the initial sizing of control surfaces based upon the initial weight estimate and the planform design.

The third group to report was the performance group. This group defined the fuel necessary to satisfy range requirements, based upon initial research by the propulsion specialist, and the data available from aerodynamics investigations.

The engine data was presented next and discussed together with its impact upon performance and range.

Weight data for the updated aircraft was then presented, together with a discussion of the materials and structural forms necessary for construction of the design. Significant problems were reviewed, such as heating or center of gravity shifts during operation.

Economics issues were then outlined to focus on the primary issue, that is, operating at a profit.

Design updates were given each week. These updates primarily focused on weight updates from the computer code used to generate the weight data.

COMPUTER CODE UTILIZATION

Students were required to research their design to the fullest extent possible. This included use of empirical relationships such as are found in literature and use of computer codes that are available on the Engineering Computer Network (ECN) and also available on the PC's located in the design laboratory.

Aerodynamic investigations were enhanced by the use of the Vortex Lattice Method code (VLM) that currently runs on a CYBER 205 computer. This code also furnishes valuable data for stability investigations. Aerodynamic studies also use the Supersonic Wave Drag program obtained from NASA Langley and a skin friction drag and a supersonic L/D program also obtained from Langley.

Performance studies were used in the subsonic regime, a small code written for the IBM PC and similar compatible machines. The FLOPS code for flight optimization and performance was used in a preliminary manner. This code is highly sophisticated and as a result somewhat difficult to use.

Structural analysis codes are now being investigated to bring capabilities on-line that are similar to those in the aerodynamics and performance area.

SATELLITE VIDEO TRANSMISSION ACTIVITIES

During the past academic year, the design class pioneered the use of live video transmissions originating from the NASA Langley Research Center. Three programs were presented from Langley: Mr. Corneilius Driver, *An Overview of SST Design;* Mr. Leroy Spearman, *Supersonic Stability and Control;* and Mr. L. Arnold McCullers, *An Overview of the FLOPS Flight Optimization and Performance Analysis Code.* These programs were taped for future use in the design course. The design class is currently reviewing future speakers for the fall semester. These video lectures are supplemented by visitors to Purdue during the semester.

SUMMARY OF HSCT DESIGN EFFORTS

Ten groups of students participated in the HSCT design effort during the academic year 1987-88. These efforts were greatly aided by Ms. Vicki Johnson of the NASA Langley Research Center. This paper will summarize significant details of this work.

The Request For Proposal (RFP) for this project was generated by the Advanced Vehicle Concepts Branch at Langley, in consultation with Purdue University personnel. The RFP (see Appendix A) requests a design that will fly a 6500-nautical-mile mission carrying between 250 and 300 passengers and travel at a cruise Mach number between Mach 2 and Mach 6. The aircraft must be able to operate from a conventional airport infrastructure and be "economical to operate." The anticipated introduction time for this aircraft is in the year 2010.

The requirement that the aircraft operate within existing airport infrastructure was a primary driver of the design, as was indicated by all the design efforts. The reluctance to choose exotic fuels led to a selection of a turbojet propulsion unit and conventional JP-X category fuels. In addition, the fact that heating effects accelerate with increasing Mach number led to the choice of Mach numbers near Mach 3 in all cases.

During the first semester, numerous problems were encountered because of the inability to obtain reliable and detailed engine data for this class of aircraft. This made it difficult to meet the range operational requirements and led to a number of associated difficulties. These difficulties definitely proved the wisdom of the old adage that the "engine is the heart of the aircraft."

Lack of reliable engine data caused the first semester design to suffer from takeoff power problems as well as excessive fuel consumption problems and associated range difficulties. By the beginning of the second semester, these problems had been overcome to a great extent, by the arrival at Purdue of "rubber engine" data from Langley. This greatly eased the burden and increased the confidence of the engine group. In addition, most groups during the second semester had little difficulty achieving the 6500-nautical-mile range requirement.

Most of the designs proposed during the two semesters carried passengers in the 260-290 passenger range. Most made extensive use of NASA wing planform data, and all foresaw the need for titanium, heat-resistant structures, with some utilization of advanced composites.

One group broke new ground and investigated an unconventional dual fuselage design. This design showed a great deal of potential for carrying large numbers of passengers and fuel. The significant aspect of this aircraft was the distance between the two fuselages and the structural connection between them so as to ensure structural integrity and to minimize flexing between the two sections.

Center-of-gravity (c.g.) placement was also a significant issue faced by the design groups. First of all, because the aircraft operates both subsonically and supersonically, there is an aerodynamic center shift with respect to the c.g. when the aircraft goes supersonic. This shift is rearward and creates a large static margin which tends to make the aircraft difficult to trim. To ameliorate this difficulty, fuel sequencing was used in the supersonic flight regime to attempt to control the c.g. position. In the subsonic flight regime the reverse is true. There is little that can be done in managing the c.g. position of an aircraft overloaded with fuel.

An examination of data generated by these groups will help to explain some of the difficulties and possibilities faced during HSCT design. First is a presentation of one of the better designs generated by a group during the fall semester. This design was dubbed "The Wave" by its creators.

THE WAVE

As with the other three design teams who considered HSCT design during the fall semester, the Wave group faced the problem of learning about the design process, while at the same time attempting to master the intricacies of the computer codes that had been acquired for this course. Their design, shown in various views in Figs. 1, 2, and 3, was an over-under engine arrangement with an arrow wing much like a proposed Lockheed design. The length of the aircraft measures 220 feet,

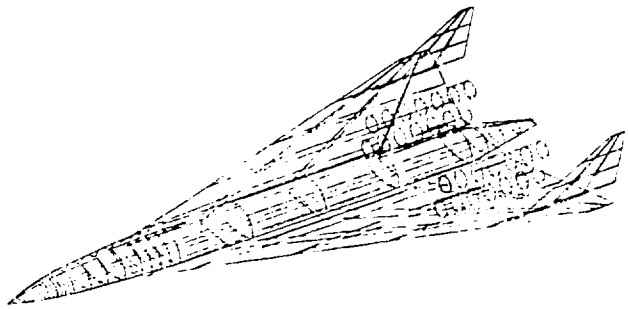

Fig. 1. The Wave Configuration

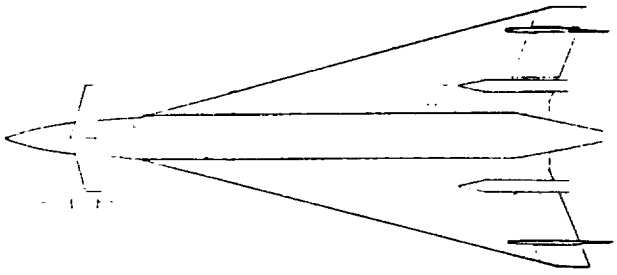

Fig. 2. The Wave Planform Configuration

Fig. 3. The Wave - Side View

while the tip-to-tip span is 95 feet. Wing area of 6530 ft^2 and a takeoff gross weight of 559,000 lbs provide a takeoff wing loading of 86 psf. The takeoff thrust-to-weight ratio was 0.39.

The primary design problem encountered by this group and others was that operational range is very sensitive to the lift-to-drag (L/D) ratio achieved at supersonic speeds. The desire to use conventional fuels and a turbojet engine led the group to choose Mach 2.8 as their cruise speed. At this speed and an altitude of 65,000 feet, the maximum trimmed L/D attained was computed to be 5.8. This fact, coupled with problems due to overland sonic boom, led the group to plan for and to achieve a 5500-nautical-mile range of the type suitable for Los Angeles-Tokyo routes.

A fairly extensive economic analysis was attempted by the Wave group. Two seating configurations were proposed. One configuration had a total of 312 coach seats, while the other had 182 business class seats and only 98 coach seats. The second configuration was preferred for marketing reasons. The cost of the aircraft was estimated to be about $180 million and unless 500 aircraft could be sold, it was unlikely ever to return all its costs without some form of subsidy. It was concluded that the efficiency of the HSCT was its own worst enemy. High speed makes it more productive. As a result, fewer aircraft are needed. However, fuel requirements at high speed make the aircraft expensive to operate and very sensitive to the price of fuel.

Some problems that affected the Wave group were fairly typical of those encountered by all the groups. The desire to fit the aircraft within the existing infrastructure of major international airports led the groups to place constraints on aircraft length and width. These constraints precluded achieving the necessary slenderness to develop high supersonic L/D values. In addition, inattentiveness to c.g. placement early in the design led to difficulties integrating the landing gear into the design. As a result, all aircraft from the fall semester had characteristic long, storklike landing gear arrangements to satisfy tipover and ground clearance requirements as well as being able to rotate at takeoff. Some designs, because of the takeoff rotation requirement, sprouted large canard surfaces to satisfy this requirement which drastically lowered cruise performance.

THE STORK

During the spring semester, the six new groups considering the HSCT design problem had the benefit of the experience of the preceding semester's activities. Some groups chose to ignore certain of these lessons, for reasons unknown, and repeated certain errors of judgement. Two features of the spring semester designs stood out. The first was the variety of different designs. One design even considered the possibility of a dual fuselage configuration. The second feature was the improvement of supersonic L/D performance. This improvement was due to the fact that the best aerodynamicists from the fall semester had been retained as paid consultants (undergraduate teaching assistants). As a result, the students learned how to use computer codes more rapidly and then were able to try different fuselage cambering and wing cambering to raise the value of L/D.

Where values of supersonic trimmed L/D were of the order of 6 for designs submitted during fall semester, these values rose to between 7 and 8.2 during the spring. Much more attention was paid to c.g. placement and control and to trade-offs between takeoff requirements and cruise. An additional factor that made the design process a bit easier and more efficient during the spring was the availability of "rubber engines" from NASA Langley. This data made it much easier to reliably size the powerplant and to integrate it with the airframe for takeoff and cruise.

Figures 4, 5, and 6 show the dual fuselage design proposed by a group who dubbed this design "The Stork." This vehicle was designed to operate at Mach 3 and cruise at an altitude of 60,000 feet. Its maximum L/D was computed to be 8.2 and was the result of optimizing the distance between the two fuselages. One potential problem with this design was excessive flexibility that might allow significant relative movement between the two sections in flight. The group tried to compensate for this by blending the wing structure and fuselage in such a way as to create significant stiffness between the two.

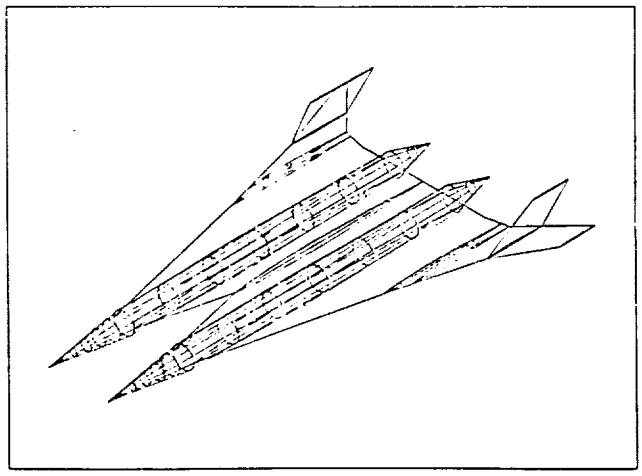

Fig. 4. The Stork

Fig. 5. The Stork - Side View

The Stork design has a relatively low wing-loading of 68 psf with a wing area of 9504 ft^2. It has the capability to fly efficiently overland at subsonic speeds and can be used on longrange routes such as New York to Tokyo. The range is estimated to be 6500 nautical miles, and it can carry a passenger load of 400. Its length of 226 feet and width of 138 feet make it suitable for conventional airport operation. In addition, the thrust-to-weight ratio at takeoff is about 0.18, making it a low-noise aircraft. The design team member assigned to do the economic analysis was skeptical of the commercial viability of this or any other supersonic transport design.

SPARTACUS

Next in order of consideration for effectiveness was a design known as Spartacus. This design, shown in Figs. 7 and 8, was the product of a six member team, who were all participants in the Purdue Co-op program. The Spartacus design weighs 625,000 lbs at takeoff and uses a thrust-to-weight ratio of 0.43, a figure that would be noticeable to the passengers. The use of the FLOPS code showed that the time to climb to 65,000 ft was 26 minutes and that, at a cruise Mach number of 2.8, the cruise leg of its operation took 4 hours and 10 minutes.

Most noticeable in the Spartacus design is the presence of a large horizontal tail surface for control of the aircraft. The group argues that this is beneficial, particularly at takeoff, for rotation. The wing loading is 95 psf and the aircraft has a range of 6500 nautical miles with a supersonic L/D of 7.7. It is projected that the aircraft can seat between 258 and 312 passengers, depending upon the arrangement chosen.

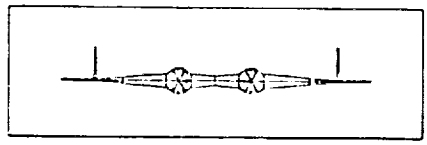

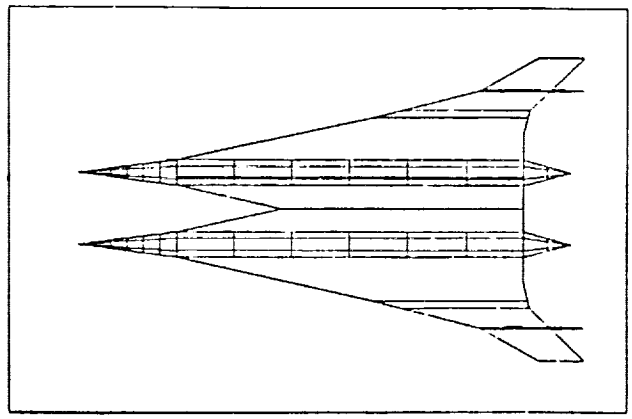

Fig. 6. Planform View of Stork

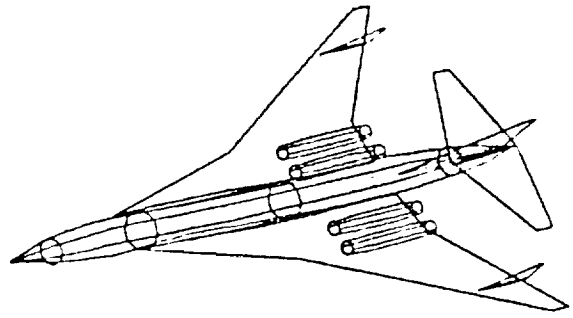

Fig. 7. Spartacus Configuration

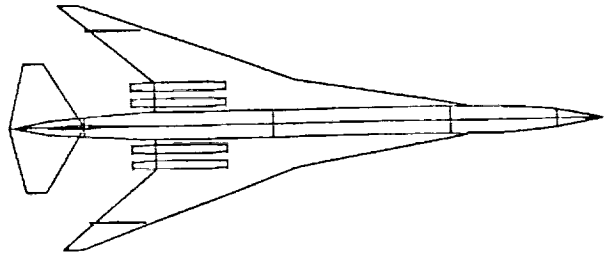

Fig. 8. Spartacus Planform Geometry

THE HAWK

The Hawk design, shown in Figs. 9 and 10, uses the NASA AST-205 as a baseline design. This design seats 276 passengers and utilizes wing and fuselage camber to achieve a maximum supersonic L/D of 6.70 at Mach 3, its chosen operating

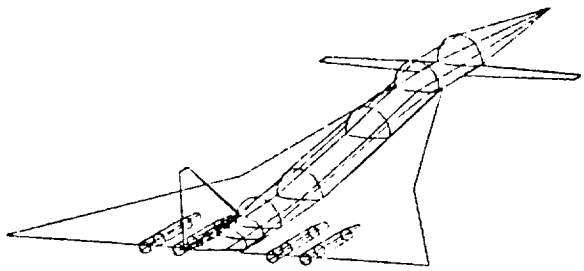

Fig. 9. The Hawk HSCT

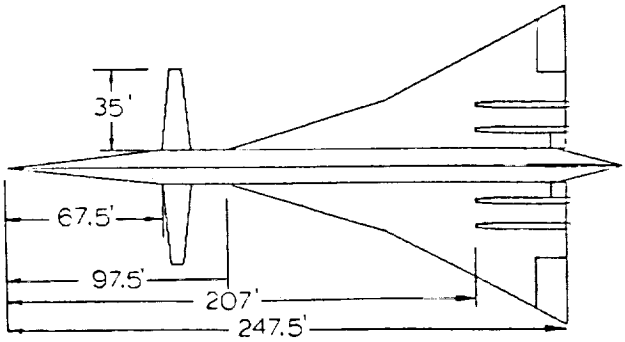

Fig. 10. The Hawk Planform

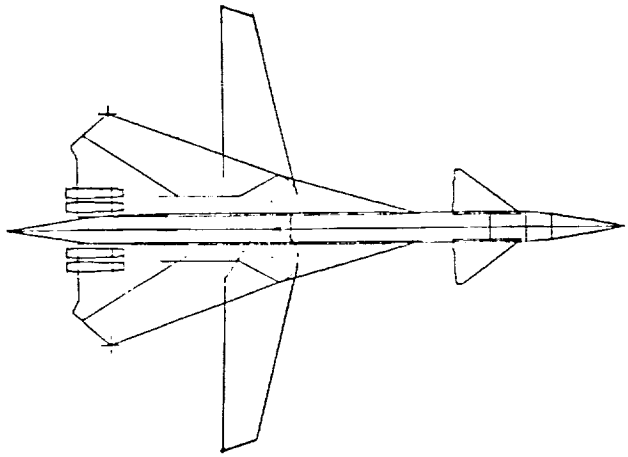

Fig. 11. The Mercury Mark II

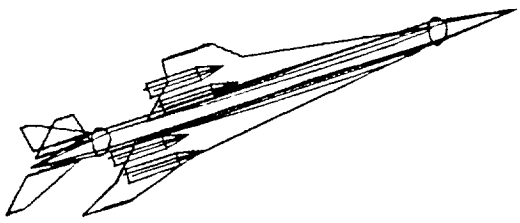

Fig. 12. The Dolphin

airspeed at 65,000 feet. This aircraft weighs 561,000 lbs and has a takeoff wing loading of 69 psf with a takeoff thrust-to-weight ratio of 0.32. As with the other spring semester designs, the NASA ASTM3-1A engine was chosen as a powerplant.

MERCURY MARK II

The Mercury Mark II design began the semester as a long, flying fuel tank that more resembled a missile than an aircraft. Once the group began analyzing their design more carefully, the wings became larger and the fuselage shorter, while the cruise airspeed was reduced. This design, shown in Fig. 11, uses a variable sweep feature to overcome the compromises required between low-speed landing and supersonic flight, as well as the requirement for overland flight. Passenger capacity is 272 passengers with a range of 6500 nautical miles. Design team members recognized that the variable-sweep feature could have a weight penalty associated with it, as well as the requirement that fuel management becomes intricate because of wing-sweep configuration changes during flight. The group did not do as detailed an analysis as was done by others in the aerodynamic area. As a result, they achieved only a supersonic L/D of 6.9. However, the aircraft is configured to carry plenty of fuel to meet the range requirements.

THE DOLPHIN

The Dolphin team used an over-under engine arrangement similar to that used by the Wave design team. The Dolphin design, depicted in Fig. 12, weighed 520,000 lbs. This team claimed the ability to carry 300 passengers a range of 6500 nautical miles and cruise at 65,000 feet. Wing loading at takeoff was 81 psf and the total trip time was about 5 hours.

SWALLOW

The group designing the Swallow HSCT created the design shown in Figs. 13 and 14. This design will cruise at Mach 2.7 at 60,000 feet and is projected to carry 24 first-class passengers and 240 passengers in coach. This aircraft is somewhat longer than other designs, 292 feet in length, with a wing span of 110 feet. The range of this aircraft is 5545 nautical miles. The design employs a fixed arrow wing with a cambered circular fuselage. The wing loading at takeoff is 102 psf. The aerodynamicist did a credible job of achieving a supersonic L/D of 8. This aircraft was one of the heavier designs, at 705,000 lbs.

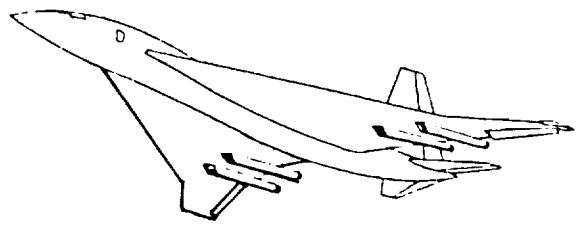

Fig. 13. The Swallow

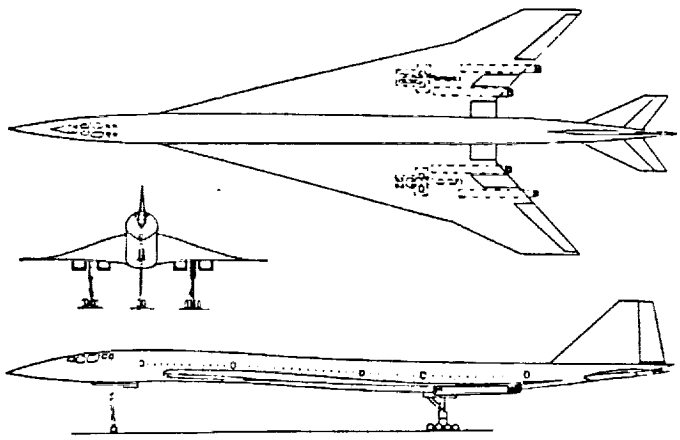

Fig. 14. Three views of the Swallow

APPENDIX A: REQUEST FOR PROPOSAL DESIGN FOR A HIGH-SPEED CIVIL TRANSPORT

Expanding international passenger markets and advances in technologies applicable to high-speed flight could result in an economically viable high-speed civil transport. It is proposed to design such an aircraft with the following characteristics:

- Mach number between 2 and 6
- 6,500 nautical mile range with modified reserves (see mission profile)
- 250-300 passengers
- Approach speed less than 160 kts
- Operate from conventional airports (balanced takeoff field length less than 12,500 ft)
- Meet FAR 25 requirements
- First flight in year 2010

Other areas of consideration should include:

Airport noise. An attempt should be made to calculate and minimize airport noise to comply with FAR 36.

Sonic boom. Sonic boom levels should be calculated and an attempt made to minimize boom to allow the possibility of overland supersonic flight.

Fare levels. The possibility of ticket cost being comparable to that for an equivalent subsonic transport (with fuel at $1.00 per gallon) should be investigated with a surcharge included if necessary.

The design cruise Mach number should be fixed based on appropriate technological and economic considerations. The primary mission considered should be all high speed. An alternate mission should be considered where part of the mission is flown at subsonic speeds (for overland flight and engine out possibilities).

In order to arrive at a final configuration capable of meeting the design requirements, close interactions between all discipline areas will be required. However, there are specific technical areas associated with the various disciplines which must be addressed. The following sections outline the disciplines and their associated technical areas.

Configuration layout. Special consideration should be given to the volume requirements of both passengers and fuel. Fuel type, volume, and location depending on Mach number should be addressed. Physical realism should be included during the configuration layout with particular attention given to landing gear placement and integration.

Aerodynamics. Good high-speed aerodynamic performance is an obvious requirement for this configuration. Takeoff and landing performance, subsonic aerodynamic performance, and stability and control for the entire flight regime should be acceptable. Finally, sonic boom should be evaluated and an attempt made to obtain acceptable boom levels.

Structures. Expected operating temperatures should be predicted and appropriate materials identified. Additionally, thermal management considerations should be addressed. The effects of all these factors on configuration weight should be identified.

Propulsion. The propulsion system and fuel type should be selected consistent with the design Mach number. Efficient high-speed cruise is an obvious requirement. In addition, off-design subsonic cruise propulsion performance should be evaluated. Finally, terminal area noise should be considered.

Performance. The aircraft should be sized to meet the design mission. Acceleration rates during the entire mission should be estimated and the effects on passengers considered. Additionally, the effect of a subsonic leg during the mission (as would exist with no overland supersonic flight or an engine out condition) should be evaluated. Finally, the sensitivity of the configuration to design range (between 4,000 and 8,000 nautical miles) should be evaluated.

Economics. A market study should be conducted to determine the need for this type of aircraft and to estimate the number of aircraft which will need to be produced. Manufacturing costs and operating costs both need to be evaluated. The sensitivity of operating costs to fuel price should be presented. The effects of design choices on the economics need to be evaluated. Also the effect of design range on both the market and economics should be considered. Finally, the effect of no overland cruise on the economics should be identified.

THE APOLLO LIGHTCRAFT PROJECT

RENSSELAER POLYTECHNIC INSTITUTE

The overall goal for this NASA/USRA-sponsored "Apollo Lightcraft Project" is to develop a revolutionary launch vehicle technology that can reduce payload transport costs by a factor of 1000 below the Space Shuttle Orbiter. The RPI design team proposes to utilize advanced, highly energetic, beamed-energy sources (laser, microwave) and innovative combined-cycle (airbreathing/rocket) engines to accomplish this goal. This second year of the NASA/USRA-sponsored Advanced Aeronautical Design effort focused on systems integration and analysis of the "Apollo Lightcraft." This beam-powered, single-stage-to-orbit vehicle is envisioned as the globe-trotting family shuttlecraft of the 21st century. The five-person vehicle was inspired largely by the Apollo Command Module, then reconfigured to include a new front seat with dual cockpit controls for the pilot and copilot, while still retaining the three-abreast crew accommodations in the rear seat. Interior arrangement and cargo space is not unlike that of a full-sized American station wagon. The gross liftoff mass of the Apollo Lightcraft is 5550 kg, of which 500 kg is the payload and 300 kg is the LH_2 propellant. The round trip cost to orbit is projected to be three orders of magnitude lower than the current space shuttle orbiter (see note 1). The advanced laser-driven "5-speed" combined-cycle engine has "shiftpoints" at Mach 1, 5, 11 and at greater than Mach 25. The Apollo Lightcraft is designed to climb into low Earth orbit in three minutes, or fly to any spot on the globe in less than 45 minutes-for the price of an airline ticket today. Detailed investigations of the Apollo Lightcraft Project during the second year of study helped evolve the propulsion system design, while focusing on the following areas: (1) man/machine interface, (2) flight control systems, (3) power beaming system architecture, (4) reentry aerodynamics, (5) shroud structural dynamics, and (6) optimal trajectory analysis. The Apollo Lightcraft concept emerged intact after this critical examination, and no technological barriers were uncovered. The principal new findings are documented in the annual report (see note 2). Advanced design efforts for the next academic year will center on a one-meter-plus diameter spacecraft, the Lightcraft Technology Demonstrator (LTD). Detailed engineering design and analyses, as well as critical proof-of-concept experiments, will be carried out on this small, near-term machine. As presently conceived, the LTD could be constructed using state-of-the-art components derived from existing liquid-chemical rocket engine technology, advanced composite materials, and high-power laser optics developed for the Strategic Defense Initiative (SDI). Lawrence Livermore National Laboratory intends to boost such a spacecraft, weighing roughly 120 kg, into low Earth orbit, using a 25-250 MW ground-based laser, in the next 5 years.

INTRODUCTION

The long-range focus of RPI's design project continues to be centered on an Apollo-sized vehicle. In the first year of this NASA/USRA-sponsored project, the student team concentrated its efforts on designing a beam-powered, combined-cycle engine that could meet (and exceed) the severe demands of a single-stage-to-orbit mission[1]. This initial effort was successful, producing an engine/vehicle concept that required only a 5-6% fuel fraction. To transport five people to orbit (~500 kg payload, including spacesuits) required only $975 of LH_2 and $2455 of laser energy. This represents a payload delivery cost of $3.11/lb, which is a factor of 1000 less than the current Space Transportation System (STS).

Efforts during the 1987/1988 school year were concentrated on the many complex *systems integration* issues involved in the Apollo Lightcraft concept. This detailed investigation evolved the propulsion system to even greater detail, while major attention was devoted to the following areas: (1) man/machine interface, (2) flight control systems, (3) power beaming system architecture, (4) reentry aerodynamics, (5) shroud structural dynamics, and (6) optimal trajectory analysis.

The Apollo Lightcraft survived this critical analysis, and emerged intact[2]. A summary of the principal new findings is presented in the following section.

Design efforts for the next 1988/1989 calendar year will center on the Lightcraft Technology Demonstrator (LTD), and associated small scale, proof-of-principle experiments. The LTD is likely to be the first full-scale realization of a single-stage-to-orbit, laser-propelled launch vehicle, having a launch mass of about 300 kg and a dry mass of 120 kg. Once in orbit, the LTD spacecraft will function as an autonomous low Earth orbit (LEO) satellite complete with a fueled attitude-control system. Roughly 18 kg is reserved for the sophisticated microcircuitry (i.e., "brain") that controls laser-launch and satellite functions.

FAMILY OF LASER-BOOSTED LIGHTCRAFT

Figure 1 shows a family of laser-boosted lightcraft which are likely to trace the development of this new propulsion technology. First to appear will be a small, 1.4-meter-diameter, unmanned drone which Lawrence Livermore National Laboratory intends to design, build and boost into orbit within the next five years. This $2M/year program is now entering

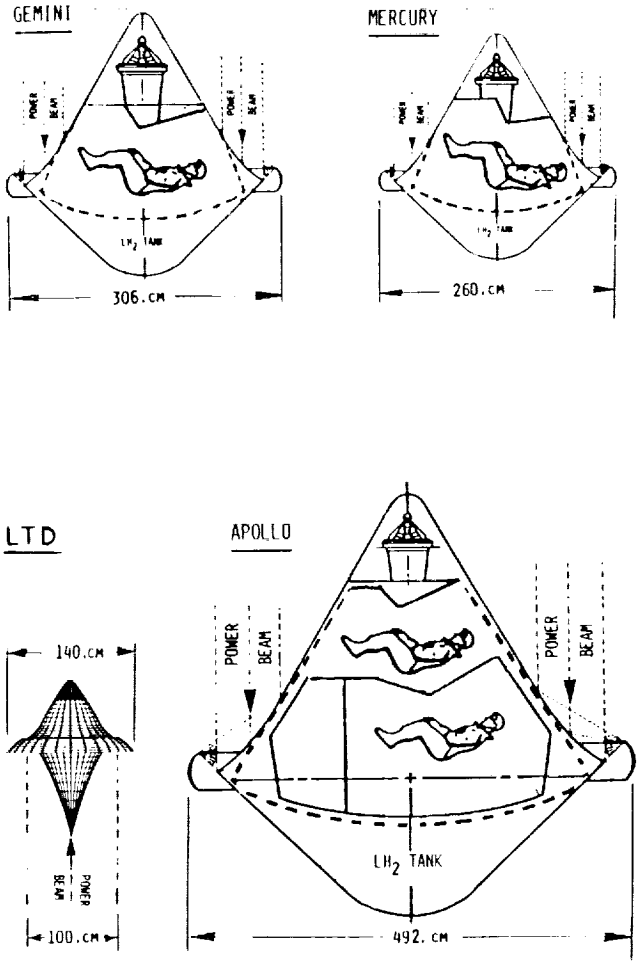

Fig. 1. Family of Laser Boosted Lightcraft

its second year. The Lightcraft Technology Demonstrator (LTD) will have a dry launch mass of 120 kg, and be propelled to space with a 25 to 250 MW ground-based laser (GBL) placed upon a 3-km-altitude mountain site. As portrayed in Fig. 2, this powerful laser could be built using existing CO_2 EDL laser technology by assembling 25 to 100 smaller units into an array. A Chandel-type beam combiner could then be invoked to link the lasers together. Redundant lasers would be built into the system so that inoperative units could be dropped out with no loss in systems utility.

As presently conceived, the LTD vehicle could be constructed using components derived from existing chemical rocket engine technology, advanced composite structures, and high-power optics being developed for SDI applications. The 1-m-diameter laser beam would be delivered directly to the LTD by a 4-m-diameter, high-power laser telescope (transmitter). The Lightcraft must reach orbital velocity within a maximum range of 800 km from the transmitter.

The other three, more advanced, lightcraft in Fig. 1 would parallel the early development of United States spacecraft, and utilize *orbital* laser power beams. It seems reasonable that since laser propulsion technology will be in its infancy, we must return to the minimum weight/volume approach to spacecraft design. Hence, the one-, two-, and five-person lightcraft are designated Mercury, Gemini, and Apollo, respectively. The Mercury Lightcraft is expected to be 2.6-m in diameter, have a mass of 1300 kg, and require four laser beams to deliver the necessary propulsive power. Each beam would carry the same power as that of the LTD, but be somewhat smaller (e.g., 50 cm) in diameter; this will probably necessitate the application of visible wavelengths to transmit the higher beam powers consumed during the acceleration run to orbit.

A two-man, 3-m-diameter, 2600-kg Gemini Lightcraft may require eight such power beams. The 5550-kg, 4.92-m Apollo Lightcraft has been designed for twelve power beams of roughly 75-cm diameter each. In last year's report, 2500 MW was proven to be adequate for the Apollo Lightcraft acceleration run, so each beam must carry approximately 210 MW[1].

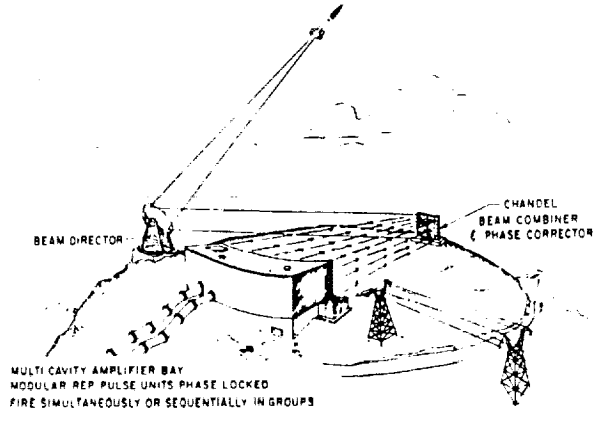

Fig. 2. Ground Based Laser System (25 to 250 MW) [After Kantrowitz]

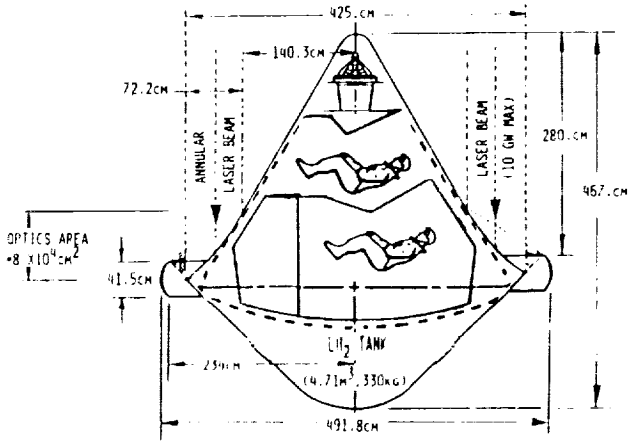

Fig. 3. Apollo Lightcraft Crew Accommodations

APOLLO LIGHTCRAFT SYSTEMS INTEGRATION

Crew Accommodations

Figure 3 portrays the Apollo Lightcraft crew accommodations. The upper cockpit level provides sufficient volume for the pilot and copilot, as well as a dual set of controls. This "front seat" cockpit of the Apollo Lightcraft is identical to that of the two-place Gemini Lightcraft. Retractable flat display screens with keyboards fold up and out of the way to facilitate entrance and egress. Twin joy sticks are employed for control, like those employed in the Manned Maneuvering Unit (MMU). The lower passenger level (rear seat) is similar to the original Apollo capsule, having three people seated shoulder-to-shoulder. The passenger level would also be provided with flat display screens, since direct viewing of the outside through transparent windows is only possible when the propulsive power beam is shut off. These flat display screens can be linked into a "super vision" system, once the Apollo Lightcraft has finished its acceleration run and the power beam has been cut off, when the vehicle is coasting through space. The "super vision" system uses fiber-optic cables, electronic image processing and the display screens to look out the 4.5-m-diameter primary optics. The optical train configuration is similar to the National Multiple Mirror Telescope. Occupants of the Apollo Lightcraft can use this system for high-resolution astronomical observation, interplanetary laser communications, or for examining promising landing sites from low Earth orbit. For the latter function, this 4.5-m mirror gives a resolution of 6 cm in the visible spectrum.

Landing Gear

A tripod landing gear with each leg individually actuated was selected because it is the minimum-weight system for a vehicle that can land/takeoff vertically, and hover. The gear is conceptually identical to that employed on the Lunar Excursion Module. As indicated in Fig. 4, each leg is equipped with a 2-ft-diameter pad which (when fully retracted) becomes an integral part of the reentry heat shield. Once lowered (i.e., extended), the gear reveals three hatches in the pressurized hull. Two are normally used for entrance and egress (as shown in Fig. 5), while the other is employed only during emergencies. The 2-ft-diameter opening is probably sufficient for most people, even with spacesuits. Obviously, larger openings are required to accommodate backpack oxygen systems for extra-vehicular activity (EVA). The entire vehicle kneels for the crew to enter, and in order to point the primary optics precisely at the laser relay satellite.

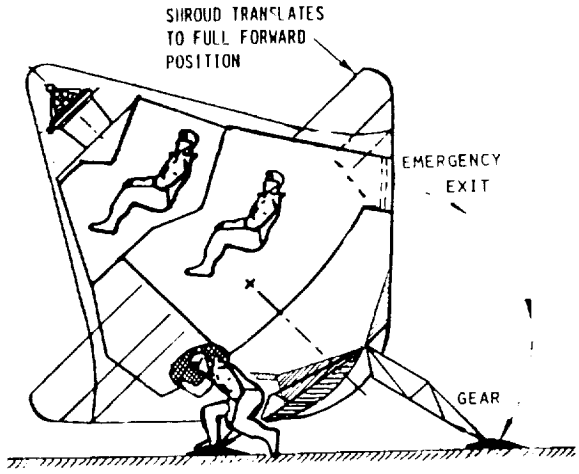

Fig. 5. Crew Entrance and Egress (Gear permits pointing to laser power satellite.)

Receptive Optical Train

Access hatches are placed in the vehicle underbody surface to eliminate the potential for damage to the delicate primary optics (PO) which comprise roughly 50% of the vehicle's upper, exterior-surface area.

Additional measures are required to protect the PO against possible dust and flying insect hazards. Electrostatic repulsion, forced airblowing, and vehicle rotation are potential solutions, possibly used in combination. Also, since a subsonic "pop-up" maneuver is employed (as described in last year's report), the

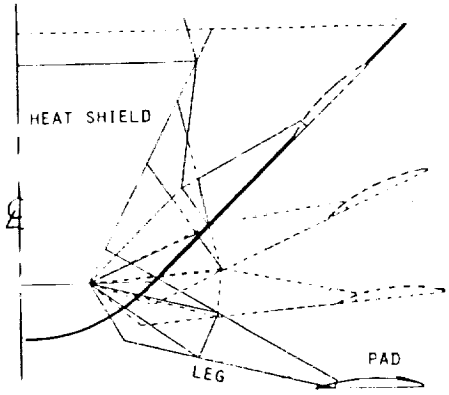

Fig. 4. Landing Gear Configuration/Deployment

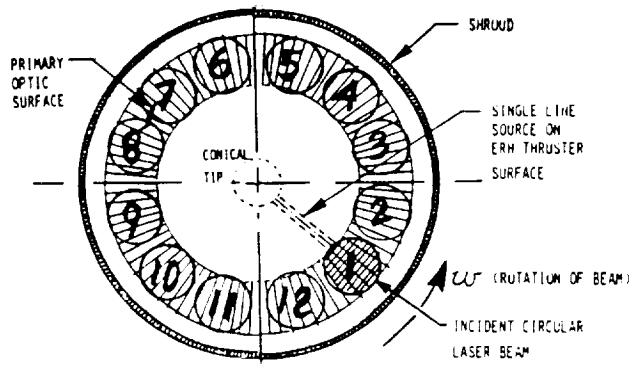

Fig. 6. Top View of Apollo Lightcraft Showing Primary Optical Surface and Single Laser Beam

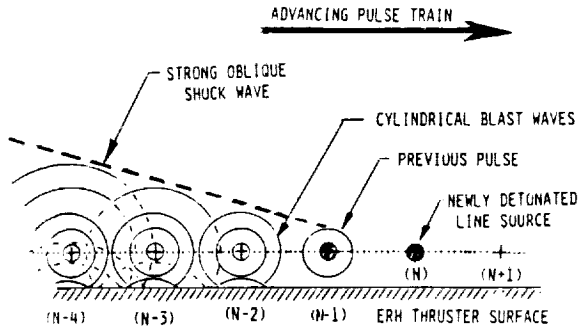

Fig. 7. Rotary Detonation Wave Engine (RDWE) Mode for Liftoff ($0 < M_\infty < 1.0$)

potential threat of aerosol and insect impact damage (abrasion, etc.) is minimized when traversing the dense lower atmosphere.

Figure 6 presents a top view of the Apollo Lightcraft, indicating the location of the PO surface. During the liftoff phase, the combined-cycle engine operates in a Rotary Detonation Wave Engine (RDWE) mode, as shown in Fig. 7. This engine mode is a variation of the External Radiation-Heated (ERH) thruster discussed in last year's report. Figure 8 is a diagram of the vehicle's bottom surface showing the location of the secondary and tertiary optics required in this propulsive mode. Basically, the primary optic is designed to receive pulsed laser beams at only the twelve specific locations given in Fig. 6. Each beam is assumed to have a roughly Gaussian intensity distribution, and three detectors (per beam) monitor the laser intensity at the beam's edge. These detectors are linked to an active feedback system to provide accurate beam pointing and tracking information.

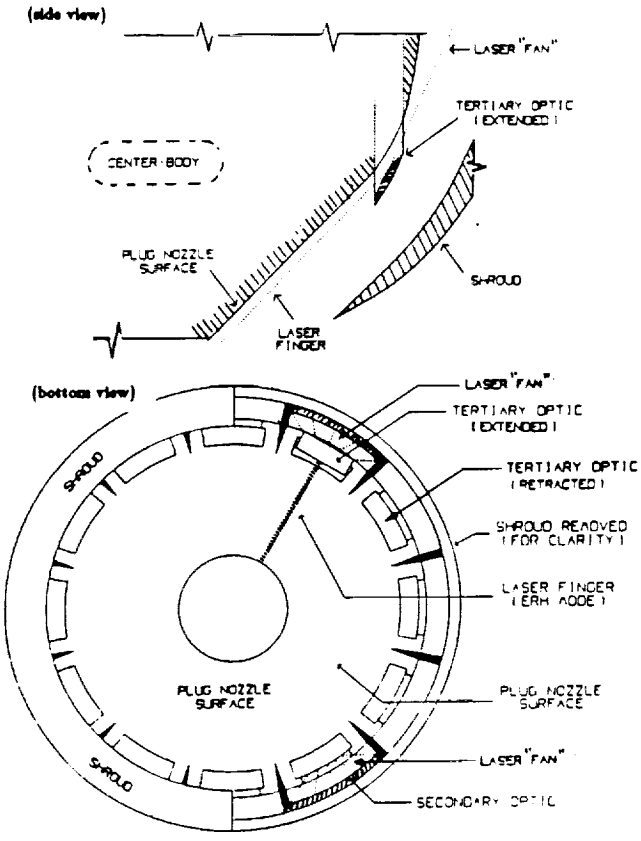

Fig. 8. Apollo Lightcraft Side and Bottom Views (Displaying Optics Used in RDWE Mode)

ERH Thruster: RDWE Mode

During the RDWE mode which is used for hover and acceleration to about Mach 1 flightspeed, each of the twelve secondary optics condenses the reflected beam onto a tertiary optic, which in turn projects a small, 2-cm-diameter laser beam across the vehicle's lower surface. Through the mechanism of inverse bremstrahlung absorption, this laser energy is transferred directly into the air, and creates in the process a high pressure (e.g., 600 atm.) "plasma finger." Each 80-cm-diameter beam is designed to create only one plasma finger.

The RDWE firing sequence can either detonate all of the available fingers simultaneously, or in some predetermined pattern (e.g., fingers 1-2-3-4-5, etc., sequentially, as shown in Fig. 7). More plasma fingers can be inserted between the fundamental twelve sites (which are tied directly to the receptive optical train) by invoking vehicle rotation. Due to the structural limitations of existing advanced composite materials, maximum rim speeds are not likely to exceed the ambient speed of sound.

During liftoff and acceleration to Mach 1, the generation of excessive noise levels can be prevented by pulsing all twelve plasma fingers simultaneously at *sub-audible rates* (e.g., below 16 Hz), or by operation in the RDWE mode at super-audible frequencies (e.g., > 10 kHz to 20 kHz). Significant noise abatement may also be possible by phased detonation of the plasma fingers, such that the outgoing sound patterns exactly cancel (i.e., an "electronic muffler").

It is interesting to note that the RDWE mode automatically compresses air into adjacent plasma-finger sites, just prior to their detonation. Hence, inherent to the RDWE operation is this "supercharging" function which can provide high thrust levels at liftoff, with zero forward velocity.

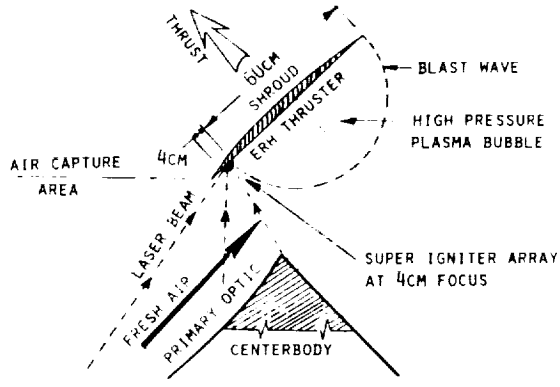

Fig. 9. "Shroud Lift" ERH Thruster Mode ($1.0 < M_\infty < 6.0$)

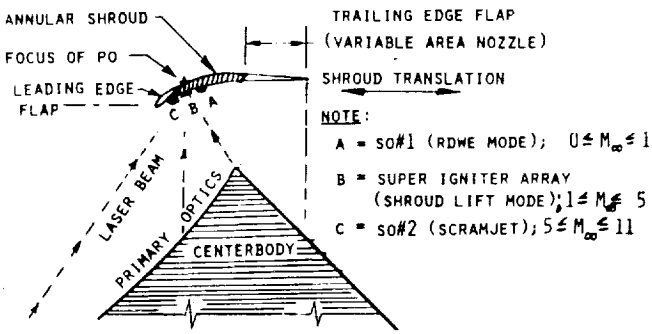

Fig. 10. Shroud Optical Functions vs. Translation

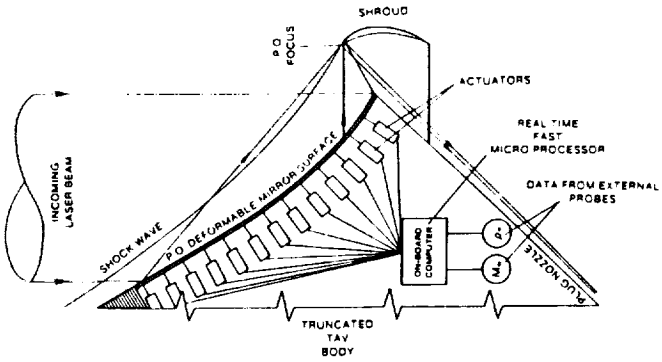

Fig. 12. Adaptive Primary Optics

Once the vehicle attains a forward velocity of Mach 0.3 to O.5, the annular shroud begins to convect large quantities of fresh, unheated air across the lower centerbody ERH thruster surface. However, this particular ERH thruster mode becomes ineffective at about Mach 3, just as the scramjet mode begins to produce thrust. Accelerating through Mach 3 was perceived as a potential problem in the combined-cycle engine proposed for the Apollo Lightcraft.

ERH Thruster: Shroud Lift Mode

To eliminate the potential problem of accelerating through Mach 3, a second ERH thruster mode was developed. Referred to as the "shroud lift" mode, this mechanism has been analyzed mathematically and exhibits excellent thrust levels from Mach 1 up to Mach 6. The new ERH thruster concept, portrayed in Fig. 9, will require the inclusion of an annular "super-ignitor array" to the inside shroud surface. This material acts as a self-excited "spark plug" to reduce the time and energy required to ignite a Laser Supported Detonation (LSD) wave at the array surface. Candidate materials are currently being investigated under the Lawrence Livermore Laboratory (LLL)-sponsored laser propulsion program.

To prepare for engine operation in this mode, the shroud is first shifted aft from position "A" in Figure 10, to position "B." This brings the super-ignitor array into the focus of the primary optics. Next, the pulsed laser beam ignites a 4-cm-wide annular LSD wave at the super-ignitor array, which resides at a location close to the shroud leading edge. The resulting 600-atm pressure toroidal plasma bubble then expands against the shroud, generating thrust, as the inlet air blows the bubble aft. When the plasma pressure falls to the local static pressure level, the impulse ends, just before the bubble leaves the shroud trailing edge (see Fig. 9). A complete description of the Mach number vs. altitude performance for this new ERH thruster mode is described in note 2.

Scramjet Propulsion Mode

The present conception of the complete combined-cycle engine is a 5-speed (1) RDWE thruster, (2) shroud-lift ERH thruster, (3) scramjet, (4) MHD-fanjet, and (5) rocket.

Shift points are now Mach 1,5,11, and above Mach 25. The scramjet mode, with its "planar heater," is pictured in Fig. 11, and has not changed in concept from last year's vision.

However, it was discovered that significant phase distortions due to aero-optical phenomena will be produced in the laser power beam as it transverses the bow shock wave. These effects are dominant mostly in the lower supersonic-flight

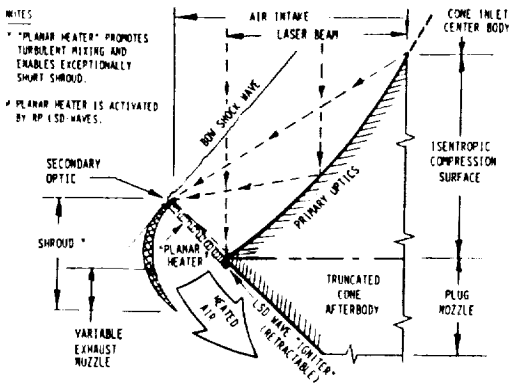

Fig. 11. Scramjet Propulsion Mode ($6.0 < MM_\infty < 11.0$)

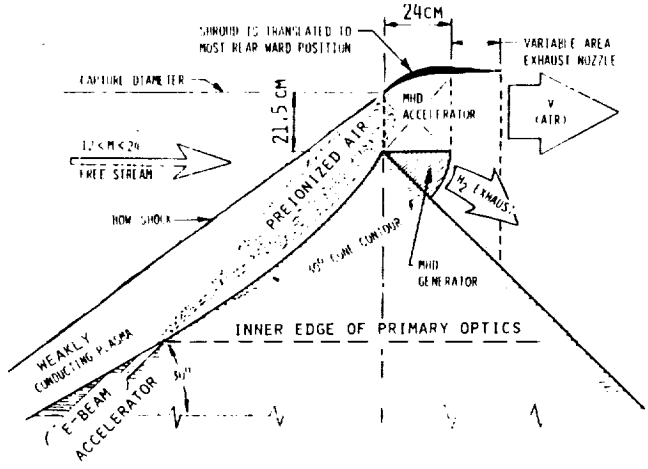

Fig. 13. Air Plasma Conductivity Enhancement for MHD Fanjet Accelerator, Using Electron Beams

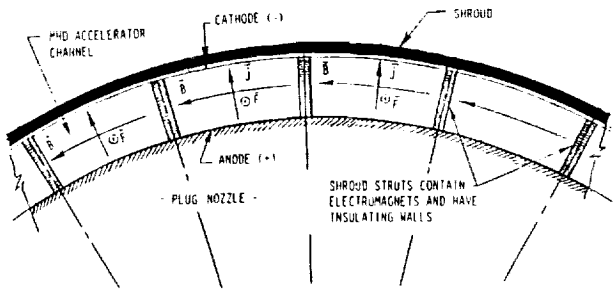

Fig. 14. Superconducting Magnet Configuration for MHD Fanjet (View from rear, looking forward)

Mach numbers typical of the ERH thruster mode, and to a lesser extent, in the scramjet and MHD-fanjet modes. As a result, it is now clear that the primary mirror must be an adaptive surface that is actively controlled throughout the acceleration run (see Fig. 12). This should present no particular difficulty, especially since these phase distortions are a direct function of flight Mach number, and can be sensed as well as corrected at the vehicle flight platform. Finally, adaptive mirror technology is advancing at a rapid rate under several Department of Defense (DOD)-sponsored SDI programs.

MHD-Fanjet Propulsion Mode

Two new developments in the MHD-fanjet engine concept bear mentioning. Most importantly, it was noted in the previous NASA/USRA report that some mechanism for augmenting the conductivity of inlet air must be found. Figure 13 portrays the most promising solution that could immediately be invoked: a large number (e.g., 24-48) of electron beam accelerators could be mounted within the vehicle forebody, just upstream of the primary optics (see Fig. 6). These devices would inject relativistic e-beams (e.g., 3 at 4 MeV) into the compressed inlet air just as it enters the MHD air accelerators. Performance of the MHD accelerators was found to be quite sensitive to air plasma conductivity.

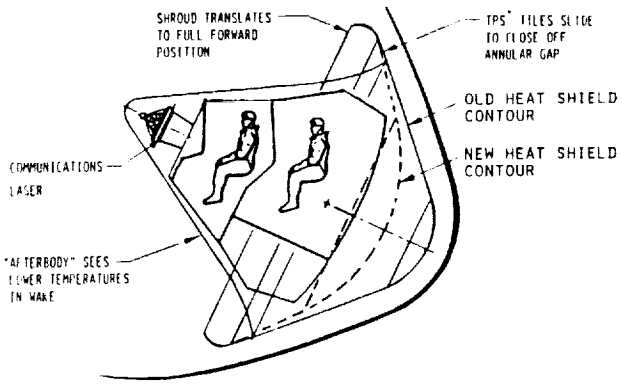

Fig. 15. Re-entry Heat Shield Configuration

Second, it is evident that from studying Fig. 14 that the optimum spacing of superconducting magnets for the annular MHD air accelerator may not exactly match the requirements perceived from structural and heat transfer considerations. Perhaps one solution would be to retract every other magnet out of the annular duct flow at flight speeds below Mach 11, when they just produce more drag.

Finally, it is fairly obvious that the revolution in low-temperature superconductors will greatly reduce magnet cooling requirements of such advanced hypersonic engines.

Aerodynamics of Reentry

An examination of the reentry heat shield contour proposed last year for the Apollo Lightcraft has indicated that a revision might be necessary. Figure 15 depicts the old 45° half-angle cone in relation with a proposed 50° blunted cone. A larger cone angle and more severe cone truncation may be required to reduce peak acceleration rates to something more in line with human tolerance.

Incidentally, this change will also improve impulse coupling in the RDWE mode, since the thrust vector will be more closely aligned with the vehicle flight axis.

Annular Shroud Structural Dynamics

It is well understood that operation of a pulsed engine at any of the natural frequencies of the engine's structure is undesirable. This could lead to an unstable dynamic situation, where the vibrations induced by the engine pulses would couple with the natural vibration of the structure. This undamped behavior would soon lead to a catastrophic failure of the system. To reduce the risk of this occurring, it is necessary to either avoid engine operation at the natural frequencies, or to pass through these frequencies quickly. In the past year, analyses were carried out to determine the natural frequencies of the Lightcraft's annular shroud. Natural frequencies were determined for both local and global modes of vibration. Of course, since the actual materials and structure of the shroud are not yet determined, these calculations are merely estimates. However, the analytic procedure developed is sound.

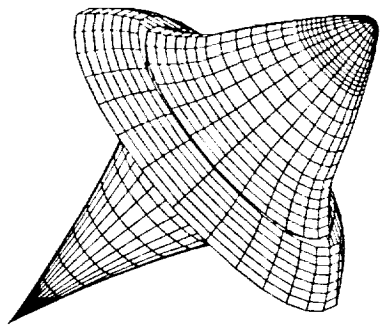

Fig. 16. Lightcraft Technology Demonstrator ($25\ MW < P_L < 250\ MW$)

Optimal Trajectory Sensitivity Studies

Last year, optimum trajectories were determined for the Apollo Lightcraft following a single relay satellite. To continue the trajectory optimization study, it was necessary to determine how sensitive the optimum trajectories were to changes in some of the trajectory parameters. Such parameters (normally held constant) as vehicle liftoff weight, vehicle drag, and maximum available laser power were examined. The trajectories were found remarkably insensitive to small changes in these operating parameters.

SUMMARY AND CONCLUSIONS

The next year's effort will focus on a detailed analysis of the Lightcraft Technology Demonstrator pictured in Fig. 16. This investigation will emphasize small-scale experiments on this near-term concept which could be built with existing technology. The LTD's "3-speed" combined-cycle engine is a much simplified version of the Apollo Lightcraft's engine; it eliminates the RDWE and MHD-fanjet propulsion modes.

A major conclusion of this year's study was the following: In order to continue climbing the steep learning curve in laser propulsion technology, emphasis must now switch to detailed engineering analysis of the most elementary propulsion system components, and to critical proof-of-concept experiments. The LTD vehicle provides just this sort of opportunity.

REFERENCES

1. Myrabo L.N., editor. The Apollo Lightcraft Project. (abstract) NASA/USRA University Advanced Design Program, Third Annual Summer Conference, June 17-19, 1987.
2. Smith W.L., editor. The Apollo Lightcraft Project. (abstract) NASA/USRA University Advanced Design Program, Fourth Annual Summer Conference, June 13-17, 1988.

omit

Space Projects

AUTONOMOUS SPACE PROCESSOR FOR ORBITAL DEBRIS REMOVAL AND FLAME AUGMENTATION ADDITIVES IN SCRAMJETS FOR THE NATIONAL AEROSPACE PLANE

UNIVERSITY OF ARIZONA

This is a brief description of the USRA-sponsored design project at the University of Arizona. Approximately eighty-percent of this effort was spent pursuing a novel engineering concept for the in-situ processing of orbital debris utilizing resources available in low Earth orbit (LEO); the other twenty-percent was devoted to discovering innovative additives for the anchoring of supersonic combustion zones that find direct use in the Aerospace Plane that is expected to use scramjets. The seriousness of the orbital debris problem is briefly described. Available "solutions" are outlined from the literature. The engineering design is briefly mentioned, with an emphasis on the positive aspects of the space environment that should be used in an economical approach. The aspects of operating in microgravity, vacuum, and in utilizing solar energy are mentioned. A quantitative computer animation was developed to provide design data. Three specific dead spacecraft were identified for an initial cleanup mission. The design concept, which includes a solar processor, remote arm manipulators, and the gradual processing of the debris, is also described. This is followed by a description of hardware construction. Operation and actual processing of simulated debris parts (aluminum, for now) are demonstrated. In the NASP task, construction of the new design for measuring the radiation from the key free radicals (as enhanced by the additives) is described. Immediate (1988) and long-range (through 1992) future plans are shown to clearly indicate the full engineering design strategy in the light of the national space program thrusts.

LIST OF SYMBOLS

V = Volume (width)(thickness)(length)
ρ = density in g/cm^3
C = heat capacity in J/g°C
H_f = latent heat of fusion in J/g
H_v = latent heat of vaporization in J/g
T_m = melting temperature in °Celsius
T_v = vaporization temperature in °Celsius
T_0 = initial temperature in °Celsius

INTRODUCTION

Orbital debris is a growing hazard affecting all space program efforts. Human activities in space have generated significant quantities of debris that pose a major threat to continued explorations. Many of these problems have been lucidly described by Kessler[1,2]. Although it is not within the scope of this USRA effort to make a thorough study of the hazard aspects of this debris, it is worthwhile to recall that a direct collision is only one aspect of the hazard. In fact, such a hit did occur during a flight of the Space Shuttle Columbia[3], causing extensive window damage. These hypervelocity impacts have the potential to vaporize metals. Occasional re-entry of some of the larger debris pieces have created significant anxiety concerning the possible dangers associated with Earth impact. The Skylab crash in Australia and the subsequent impact of a Russian spacecraft in Canada provide two examples. The United States Space Command has created a good database representation of the debris objects in orbit. Several large pieces are evident. Even astronomers, who argued for telescopes in low Earth orbit (LEO) to search the pristine sky, away from polluted terrestrial sites, have been painfully surprised to see the sky view temporarily obstructed by orbiting objects[4]. If these past encounters with debris are considered bad, the future looks much worse. Systematic projections have shown that by 1990 the probability of collisions is almost double what it is today. Many of the more recent activities in LEO will not alleviate this problem.

Taking a more constructive point of view, a concept for the utilization of the resources in LEO to clear the debris was presented by Ramohalli in 1986[5]. The concept uses solar energy to process the materials and either retrieves, or burns up in reentry, the larger pieces of debris. Finally these spacecraft would self-process to a compact mass to be retrieved by the Shuttle or re-enter the Earth's atmosphere to burn up, or splash down harmlessly. A quantitative computer animation showed the feasibility of this approach[6]. One point of some importance must be made here. It can be argued that larger pieces are not really a hazard and that the problem is due mostly to the innumerable smaller particles. Future spacecraft can always avoid large debris, but smaller particles are more unpredictable and essentially untrackable. Hence, the argument goes, we are solving the wrong problem. We disagree. It is certainly true that the large, well-characterized orbiting debris seem to pose a small threat to space operations at this time. But even a single collision can multiply the number of fragments enormously; thus, by ignoring the larger debris, we will have lost the opportunity to clear large compact masses. Recent operations in space have been shown to create an incredibly large number of small particles with a single collision.

This paper presents the first step in a well-planned engineering design activity that will eventually lead to the

development of technologies to clear orbital debris. At the time of this report, the concept has evolved, the first prototype has been designed, the first hardware built and processing using solar energy has been demonstrated to be feasible. In the National Aerospace Plane (NASP) contribution, we have proven the design of an apparatus for measuring the enhanced radiation associated with the flame stability enhancement proved earlier[7]. This paper ends with a summary of future activities.

MISSION SPECIFICATIONS

The debris processor is to be launched from the Space Shuttle. Once launched, the processor will maneuver to a piece of debris, cut the piece into manageable pieces and then store them in an attached collection bin. The processor will then maneuver to another piece of debris and the cutting process will be repeated. This pattern will continue until the collection bin reaches its capacity. With the bin full, the craft will either be retrieved by the Shuttle or directed to a splashdown recovery.

An initial mission was studied in great detail by Ramohalli and Cassidy[6] and a computer simulation was generated. The proposed initial mission consists of the collection of three well-known pieces of space debris followed by a splashdown recovery. The three candidates for the first mission are the Cosmos 631 satellite, the Cosmos 631 satellite booster and the Cosmos 655 satellite. The mission will begin with the removal of the outermost target. Once this piece is processed, the craft will maneuver to the second piece in the next lower orbit. The craft will maneuver by Hohmann transfer so that maximum fuel efficiency will be achieved. The craft will process the second target then maneuver to the final craft (using a Hohmann transfer once again). Once the final target is processed the processor will be guided to a splashdown recovery. To carry out the mission, a state-of-the-art propulsion system will be employed which will provide a specific impulse of 300 sec. The initial mission will require approximately 191 kg of propellant.

DESIGN SPECIFICATIONS

Solar focal point cutter

A solar focal point cutter has been developed which utilizes the sun's energy to dismember orbital debris. The cutter was designed to utilize the abundant solar energy available in LEO. To cut a material using focused light, energy must be input to a point faster than it can be conducted, convected, reflected, or re-radiated away. In space the only mode of heat transfer from a body is radiation, although conduction is responsible for removing heat from the focal point. The rate of conduction from the focal point is determined from the equation:

$$\dot{q} = kA_c V(\partial t/\partial r) \qquad (1)$$

where k is the thermal conductivity coefficient (for Aluminum 237 W/mK).

The total amount of energy required to produce a kerf (or cut) by complete vaporization is given by the equation:

$$E = \rho V[C(T_m - T_o) + C(T_v - T_m) + H_f + H_v] \qquad (2)$$

Equation (2) was used to estimate the heat flux (energy/unit area) required to vaporize various thicknesses of pure aluminum. It was estimated that a heat flux of 5493 W/cm^2 is needed to vaporize a 1/16-inch piece of aluminum (the absorptivity of aluminum was estimated to be 0.3 in the calculation). From equation (2) it follows that the main consideration for cutting using concentrated solar energy is the energy flux. For this reason the focal point cutter was designed to collect and concentrate large amounts of solar energy into small focal point areas.

Robotic Manipulator Arm

A robotic manipulator arm is being developed which will allow pieces of debris to be positioned and moved during the solar cutting process. The final arm design will have to meet several requirements. The movement of the arm should not interfere with the operation of the focal point cutter. Hydraulic actuators cannot be used because that hydraulic fluid leakage would be difficult to control in the vacuum of space. The arm should position the debris so that the concentrated light is perpendicular to the plate in order to minimize the cutting

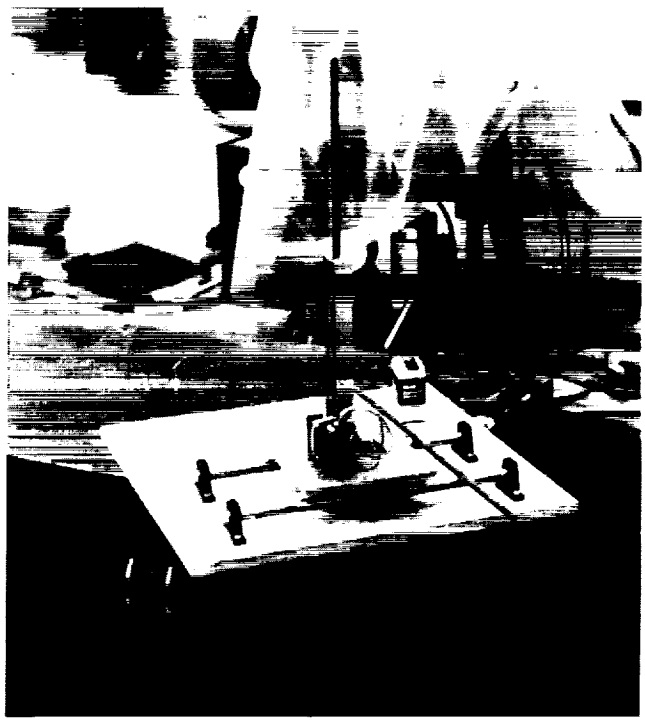

Fig. 1. The first design of the Cartesian remote arm manipulator. (This design is currently being revised to operate in polar coordinates.)

time. Materials used in the robotic arm will be limited due to space environment considerations (vacuum, low temperature, radiation). A Cartesian robotic arm was constructed and operated. This design is currently being altered in order to employ a polar-coordinated system of motion. The Cartesian arm is shown in Fig. 1.

DESIGN CONFIGURATION

The developed solar focal point cutter uses a system of mirrors and lenses to collect and focus solar radiation in order to cut pieces of space debris. Several hinged joints are incorporated into the cutter design (Fig. 2) so that the cutter can be compacted into a small volume for transport aboard the Space Shuttle. The collapsible feature also greatly decreases the probability of a direct collision with a meteorite when maneuvering under its own power by allowing the frontal surface area to be reduced. Gold mirrors were used in the prototype since they reflect infrared radiation much better than silver mirrors. This greater ability to reflect infrared radiation isn't important on Earth, but is extremely important when used in space where infrared radiation is abundant. Fresnel lenses were used since their flat geometries make them lighter than corresponding converging lenses having similar focal points and focal lengths. These lenses are also relatively inexpensive. Aluminum was used throughout the design for the

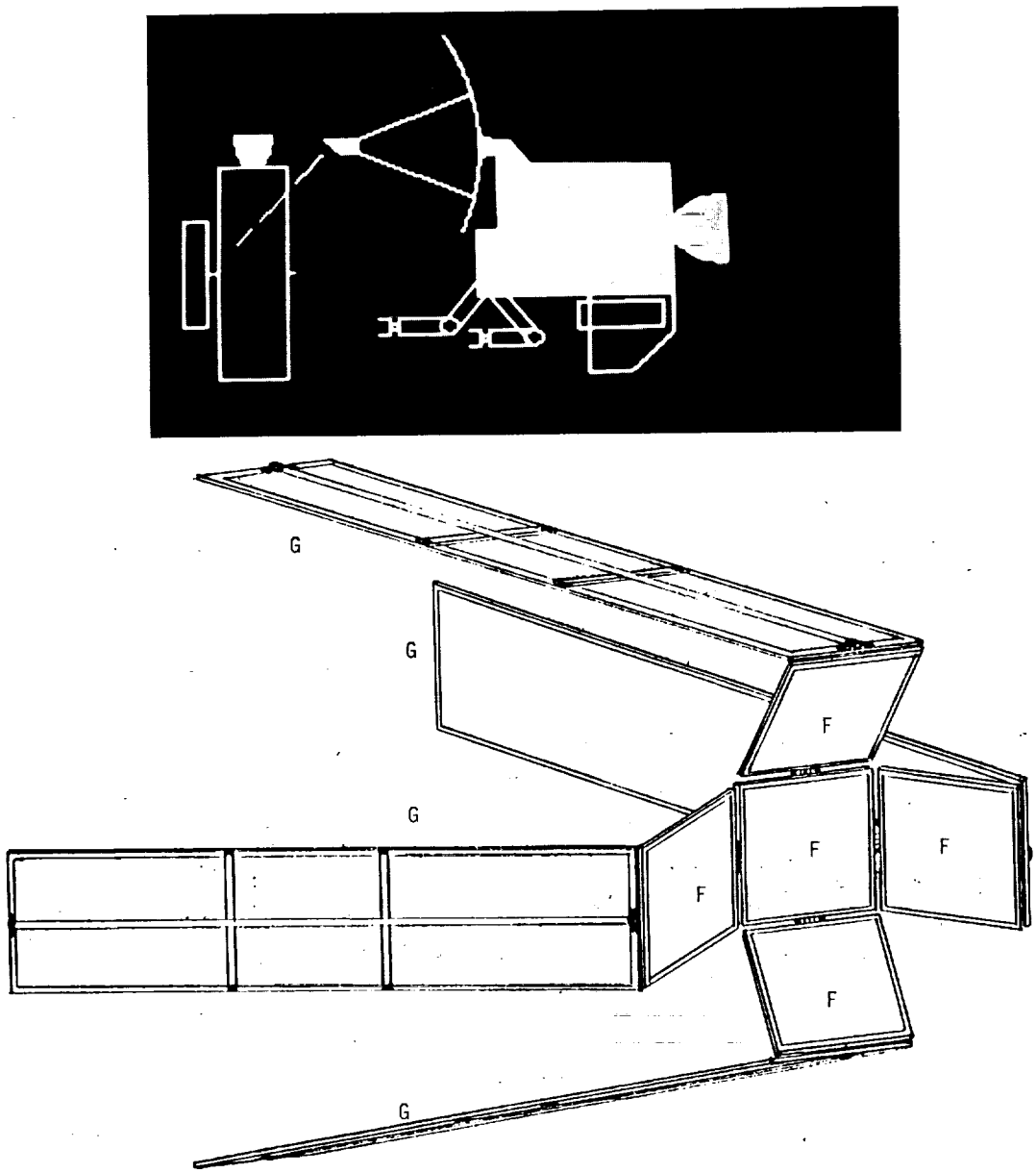

Fig. 2. The fundamental design of the solar concentrator. The combinations of Fresnel lenses (F) and the gold film reflectors (G) represent innovations.

support structures and the mirror and lens framework. Aluminum was selected because it is lightweight, rigid, and relatively inexpensive. Figure 3 shows a photograph taken of the assembled focal point cutter (note that in this photograph the table is used only to hold the cutter and is not part of the actual solar cutter).

PERFORMANCE

Tests were performed by placing different metal samples at the compound focal point of the cutter. The cutter was successful in vaporizing a hole in a 0.005-inch-thick aluminum can. A hole was melted in an 0.009-inch piece of tin, but the hole closed upon cooling (which should not be a problem in the hard vacuum of space). A piece of 1/8-inch solder was melted when tested. Figure 4 shows the results of the solar cutter tests. In order to verify the success of our special collector design, a single Fresnel lens was used to duplicate the solar cutter tests. The single Fresnel lens could not melt the 0.005-inch aluminum can.

SUMMARY AND FUTURE WORK

This USRA sponsored engineering design work has the ultimate goal of developing an autonomous craft for clearing orbital debris; it is hoped that the craft can qualify for a Getaway Special on the Space Transportation System (STS). In a planned gradual march toward this goal, the first steps have been taken. The fundamental mission has been identified. The space resources have been quantified. The propulsion requirements were calculated. Using a standard, state-of- the-

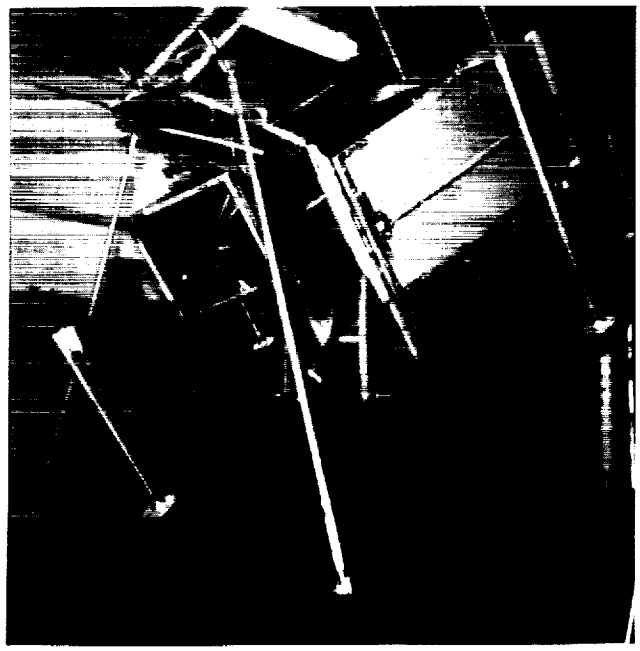

Fig. 3. Photograph of the completed tabletop hardware showing the focal point cutter.

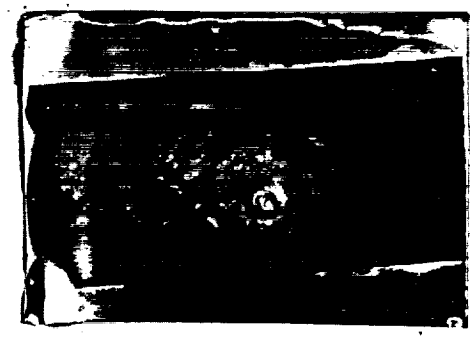

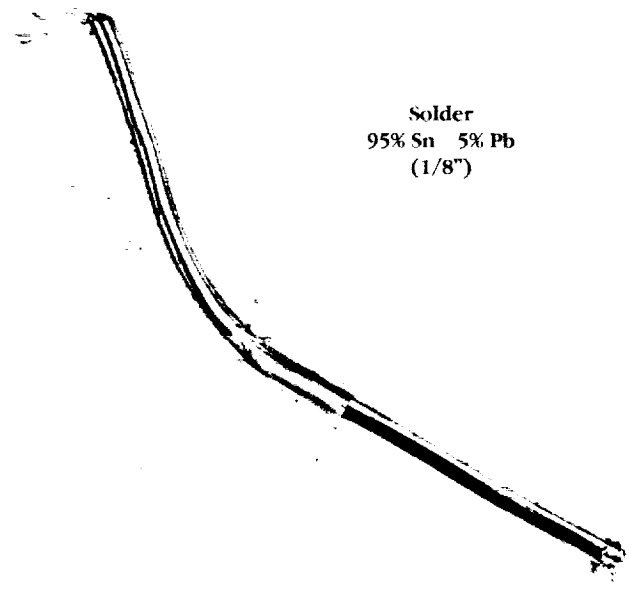

Fig. 4. Examples of the successful operation of the focal point solar processor.

art (300 sec. specific impulse) propellant system, a three-rendezvous mission was envisioned. The inclination, altitude, mass, and general configuration of three satellites were read from the Space Command database. The outermost debris object was identified for processing first, from the autonomous craft launched from LEO. The launch to LEO is assumed to be accomplished with the STS or an Expendable Launch Vehicle (ELV). The outermost orbit is chosen first to minimize the propellant requirements with the low initial mass. After solar processing, the debris- processing vehicle executes a Hohmann transfer to reach the next lower orbit and the debris removal operations continue. After the processing of the third piece of debris, the craft self-processes for a splashdown, STS retrieval, or burnup upon reentry into the Earth's atmosphere. A quantitative computer animation provided the first design data.

The mechanical execution was divided into four stages and two tasks. The stages are concept demonstration, tabletop working model with manual operation, prototype hardware with autonomous operation, and "flight-ready" hardware with space-qualified construction. The emphasis is on the basic engineering design philosophy rather than on delivering a piece of hardware. The two tasks that proceed in parallel are the focal point solar processor and the robotic manipulator.

At the time of this report (May, 1988) the initial feasibility demonstration is complete. The tabletop working model is completed for the solar processor. The robotic manipulator is progressing and is expected to be complete by the end of the summer. Cutting of aluminum, stainless steel, and bending (forming) of a metal rod are all demonstrated. The hardware performs as designed.

The autonomous robotic operation is being developed from a fundamental point of view. Pattern recognition, tracking, maneuvering, and processing are all considered separately drawing on the available technology and are being integrated economically. High-tech materials and innovations are being planned. One example is the innovative use of Fresnel lenses and gold film reflectors to maximize the use of the infrared portion of the solar spectrum. This provides the maximum thermal energy for the focal point processing and also provides for easy folding (stowing) and deployability. The small frontal area also minimizes the probability of a meteorite impact.

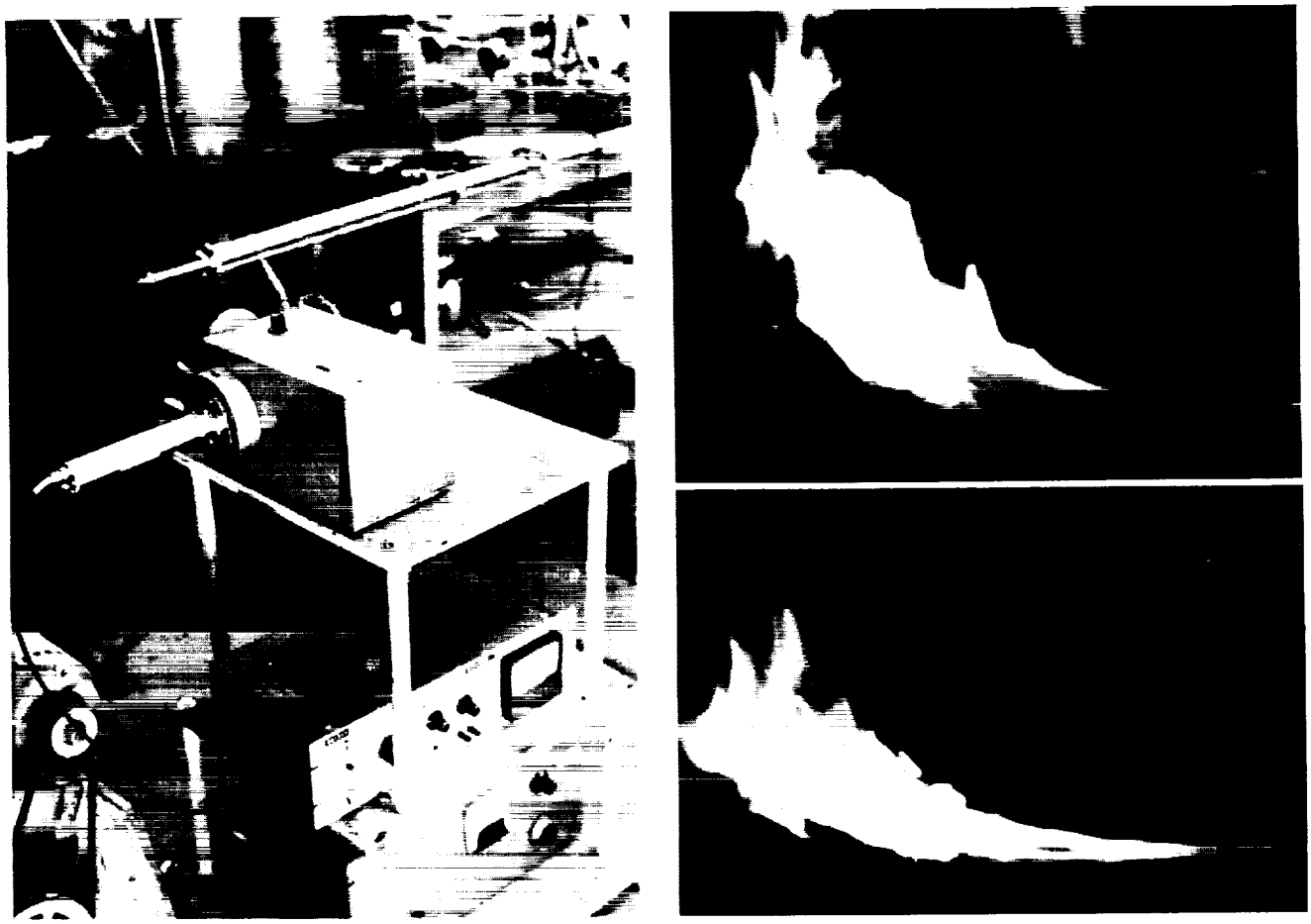

Fig. 5. Flame augmentation design for scramjets. The basic engineering design showing the flame exit (tube), the photomultiplier tube assembly, the scanner, amplifier and the radiation analyzer. The platform design is particularly noteworthy, and represents a self-locating aligner. Examples of two flames without and with the Free Radical donor injection.

A graduate student is currently being trained at JPL where the details of space-qualified hardware will be learned.

The fully operational hardware is expected to be developed by the end of the year (December, 1988). The automation, or autonomy, in operation will be the main theme of design engineering in 1989. The space qualification and space hardware use will take place in 1990 and the Getaway Special hardware will be tested and qualified in 1991.

In the minor program of NASP flame anchoring, an apparatus was designed for the identification of the key free radicals in open jet turbulent flames (Fig. 5). The apparatus concentrates the flame radiation to a photomultiplier tube and scans in the wavelength range of 3000 Å and 9000 Å. At the time of this report (May, 1988) strong signals were seen in the OH band as expected and in direct support of the earlier experiments at the University of Arizona that demonstrated augmentation of stability through donor injections. It is expected that the design of this apparatus will evolve to autonomously inject the chemicals to suit varying flight conditions of the scramjet engine.

ACKNOWLEDGMENTS

The authors are grateful to the entire staff of USRA for support. They are also thankful to Mr. James Burke of JPL for advice and help.

REFERENCES

1. Kessler D.J. Orbital Debris, NASA Conference Publication 2360, 1985.
2. Kessler D.J. Earth Orbital Pollution, *in Beyond Spaceship Earth*, Sierra Club Books.
3. Kessler D.J. Orbital Debris Issues, in *Advances in Space Research*, pp. 3-10, Pergamon Press, 1985.
4. *Sky and Telescope*, p. 213, September, 1986.
5. Ramohalli K.N.R. Autonomous Space Processing for Cleaning Space 'Junk,' NPO Item No. 6465 Docket No. 16951, April, 1986.
6. Romohalli and Cassidy. An Economical Space Processor for Orbital Debris Removal. XXXIX IAF Congress, October, 1988.
7. Schirmer A., Green J., and Ramohalli K. Experimental Augmentation of Turbulent Flames Through Free Radicals Delivered in situ, *Combust. Sci. and Tech. Vol 51*, 1987.
8. Winston R. and O'Gallagher J. *Optics in Nonimaging Concentrators*, Academic Press, Chicago, 1987.

DESIGN OF THE UNMANNED MULTIPLE EXPLORATORY PROBE SYSTEM (MEPS) FOR MARS OBSERVATIONS

AUBURN UNIVERSITY

The unmanned Multiple Exploratory Probe System (MEPS) is designed for Mars observations in preparation for manned missions to the planet early in the 21st century. MEPS will test vehicle systems, provide important data about the Martian surface and atmosphere, and assist the planning of manned missions. This mission will be a precursor to the manned missions. MEPS will consist of six primary systems. A Command Information Center (CIC) will be employed as an onboard mission control, communications link, and observation post. The Space Transportation Main Engine (STME) will be used to provide the thrust for Earth-Mars transit following vehicle construction near the Space Station. A polar lander/Orbital Transfer Vehicle (OTV) will be deployed during transit to achieve a polar orbit about Mars. A secondary propulsion will be used to place MEPS into orbit about Mars; this system and the aerobrake will circularize the orbit. Following orbit circularization, a satellite will be deployed to observe the Martian surface and atmosphere and to study the space environment. Polar and equatorial lander systems will land on Mars with rovers to collect surface and atmospheric samples while on-board laboratories will provide initial sample study. Two solid rocket booster/payload vehicles will launch samples into a low Mars orbit. The OTV will rendezvous with each payload capsule and then transfer the samples to Earth for hands-on observation.

INTRODUCTION

In August of 1987 the Ride commission presented to Dr. James Fletcher several recommendations for future NASA goals. One goal is very encouraging for the American space program—a manned mission to Mars by the turn of the century. However, just as Apollo required Ranger and Surveyor to lead the way to the Moon, any manned Mars mission will need precursor, unmanned missions to test vehicle systems, observe Mars for possible landing sites and probable dangers, and expand the current database initiated by Mariner and Viking. A design study into such an unmanned mission has resulted in the Multiple Exploratory Probe System (MEPS).

MISSION DESCRIPTION

Figure 1 presents the vehicle configuration for the MEPS mission while Fig. 2 shows the mission profile. Designed for modular construction, MEPS is composed of six primary systems—main propulsion, polar lander/OTV, secondary propulsion, command information center/satellite, equatorial lander, and aerobrake. With the exception of the aerobrake, each system is enclosed during interplanetary transport and descent to the Mars surface by a thin-walled cylinder supported by bulkheads and stringers. These cylindrical modules are 25 feet in diameter and will be completely constructed on Earth for transport to Low Earth Orbit (LEO) using Heavy Lift Launch Vehicles (HLLVs). The modules will be placed in an approximate 270-nautical-mile orbit near the operational Space Station while astronauts performing Extra-Vehicular Activities (EVAs) will assemble the vehicle. The modules will be joined using 5-foot connectors similar in design to the module enclosures; the aerobrake will be connected to the equatorial lander using a 10-foot connector. Specially designed pins using a tang and clevis composition will provide permanent attachments for the vehicle components. These pins do not require tools, thus minimizing EVA time.

One module is extremely important to the success of MEPS—CIC. The CIC is an onboard Mission Control; responsibilities include systems maintenance, data collection and processing, trajectory maintenance, guidance and control, propulsive burn control, and module deployment. Computers with some degree of artificial intelligence will be employed, using special flight software to accomplish all mission tasks. The CIC will provide the communications link between Earth and MEPS, and between several of the MEPS systems. Observation equipment will be located within this module for mapping of the Martian surface, measurement of the heat budget of Mars, and study of the space environment during transit and while in Mars orbit. A solar array panel and auxiliary rechargeable batteries will provide the required power for MEPS.

Once construction has been completed and all systems have been remotely checked by ground-based technicians and the CIC, MEPS will be moved to the ecliptic plane using orbit transfer vehicles (OTVs). A propulsive burn by the main engine will be employed to begin the Earth to Mars transit. The propulsion system used for departure is the STME. This engine is still under design, but is projected to be more reliable and cost-effective than the Space Shuttle Main Engine. Design

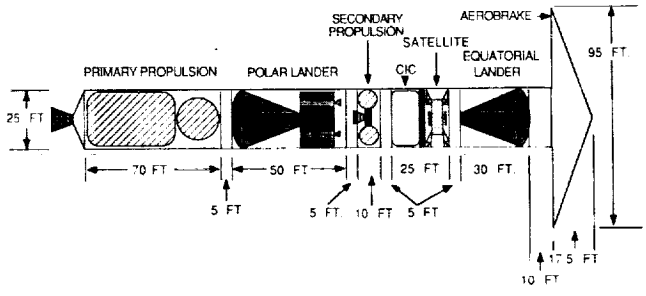

Fig. 1. MEPS Vehicle Configuration

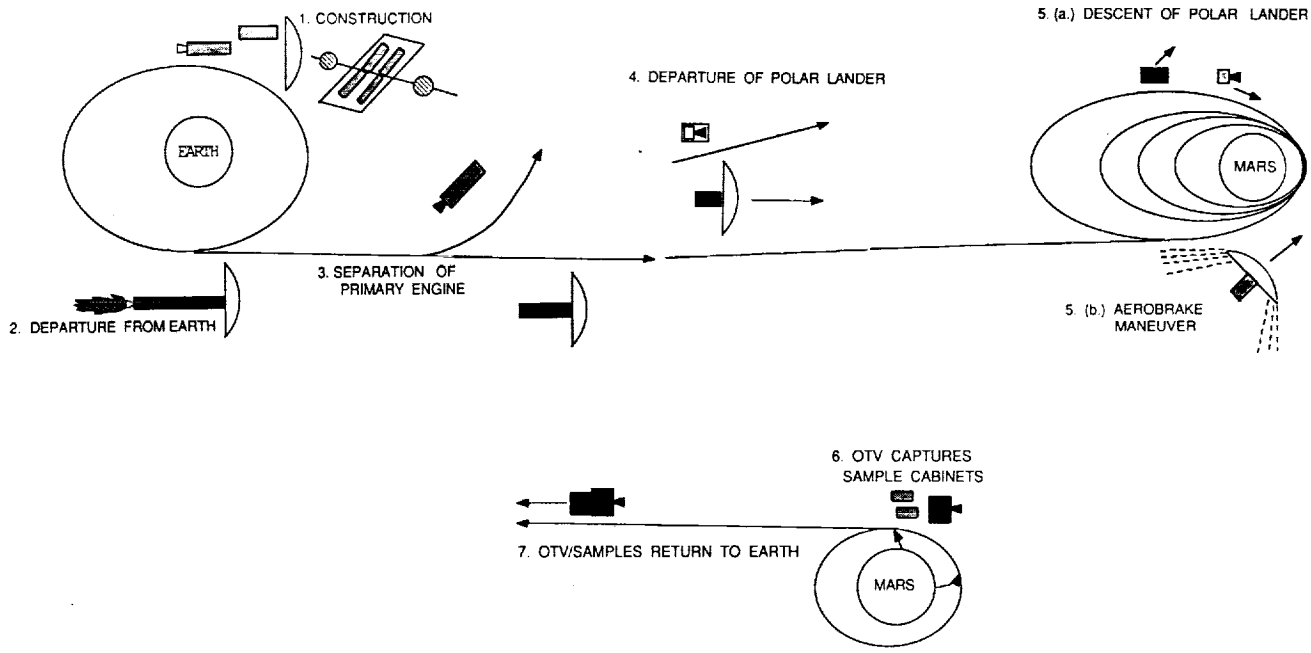

Fig. 2. MEPS Mission Profile

points include reusability, space applications, and space operation; liquid hydrogen and liquid oxygen will be used as the propellant[1]. Once the STME has put MEPS on the trajectory to Mars, the entire propulsion module will be released and deboosted into a high Earth orbit for retrieval and reuse.

The transfer has been analyzed using the patched-conic approximation, which accounts for an elliptic path between planets and a hyperbolic passage near the target planet. A Hohmann, or minimum energy, transfer will be used, requiring 285 days for transit.

At approximately the halfway point in the transfer the polar lander and an accompanying three-stage orbit transfer vehicle will be deployed. Following separation, this system will enter a trajectory for polar orbit insertion about Mars. Upon approach to Mars the first stage of the OTV will perform a burn to insert the system into an elliptic polar orbit.

The reasoning behind the separation at this point in the mission is the savings of weight. If the lander system were released from the vehicle after attaining orbit about Mars, a plane change of at least 60° will be required to transfer into a polar orbit. Since the magnitude of the propulsive burn is proportional to a trigonometric function of the inclination angle, the greater the angle the greater the burn, and thus the more fuel required. This maneuver not only requires more fuel, but also increased structure to support the extra weight during transit and aerobraking. By performing the maneuver during the transit minimum energy will be required because the plane change will be relatively small[2].

During transit of the polar lander the remainder of the MEPS vehicle will be approaching Mars at the nominal inclination. The first of four propulsive burns by the secondary propulsion system will be initiated to place MEPS into a high-eccentricity elliptic orbit about Mars. The propulsion system will consist of three engines using storable propellants; two of these engines are directed forward to retrofire for the first two burns and during braking. Following systems checks a second impulsive burn will be applied at apoapsis of the orbit to lower the orbit periapsis into the atmosphere. Upon approach of the periapsis the aerobraking will begin.

Aerobraking is the process of obtaining a circular orbit about a planet by gradually reducing the vehicle's elliptic orbit through atmospheric passage. MEPS will employ a 95-foot 70° right circular cone aerobrake for orbit circularization. The inner 25-foot diameter will be rigid and composed of graphite polyamide honeycomb and ceramic foam tiles. The remaining brake will be a flexible blanket of sheets of interwoven ceramic fibers alternated with ceramic felt filler[3].

A computer program was written to aid the aerobraking analysis. Using the assumptions of constant drag, which can be achieved by firing the secondary propulsion system, and constant atmospheric conditions at periapsis altitude, the program models the braking process for each orbital pass. At the desired periapsis altitude (51.8 nautical miles) the braking required to obtain a 270-nautical-mile apoapsis will take 21.9 days. When this apoapsis is achieved, the third propulsive burn will raise the periapsis out of the atmosphere to 270 nautical miles in order to circularize the orbit. If necessary, a final burn will be applied at the periapsis to adjust the apoapsis.

Following orbit circularization the aerobrake will separate and the CIC will prepare to deploy an observation satellite and the equatorial lander. The satellite is located within the CIC module to aid in systems maintenance. The satellite will be designed for a five year service life, using a solar array panel and rechargeable batteries for power. The satellite will employ

a payload assist module to achieve an observation orbit of 380 nautical miles. Experiment packages will allow surface mapping, observation of polar cloud cover and dust cloud/dust storm formations, determination of the water vapor and carbon dioxide distribution in the atmosphere, study of the distribution and temperature of atmospheric gases, and studies of the space environment to be performed. All data will be collected and stored within the satellite until relay to the CIC; the CIC will store the data until transmission to Earth receiving stations.

Following deployment of the equatorial lander from MEPS, and of the polar lander from the OTV, the two landers will enter the atmosphere. Using atmospheric drag, parachutes, and retro-thrusters, the systems will land safely on the martian surface. The two landers make up the Mars surface exploration system, which has been developed for two purposes: to obtain scientific data about the geology, atmospheric chemistry, and meteorology of Mars, and to carry soil, rock, and atmospheric samples back to Earth.

Two rovers are located in each lander, as well as an automated laboratory and a sample return vehicle. Each rover is designed with tracks for mobility, equipment for gathering samples, and artificial hardware and software for complete automation. The rovers will travel 0.3 miles per day, gathering samples and photographing the surface during its traverse. The Viking mission to search for life will continue, as well as obtaining core samples, seismometer readings, and geochemical and climate data. Adaptations of Viking systems will be used.

The rovers will return to the lander to unload samples. Some samples will go through laboratory processes such as biologic and organic experiments and spectrometer readings. Data will be stored before transmission to the CIC and, ultimately, to Earth. In addition, the transmission link can be used by Earth-based observers to override rover programs to send the rovers to any area of interest.

Robot arms will move canisters of samples from the rovers to the Sample Return Vehicle (SRV), a solid rocket booster with a payload capsule. The vehicles will launch from the landers and enter a low Mars orbit. The payload from the martian pole will rendezvous with the OTV; the second stage of the OTV will then provide the propulsive burn for the inclination change to the ecliptic plane. After both SRVs have been captured, the third stage will perform a burn to transfer the vehicle to Earth.

The time frame for MEPS is the late 1990s. Detailed analysis of the MEPS mission will continue until the early 1990s. Construction will begin soon after the Space Station becomes operational (approximately 1995) and will require 2.5 years. The initial transfer burn is scheduled to take place in late 1998, MEPS will arrive at Mars in September 1999, and the samples will return to Earth by 2001. The rovers, satellite, and CIC will continue operations as long as possible.

CONCLUSIONS

Unmanned systems have always been used to forge a path for manned missions. The multiple system design of MEPS will allow maximum collection of data concerning all phases of a Mars mission during a single trip. The success of MEPS will ensure success of the manned Mars missions of the early 21st century.

REFERENCES

1. McNeely R. Professional Engineer, Preliminary Design, Propulsion Group, Marshall Space Flight Center, Huntsville, Alabama. Personal communication.
2. Cicci D.A., Ph.D. Professor, Aerospace Engineering Department, Auburn University, Auburn, Alabama. Personal communication.
3. Willcockson W.H. OTV Program Manager, Martin Marietta-Denver Aerospace, Denver, Colorado. Personal communication.

THE SPACE STATION INTEGRATED REFUSE MANAGEMENT SYSTEM

UNIVERSITY OF CENTRAL FLORIDA

The University of Central Florida's design of an Integrated Refuse Management System for the proposed International Space Station is addressed. Four integratable subsystems capable of handling an estimated Orbiter shortfall of nearly 40,000 lbs of refuse produced annually are discussed. The subsystems investigated were (1) Collection and Transfer, (2) Recycle and Reuse, (3) Advanced Disposal, and (4) Propulsion Assist in Disposal. Emphasis is placed on the recycling or reuse of those materials ultimately providing a source of Space Station refuse. Special consideration is given to various disposal methods capable of completely removing refuse from close proximity of the Space Station. There is evidence that pyrolysis is the optimal solution for disposal of refuse through employment of a Rocket Jettison Vehicle. Additionally, design considerations and specifications of the Refuse Management System are discussed. Optimal and alternate design solutions for each of the four subsystems are summarized. Finally, the system configuration is described and reviewed.

INTRODUCTION

Accumulation of refuse is merely a minor inconvenience in everyday life. From a macroscopic viewpoint, this problem has become significantly greater in proportion to increases in population. Moreover, refuse collection, recycling, and disposal for the purposes of a permanently manned Space Station is a virtually unexplored problem. Until now, there has been no real need to study the waste problem for space missions due to the limited duration of operations and payload capabilities for returning relatively small amounts of waste back to earth. Because the Space Station is to be a permanent, multipurpose facility, there exists a need to address the refuse problem in a "comprehensive, long-range resource management framework"[1].

The potential Space Station refuse problem has been estimated considering a waste return requirement of approximately 120,000 lbs/yr and a shuttle return capability of about 80,000 lbs/yr[2]. The difference between the return requirement and the Shuttle return capability highlights the magnitude of this overwhelming problem. Nearly forty-thousand pounds of excess refuse will accumulate over the first year of manned operation[3]. If the shuttle alone is to be relied on to remove Space Station refuse, then its payload capacity during its return to Earth will be entirely utilized for the transportation of refuse to the detriment of other payload requirements. Simply stated, the Space Shuttle's return capacity will fail to accommodate the annual buildup of refuse on the Space Station. This consequence may be unavoidable "unless an orbit waste processing reuse-recycle and other alternatives to Shuttle deorbiting are implemented"[1]. It must be noted that available Space Station refuse data are based on hypothetical conditions and are therefore only estimates[1]. Nonetheless, the needs of Space Station require the development of an effective and efficient refuse management system tailor-made for the space environment.

REQUIREMENTS

System Specifications

The Space Station Integrated Refuse Management System (SSIRMS) involves the control of generation, storage, collection, transfer, processing, and disposal of refuse that is in accord with the best principles of public health, economics, engineering, conservation, aesthetics, and other environmental considerations. To this end, techniques must be developed to satisfy the crew and laboratory refuse accumulation, and which, in addition, interface with the Space Station's various subsystems. The system must accommodate the accumulation of a range of diverse waste materials. Hard plastics, metals, papers, pharmaceuticals, ceramics, ball bearings, and semiconductor waste products were considered in the system design. Power requirements were kept to a minimum. Automation was deemed to be a driving factor in eliminating unnecessary crew involvement. Finally, much attention was given to the performance requirements of refuse collection and transfer, sanitization and disposal, and the associated propulsion and power systems.

System Profile

The Space Station Integrated Refuse Management System has been designed to successfully reuse or dispose both biologically active and inactive materials. In accordance with NASA Standard 3000, the treatment of metabolic bodily wastes was excluded from the yearlong study. To facilitate the monumental task of addressing all aspects of refuse management, four design areas have been defined. To fulfill the mission of recycling or reusing refuse on the Space Station, the task of successfully making use of any existing potential energy or material properties that refuse may possess was established. The second area of concern dealt with the collection and

transfer of all materials to either be reused or completely removed from the station environment. Third, design of an expendable jettison vehicle for refuse containment and transport out of close proximity of the Space Station was conducted. Lastly, numerous jettison vehicle launch scenarios were analyzed. Selection of a proper disposal site and the development of a system to propel the vehicle to that site were completed.

The SSIRMS has been designed with both the existing technology of the 1980's and the assumed technology level that will have been developed through post-initial operating capability of the Space Station.

CONFIGURATION DESCRIPTION

The first step in any refuse management system (Fig. 1) is that of collection and transfer. The design of a Space Station subsystem capable of collecting and transporting refuse from its generation site to its disposal and/or recycling site was accomplished. Refuse canister transport, receptacle designs, storage systems, and power supply were among the topics researched. The subsystem design selected is of a multi-disposal site configuration. Each site contains a compactor, access to the transfer flow path, and a supply of bags, labels, and capsules. Materials research warranted the use of high density polyethylene bags to be placed sparsely throughout the modules and within the compactors for convenient waste disposal. Following compaction and evacuation of the refuse, the packages are manually inserted into cylindrical capsules constructed of polypropylene. The capsules are then introduced to a special transfer system referred to as the "bank shuttle network." The network, similar to those used in commercial bank applications, can be used to transport capsules to an external storage, recycling, or disposal facility. Airflow in the bank shuttle system will be generated by a blow-motor vacuum pump which receives power from solar panels placed along the Space Station structure. In the event of a power failure, hand pumps will be available at each of the waste handling facilities. A selected storage design consists of an exterior rack unit to house excess refuse generated from any of the proposed multi-disposal site arrangements. General sanitization, airborne, and surface contaminant control were addressed. Combinations of room arrangement, microbiological filtration, and application of germicidal vapors and gases

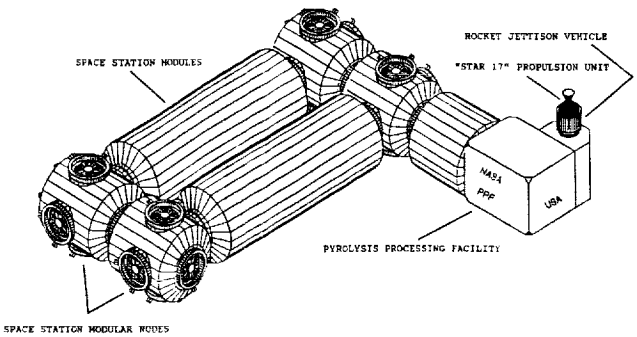

Fig. 1: Space Station (partial view) with proposed waste recycle facility and jettison vehicle.

were employed for an optimum solution. Focus was also placed on inventory control which incorporates the use of color coding and bar coding to maximize simplicity and automation, respectively.

The objective of producing a technically self-supporting recycle/reuse system led to the design of the Pyrolysis Processing Facility (PPF). Pyrolysis is the destructive distillation of a carbonaceous material in the presence of heat and the absence of oxygen. The facility is composed of (1) refuse size reduction, (2) pyrolysis reactor design, and (3) power generation.

Before implementing the pyrolysis process, it is necessary to first reduce the size of the refuse which will in turn increase the efficiency of the system. A number of refuse size reduction concepts were evaluated with respect to overall system performance. Reduction devices such as hammermills, wet pulpers, rasp mills, grinders, and shredders were investigated. The chosen shredding device is composed of diametrically-opposed, counter-rotating blades that are self-cleaning and have the ability to reject materials that would otherwise damage or shut down the system. Previously developed by Foster-Miller Associates, this unique shredding system shows great promise based on results obtained during extensive testing for microgravity applications.

Analysis of pyrolysis reactor designs included, but were not limited to (1) fluidized bed, (2) rotary kiln, (3) hot wire, and (4) cyclonic entrained-flow devices. Virtually all of the pyrolysis reactor designs are extremely efficient, pyrolyzing up to 96% of the refuse material introduced. The optimal design selection is the cyclonic entrained-flow pyrolysis reactor. This device involves a very high throughput reactor in which refuse particles are introduced into a cyclone or vortex tube at high velocities. The circular wall area of the cyclone is externally heated and the particles follow a spiral path through the reactor. The constant contact with the thermally activated wall combined with the high velocity of the particles make this an efficient and complete pyrolyzing process. The reactor is ideal for space applications. Problems resulting from a lack of gravity will not be a factor as the reactor creates its own gravitational environment. Innovative reactor design has reduced temperature requirements from 1500°C to 600°C. This reduction in temperature also leads to a reduction in power generation requirements.

Research has indicated that power allotments on the Space Station have nearly been exhausted, and the availability of any "excess" power will be scarce at best. It is for this reason that power generation was included as a major design aspect. Several power generation systems were considered to supply power to the PPF. The systems include (1) hybrid electrical, (2) modular radioisotope thermoelectric, (3) heat pipe Rankine, (4) thermionic, and (5) electrostatic parametric power generation. Analysis of the possible solutions has indicated that a combination of an electrostatic parametric generator coupled with a heat pipe Rankine cycle will best meet the requirements of supplying power to the Pyrolysis Processing Facility.

The objective of removing refuse from the Space Station environment subsequent to recycling was fulfilled with the

design of an expendable jettison vehicle. The primary design goal concerned the safe containment of refuse while the vehicle is docked at the Station. A second goal was to insure prompt destruction of the vehicle and its contents upon reentry into the Earth's atmosphere. To undertake such a mission a vehicle was designed which employs a rigid, aluminum alloy cylinder to be launched via an expendable rocket. The vehicle will be assembled and mated with its propulsion unit on Earth. It will then be placed into low Earth orbit, be retrieved by an orbital maneuvering vehicle, and placed into its desired location on the Space Station. The vehicle designed is 4.5 feet in diameter and 3.5 feet in length. The interior features pigeonhole storage racks that will accommodate six canisters of compacted refuse. Studies of worst case scenarios describe the need for a maximum of ten vehicles annually. In addition to vehicle design, debris casualty risks and environmental effects associated with atmospheric reentry were investigated.

PROPULSION SYSTEM DESIGN AND INTEGRATION

To insure prompt destruction of the jettison vehicle, designs for the propulsion system and for vehicle integration were required. Additionally, the selection of a proper disposal site for the vehicle and its contents was of utmost concern. Four major disposal sites were researched in detail. These sites are (1) the sun, (2) the Moon, (3) the Earth-Moon libration points, and (4) the Earth's upper atmosphere. Propulsion systems and launch scenarios for each of the four sites were evaluated. Of the candidate systems, reentry into the Earth's atmosphere for refuse incineration was determined to be the most attractive solution. Propulsion for the vehicle was selected in accordance with mass limitations and the total change in velocity requirement of 280 ft/sec. Interfacing a Morton Thiokol Star 17 expendable rocket to the jettison vehicle will optimally provide the propulsion/disposal system. The assembly is referred to as the Rocket Jettison Vehicle (RJV).

Preliminary studies cited the need for transporting numerous RJV's to the Space Station via the Orbiter fleet. To alleviate any dependence on the Shuttle, the project scope was broadened to encompass a range of expendable launch vehicles (ELVs) for the sole purpose of transporting RJVs to the Space Station. The Titan 3 commercial rocket was selected to complete this task. Subsequent to filling an RJV with compacted refuse, either an orbital maneuvering vehicle or a proposed cold gas system would remove the RJV from close proximity of the Space Station. It would then initiate spin with proper launch attitude. Finally, the launch of the Star 17 rocket, which incorporates guidance and navigation controls, will deliver the refuse payload into the upper atmosphere to achieve complete destruction within one low Earth orbit.

ECONOMIC ANALYSIS

Cost is a major determining factor in most decision making models. Cost goals for the Refuse Management System included the investment cost of human and material resources for design preparation, construction, enplacement, and maintenance. Incremental and marginal benefits associated with changes beyond a base level or reference design were used in this study due to the problem of choosing between several viable alternatives. Because the project was based on a current technology level, relatively accurate cost estimates could be made. For example, Shuttle launch costs are approaching $5,000/lb. Thus, 40,000 lbs of refuse equates to $200 million in Shuttle launch costs to Low Earth Orbit per year. Use of the Titan 3, as opposed to the Shuttle, will cut launch costs approximately in half. Cost comparisons such as these ranked second among all design considerations for the yearlong study. Crew safety was rated highest.

CONCLUSIONS AND RECOMMENDATIONS

The Space Station Integrated Refuse Management System is capable of handling the projected Orbiter shortfall of approximately 40,000 lbs of refuse annually. The SSIRMS consists of four integratable subsystems that will minimize contamination risks, crew involvement, and dependence on the Shuttle for refuse management.

The Collection and Transfer subsystem is designed to be as automated as possible requiring only that the crew place waste into bags and activate switches which cause the collection and transfer process to begin. The subsystem was designed to provide for a contamination-free environment, yet in the event of a possible contamination occurrence, workstation isolation would prevent the spread of contaminants.

Equipment suggested for use in the design has been previously manufactured or has been determined to be highly feasible to construct. Because of the availability of the needed hardware, the cost of the subsystem design should be relatively low in comparison to alternative waste management systems.

To completely integrate the Collection and Transfer design with the remaining subsystems, further study is recommended in the areas of (1) component dimensions, (2) costs, (3) alternate means of canister transport, and (4) subsystem weight.

The design of a self-supporting Pyrolysis Processing Facility was achieved. The facility consists of a shredder system, a cyclonic entrained-flow pyrolysis reactor, and a hybrid power generating system. Recommendations include the need for an in-depth computer study to determine the relative merit of pyrolysis oil as a rocket fuel, and the need for a detailed cost analysis.

In terms of the complete disposal of Space Station refuse, it was concluded that a jettison vehicle would provide the means for transporting wastes to a fiery destruction in the Earth's upper atmosphere. Further investigation is recommended in the areas of (1) orbital mechanics, (2) prototype vehicle development, and (3) vehicle testing under simulated launch conditions.

Low cost and ease of operation make the delivery of the Rocket Jettison an attractive choice for Space Station refuse management. While paper, plastics, and other incinerable materials have negligible environmental effects on the Earth,

hazardous materials and heavy metals may justify the need for an alternate disposal site. For now, research has shown the Moon to be the best alternate and redundant site.

It is concluded that the transportation of cargo should be accomplished using unmanned vehicles such as the Titan. Also, assembly on Earth of the RJV system proves economical and practical. Extensive extra-vehicular activity and sophisticated attachment design would consequently be eliminated.

Above all, an environmental impact study should be performed to predict the consequences of sending refuse through the atmosphere or to any alternate site. The incorporation of guidance controls, artificial intelligence capabilities, and spin tables needs to be addressed. Further research concerning the availability of alternative off-the-shelf rockets to interface with the required performance parameters should be pursued.

REFERENCES

1. Rasmussen, Johnson, Bosley, Curran, and Mains. *OSSA Space Station Inventory*, NASA Publication, NASA Ames Research Center, CA., January 1987, pp. 3-7.
2. *Space Station Trash Disposal Using Tethers*, Marshall Space Flight Center Study, February 1987.
3. Brunner, Calvin. *Incineration Systems*, Van Nostrand Reinhold Company, Florence, KY., 1984.

DESIGN AND MANUFACTURE OF SOLID ZrO_2 ELECTROLYTE

CLEMSON UNIVERSITY

BACKGROUND

Oxygen anions in cubic zirconia (zirconia stabilized in the cubic phase by small additions of CaO, MgO, or Y_2O_3) diffuse very rapidly through the zirconia crystalline structure. This is because these additions create oxygen vacancies. (Oxygen vacancies are places in the zirconia crystal structure which would ordinarily be occupied by oxygen anions if the zirconia were pure. These places are empty in the impure stabilized zirconia structures.)

An electric field will "pump" oxygen from one side of the electrolyte to the other. A negative electrode will donate two electrons to an oxygen atom, thus creating an oxygen anion. The electric field then pushes this anion toward the positive electrode on the opposite side of the solid electrolyte. When the oxygen anion reaches the positive electrode, it loses the additional electrons and becomes an oxygen atom again.

These processes are most efficient in electrolytes which are actually very thin membranes. The challenge is to produce thin continuous membranes which are strong enough mechanically to withstand the pressure differential across the membrane. A high ratio of surface area to thickness is also desirable. It is also important that the material be leak proof. Molecular gases must not be able to diffuse through the electrolyte.

Several universities at the NASA/USRA Third Annual Summer Conference reported that they would build systems which would decompose CO_2 gas in the martian atmosphere. (For example, see *Mars Oxygen Demonstration Project Design Summary Report*, Joseph A. Verne, Old Dominion University, 1987.) An essential component of these systems was a solid yttria stabilized zirconia (YSZ) electrolyte cell. Discussion with these universities revealed that optimizing the design of such an electrolyte was highly desirable but there was relatively little commercial interest in doing so. Thus, the design and fabrication of such an electrolyte would be a challenging and worthwhile project for ceramic engineering students at Clemson University.

PROJECT ASSIGNMENT

The following project assignment was given to the students: "Design and build a suitable YSZ solid electrolyte cell. Describe advantages of the design and fabrication method. Finally, to the limits of available resources, fabricate the design. Explain why it would be superior to other designs."

CONDUCT OF CERAMIC ENGINEERING 425/625

The basis of this class was a lecture and laboratory combination. The first few sessions dealt with zirconia, the structure of zirconia, and how to stabilize zirconia.

It is very important that the engineering designer knows how his project fits with the rest of the project. For this reason, the class spent considerable time studying the conditions on the martian surface. The necessity of having an oxygen generating apparatus to take on a mission to Mars soon became obvious. Students were encouraged to review reports generated by Old Dominion University.

The class formed into teams, each having three members. Each team submitted a progress report every two weeks, with occasional oral reports. The whole class met to trade information on fabrication techniques and where to find various supplies.

Each team showed evidence of experimental work by presenting the results of attempts to form a cell that the team had designed. The team that submitted the best design presented its report at the Fourth Annual Summer Conference, held in Cocoa Beach, Florida. Summaries of the five teams follow.

EXTRUSION

Extrusion is similar to squeezing toothpaste from a tube. Ceramic material with a clay-like character is placed in a cylindrical chamber and squeezed out through holes in a die at the end of the chamber. In this case, the plastic material is a ceramic powder-water mixture with minor additions of binders.

Ceramic engineers use extrusion for forming intricate thin wall tubes for catalyst supports. There are several commercial companies with the technical expertise to make thin walled multicell tubes. Tubes such as these could satisfy the requirements of the solid electrolyte configuration very well. Unfortunately, the expertise for forming these tubes is proprietary and not obtainable from open literature.

Raw Materials

Reactive alumina
A-152 (Alcoa Chemicals) alumina
Partially stabilized zirconia (TX-3Y, Toya Soda)
Stabilized zirconia (Tosoh)
Methocel binder (213-3O, Dow Chemicals)
A-152 alumina

Actual Success

This group found that the extrusion process was already performed commercially. The group concentrated on establishing the important parameters necessary to form the solid electrolyte material.

Because of the expense of YSZ, this group experimented mainly with alumina and learned that the following parameters were important if they were to obtain uniform results:

1. A wide range of particle sizes must be present.
2. Pressure in the extrusion chamber is important.
3. A binder is necessary to give the unfired material strength.
4. Other agents are necessary to regulate plasticity.
5. The drying very slowly and carefully is essential.
6. Firing carefully in order is necessary to prevent cracking.

Comments

The extrusion process is a very strong candidate for making complex solid electrolyte tubes. With enough money, several companies could become interested in producing a satisfactory product without much further research.

SLIP CASTING

Slip casting is the common method for forming vases and "art pottery" in ceramic shops. A slip is a creamy mixture of ceramic powder, water, and other additives. The additives keep the ceramic powder in suspension and modify the flow properties of the mixture. The slip casting process consists of pouring the slip into a porous mold (usually plaster) and waiting until a leathery "skin" of material has formed on the mold surface. When the "skin" is thick enough, the remaining slip is poured out of the mold. The material remaining in the mold must lose some of the fluid. After the skin has dried sufficiently, it becomes more rigid and shrinks away from the mold surface.

Raw Materials

Reactive alumina
Partially stabilized zirconia (TX-3Y, Toya Soda)
Stabilized zirconia (Tosoh)
Ethanolamine (for rheology adjustments)
Polyvinyl alcohol (PVA) binder
Methocell
Cellulose ether

Actual Success

This method of forming ceramic shapes is a traditional method. Consequently, ceramists have extensively studied slip casting and can easily make simple shapes to close tolerances. The shape proposed by this group was not simple, however, and difficulties arose because of cracking. The group also encountered difficulty when trying to separate the shape from the plaster mold.

The group finally succeeded in reducing the cracking. This was accomplished by grinding the zirconia for several hours in a ball mill. The slip became thixotropic and the wall thickness of the finished cell became uneven as a result.

Comments

The slip casting process has a great deal of potential for producing a cell. Proponents of slip casting, however, must successfully overcome the problems of uneven casting and cracking. These problems are solvable, however, and slip casting is a possible means for producing these cells.

TAPE CASTING

Tape casting is a primary method for forming long, flat, extremely thin "tapes" of ceramic materials. The process uses a slurry of ceramic powders, binders, plasticizers, and dispersants,combined with a nonaqueous solvent. A device (doctor blade) spreads this slurry on a surface where the solvent evaporates. The result is a very thin, flat, flexible layer of mostly ceramic powder which on firing becomes a hard ceramic material.

The advantage of this process is the ease of producing very thin ceramic shapes, which are very desirable for this project.

Raw Materials

Polyvinyl butyral (binder, Butvar 98)[2]
Menhaden fish oil (deflocculant)
325-mesh alumina
Fine alumina powder
Submicron alumina
Toyo Soda zirconia
Octyl phthalate (plasticizer, Santicizer 160-Monsanto)
Polyethylene glycol (plasticizer)
Ethyl alcohol (solvent)
Trichloroethylene (solvent)

Actual Success

Tape casting has been a traditional "high tech" ceramic manufacturing process. It requires sophisticated control and is a more complicated manufacturing process. The potential for manufacturing uniformly smooth, flat, precisely dimensioned plates makes this extra effort very cost effective.

This group was probably the most successful of all the groups in the class. In fact, we intend to perfect this process for manufacturing ZrO_2 electrolytes in future classes. A significant finding by this group is that the green tapes are capable of being "glued" together into a more complex shape. This finding will make tape casting even more attractive. This process will likely be more successful than the others in producing a desirable cell. This group represented Clemson at Cocoa Beach in June, 1988, because of their success.

SOL GEL

The sol gel technique is the most recently developed of any technique tried by this class. The group tried to form monolithic plates of yttria stabilized ZrO_2 by causing an organometallic salt of Zr (zirconium n-propoxide) dissolved in

2-propanol (propyl alcohol) to hydrolyze. The group also tried other materials such as zirconium acetate dissolved in H_2O.

The main idea of the sol gel technique is first to form a gel of zirconium oxide together with the stabilizing oxide (yttria, calcia or magnesia). Next, the water is removed from the gel and the dehydrated gel is fired to form a solid ceramic material. The advantage of this technique is that it forms a chemically homogeneous, fine-grained, reproducible material.

Raw Materials

2,4 Pentanedione
2-Propanol
Calcium hydroxide
Concentrated nitric acid
Diacetin
Distilled water
DMF
Hydrochloric acid (optional)
Yttrium nitrate
Zirconium acetate sol
Zirconium n-propoxide

Actual Success

In contrast to some of the other techniques, the sol gel process is relatively new. The group was actually able to make thin membranes by this technique. Note, however, that the degree of control was not as good as the tape casting process. The group gained experience with differing mold surfaces. At first, the specimens cracked when the group tried to dry them. The group partially overcame this problem by using various drying additives.

Comments

This technique may merit further study if it is found that ultra-fine grain size is desirable. Unfired pieces made from this material may be difficult to handle.

INVESTMENT CASTING

Investment casting as described here, refers to using a disposable mold. Substances which either evaporate or quietly oxidize at high temperatures are materials possibly suitable for making molds. Plaster and similar materials may partially decompose, thereby reducing to a powder. These are also satisfactory in some cases.

It is important that the products of decomposition or combustion not affect or contaminate the ceramic materials. Also, swelling or excessive thermal expansion can lead to cracking of the part.

The objective is to form the ceramic part in the mold. The unfired part remains in the mold during the firing process. The mold either disintegrates or disappears during the firing process, leaving the ceramic part free.

Raw Materials

Acetone
Aluminum Oxide
Carbon steel furnace electrode (mold material)
Darvon C
Distilled Water
Methylcellulose
Plaster (mold material)
Polyvinyl alcohol (PVA)
Yttria (12 mol.%)stabilized zirconia

Actual Success

This group was hampered because investment casting depends on very many factors, especially impurities in mold materials. Interfacial tension between the mold materials and the ceramic slip is strongly materials dependent. It is often dependent on low impurity levels in one of the materials. In spite of all this, the group actually fabricated some tubes and geometric shapes by this method.

Comments

Investment casting as a technique requires further development than the other techniques addressed by the class. There needs to be much more control over the process before investment casting is a practical process.

SUMMARY

Clemson University students definitely benefitted from this experience with USRA/NASA. The challenge that this project gave the students was both exciting and attention-getting. Students spent far more time per credit hour on this project than on their other courses.

This project advanced the art of making efficient oxygen generators as well. Clemson students are now well on the way to designing a solid electrolyte with a large active surface area and comparatively small volume. Previous devices have had to endure the limitation of using only simple shapes such as tubes. The results of this project have demonstrated that better configurations are not only possible but practical.

N93-71989

THE DEVELOPMENT OF A CISLUNAR SPACE INFRASTRUCTURE

UNIVERSITY OF COLORADO, BOULDER

The primary objective of the University of Colorado Advanced Mission Design Program is to define the characteristics and evolution of a near-Earth space infrastructure. The envisioned foundation includes a permanently manned, self-sustaining base on the lunar surface, an L1 space station, and a transportation system that anchors these elements to a low Earth orbit (LEO) station. The motivation of this project was based on the idea that a near-Earth space infrastructure is not an end but an important step in a larger plan to expand man's capabilities in space science and technology. The presence of a cislunar space infrastructure would greatly facilitate the staging of future planetary missions, as well as facilitating the full exploration of the potential for science and industry on the lunar surface. This paper will provide a sound rationale and a detailed scenario in support of the cislunar infrastructure design.

LIST OF ACRONYMS

CELSS: Controlled Ecological Life Support System
ECLSS: Environmentally Controlled Life Support System
EPOTV: Electric Propulsion Orbital Transfer Vehicle
ESA: European Space Agency
EVA: Extra-Vehicular Activity
FRG: Federal Republic of Germany
GEO: Geosynchronous Earth Orbit
GNP: Gross National Product
HEO: High Earth Orbit
HPV: Human Powered Vehicle
L1: Libration Point between the Earth and Moon
LEO: Low Earth Orbit
OMV: Orbital Maneuvering Vehicle
OTV: Orbital Transfer Vehicle

INTRODUCTION

Recently, both the National Commission on Space report and Dr. Sally Ride's report to the NASA Administrator have advocated returning to the Moon. The University of Colorado Advanced Design class undertook an evaluation of how such a mission might evolve. The primary goal was to define the evolution of a near-Earth space infrastructure having manned lunar activities. The approach was to be programmatic and was to avoid Apollo-like, highly-focused, technology demonstration characteristics.

A multiphased program was developed by grouping mission activities within levels of increasing infrastructure support. The activities include those conducted in orbit, as well as those performed on the lunar surface. When defining mission scenarios, weighted consideration was given to the economic feasibility, flexibility, scientific interest, safety, and required hardware of these missions. A preliminary design of key components and/or systems of the infrastructure are presented.

It was desired that each phase of the program based on clear, supportable rationale. A set of metrics was developed to evaluate continued program growth. Predetermined breakpoints provided for program evaluation. Additionally, the impact of such a program and associated space infrastructure on the nation's economy was assessed.

INFRASTRUCTURE

An infrastructure is traditionally defined as "the basic facilities, equipment, services and installations needed for the growth and functioning of an organization" (*The American Heritage Dictionary*). Examples of such an infrastructure are found in the highway systems, the railways system, and the detailed network by which goods and services are distributed throughout this country. In today's society, the facilities, equipment, and services are taken so much for granted, that the infrastructure has become virtually transparent. It is not until a disaster or crisis occurs that the infrastructure becomes visible. Natural disasters such as floods, tornados, and earthquakes often disrupt portions of our infrastructure. The oil embargo of 1973 disrupted a major supply line that was a large part of the oil distribution infrastructure. Gas prices rose dramatically as the United States was forced to look elsewhere for oil. This example illustrates the importance of a strong infrastructure. Certainly prices increased, but the oil distribution infrastructure was flexible enough to continue to operate throughout the crisis. The embargo did not result in a complete halt of the country's oil-dependent activities. The infrastructure ensured a certain degree of programmatic safety. It allowed a parallel or alternative progression of events. This was opposed to a situation where there is little infrastructure and where critical services are completely lost in times of natural disaster.

A space infrastructure provides a sort of "scaffolding" in anticipation of future program expansions. Development of a sound infrastructure for the space program will provide the foundation for the future development and exploration of space. It is necessary to build this infrastructure so that it may be the foundation from which future space activities can flourish. The infrastructure must be capable of expanding to adequately support innovative and more technologically advanced missions than are presently imagined. Historically, it has been shown to be difficult to predict scientific breakthroughs or their implementations, but it has been possible to show that all of these things occur only when the infrastructure is capable of supporting them. Thus, a space infrastructure program should be developed which will promote unexpected advances and that will allow all the benefits of these advances

to be realized. The thesis developed herein highlights a space program founded on an infrastructure basis that will be strong, cost efficient, and most importantly, flexible.

RATIONALE

The United States and the Soviet Union are no longer the only nations with strong space programs. Western Europe, Japan, China, and India each participate in space-related activities. American successes such as Apollo, Titan, Saturn, Voyager, Skylab and the Space Shuttle are being overshadowed by names from other nations, such as Soyuz, Ariane, Energia, Vega, Mir and Hermes. Without the development of a near-Earth space infrastructure, the United States could soon lose its historic stature as a leader in space technology. Similar occurrences could happen in other technological arenas. Consequently, the United States and specifically NASA's expertise may one day be no longer in demand.

The University of Colorado Advanced Design Program proposes a near-Earth space infrastructure consisting of a lunar base, a manned L1 space station and a fleet of associated transportation vehicles. A near-Earth space infrastructure has the potential to generate great economic and scientific returns, as well as less-tangible benefits such as increased national pride and greater American stature in world politics. It is expected that a near-Earth space infrastructure would be beneficial to the future of the United States by providing a degree of economic return similar to that attained by the Apollo program. An American presence in Earth orbit would advance research in areas such as Earth studies, materials processing, and variable gravity experiments, as well as astronomy and solar studies. Although the direct benefits of a space initiative are difficult to assess, the United States must make an investment now in the technological future offered by space. The U.S. has exhausted many of the advantages gleaned from the infrastructure put into place by previous generations. It is time to build the infrastructure from which the United States of the 21st century will flourish. This investment will aid America in maintaining leads in science, technology and industry.

METHODOLOGY

The evolution of the proposed infrastructure is illustrated in Fig. 1. This preliminary scenario timeline consists of specific mission target dates that can accommodate changes depending on both funding and available technologies. The timeline is subject to any initial delays dependent on the date of program initiation. The infrastructure development program is checked periodically by means of breakpoints. These breakpoints, or milestones, are used to evaluate the progress and success of the program. Additionally, they will establish a series of questions that will drive the future of the program.

The evolution of the program is controlled by four goals. These goals relate to safety, cost, mission efficiency and program evaluation. The grouping of mission objectives into phases that require similar levels of infrastructure support is optimized using these goals and expected levels of available technology.

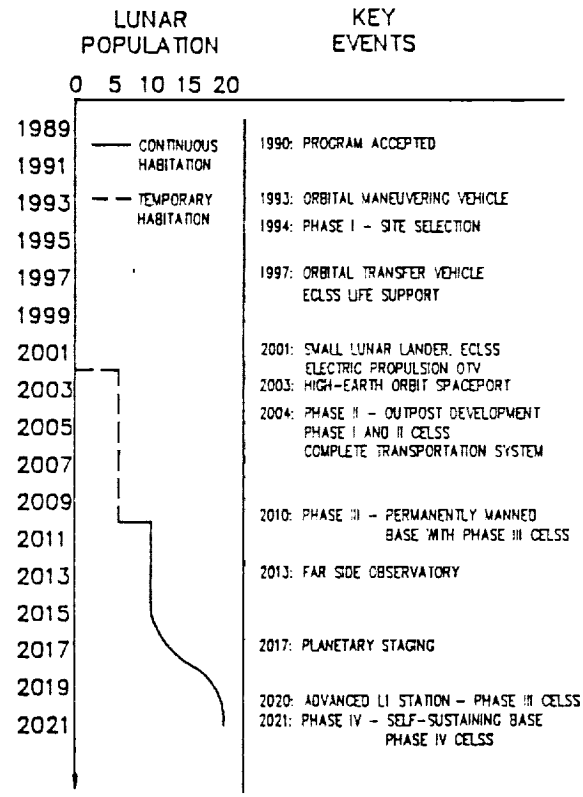

Fig. 1. Timeline

The first goal is to maximize human safety. This is addressed by minimizing transit times between destinations, by providing adequate radiation protection against solar flares, and by maximizing the use of automation and robotics to reduce risks to humans. Cargo will be transported without human crews. As the number of human missions increases, the infrastructure will enhance human safety by providing a safe haven and resupply depot in the lunar vicinity at an L1 space station

The L1 station provides for greater flexibility within the transportation infrastructure. For example, emergencies on the Moon could receive assistance from the L1 station in approximately one day. Assistance from LEO would take almost four days.

Low cost is the second goal. Incorporation of previously designed space hardware, such as that proposed for use on a LEO space station will help reduce program costs by eliminating additional research and development costs. Recycled hardware will minimize acquisition costs. The L1 transportation node reduces overall transportation costs by providing a staging point near the Moon. This location was chosen to minimize overall ΔV expenditures. It also allows the consolidation of crews and cargos in order to reduce overall transportation activities and costs. Electric propulsion cargo vehicles take advantage of low propellant usage to further reduce operating costs.

The development timeline of the infrastructure was scheduled using a reasonable, yet aggressive and ambitious policy. This provided realistic dates for breakpoints while minimizing cost overruns which might occur if (for example)

a contractor fell behind in development or production schedules. Funds will be committed on a phased basis. This reduces the financial investment for any given phase. Overall funding cost effectiveness should make follow-on program funding more attractive for congressional approval.

The infrastructure was designed in an open-ended manner. The inherent flexibility enables the continuance of a project should it experience a setback. Open-endedness means that a failure becomes merely a decision point and not a dead-end. The most important characteristic of an open-ended design is that the goals of the design form the foundation for further expansion without specifying the direction the expansion must take. Thus, single "final pathways" and bottlenecks are avoided.

Mission efficiency demands the logical planning of both scientific experiments and mission objectives. Experiments for each phase are selected to take full advantage of the available support from the infrastructure. For example, early infrastructure support enables new scientific information and demonstrations of economical feasibility of using lunar materials for future expansion of the infrastructure. These mission objectives also imply what type of support is needed. For example, during the Outpost Phase, robotic vehicles are required to support various construction activities at the base. When no longer needed for construction, a simple changeover of modular components could convert a construction vehicle into an automated core sample return vehicle.

Finally, the fourth goal is that the missions must provide the means to evaluate further expansion of the infrastructure and continuation into the next phase of development. For example, if processing of lunar materials is infeasible (from a cost or technology standpoint) then it is probable that the program would not continue into Phase III, Permanent Base, and power requirements may not justify a nuclear power plant.

Evaluation of design performance at any particular stage of development is accomplished by a set of specific criteria and metrics. The evaluations take place at specified breakpoints and the design current status is compared logically to the predicted status for a given point on the overall timeline.

The methods by which the goals of the program will be achieved are dependent upon the technologies available throughout the period of system evolution. Some of the more important technologies which will enable the system are life sciences and life support, transportation systems, propellant storage and transfer, space construction techniques, automation and robotics, power generation, and space suits.

Four assumptions were made in establishing the cislunar infrastructure scenario: (1) a reliable transportation system exists between Earth and LEO; (2) there is a functional LEO space station; (3) a heavy lift launch vehicle exists; and (4) on-orbit construction capabilities exist.

HEO ACTIVITIES

A high Earth orbit (HEO) platform is needed to support the in-orbit activities and services that are necessary to promote safe and efficient planetary exploration. For safety, flexibility and cost efficiency, a platform will be placed in a halo orbit about the first Earth-Moon libration point (L1). The manned L1 station will act as a staging point between LEO and the Moon. The use of the L1 station for cargo and fuel storage along with refueling capabilities, will aid in a more cost efficient transportation infrastructure. Other activities such as satellite servicing, geosynchronous orbit cleanup, and a transportation control center provide additional justification for an L1 station. The L1 station is also an excellent location from which to base future planetary missions. Prior to full HEO activities, the L1 site acts as a "parking orbit" for expended external tanks from the Space Shuttle, for obsolete GEO satellites and other space hardware for which the costs of transport to orbit have been paid. The role of this hardware in future missions is only partially predicted.

LUNAR BASE ACTIVITIES

The Moon will provide a focal point for advanced astronomy and planetary studies, as well as lunar resource processing.

Advancements in sciences will be enabled through the use of lunar-based observatories to study the universe while a better understanding of the solar system will be aided through seleneological studies conducted on the Moon. The scientific benefits of lunar-based astronomy should far exceed those of comparable astronomical observations made from Earth. Because the Moon is not shielded by an atmosphere, all wavelengths of electromagnetic radiation (X-ray, infrared, gamma ray and ultraviolet) will reach the lunar surface, hence they can be studied in much greater detail. Additionally, radio-interference from Earth can be shielded by the Moon, making radiotelescopes located on the farside lunar surface more effective.

Production of lunar resources will help reduce a dependence on Earth-based supplies. Lunar-derived oxygen, water and propellants are determined to be key lunar products. Carbothermal reduction is a candidate process to extract oxygen and water. The by-product would be spun lunar fiberglass, useful for lunar construction. In addition, mining and materials processing may provide the lunar base with raw materials to be used in future expansions of lunar activities, as well as space activities. A Controlled Ecological Life Support System (CELSS) will fulfill the requirements for long term human space missions by reducing the total mass required to be transported from Earth. The lunar CELSS will provide the "seed" to start up other life support systems, such as those needed for an advanced L1 station or a manned Mars mission and base.

TRANSPORTATION SYSTEM

The programmatic needs of the transportation systems were considered when selecting transportation system components. Modular components were utilized to reduce costs, to enhance efficiency, and to provide flexibility. The transportation fleet will consist of a variety of manned and unmanned vehicles. A staging node at L1 is proposed in order to reduce overall transportation costs by providing an intermediate staging point easily accessible from LEO, GEO, and lunar orbit. A halo orbit at L1 has the additional advantage of providing access to all orbit inclinations at the Moon and Earth.

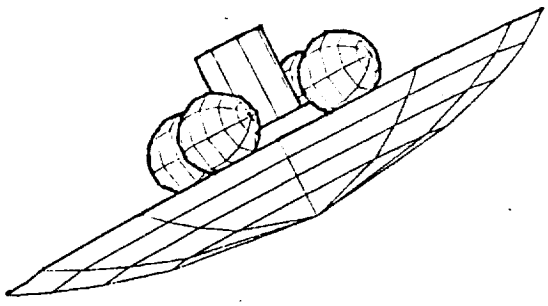

Fig. 2. Manned Orbital Transfer Vehicle

Modular manned orbital transfer vehicles will utilize aerobraking technology and cryogenic liquid oxygen/hydrogen based propulsion to transfer crews and time-sensitive cargo throughout cislunar space. Additional manned transportation will be provided by two types of lunar landers. One lander is used to bring modest amounts of equipment and small crews from L1 to the lunar surface. Cargo and larger crew transportation requirements will be satisfied by a larger lander which travels between lunar orbit and lunar surface.[1]

The manned orbital transfer vehicle, depicted in Fig. 2, is composed of several modular components. The central component is a structural frame with main engines, reaction control, propellant tanks, batteries, limited communications, and a control system capable of remote or preprogrammed operation. An aerobrake may be attached to this frame in order to save ΔV expenditures on trips to LEO. Trips from L1 to GEO or to lunar orbit cannot use aerobraking because no atmosphere exists at the destination to provide the frictional forces necessary to "brake" the vehicle. Therefore, for these trips, the aerobrake would be removed and left at L1 to save weight, thereby saving propellant.

A habitation module that can support three crew members, could be fixed to the frame. A crew of six would be transferred by using two habitation modules end to end. Some life support requirements and most of the power requirements would be derived from a life support module. This module uses an oxygen/hydrogen fuel cell to provide 7 kW of continuous power and 21 man-days of potable water. It also would contain tankage for removal of wastes.

By using modular equipment, spacecraft can be tailored to meet most specific mission needs and thus optimize the spacecraft for greater economy. Yet this configured modular approach does not require special spacecraft for each different mission. Additionally, OTV's without crews or habitation modules can be used for insertion stages for increased payload capability. These insertion stages would be remotely operable or preprogrammed for return trips to LEO or for unmanned emergency sorties.

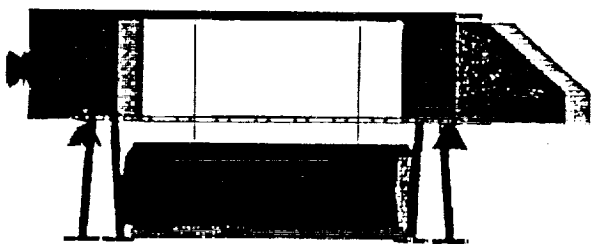

Fig. 3. Cargo Lunar Lander

The smaller lunar lander would be a single stage vehicle approximately twice the size of the Apollo Lunar Module with a 9 metric ton dry weight. This lander could be configured to support three crew members and many scientific payloads for exploration missions. Later, as the lunar base becomes more developed, fewer scientific payloads will be transferred using this lander, and it would be equipped to transport four or five crew members. This lander would shuttle between the L1 staging node and the lunar surface.

The second lunar lander would be substantially larger, and is illustrated in Fig. 3. It would be capable of landing 25-30 metric tons of payload on the lunar surface, as well as a crew of up to six. Due to the size of this vehicle, it would operate only between low lunar orbit and the lunar surface. Cargo destined for the lunar surface would be sent directly to lunar orbit from LEO. Crews would be transferred to L1 from LEO and then to lunar orbit.

All manned transportation vehicles would use liquid oxygen/hydrogen propellants. Additionally, all would use the life support modules to provide power and water supplies. Use of common and standardized equipment reduces costs by requiring only one type of fuel to be transferred and stored. This also enhances flexibility since redundant vehicles are used extensively throughout the transportation system.

Unmanned vehicles consist of two basic types. Small orbital maneuvering vehicles (OMV's) will shuttle between the L1 station and GEO to retrieve and redeploy satellites requiring service. A nuclear electric ion propulsion vehicle will transfer cargo and propellants from LEO to L1 or to lunar orbit. These electric propulsive orbital transfer vehicles (EPOTV) would take less than one year for a round trip.

Cargo to the Moon and propellant to the depot at L1 would be transferred by a fleet of electric propulsion vehicles. An Electric Propulsion Orbital Transfer Vehicle (EPOTV) is shown in Fig. 4. These vehicles would use 300 kW solar electric ion propulsion with xenon or argon propellant. They would be capable of transporting 25-30 metric tons to lunar orbit. Ion propulsion provides a substantial savings in propellant expenditures compared to traditional chemical propulsion systems such as liquid oxygen/hydrogen. Lower propellant expenditures will lower cost. The primary disadvantage of EPOTV systems is the long transit time required. Proper staging of equipment can overcome this disadvantage. As power and propulsive technology progresses, later versions would be nuclear powered at one megawatt or more, and may have increased cargo capabilities. Such a vehicle may be adapted to use a variety of propellants derived from waste and/or space debris.

Another unmanned vehicle is the Orbital Maneuvering Vehicle (OMV). This is a remotely operated spacecraft used to retrieve and transport GEO satellites, perform servicing operations and other operations within the robotic capability of the spacecraft. Salvage and rescue missions are candidate operations that could be performed by such vehicles. The dry

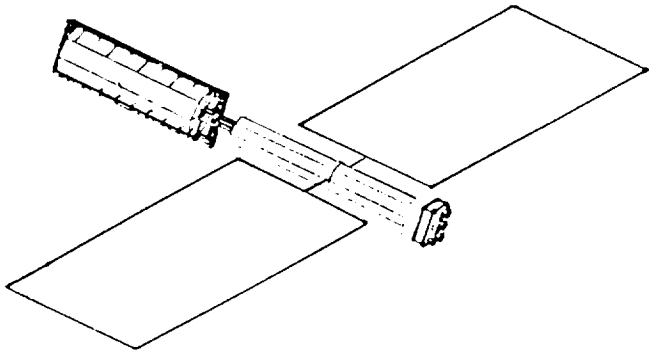

Fig. 4. Electric Propulsion OTV

weight of each OMV would be approximately five metric tons. Since they are used in missions requiring low ΔV expenditures, aerobraking is not used and weight is kept to a minimum. Also, this small spacecraft could be used for robotic functions in lunar orbit, at the LEO station, or the L1 station.

INFRASTRUCTURE DEVELOPMENT

The lunar base configuration was designed considering maximum crew safety, ease of construction, modularity, adaptability to different missions, durability, and cost. The driving factors in determining the size of the base were required habitation area, experimental and research activities, and the volume of the environmentally controlled life support system (ECLSS).

The lunar base design was developed in incremental steps beginning from the remote-sensing site selection and moving toward the ultimate goal of a self-sustaining lunar base. Lunar surface development occurs in four distinct phases. The development of the L1 station parallels the progress of the lunar base.

Phase I, Remote-Sensing and Site Selection, will encompass a variety of remote-sensing exploration missions, as well as manned missions to two remote locations. This phase will determine the location of an initial outpost. Phase I could begin as early as 1994 with the Lunar Geoscience Observer mission currently proposed by NASA, but awaiting funding. Remote sensing of the lunar surface will aid in selecting a safe and promising site for the future lunar outpost. From the data gained using this satellite, approximately ten of the most promising sites for a lunar outpost will be chosen. Further evaluation of these sites will be performed by a cluster of small probes. Each cluster mission will cover an area of approximately 1000 square kilometers. Each cluster consists of two fully-instrumented soft landers and ten small probes which hard land on the surface. Data from the hard landers are relayed to the soft lander for transmission back to Earth. This data will be used to select two sites for further evaluation by a manned mission.

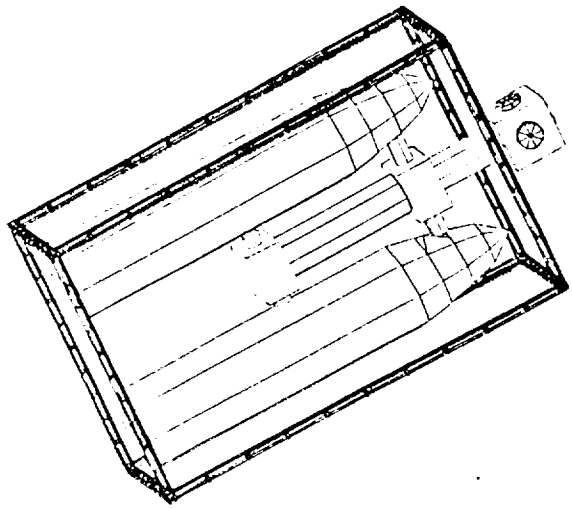

Fig. 5. Initial L1 Station

Continued lunar expansion will be evaluated at this point. In addition to the data obtained, financial support must be available, as well as a transportation system capable of supporting the Outpost development phase. In particular, the large lunar lander must be available. It is anticipated that expansion would continue into Phase II to allow for manned scientific studies on the lunar surface.

Phase II, Outpost Development, consists of establishing a man-tended outpost on the moon to provide for a series of ten to fourteen-day missions. The purpose of these missions will be to perform science experiments and to research lunar processing capabilities. Concurrent with the lunar development is the addition of a modest space station located at L1 to serve as a transportation and staging node, as depicted in Fig. 5.

A transportation node at L1 provides a staging point for manned lunar missions and a more cost-effective location from which to service GEO satellites. For example, two crews can be transported to L1. The crews will ready the lunar lander for one crew to use for a lunar mission while the second crew remains at the station to repair GEO satellites. Additionally, robotic lunar exploration is enhanced by control of such missions at the L1 station exploiting the lower transmission delay times. Constructing the station with external tanks and components developed for the LEO station reduces the cost of building such a station.

The lunar base will be powered by a 100-kW solar array with backup fuel cells. Other hardware staged to this point include a habitation module, multi-purpose lunar surface vehicles and a sandbagging device to bag regolith for shielding purposes. Radiation protection will be provided by a regolith "tent" supported by a truss structure. Such a structure is shown in Fig. 6.[2]

Lunar activities would vary widely depending upon current mission objectives. Construction activities include deploying solar arrays, sandbagging to construct the radiation shield, and other activities to establish the outpost. Selenological studies of the Moon would be performed by studying core samples returned by robotic missions as well as by studying mineralogical debris from craters. Although much was learned from the Lunar Geosciences Observer, new remote sensing packages will be carried by the lunar landers to take data during orbital phases of those missions. Chemical analysis of the soil will be

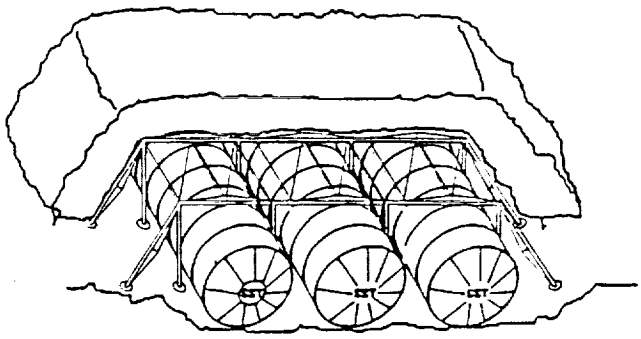

(ADAPTED FROM KAPLICKY AND NIXON, 1985)

Fig. 6. Regolith Shielding Tent

conducted to evaluate potential processing of raw materials. Several candidate processes to obtain oxygen and water from the lunar regolith will be evaluated to determine the most efficient process. Candidate volatile recovery processes would be assessed for feasibility of simultaneous materials production such as the production of fiberglass beams. Also, basic astronomy facilities may be placed near the base during this time period.

In addition, the effect on humans living in a 1/6-*g* environment will be assessed. Human factors involved in working on the lunar surface will be evaluated in order to develop a more efficient permanent base if one is to be built. These assessments will also help to develop better operational procedures to maximize productivity and psychological well-being of the outpost personnel.

The success of Phase II activities will provide the means to assess the practicality of continued lunar development. Key considerations are the following: lunar oxygen production rates, CELSS efficiency, and demonstrated potential for further scientific and economic gains. These considerations will determine if a permanently-manned base is justified. Perhaps the construction of another outpost at a different location would be needed to perform additional studies before committing to a permanently manned facility. Studies beyond the scope of these missions must be planned before further expansion of lunar facilities is warranted.

Phase III, Permanently-Manned Base, should lead to lower space program operational costs by beginning the development of large-scale processing activities to provide water, propellants, and other materials from lunar resources. A nuclear power plant will provide the energy required for the anticipated increased level of processing. Two more habitation modules, increased ECLSS and CELSS capability and closure, and a larger crew on the lunar surface are required to support the expanded lunar operations. A farside observatory will be constructed during this phase, if not already initiated by this time.

This phase strives to establish economic uses of the Moon. It would be hard to justify substantial investments if there is not a clear economic or technological return to the program. Lunar derived propellants, oxygen and water for life support, and materials for construction of larger habitat volumes are candidate technologies for economic return.

Phase IV, Self-Sustaining Base, results from the continued success of Phase III operations. Integrating more systems, new processes and better technologies (such as CELSS) into the base, promotes greater independence from Earth based supplies. These benefits will enhance operations within the entire infrastructure. Transportation costs will become lower due to the availability of lunar-derived propellants and/or future reductions in Earth-to-orbit costs. Structural materials manufactured on the Moon may be used for base expansion, new outposts, space station expansion, and materials to support the construction of equipment for manned Mars missions.

An advanced L1 station, illustrated in Fig. 7, becomes justified as lunar activities and capabilities are expanded. The construction of an advanced L1 station is warranted as the permanently-manned Phase III matures. An advanced L1 station will probably rotate to generate artificial gravity, will use CELSS for most life support needs, and will serve as a staging location for manned Mars missions.

This sequence represents an economically feasible expansion of the space program activities. Compression of this schedule can only be made with a firm commitment in resources and technology development. A more probable scenario is the lengthening of this schedule. Logically, the nation's capabilities must expand in a manner that provides a clear means to evaluate further growth. These evaluations should provide a clear rationale concerning what the next phase will provide both economically and scientifically. Perhaps the most important breakpoint is the one between the outpost and permanently manned phases of operations. Additional outposts may be preferable to expanding one base; however, this can only be truly evaluated by well designed missions during the outpost phase.

A manned Mars mission is inevitable, but it is impossible to establish a specific timeframe. Such a mission would have considerable impact on the proposed infrastructure program

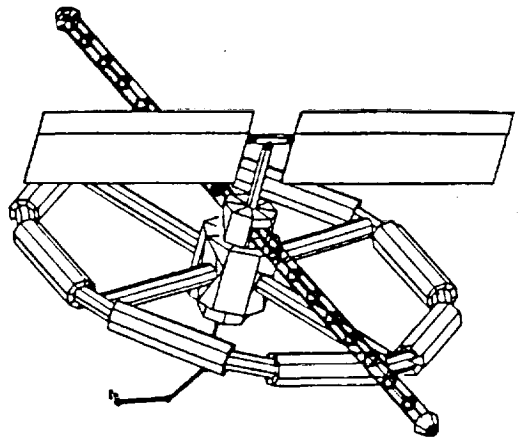

Fig. 7. Advanced L1 Station

and vice versa. Limited space program funding could make these programs competitors. Commitment to an early Mars mission (perhaps including Soviet cooperation) would require stretching the timeline for development of the lunar infrastructure. An early Mars mission would most likely be staged from LEO with all Earth-derived materials. It would not realize the potential benefits of a mature cislunar infrastructure for staging. Fortunately, many of the technological challenges targeted for development in the infrastructure program are applicable to a manned Mars mission. A Mars mission staged at a later date may be a better choice. Long-term operations in space will help establish and demonstrate the required system reliability needed for a manned Mars mission. In addition, the potential economic savings from the use of lunar-derived propellants and materials could provide a less expensive Mars spacecraft to depart from L1 rather than LEO. Finally, electric propulsion staging of fuel to Mars could take advantage of similar technologies developed and proven in cislunar space.

SPECIAL FEATURES

Many elements of the infrastructure have been discussed, however there are several features that require additional description. These are the CELSS, training simulators, a human powered short range lunar vehicle, and space suits.

The first of these features, CELSS, is an advanced life support system utilizing regenerative techniques, both biological and physiochemical, to recycle wastes and to produce consumables. Currently such a system does not exist; however, the successful development of CELSS will be crucial to the design and operation of advanced space missions (i.e., a permanently manned lunar base or future manned missions to Mars). For a lunar surface base, this life support system will provide consumables and will process wastes from the human crew.

Life support will be necessary for a variety of scenarios during the lunar surface development, that is, from a series of short-stay missions to permanent habitation. CELSS development will reflect these varying degrees of life support requirements by embracing a phased-growth approach. In order to develop the regenerative life support technologies that CELSS entails, it is necessary to provide a framework in which the various subsystems can be used as the technologies become available. A four-phase development design has been proposed which will provide a regenerative life support system for all stages of the cislunar infrastructure development.[3] The phases of CELSS development do not directly correspond with the infrastructure development phases.

Phase I will close the hygiene water loop. Since hygiene water constitutes approximately 77% of all the consumable mass, which consists of potable water, hygiene water, oxygen and food solids, this is a considerable savings. Since the purity of hygiene water is not critical, it may be easily filtered using filter setups (0.22 micron nitrocellulose) currently available commercially.

Phase II will see the evolution of CELSS into a full-scale waste processing system. The goal will be to purify urine and fecal water to produce potable water, which is approximately 17% of the consumable mass. The methods employed during this phase will be dependent on actual mission length. For short stay missions (10-14 days), the waste will be sterilized and converted back to water and carbon dioxide using a supercritical water oxidation (SCWO) system. Waste processing for the permanently-manned lunar base will be done with a biological reactor, with SCWO being done on a limited basis. Once wastes are processed by either of these methods, the effluent water will be purified in fuel cells using an electrolysis subsystem to convert recaptured water into hydrogen and oxygen.

Phase III will be characterized by the implementation of an algal growth facility. This algae will feed on the nutrient-rich effluent water produced in Phase II and will serve as a means to convert carbon dioxide to oxygen. Algae is also a rich source of protein which will have potential as a food source for the crew.

Phase IV, the final phase in the CELSS development, will make a logical addition to Phase III by growing higher plants and supporting aquaculture. The growth of higher plants will not only increase the production of high quality food products, but will also increase oxygen production. The aquaculture will provide variety in the crew members' diet. It will also be closely tied to the algal subsystem, as the algae will provide food for the aquaculture.

This phased approach to a CELSS development promotes logical advancements which will directly satisfy each portion of the infrastructure development. Life support needs are based on both mission length and crew size.

A second feature is development of on-orbit and lunar surface high-fidelity simulation facilities. Current training philosophy entails repetitive practice of required skills to ensure the necessary skill level is attained. Once on the moon, crews may spend greater times performing duties other than flying spacecraft. This implies a potential reduction in skill efficiency. A simulator will be required at the base to allow continuing practice of upcoming missions, emergency procedures, and novel practice for emergency missions.

This capability could be enabled in one of two ways, or a combination of both. First, a portion of a habitation module could be dedicated to simulation. The second method would use a dual mode transportation vehicle. This vehicle could be used in a "simulation" mode to practice a mission or in an

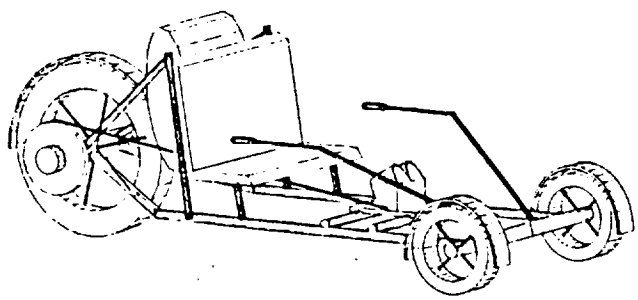

Fig. 8. Human Powered Vehicle

"operate" mode which would allow use of the actual controls and indicators onboard the lunar lander to simulate a mission. Thin visual display boards would be placed over the window areas. Greater computer power also would be needed onboard.

The advantage of the dual mode transportation vehicle option would be that if multiple lunar sites were used, a simulator would automatically be available at each site. Also the computer power to support simulation could be applied to performing rendezvous predictions or other orbital maneuvering calculations without ground, lunar base, or space station support. The disadvantages are increased weight of the displays, computers, and dual mode circuitry, all of which implies greater propellant consumption. A trade-off study of these options will be necessary to evaluate simulation technology levels at the time of final design. Another choice could be a hybrid of the two, using transportation vehicle controls tied to lunar based computer support and utilities.

Additionally, an Orbital Transfer Vehicle (OTV) simulator would become necessary. Crews in space for long duration may find the need to review emergency procedures, docking maneuvers or other operations. Such a simulator could be located in a space station node outfitted with a high-fidelity simulator thus keeping OTV weight to a minimum.

A human-powered vehicle (HPV) has been proposed. This vehicle was designed to fulfill the need for short range transportation on the lunar surface.[4] Such a need will undoubtedly arise with the advent of a lunar outpost and increased lunar activities. The HPV, shown in Fig. 8, is a three-wheeled vehicle which was modelled after an Earth-type mountain bicycle and a recumbent bicycle. As the name implies, it is will be powered by the astronauts themselves. Hence, special design considerations have been given to space suit flexibility, durability, lunar surface terrain, and human safety. Not only will the HPV provide shortrange transportation, it will also be a source of exercise and entertainment for the astronauts.

In order for external lunar activities such as an HPV mission to be effective, a new space suit design modified for the Moon's harsh environment is warranted. These suits must be durable enough to withstand the abrasiveness of the lunar soil and prevent clinging of the soil to the suit. A high-powered vacuum cleaner at the airlock could aid in the removal of lunar soil.

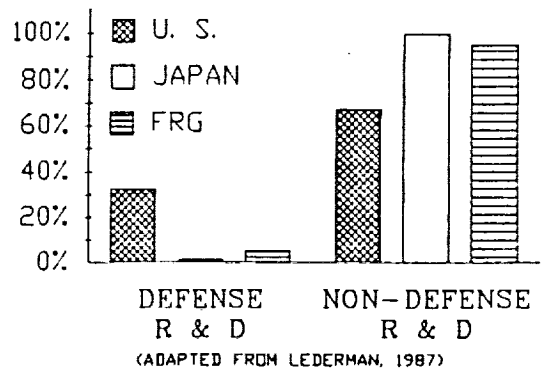

Fig. 9. Relative R & D Expenditures

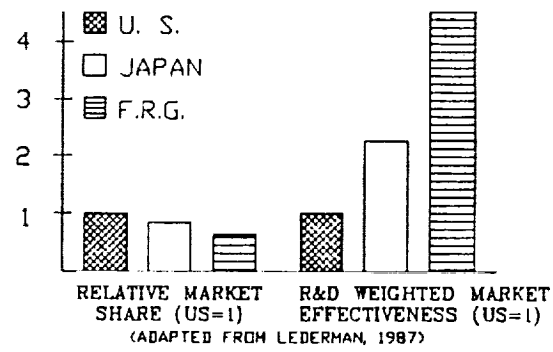

Fig. 10. Relative Shares of Technology-Intensive Exports

Additionally, the suit must be able to operate in a wide range of thermal environments, to be flexible, and to require no prebreathe. The suit should allow considerable use between maintenance periods and possibly automated rejuvenation of suit life-support systems. On-orbit Extra-Vehicular Activity (EVA) space suits have similar requirements to satisfy space construction, transportation vehicle servicing, satellite servicing, and other space activities. Current space suit design allows only limited use between servicing, is not flexible, and requires prebreathe. Technological improvement of these suits is imperative in order to allow humans to efficiently operate outside their habitats or vehicles.[5]

ECONOMICS

Is it possible to commit large expenditures to such a program at a time when the economic climate of the government is one that emphasizes budget reductions in order to balance the budget and to reduce the deficit? Perhaps a better question is whether the United States can afford not to pursue such activities. In order to stay competitive in world markets at the turn of the century, the United States must make a commitment to technological research and development.

After the Soviet Union, Japan and the Federal Republic of Germany (FRG) are America's closest competitors in technological arenas. During the years 1983-1986, the gross national product (GNP) of the United States was almost three times that of Japan and over five times that of FRG. Research and development (R&D) spending in all three countries was approximately 2.8% of GNP. However, the distribution of such funds and the output of the respective economies vary. Figure 9 illustrates the strong American commitment to defense R&D; however, only 10% of this amount is devoted to research. Japan and FRG spend the majority of their R&D funds in non-defense activities.[6]

Each economy provides different products to the world market. In order to measure the successful utilization of R&D expenditures, technology intensive exports were selected as the metric. The country with more state-of-the-art technological products for world markets should have a greater share of export business. The left half of Fig. 10, Relative Market

Share, illustrates the ratio of technology-intensive exports for Japan and FRG relative to the U.S. export market. Japan's world export market is approximately 80% of the U.S. market. Although the United States has a larger share of the world market in absolute terms, it is not as effective as Japan and FRG per R&D dollar expended. The right half of Fig. 10, R&D Weighted Market Effectiveness, weights the export markets of Japan and FRG to the amount of R&D funds expended. This weighted market share is normalized to the U.S. R&D weighted market share. Per R&D dollar, Japan is 2.3 times more effective and FRG is 4.4 times more effective in generating technology-intensive exports than is the United States.

Clearly, the United States is currently losing its technological edge. Japan is becoming increasingly competitive in computer technology. The European Space Agency (ESA) is closing the technological gap between its space program and the U.S. space program. Already, ESA competes very well for Western launch services. In the next decade, ESA plans to have developed a small shuttle. Japan has similar designs to compete in the world market for launch services, manned spaceflight, and possibly a space station. Where at one point the United States was the undisputed leader in space technology, the turn of the century could find the U.S. trailing behind Russia, ESA, and Japan, as well as various other countries trying to form space programs.

Failure by the United States to commit the necessary resources could result in further lagging of technological growth in this country. This would further reduce exports and weaken the country's economy. The proposed program to develop a cost efficient space infrastructure and to explore the Moon could prevent this pessimistic scenario from occurring by increasing the nation's commitment to research and development.

Commitment to increased space program funding will provide benefits throughout the nation's economy. Immediate effects will be increased employment to support the development of these projects and concurrent growth in local support service economies to support the increased employment. Universities will receive more funding to support higher education and enhance graduate education. Other sectors of engineering and science may benefit from quality graduate education supported by funding of universities for space application studies. Thus, space is a technological target that may embrace a broad advance in American competitiveness into the next century.

Space technology requires a multi-disciplinary effort. Therefore, funding will support a wide range of activities, thereby increasing the potential applications of new developments into other sectors of industry. Perhaps the greatest impact will be in the area of automation and robotics. This technology is vital to efficient space operations. However, this technology has enormous potential in industry to yield products less expensively and with greater quality than is currently possible.

Robotics innovation will undoubtedly become more popular in world markets. Other areas of technological interest stimulated by the space program include artificial intelligence, medicine, new high-strength low-weight alloys, and computers.

The Apollo program was politically motivated; it was pursued in order to maintain the technological edge of the United States. Approximately $40 billion were invested in this program, resulting in an estimated $200 billion worth of benefits. Return on this investment is continuing today. The proposed space infrastructure should provide similar returns to the economy as a whole. Although not all of the specific products can be anticipated at this time, an investment in the future must be made to provide the framework for future innovation. Continued pursuit of products that show only a short-term return on investment will not be in the interest of the U.S. economy as a long-term world leader in technology.

CONCLUSION

The University of Colorado Advanced Mission Design Program has defined the evolution of a cislunar space infrastructure and has designed many of the infrastructure components. Technological advances, scientific gains, economic returns, greater political stature, and national pride justify the development of such an infrastructure.

Specific activities will take place through the use of an L1 space station, a lunar habitat, and an extensive transportation system. The development and construction of the infrastructure are phased such that specific breakpoint criteria must be satisfied before the next phase can begin. By advancing logically and methodically, a solid foundation will be established upon which a credible and successful program may be built.

Development of the infrastructure begins when the program is accepted. Around 1990, research and design of technologies, as well as hardware and programmatic considerations will be accelerated. This scenario continues through 2021, when the lunar base becomes self-sufficient. At this point the open-ended nature of this design, becomes an important stepping stone for more aggressive projects, such as a manned Mars mission.

REFERENCES

1. Johnson S., Kliss M. and Luttges M. A Transportation Infrastructure for 21st Century Activities of the U.S. Space Program, (Paper LBS-88-178), *Lunar Bases and Space Activities in the 21st Century*, 2nd Symposium, Houston, Texas, April, 1988.
2. Kaplicky J. and Nixon D. A Surface-Assembled Superstructure Envelope System to Support Regolith Mass-Shielding For An Initial-Operational-Capability Lunar Base, in *Lunar Bases and Space Activities of the 21st Century*, (W.W. Mendell, Ed.), pp. 375-380, Lunar and Planetary Institute, Houston, 1985.
3. Banks G. and Rose S. A Phased Approach to the Evolution of CELSS For Long-Term Space Habitation, Houston AIAA 13th Annual Technical Symposium, May, 1988.
4. Leech H. and Ryan K. Short-Range Lunar Transportation: A Human Powered Vehicle, AIAA Region V Student Conference, April 15, 1988.
5. Buck C. A Novel Approach to the Design of An Extra-Vehicular Mobility Suit, AIAA Region V Student Conference, April 15, 1988.
6. Lederman L.L. Science and Technology Policies and Priorities: A Comparative Analysis, *Science*, *237*, 1987.

DESIGN OF COMPONENTS FOR GROWING HIGHER PLANTS IN SPACE

UNIVERSITY OF FLORIDA

The overall goal of this project is to design unique systems and components for growing higher plants in microgravity during long-term space missions (Mars and beyond). Specific design tasks were chosen to contribute to and supplement NASA's Controlled Ecological Life Support System (CELSS) project. Selected tasks were automated seeding of plants, plant health sensing, and food processing. Prototype systems for planting both germinated and nongerminated seeds were fabricated and tested. Water and air pressure differences and electrostatic fields were used to trap seeds for separation and transport for planting. An absorption spectrometer was developed to measure chlorophyll levels in plants as an early warning of plant health problems. In the area of food processing, a milling system was created using high-speed rotating blades which were aerodynamically configured to produce circulation and retractable to prevent leakage. The project produced significant results having substantial benefit to NASA. It also provided an outstanding learning experience for the students involved.

INTRODUCTION

This project is being conducted in cooperation with the personnel of the NASA Controlled Ecological Life Support System (CELSS) project at the Kennedy Space Center. The overall goal of the project is to design unique systems and components for growing higher plants in microgravity during long-term space missions. The plants will be used for food and atmospheric regeneration.

The goals of the first semester were to obtain a comprehensive overview of the requirements of the integrated system, to identify promising design topics, to perform preliminary design on the identified promising tasks, and to determine the practicality of various candidate systems and components for detailed design and prototype fabrication efforts. The areas selected for in-depth study and preliminary design efforts were (1) automated seeding and tissue culture, (2) adaptable-geometry growth chambers, (3) plant health monitoring systems (including the areas of leaf finding, nondestructive tissue analysis and leaf diagnosis, and sensors), (4) expert systems for automated, intelligent sensor interpretation, intervention, and control, and (5) food preparation and waste processing.

After initial study and preliminary design, the candidate design tasks were ranked for appropriateness on the basis of the background and interests of the class, potential importance to NASA programs, availability of resources to be applied to the effort, and the likelihood of successful design and fabrication. The projects chosen for study during the second semester were (1) automated seed separation, manipulation, and placement; (2) automated sensing and interpretation of plant health; and (3) automated food processing, particularly milling.

Three project groups were formed to address these topics, design criteria were refined, and detailed design and prototype fabrication was initiated.

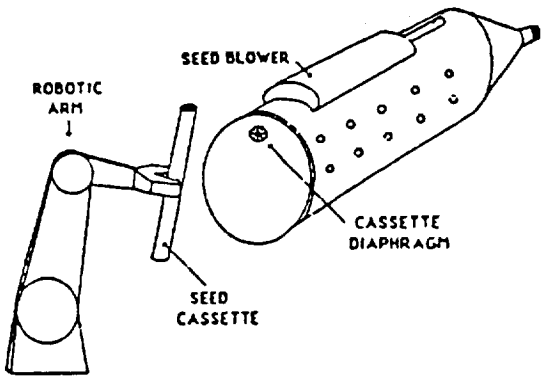

Fig. 1. MBS-1

CONCEPTS AND DESIGNS

Automated Seed Manipulation and Planting

The Automated Seed Manipulation and Planting group addressed the development of a system for safe seed separation, acquisition, and planting operations. The seeding systems constructed and tested during the spring semester, 1988, were diverse and indicated promise for future development.

The mechanical division fabricated three seed separators utilizing pressure gradients to move and separate wheat seeds. These separators are called "minnow buckets" and use air and/or water to generate the pressure gradient. Figure 1 shows the Minnow Bucket Seeder-1 (MBS-1) which traps seeds in machined holes on the inside wall. A cassette is then inserted and aligned to a row of holes. Negative pressure is applied and the seeds are implanted in the cassette. The cassette is then withdrawn and delivered to the growth chamber. MBS-2, depicted in Fig. 2, utilizes tube transfer to move the seeds from the inside chamber to a cassette or planting tray. The tube transfer mechanism consists of a spring-loaded bracket to ride along the inside wall and collect the seeds and a rotating block to move the spring-loaded bracket. MBS-3 uses water as a medium and seeds were removed through tubes out the sides of the container. A seed separator, Fig. 3, was designed and built to separate seed and water which allowed for the planting of germinated seeds.

Electrostatic fields were employed in the seed separator constructed by the electrical division. This separator operates by forcing a temporary electric dipole on the wheat seeds and

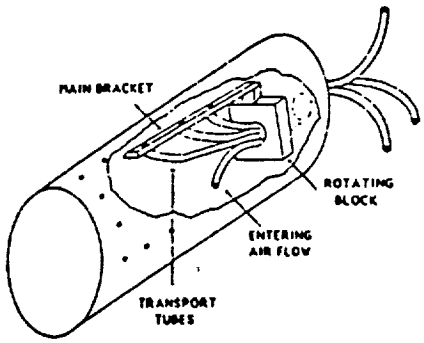

Fig. 2. MBS-2

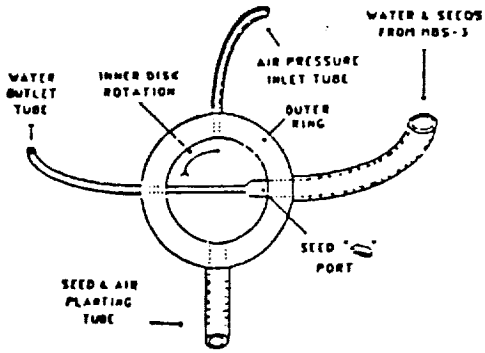

Fig. 3. Seed Separator

uses charged electrodes to attract and move the seeds. Allowing seeds to align in the field lines, seed placement is accomplished by seed flow over the cassette opening and then by blowing those seeds into the cassette (Fig. 4).

Seed delivery to the hydroponic growth tray is accomplished by the seed cassette. The cassette is compatible with all the seed separators and consists of a plastic tube threaded with millipore filter paper. During planting operations, the seeds are placed in an empty cassette. The loaded cassette is then placed in the growth tray and nutrient solution provided. The solution wets the filter paper and capillary action draws the nutrients up to feed the seeds.

The aforementioned seeding systems were then tested and produced encouraging results. The seeds were effectively separated and the cassette showed that it can support the growth of wheat plants. Problems remaining to be investigated include improving the success of delivering the seeds to the cassette and providing adequate spacing between seeds for the electric separator.

Plant Health Sensing

The Plant Health Sensing group investigated many different plant health indicators and the technologies used to test them. The project selected focused on measuring chlorophyll levels using absorption spectroscopy.

The spectrometer shown in Fig. 5, measures the amount of chlorophyll in a leaf by measuring the intensity of light of a specific wavelength that is passed through a leaf. The three wavelengths of light used corresponded to the near-IR absorption peaks of chlorophyll a, chlorophyll b, and chlorophyll-free structures. Interference filters, mounted on a rotating disk and placed in a beam of collimated light, are used to select a specific wavelength of light. A computer positions the disk to select the proper filter. A lens then focuses the filtered light onto the end of a fiber-optic light guide, which carries the light to the detector clamp. A leaf is placed between the blades of the clamp and a photodetector is located directly opposite the end of the light guide. The computer measures the voltage produced by the detector and stores the data on a disk file for analysis (Fig. 6).

Experimentation showed that the sensor is indeed measuring levels of chlorophyll a and b and their changes before the human eye can see any changes. The detector clamp, (Fig. 7), causes little damage to the leaf and will give fairly accurate readings on similar locations on a leaf, freeing the clamp from having to remain on the same spot of a leaf for all measurements. External light affects the readings only slightly, thus, measurements may be taken in light or dark environments.

Future designs and experimentation will concentrate on reducing the size of the sensor and adapting it to a wider range of plants. Additional research may allow the sensor to be used in conjunction with an expert system to diagnose particular stresses and propose specific treatment.

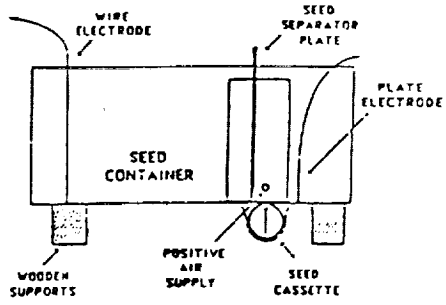

Fig. 4. Electrical Seeder

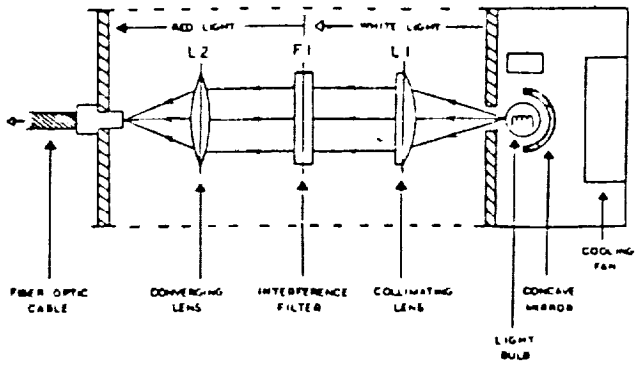

Fig. 5. Spectrometer

C-2

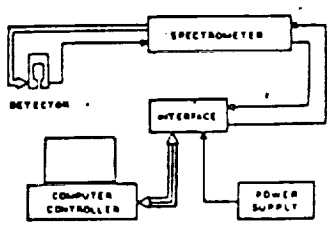

Fig. 6. Sensor Diagram

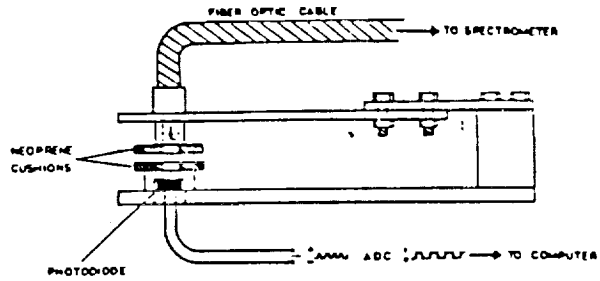

Fig. 7. Detector Clamp

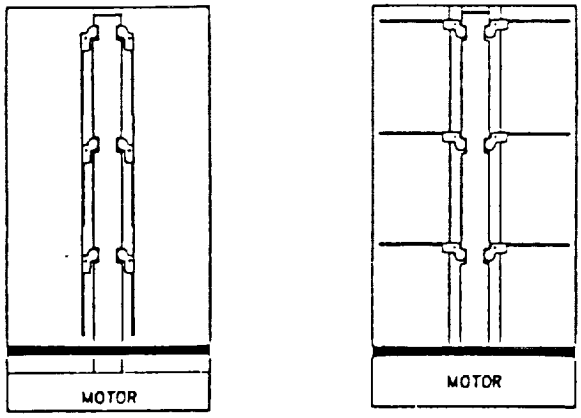

Fig. 8. Deployable Blades

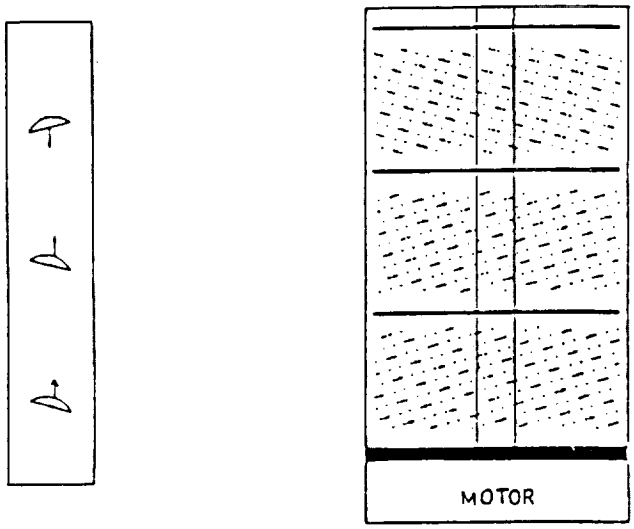

Fig. 9. (A) Blade Angle, (B) Induced Flow

Food Processing

The food processing group developed a system for food processing in microgravity. Key problems addressed in the design of the system were blade insertion, particle confinement, and blending efficiency. A prototype wheat milling system developed by members of the food processing group consisted of a blending container, a set of deployable/retractable blades, and a particle confinement system (Fig. 8).

A shaft containing the blades is inserted through a one-inch diameter opening in the blending container and the blades are deployed only after the shaft is fully inserted. The particle confinement system consists of a rotating disk which covers the blending container opening when no processing is being performed.

Angles of attack, as depicted in Fig. 9A, were given to the blades to improve the blending efficiency by inducing a turbulent flow of the wheat around the blades (Fig. 9B). Testing of the prototype produced favorable results with the system meeting several of the key design criteria. Suggestions are presented for solving some of the problems encountered during testing.

The wheat milling system developed by the food processing group is intended for implementation in a circular track food processing system.

CONCLUSION

The EGM 4001 Design Class designed and fabricated three elements of a bioregenerative system for higher plant growth as well as a processing system for particle reduction. The bioregenerative areas included automated seed separation and manipulation along with plant health sensing using comparative chlorophyll levels of sick and healthy plants. The processing area studied the problem of particle reduction and flow in microgravity.

Several useful products were produced by this effort. The seed separation and manipulation group created four types of seeders. Three of these designs employed the air or water pressure gradients to trap or move seeds while the other system utilized an electrostatic field to separate seeds. The plant health sensing group fabricated an absorption spectrometer to measure and compare chlorophyll levels of plants. The food processing group built a milling device which incorporated aerodynamic blades to induce flow against gravity.

Overall, these projects were highly successful in that they produced novel and workable designs for components essential to the growth and utilization of higher plants and atmospheric regeneration during long term space missions.

DESIGN OF A LUNAR TRANSPORTATION SYSTEM

FLORIDA A&M UNIVERSITY/FLORIDA STATE UNIVERSITY

INTRODUCTION

The establishment of lunar bases is the next logical step in the exploration of space. Permanent lunar bases will support scientific investigation, the industrialization of space, and the development of self-sufficiency on the Moon. Scientific investigation and research and development would lead to applications utilizing lunar material resources. By utilizing these resources, the industrialization of space can become a reality. The above two factors coupled with the development of key and enabling technologies would lead to achievement of self-sufficiency of the lunar base.

An important element in lunar development is the transportation infrastructure. Transportation is characterized by the technology available in a specific timeframe and the need to transport personnel and cargo between the Earth and Moon and between lunar bases. In this study, attention is focused on the transportation requirements during the establishment of the first-generation lunar base. It is foreseen that in the early years of habitation, lunar bases will serve as facilities for scientific research, economic exploitation, and as the first steps in colonization of the Moon.

Lunar development will begin with a research station. This station will expand while additional stations are installed at locations of scientific interest. Many beneficial locations exist on the lunar surface. The first research station will evolve into a production facility that must be connected with the remote outer stations by a transportation system. The growing production capacity of the main station will then require raw materials from distant regions, and as self-sufficiency increases, products produced at the main base must be transported to the other stations. This will increase cargo transportation demands. A typical growth function shows that the number of lunar inhabitants will increase to about 1000 in 25 years and to about 10,000 in 50 years, beginning with the year 2010[1]. The establishment of such lunar colonies will require that an efficient mechanism be established for the transportation of personnel and cargo both over short and long distances. Hence a study was undertaken to better understand the seleno-physical and economic factors as they affect the problems associated with lunar transportation at a conceptual level, both in the range of less than ten kilometers and more than ten kilometers. Attention was focussed on specific design(s) to be pursued during subsequent stages in advanced courses. Some of the objectives in the project included: (1) minimizing the transportation of construction material and fuel from earth, or maximizing the use of the lunar material; (2) use of novel materials and light weight structures; (3) use of new manufacturing methods and technology such as magnetically levitated, or superconducting materials; and (4) innovative concepts of effectively utilizing the exotic lunar conditions, i.e., high thermal gradients, lack of atmosphere, zero wind forces, and lower gravity, etc.

The designs were to be conceptual in nature but aimed at long and short distance movement of men and materials. The designs are applicable to the timeframe which encompasses the first and second half of the 21st century as the lunar colony continues to grow.

DESIGN CONSIDERATIONS

The Moon's geophysical and environmental conditions are dramatically different from those of Earth and thus present a real challenge in the design of any facility[2]. The following characteristics influence the design of a transportation system for the lunar surface.

The Moon has a gravitational field of about one-sixth of that measured on the Earth's surface. Due to the low gravity, much larger structures can be built on the Moon. The low gravity allows use of materials of lower strength than on Earth for structures of equivalent size.

The Moon has a slow rotation period of 28 days, so lunar days and nights each last for 14 Earth days, therefore, solar energy systems should be equipped with some means to store energy during the long lunar night.

Moonquakes are much rarer and much shallower than Earthquakes. Seismic waves are intensely scattered near the lunar surface. The energy of the waves arriving at a given point is diffused so that the damaging effects are less than those of a comparable event on the Earth.

The lunar atmosphere is a collisionless gas. This will eliminate engineering problems associated with drag forces and wind but might cause difficulty in lubricating moving parts. A number of scientific experiments requiring hard vacuum can be conducted on the Moon.

The drastic changes in surface temperature pose a problem in the selection of materials for various lunar structures. The materials chosen must withstand steep thermal gradients of about 5 K per hr.

The magnetic field of the Moon is very weak, about one thousand times less than that of the Earth.

The Moon is radioactive. Since the Moon has a small magnetic field and no appreciable atmosphere, solar and nuclear particles strike its surface unimpeded. The Moon receives high-energy cosmic rays, solar flare particles, and solar wind particles. Solar flare particles are dangerous to electronic devices and harmful to people.

Since there is no atmosphere to slow down cosmic particles, even the smallest particles impact the surface at cosmic velocities. These particles could damage some structures and instruments on the lunar surface.

The lunar regolith is a layer of debris generated by meteorite impacts. It contains rock and mineral fragments and glass form by impact melting. Regolith is an excellent thermal insulator.

CONCEPTUAL DESIGN

Short Range Design

In this range (< 10 km) a Multipurpose Lunar Transportation Vehicle (MPLTV, as shown in Fig. 1) is considered.

The MPLTV is an improvement on the original Lunar Rover design and conforms to the following design criteria: (1) ease of operation and versatility, (2) maximum payload capabilities, and (3) non-terrain limiting.

In order to meet the above criteria the MPLTV is designed to be a segmented vehicle. The front portion of the vehicle consists of the power and drive systems with some small amount of load-carrying capability. The second portion is called the Multi-Purpose Lunar Trailer (MPLT). The MPLTV can be configured in a number of ways to best aid the specific task at hand. Coupling and uncoupling of the MPLT and the MPLTV is done with an electromechanical device. This device will allow the MPLT to be engaged or disengaged without the operator having to leave the MPLTV.

The MPLTV will be designed to maneuver in a variety of different lunar environments without strict limitations. The original Lunar Rover was severely limited by terrain because the wheels could not withstand high-impact loads and also because the wheels lost traction on lunar soil if subjected to an inclination greater than 20°. The tracks designed for the MPLTV can surmount these constraints. These tracks can withstand high-impact loads and maintain traction even during 60°-inclined climbs in loose soil, as shown during experiments on Earth.[4] A prepared surface is not necessary because by their very nature tracked vehicles lay down their own road. Another advantage of tracked vehicles is that they have a much greater surface contact area as compared to wheeled vehicles. This feature has a disadvantage in that the resistance to rolling is 2.5 times greater than wheels in soft soil. The advantage is that any load which the track supports is distributed over a much greater area. From calculations it has been determined that the ground pressure for the MPLTV is 2.85 psi (39,233 Pa) while the same load supported by 4 wheels, not taking into account their deformation, is 41.6 psi (286,832 Pa). Through these features it can be said that MPLTV will be able to best meet the demands of a first generation lunar base.

Steering Mechanism

The MPLTV uses a newly introduced steering mechanism called the Gleasman all-gear steering system. The Gleasman system, shown in Fig. 2, is very simple and uses commercially available parts. If these parts are manufactured out of materials

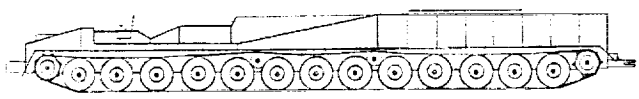

Fig. 1. Multipurpose Lunar Transportation Vehicle

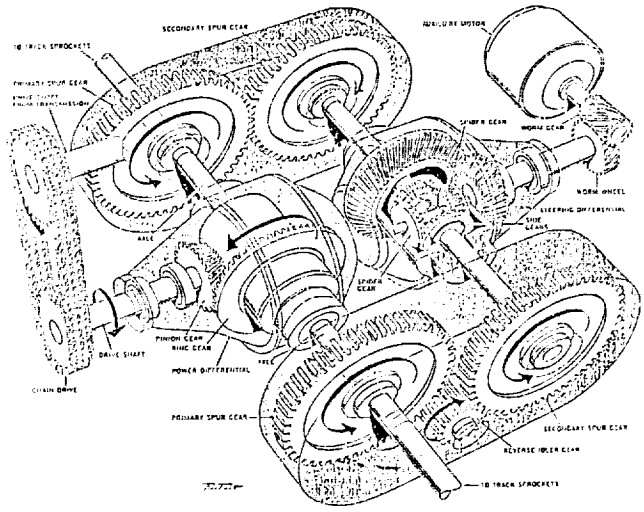

Fig. 2. Gleasman Drive and Steering Mechanism

that can withstand the extreme temperatures of the lunar surface, then the system can be put to use on the Moon. The Gleasman system is very reliable and durable as shown in field tests conducted by the United States Army[4]. The cost of the system is about one-tenth that of an ordinary steering system in a tank.

The system uses two standard differential worm and spider gears and consists of a minimum number of parts. The system works in the following way: A power differential applies power to the vehicle to move in a straight line. The steering differential is mounted parallel to the power shaft and is in front of the power differential. The input to this steering differential is through a worm wheel that is turned by a worm gear powered by an auxiliary motor. This motor is controlled by a rheostat on the steering wheel. When the vehicle travels in a straight line, the steering is steady and the worm gear does not move. Because the steering differential is controlled by the worm wheel, which cannot turn a worm gear, it is locked. To make a turn, the speeds of the two driving sprockets must be varied so that the tracks can move at two different speeds. This is achieved through the use of the steering differential. The motor and the worm gear act on the steering differential like a driveshaft in a car. The more the operator turns the wheel, the more the worm gear turns the worm wheel. This effective torque then turns the entire front steering housing. When this housing begins to rotate, the spider gears inside the housing rotate thus causing two side gears mounted on the axle ends to rotate. The rotating spider gears force one side to move forward and the other to move backward. Since the axle shafts are already moving in opposite directions with the help of an idler gear, this turning action merely decelerates one side and accelerates the other side. This action is transmitted to the tracks through sprockets so that one track speeds up while the other slows down.

In the Gleasman drive there is no wastage of power and the vehicle can turn about its own center thus improving maneuverability. Because of these advantages coupled with low cost, the Gleasman system appears to be an excellent candidate

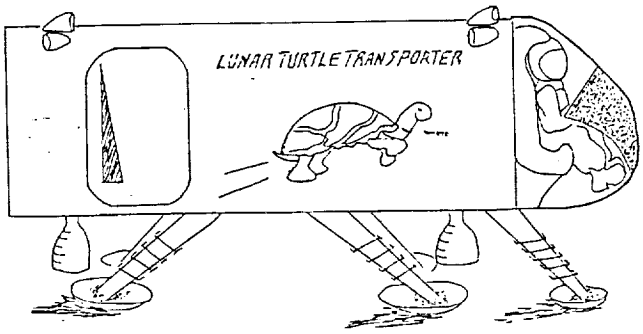

Fig. 3. Lunar Turtle Module

for use on the MPLTV. The power for the vehicle is supplied by a nuclear reactor or fuel cells with energy storage capabilities of silver zinc batteries.

Long Range Design

In this design the Lunar Turtle Module (LTM, as shown in Fig. 3) is considered to transport passengers and materials over longer distances.

The LTM is a versatile transportation vehicle that operates above the surface of the Moon. The proposed vehicle would operate using vectored thrust produced by liquid chemical rocket engines mounted on the underside of the vehicle. Initial launch is achieved with the help of a catapult system. Rotations may be obtained using small thruster rockets mounted to the sides of the LTM. Landing is achieved using the Moon's gravitational forces and the underside rocket engines are used for vehicle descent. The cockpit is designed to allow maximum comfort, visibility, and vehicle control. The cargo hold is equipped for multiple task functionality allowing for the transportation of cargo and/or people.

Cargo Bay

The LTM is provided with a reasonably sized cargo bay. The cargo bay is 22 ft long, 10 ft wide, and 8 ft high. In order to maximize storage space, the cargo bay is designed as a rectangular volume. The LTM can be used for transportation of men and/or materials. The cargo bay will not be climate controlled, hence the passengers will have to wear environmental suits. Located at the front of the cargo bay is the air lock system leading to the cockpit. The inner walls are to be a honey comb structure using Aluminum 5052. The outer surfaces are to consist of Aluminum 2024-T6 coated with Kevlar. The floor of the cargo bay will consist of sections of Aluminum 2024-T6 sheets supported by a substructure to allow access to the storage area underneath. Tie down capabilities to prevent movement of materials are provided on the floor and walls.

Cockpit

The cockpit of the LTM is to be pressurized and will utilize an existing airlock design. The University of Texas at Austin design team came up with a minimum loss airlock for use in low gravity which allows one man to enter at a time[6]. The weight of this system is 59 lbs. The cockpit consists of a control panel and two pilot seats. Glass floor and ceiling panels are used to ensure maximum visibility. The substructure and outer skin are to be made primarily with the same aluminum alloy used for the rest of the LTM. Entrance to the cockpit will be through the airlock chamber door located in the cargo bay. Onboard equipment will be powered by silver zinc batteries. These batteries have an energy efficiency greater than 70% and a life cycle of greater than 2000 cycles. The silver zinc batteries offer quick recharge capabilities and can operate at temperatures encountered in the lunar environment.

Propulsion Systems

The LTM uses a liquid chemical rocket engine, possibly one which uses liquid oxygen as the oxidizer and liquid hydrogen as the fuel, since the Moon contains both of these elements. For maneuvering, it is recommended that cold gas rockets be used. Rockets of this type are lightweight and of simple construction. These rockets will be placed in the upper corners of the LTM and will be used to orient the vehicle. The thrust required will be shared by four engines. Calculations were made considering a maximum lunar weight of 7000 lbs and a total fuel rate of 1.5 lbm/s. These assumptions were made so as to approximate the calculation of nozzle velocities and areas. An exit velocity of 10,800 fps and a nozzle diameter of 5 inches were determined. It is proposed that solid propellant rockets be used to supply the extra boost needed to reach the planned destination.

Launch

In determining the best way to launch the LTM, several methods have been considered. To minimize fuel and to take advantage of low gravity, a catapult system is proposed. To further flight distances an extra solid booster mounted to the LTM may be ignited. During the boost phase, control of the vehicle to prevent spinning and/or veering off course is achieved by the use of four retro-rockets externally mounted at the top of the LTM. For landing, the retro-rockets are used for slowing the LTM.

Other Designs

A common but innovative design called the lunar lift was also considered, which involves a cable and pulley network for hauling materials and men, powered by a thermo-electric module buried under the lunar surface. The thermal module is a thermoelectric device that utilizes a temperature differential to generate power. The underlying design of a thermo-module is based on the Seebeck effect. In the lunar lift system, a thermo-module/heat-pipe bank will charge the batteries that will run the electric motor. Such a power generation system can also be used in other designs. Design of an underground superconducting rail system using a repulsive magnetic force was also considered. Use of high-temperature superconducting material in conjunction with

highly powerful magnetic material can be an effective answer to the problem. However the problem of propulsion and control is still a major issue.

Another design of a surface-based vehicle is a lunar van with a self-sustaining oxygen supply with a range of 120 km and a payload of 3600 kgs. This land-based vehicle is of square boxed construction, taking advantage of lack of atmosphere and hence zero drag. The box is made up of aluminum-Kevlar-aluminum composite material. The wheels are magnetically levitated and are of adjustable height to compensate for rough terrain. Another design is a fast moving surface-based vehicle suspended above a trackway by the use of superconducting magnets. The power requirements for such vehicles are considerably lower than on Earth because of reduced weight and lower wind loads.

SUMMARY AND CONCLUSION

Transportation needs on the Moon can be met through the use of a multipurpose lunar vehicle for short ranges and the Lunar Turtle Module for long ranges. The power requirements can be met through the use of advanced concepts such as fuel cells augmented by banks of thermal modules.

The proposed systems are conceptual in nature and further detailed modeling, analysis, construction, and testing are needed before the final design can be achieved.

ACKNOWLEDGMENTS

The authors acknowledge the enthusiastic efforts by all the students in the introduction to design course in which most of the designs were conceived. Special appreciation is given to Shawn Greenwell, Paul Schwindt and Jennifer Lander for their relentless work.

REFERENCES

1. Apel U. Simulation of Lunar Surface Transportation, Symposium '86; The First Lunar Development Symposium, Lunar Development Council, Pitman, NJ, 1986.
2. Taylor G.J. The Lunar Environment, Symposium '86; The First Lunar Development Symposium, Lunar Development Council, Pitman, NJ, 1986.
3. Ogorkiewicz R.M. Design and Development of Fighting Vehicles, Doubleday, Garden City, New York, 1967.
4. Gleasman Corporation, Fastrac Brochure, Austin, TX, 1987.
5. Bargo Jr., M. All Gear Steering, Popular Science; July 1985.
6. Foster T.S, Kok S.N., Payne R.A., Wong Y.F. "Design of a Minimum Loss Airlock for Use In Low Gravity, High Vacuum Space Environments", The University of Texas at Austin, Austin, Texas, 1986.

LUNAR LANDING AND LAUNCH FACILITIES AND OPERATIONS

FLORIDA INSTITUTE OF TECHNOLOGY

INTRODUCTION

A preliminary definition of a lunar landing and launch facility (LLLF or Complex 39L) has been formulated. A Phase III lunar base is considered[1,2]. Without specifying specific lunar base scenarios, three traffic levels are envisioned: 6, 12, and 24 landings/launches per year. A single, multipurpose vehicle for the lunar module is assumed. The design and specification of the vehicle and of the lunar base are outside the scope of this study. However, these two items will impact those items considered within the scope of this study because of interactions at the system boundaries. The scope of this study is graphically portrayed with the systems diagram presented in Fig. 1. Major functions or facilities are represented by blocks in the system diagram. The dashed line represents the boundary of Complex 39L; and thus, the scope of this study. Figure 1 contains a simplified version of the overall system. Obviously, other items could be included; e.g., lunar surface transportation and electromagnetic launchers. A discussion of items on or outside the dashed lines which impact the design of items within the boundary will be included. Based upon this diagram, nine major design items or areas are considered. These items are:

1. Landing/Launch Site Considerations
2. Structure, Shelter, Safety, and Environmental Needs
3. Landing/Launch Guidance, Communications, and Computing Needs
4. Lunar Module Surface Transport System
5. Heavy Cargo Unloading/Loading Systems
6. Personnel Unloading/Loading Systems
7. Propellant Unloading/Loading Systems
8. Vehicle Storage
9. Maintenance, Repair, Test and Check-Out Requirements

Initially, a general, conceptual description of each of these items is given. Then, preliminary sizes, capacities, and other relevant design data for some of these items are identified. The Earth-Moon transportation infrastructure and the baseline lunar module design are summarized in Figs. 2 and 3, respectively.

MAJOR DESIGN ITEMS

1. Landing/Launch Site Considerations

The lunar module will touch down vertically on a landing/launch pad. It is desirable to have a paved landing/launch pad to satisfy lunar module transportation requirements. Loose particles on the pad can become dangerous projectiles in the presence of engine blast from the lunar module. With a paved pad this problem is greatly diminished. The ideal site would be a large expanse of flat rock which could be cleared of lunar dust and used without any further preparation. The next-best option would be to locate an area where the lunar regolith could be excavated to uncover a suitable hard rock site. From lunar surface studies it is unlikely that such an ideal site can be found[3]. Thus it becomes necessary to prepare a landing pad using other means. Concrete prepared using lunar regolith, lunar gravel, or bags of lunar regolith are three possibilities. For this study a paved landing pad is assumed.

The landing pad (Fig. 4) will be circular with a diameter of 50 m (approximately four times the diameter of the lunar module). This diameter was determined by making comparisons with terrestrial vertically landed vehicles. A similar figure (100 m) was arrived at independently by Eagle Engineering[4] from consideration of cruise missile technology. A circular area with a radius of approximately 250 m will be cleared of large rocks and equipment to guard against possible navigation errors and harmful blast effects. The landing pad will be marked with lights similar to a terrestrial airport to assist lunar module pilots with navigation and provide the necessary illumination for television cameras used by controllers in the communication and control facility. These lights will be the only equipment within the 250-m radius during landing or launch. This equipment must be capable of withstanding engine blast effects, through use of replaceable lens covers on cameras, for example. The number of landing/launch pads will depend on the flight schedule and the time required for pad maintenance. Figure 4 shows one pad, though more may be required.

2. Shelter, Structure, Safety, Environmental Needs

It is assumed that the lunar module will spend a significant period of time on the lunar surface. This period could be from 2 weeks to 2 months. When not in use, the vehicle's

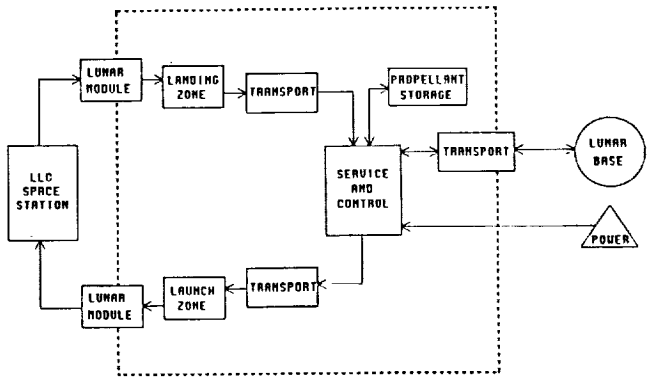

Fig. 1. Lunar Landing and Launch Facility (LLLF or Complex 39L) Systems Diagram

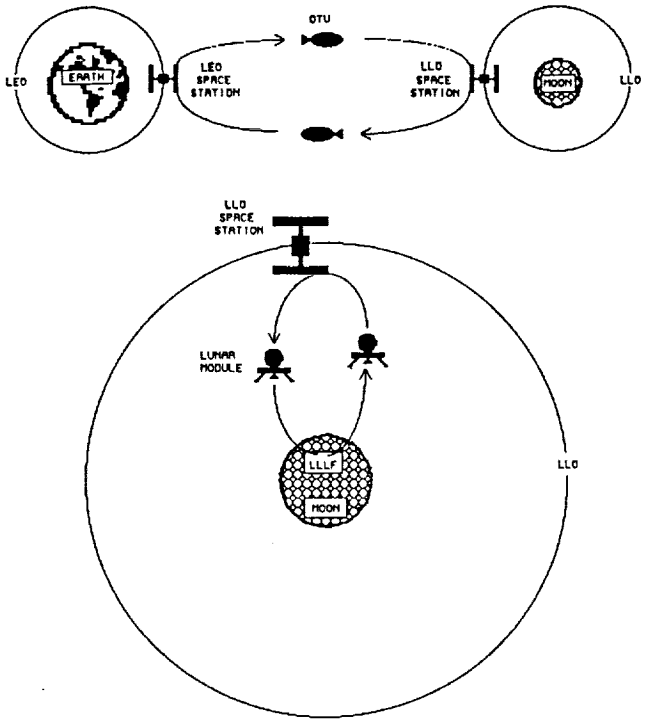

Fig. 2 Earth - Moon Transportation Infrastructure

ENGINE DATA:	
Isp (s) :	470
Number of engines :	2
Thrust per engine (N) :	33400
Mass of each engine & its thrust structure (kg) :	95
Mass ratio Oxygen/Hydrogen (kg) :	5.5
APPROXIMATE MASS (kg):	
Dry mass :	1000
Landing gear mass :	1800
Oxygen tank mass :	100
Hydrogen tank mass :	400
TOTAL MASS :	3300
APPROXIMATE PROPELLANT CAPACITY (kg):	
Oxygen :	21000
Hydrogen :	4000
TOTAL PROPELLANT CAPACITY :	25000
APPROXIMATE DIMENSIONS (m):	
Height :	10
Diameter :	13
APPROXIMATE PAYLOAD CAPACITY (kg):	
Maximum payload capacity :	15900
Liftoff payload capacity :	15900
Manned capsule (crew of 6) :	6900

Fig. 3. Baseline Lunar Module Design

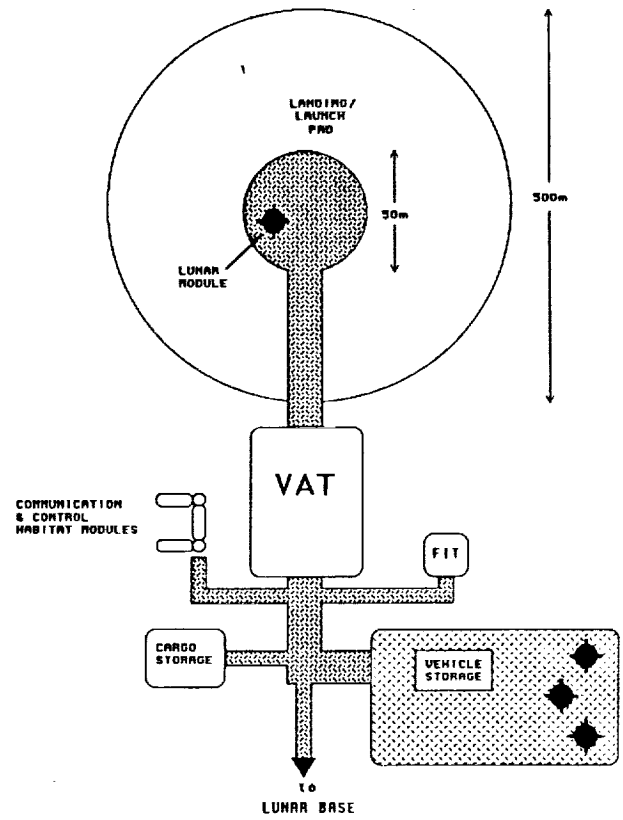

Fig. 4. Complex 39L Plot Plan

temperature should be controlled by removing it from direct sunlight. This decreases the boil-off of cryogenics and also provides a constant thermal environment. The module will be serviced by personnel wearing space suits. The shaded environment will decrease both visibility problems and life support requirements[5]. Other equipment such as robots and tools will benefit from such an environment.

A quonset hut structure is proposed for the shelter (Fig. 5). This structure is referred to as the vehicle assembly tent (VAT). The facility will be large enough to contain four lunar modules. The dimensions are 50 m long, 36 m wide, and 18 m high at the center line. Entrances, 15 m high and 16 m wide, will be located at each end of the structure. A framework will be constructed of a material such as 2014-T6 aluminum[6]. Highly reflective panels made of a mylar/evaporated aluminum laminate will shield equipment inside the VAT from incoming thermal radiation. These panels are expected to reflect approximately 90% of the thermal solar spectrum[7]. Other panel materials and laminates are being investigated. Initial calculations with one layer of panels yield a surface-level temperature inside the VAT of approximately 0° C during the lunar day. It was found that using two layers of panels separated by 0.1 m gave a decrease in surface temperature of only 8° C. The panels will be sized so that a single person wearing a space suit could replace one easily. An initial size of 2 m × 2 m will be assumed. The panels will attach to the frame at points approximately every 0.5 m. Approximately 850

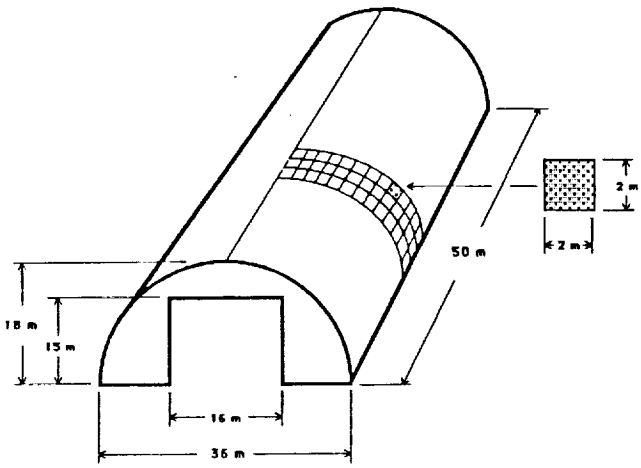

Fig. 5. Complex 39I. Vehicle Assembly Tent (VAT)

panels will be required. When a panel has degraded or been damaged it will be replaced with a new or refurbished panel. Movable flaps will be used to cover the entrances at each end of the structure. They will serve to block glare and possible particles from engine blast. These will be made of the same material as the panels and will function similarly to a typical stage curtain. They will cover an area of 240 m^2 at each end. A total mass of approximately 10 metric tons has been derived for the proposed structure.

Most servicing and unloading/loading operations will be performed in the VAT. Artificial lighting, etc., must be provided where personnel are working. This is not a pressurized facility and personnel must wear environmental suits. This facility will not block radiation that is potentially dangerous to humans, consequently, the amount of time humans can work in this environment will be limited[8]. Personnel will be able to work in the VAT approximately 33 hours per week without exceeding earth-based exposure limits (5 rem/yr). All surface activity must be discontinued during periods of solar maxima (large solar flares). It may be determined that all surface operations will be best performed during the 14-day lunar night. Electronic devices will also be affected by high doses of radiation resulting in hardware and software failures. Electronic equipment should be specially designed for lunar applications.

One of the major environmental problems is damage caused by engine blast during lunar landing and launch. The facility is located a distance of somewhat greater than 250 m from the nearest landing pad, which should be sufficient to eliminate damage from large particles (> 0.5 mm). Delicate equipment should be protected during landing and launch operations by use of a shield or protective blanket. For safety all personnel on the surface within ~ 3-5 km of the pad will be required to remain behind a protective barrier until the landing or launch operation is complete. It is possible that a large barrier could be constructed between the pad and the VAT. This could be a pile of lunar regolith or a wall made from bagging lunar regolith.

3. Landing/Launch Guidance, Communications, Computing Needs

The lunar module will be manually controlled by two pilots. Assistance will be provided by a surface communications and control facility similar to that of a terrestrial airport. It has been determined that currently available terrestrial navigation systems can be applied to achieve high degrees of landing and positioning accuracies[4]. Onboard systems will utilize terrain matching systems during periods when the base is out of view. Terrain matching radar technology is used with high degrees of accuracy in modern cruise missiles. An accurate map of lunar surface features will be required. When the lunar base is in view of the lunar module, surface-based transponders will be used. Transponders will be placed on the surface to provide high-resolution triangulation. They should be detectable by the lunar module radar system at a distance of 200 km. It is assumed that five transponders will be used. Three transponders will be placed 120° from each other at a distance of 100 m from the center of the landing pad. Two other transponders will be placed 1.5 km downrange and 1.5 km crossrange respectively. A surface-based radar system consisting of a dish approximately 1 m in diameter will be used to track the transponder aboard the lunar module. This will enable the operators in the communication and control facility to follow the lunar module and to abort unmanned flights if necessary.

4. Lunar Module Surface Transport System

The lunar module will be transported from the landing/launch pad to the VAT. A battery-powered lunar forklift is envisioned. A dolly will be placed under each footpad and a harness will be attached to the lunar module or dollies. The lunar module will then be towed by the forklift into the VAT. The forklift and the dollies will function best if the towing surface is paved and level. It is assumed that the vehicle will be operated by a person in an environmental suit, though this is an area with potential robotic application that should be investigated. This same system will be used for transporting lunar modules to vehicle storage.

5. Heavy Cargo Unloading/Loading Systems

Heavy cargo items such as habitat modules, construction equipment, nuclear reactors, and lunar oxygen (LUNOX) production modules will be transported to the lunar base on a regular basis. These items will be attached to the lunar module and may or may not be stored in containers. The lunar module will be transported into the VAT fully loaded with payload. Once in the facility the module will be unloaded. We envision the use of a bridge crane. The crane will encompass an area of 15 m by 30 m at a height of 15 m. For a preliminary design a maximum load of 45 metric tons is assumed sufficient. The center beam is designed to deflect less than 0.05 m when the maximum loading is applied at its center point. It was found that a standard 24 × 62-m-wide flange beam constructed of 4340 low-carbon steel will meet these design requirements[9]. This is a baseline design and other construction materials are

being investigated. It is assumed that the entire structure will be constructed of the same members. This gives a total crane mass of approximately 20 metric tons.

Unloading and loading operations will begin by detaching (unstrapping) a payload from the lunar module. The crane will then be positioned and attached to the payload. The payload will be lifted, transported away from the lunar module, and lowered onto either a lunar transport vehicle, a dolly, or the lunar forklift. If the transport vehicle is not available to take the payload directly to its destination, then the payload will be transported to cargo storage at Complex 39L to await further processing. The lunar forklift will be used to tow the dollies or to lift the payloads directly. Complex 39L cargo storage will be a separate tent structure similar to the VAT, located nearby (Fig. 4). The lunar module will be loaded in an inverse manner.

6. Personnel Unloading/Loading Systems

Three modes of personnel unloading/loading are envisioned. The first mode requires Extra-Vehicular Activity (EVA) similar to that used in Apollo missions. The personnel will don space suits and exit the lunar module by climbing down a ladder that is attached to one of the module legs. This can be done either on the landing/launch pad or in the VAT. If personnel exit or enter the vehicle on the pad they must either walk or be transported to or from the pad. It would be advantageous for several reasons to have the personnel exit the vehicle after it has been towed to the VAT. The main reason is a decrease in the amount of total EVA time required.

The second mode of unloading/loading is for the personnel to remain in the module until it has been transported into the VAT. They will then disembark into the pressurized compartment of a lunar surface transport vehicle. The personnel will be transported to the habitat modules or wherever their final destination may be. This is a "shirtsleeve" transport operation where space suits are not required. This mode will require a pressurized transport and an airlock mechanism to connect the two vehicles.

The third mode of unloading/loading is for the personnel to remain in the lunar module until it has been transported into the VAT. Here, the manned capsule of the lunar module will be detached, lifted by the bridge crane, and either placed on a dolly or on a lunar surface transport vehicle. The entire manned capsule will then be transported to the habitat modules where the personnel can disembark through an airlock. This mode, like the second mode, does not require EVA. However, a separate pressurized transport will not be required as in the second mode. This example illustrates the integration (modularity) that we believe is necessary for a successful lunar base.

7. Propellant Unloading/Loading Systems

The lunar module will land at Complex 39L with some propellant remaining in its fuel tanks. Assuming no LUNOX is available this will be all the hydrogen and oxygen required for the return flight to low lunar orbit (LLO). The propellant can either be left in the fuel tanks or transferred into propellant storage tanks. If boil-off from the cryogenic tanks is significant, it would be preferable to store the cryogens in larger tanks with active cooling systems. Hydrogen and oxygen storage tanks will be located at Complex 39L.

The storage requirements are set by the number of people residing at the base. As a design criteria we require that enough propellant be stored to evacuate the entire lunar base population. For a population of 30 this would require storage of approximately 150,000 kg of oxygen and 30,000 kg of hydrogen. If one spherical tank is used to store each cryogen this would require tank diameters of roughly 6.0 m and 9.0 m for oxygen and hydrogen, respectively. Multiple tanks of differing geometries may be used.

The storage tanks and pumps will be located in a separate tent near the VAT. This tent is referred to as the fuel inventory tent (FIT, Fig. 4). The lunar module will be defueled/fueled by removing the propellant tanks from the module with the bridge crane, placing the tanks on dollies, and transporting them to the propellant storage tent in the same manner that cargo is transported. All propellant transfer operations will be performed in the FIT.

8. Vehicle Storage

A long-term vehicle storage area will be provided at Complex 39L (Fig. 4). This will be an area near the VAT that has been cleared of large objects. It is assumed that some surface preparation will be required for transportation purposes, but it is unlikely that the paving requirements will be as stringent as for the landing pad. At this phase in lunar base development we envision an area large enough to contain six lunar modules (approximately 1000 m^2). Any increase in quantity of the lunar module fleet and landing/launch rates will necessitate enlarging this area.

The lunar module will be transported to vehicle storage if it has been damaged beyond repair, exceeded its operational life, or will not be used for a long period of time. The lunar

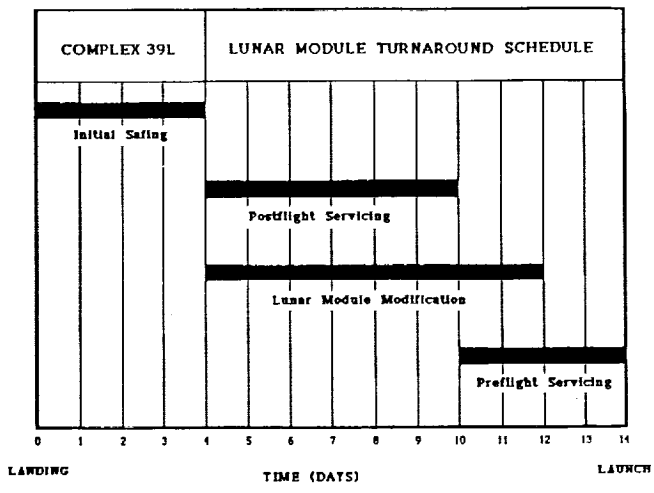

Fig. 6. Lunar Module Turnaround Schedule

modules will defuel prior to storage. The module will be towed by the lunar forklift to a storage location as discussed previously. A dome tent will then be constructed over the module. This tent will consist of the same panels used in the VAT, attached to a metal or composite support frame. The tent is used to achieve a constant thermal environment and to protect the module from potential particle bombardment. The tents must be designed to enable assembly by a few personnel in environmental suits.

9. Maintenance, Repair, Test and Check-out Requirements

The lunar module is a reusable vehicle and will require regular maintenance with each flight. Vehicle maintenance will include but is not limited to vehicle test and check-out, lubrication, recharging of environmental systems, recharging or replacing batteries, regenerating fuel cells, modular parts replacement/repair, and system modifications. Unlike presently operated reusable terrestrial space vehicles, the lunar module should require minimal maintenance. For our highest frequency flight schedule (24 flights/yr), the lunar module maintenance turnaround time is two weeks (14 days).

When a lunar module component malfunctions or is damaged, it can either be repaired or disposed of. Repairs can be performed onsite, at one of the space stations, or on Earth. In many cases it will be desirable to repair the component at Complex 39L. Lunar module mechanics will be constrained by space suits, thus making detailed repairs difficult if not impossible. Smaller components (computer systems, circuit boards, etc.) can be brought into the Communications and Control Facility to be worked on in a shirtsleeve environment. Detailed repairs on larger components (engines, fuel tanks, etc.) will require a large pressurized facility. Such a facility is beyond a Phase III lunar base, and repairs of this nature will not be possible at Complex 39L.

Four main lunar module turnaround procedures are envisioned. These procedures are Initial Safing, Postflight Servicing, Lunar Module Modification, and Preflight Servicing. The following is a preliminary description of some of the operations that will be performed during each these procedures.

Initial Safing operations will include transportation of the lunar module into the VAT, unloading or draining fuel tanks, attachment of ground power and purge lines to the lunar module, purging main engines and fuel lines to remove possible moisture resulting from hydrogen/oxygen combustion, and unloading payloads. Also, the lunar module crew will disembark sometime during the initial safing procedure. This preliminary list of required operations can easily be expanded upon.

After Initial Safing is complete, postflight troubleshooting will identify anomalies that may have occurred during launch, flight, or landing. An umbilical containing electrical, communication, instrumentation, and control lines is connected to the vehicle. Visual and electrical inspections will be performed on the lunar module. Along with postflight inspection, routine servicing will include lubrication, recharging of environmental systems, recharging or replacing batteries, regenerating fuel cells, and other required routine maintenance tasks.

Fig. 7. Lunar Landing and Launch Facility (LLLF or Complex 39L) Design Matrix

	CONSTRUCTION				OPERATION				MAINTENANCE			
	SPECIFICATION	MASS	POWER	MANPOWER	SPECIFICATION	MASS	POWER	MANPOWER	SPECIFICATION	MASS	POWER	MANPOWER
LANDING / LAUNCH SITE CONSIDERATIONS												
SHELTER, STRUCTURE, SAFETY, ENVIRONMENTAL NEEDS												
LANDING / LAUNCH GUIDANCE, COMMUNICATIONS, COMPUTING NEEDS												
LUNAR MODULE SURFACE TRANSPORT SYSTEM												
HEAVY CARGO UNLOADING / LOADING SYSTEMS												
PERSONNEL UNLOADING / LOADING SYSTEMS												
PROPELLANT UNLOADING / LOADING SYSTEMS												
VEHICLE STORAGE												
MAINTENANCE, REPAIR, TEST & CHECK-OUT REQUIREMENTS												

Lunar Module Modifications will then be made if necessary. Modifications may include replacing damaged components discovered during the postflight inspection, adding or removing equipment necessary to meet future mission requirements, and replacement of outdated hardware with new designs to enhance vehicle performance. Lander modifications, if extensive, can be performed over a long period of time while the craft is in vehicle storage. However, many modifications will be performed in parallel with routine servicing.

The lunar module will then be prepared for launch. This Preflight Servicing will include installation of flight supplies and payload, attachment of fuel tanks, loading of personnel, visual and electronic check-out of lunar module systems, detachment of ground umbilicals, and transportation from the VAT to the launch pad. Other related operations may be necessary.

A sample Lunar Module Turnaround Schedule (Fig. 6) was developed using the four main procedures just described. This figure is based upon preliminary estimates regarding the time required to perform each of the four main procedures.

CONCLUSION

Short descriptions or specifications of nine designated design items have been presented. The next stage in the design process will be to determine preliminary estimates for the major resource requirements of the system. Three major resources which were identified are mass, power, and manpower. The cost of commissioning and operating the lunar base will be directly related to the resource requirements. While mass and power requirements can generally be determined by standard engineering methods, assessments of manpower requirements can be difficult. One assumption that is made is that all EVA operations will be undertaken by at least two people. This is a safety consideration which mimics the buddy system that is used in scuba diving.

A design matrix has been developed (Fig. 7). The rows of this matrix consist of the nine major design items. Specifications, mass, power, and manpower determine the columns. Three main resource requirement areas are recognized and are referred to as: Construction, Operation, and Maintenance. The Construction area represents the resources that will be required during the construction phase of the landing and launch facility. This will include but not be limited to clearing a site of large debris, landing/launch pad preparation, construction of various tents, and assembly of cranes and other structures. The Operation area represents the resource requirements for the steady-state operation of the facility. The Maintenance area represents the facility maintenance requirements, e.g., refurbishment of landing/launch pads, tent structures, and other hardware (forklifts, cranes, etc.). A matrix element is checked off when the design work corresponding to that element has been completed.

REFERENCES

1. Roberts B.B. "Lunar Bases in the 21st Century: The First Step Towards Human Presence Beyond Earth," NASA/Johnson Space Center, March 1987.
2. Ride S.K. *Leadership and America's Future in Space: A Report to the Administrative National Aeronautics and Space Administration,* Washington, D.C., 1987.
3. Taylor S.R. *Planetary Science: A Lunar Perspective*, Lunar and Planetary Institute, Houston, TX, 1982.
4. Eagle Engineering Inc., Lunar Base Launch and Landing Facility Conceptual Design, NASA Contract No. NAS 9-17878, EEI Report 88-178, March, 1988.
5. Eagle Engineering Inc., Lunar Surface Operations Study, NASA Contract No. NAS 9-17878, EEI Report No. 87-172, December, 1987.
6. *Engineering Data for Aluminum Structures*, The Aluminum Association, 750 Third Avenue, New York, NY, 1975.
7. Incropera F.P., DeWitt D.P. *Fundamentals of Heat and Mass Transfer*, John Wiley & Sons, New York, NY, 1985.
8. Adams J.H., Shapiro M.M. Irradiation of the Moon by Galactic Cosmic Rays and Other Particles. *Lunar Bases and Space Activities of the 21st Century*, Lunar and Planetary Institute, Houston, Texas, pp. 315-327, 1985.
9. Bowles J.E. *Structural Steel Design Data Manual*, McGraw-Hill Book Company, New York, NY, 1980.

THREE-LEGGED MOBILE PLATFORM: SKITTER

GEORGIA INSTITUTE OF TECHNOLOGY

Described herein is a system of equipment intended for site preparation and construction of a lunar base. The proximate era of lunar exploration and the initial phase of outpost habitation are addressed. Drilling, mining, and beneficiation of lunar soil prior to pilot-plant oxygen extraction and other soil processing techniques are included within the scope of this system's capabilities. The centerpiece of the design is the SKITTER mobile walking, site preparation, and construction platform. The SKITTER system is modular in nature and includes a series of interchangable implements whose individual use tends to be seasonal or intermittent. The concept is analogous to the farmer's tractor and implement set. The proposed system is mechanically simple and weight efficient and the individual implements are designed to take advantage of the lunar environment while operating within the constraints imposed by that environment. The system's implement interfaces can also be used for transporting containerized cargo on the lunar surface. A proposed lunar orbit to lunar surface landing pod might also be used to deliver the walker and crane boom combination in a ready-to-work configuration.

INTRODUCTION

Conceptual design is currently in progress for a system of equipment to conduct site preparation and construction on the lunar surface. This effort is centered in the Engineering Design Laboratory at the Georgia Institute of Technology in conjunction with the NASA/USRA Advanced Design Program. Proof-of-principle models have also been developed to validate certain new technologies and concepts to be utilized.

Previously, little attention has been directed to the phase of lunar surface activity that begins once equipment has landed and ends when the initial habitats become usable. Even then, the hopper must be filled before the first oxygen extraction plant can become operational. Artistic renderings up to the present time have typically envisioned terrestrial types of equipment (such as the bulldozer and the backhoe) being used. An engineering design approach to the mission, however, shows the impracticality of such equipment that has not been uniquely designed for the lunar environment. In particular, such traditional equipment typically depends on its earthly weight for counterbalance and for reaction to the application force.

Deliverability to the Moon and the absence of human operators during the unmanned phase of exploration and surface preparation place additional constraints on the design and implementation of any construction equipment. Design principles subsequently emphasized in this program included the following:

- Mechanical simplicity
- Fault and accident tolerance
- Minimal weight
- Robotic maintenance and repair
- Commonality of parts
- Standardization for compatibility
- Reloadable, task-specific control software
- Localized bearing of forces within the system to avoid load transfer to supporting structures
- Adaptability to mission changes
- Modularity for weight and damage control

THREE-LEGGED MOBILE PLATFORM: SKITTER

A three-legged walker is proposed as a mobile work platform for most of the activities involved in lunar base site preparation and construction. Initially named SKITTER because of the envisioned ability to "skitter" over the surface of the Moon, it may also be defined as a Spatial Kinematic Inertial Translatory Tripod Extremity Robot (SKITTER). Utilizing the principle of dynamic stability and taking advantage of the Moon's low gravity, the system is capable of walking in any radial direction and rotating around a point. The current light-weight configuration is intended to clear the surface by some four meters.

When used as a carrier for a series of specialized implements, it will enable or enhance the stability and dexterity of each implement to provide a mechanically simple and weight-efficient means of carrying out such tasks as digging, drilling, leveling, hoisting, and mining. SKITTER is also designed to transport lunar soil or containerized cargo. It is further designed for landing with a crane or robotic arm implement attached, and detaching its Viking-like landing pod.

A working proof-of-principle model of SKITTER was designed and demonstrated at the NASA/USRA Summer Conference held in Washington D.C. in 1987. During the following year, efforts by some of the participating students have been concentrated on the design of a more comprehensive model, SKITTER II. These efforts are described in the following paragraphs:

3-D Graphic Simulation

Extensive analysis was conducted on the kinematic and dynamic characteristics of SKITTER. As a result, two user-friendly programs were written such that any physical trait of the platform (i.e., mass, inertia, length) or constants (i.e., gravity) could be easily varied to optimize the system.

*SKIT*TORQUE is a program written to simulate platform operations during either the "lean" or "jump" modes of operation. The solution methodologies corresponding to these

kinematic problems were implemented in a computer program in order to solve for the angular velocity and acceleration components of each joint. The determination of these values was necessary for completely solving the dynamic problem. To accomplish this, the Newtonian force equations were derived for the linkage so that the torque about each of the joints could be solved for as a function of its position.

Computer graphic simulation is an excellent engineering tool for analyzing and designing spatial mechanisms. SKIT-3D is a three-dimensional graphic simulation program which allows the user to visualize SKITTER's spatial configurations by controlling system, leg segment, or actuator movements of a screen representation of the platform. User input is in the form of incremental positioning, direct positioning, or time-based data files which can be used for platform animation. Output is directed to a screen, plotter, or dump device.

Platform Structure

Two student groups worked on the task of optimizing the platform structure. Ease of assembly and weight reduction were the primary design constraints. One group approached the problem by using a tubular truss structure and modeled femur, tibia, and central body components as well as joint connections using the SUPERTAB finite element modeling routine. The final iteration of this design cut the initial SKITTER I weight by approximately fifty percent. The second group approached the problem by using a monocoque design. By utilizing composite materials, this group was able to cut the initial weight of SKITTER I by fifty percent.

IMPLEMENTS

Utilizing the dexterity of the three-legged walker permits each task-specific implement to be designed with greater mechanical simplicity and minimum weight. Each implement is self-sufficient in that it includes its own power, controls, and communication devices.

SKITTER is designed with two triangular interfaces of identical size, one on the upper interface of the body and one on the lower. Most of the implements that have been designed by the students are anticipated to attach interchangeably to the lower interface. Commonality of the locking system will allow successive implements to be selected, utilized, and then replaced in storage. Cargo pods and the Viking-type landing pod can likewise utilize the bottom interface.

Digger

This implement will be used for general excavation and soil handling for surface reconfiguration. This includes digging, trenching, and leveling. The digger will also support lunar resource pilot plants by mining and loading of soil. The digging implement is comprised of a moderate length arm and a powerful end-effector. The end-effector consists of two independent clamshell-type buckets arranged back to back so as to generate equal but opposite forces for either digging or clamping. The major loads and stresses are subsequently handled by the end-effector. By utilizing the principle of opposing forces, the emplanting and scooping function can be achieved with little reliance on the force of gravity. The arm can be used to impact the bucket tips into the soil to break up crust and aggregates prior to digging and scooping. Leveling is accomplished by planting one bucket and then moving the other. The reverse surfaces of the buckets can act together to clamp on a boulder for its handling. The implement utilizes the walker's dexterity to extend its work envelope, especially where deep holes or trenches are required.

Since the buckets scoop away from one another, they can be unloaded one at a time into the bulk transport vehicle. A conveyor or hopper associated with a pilot plant can also be loaded directly.

Fluid conduits, fiber optic and electric cables can be emplaced by trenching and backfilling with the implement.

Drill

The drill implement includes a rack and changer mechanism for storing and handling the drill string rod elements. A variety of drill bits and sample acquisition devices will be available on the rack to best address each given task. Rotary and short-stroke vertical actuators power the down-hole activities. The walker provides a stable platform and the large, generally vertical motion for inserting and withdrawing the drill string as the work progresses. The walker also provides the tilt and off-hole motions required by some of the drilling and sample acquisition techniques.

The use of heat pipes facilitates limiting the maximum temperature of the drill bit. The heat is thus conducted to the lower portion of the drill string. A significant portion of the heat generated as the drill progresses is contained in the cuttings. By removing the cuttings quickly, the bit temperature management is enhanced.

Cutting removal from the bit location is accomplished by an enclosed staircase-like device. This device incorporates vertical fences arranged radially at intervals along a generally helical auger flight. By accelerating the device vertically upward, the cuttings achieve a given vertical velocity. As the device stops, the cuttings ricochet off the underside of the helical ceiling above. The cuttings advance one or more fences up the staircase. A net upward progression of the cuttings continues with successive strokes of the device. A proof-of-principle model has successfully demonstrated this staircase auger concept. The low lunar gravity is expected to enhance this process. Cutting removal at an extended depth may be accomplished by a continuous staircase or to a coaxial bail that is intermittently raised to the surface. Uses of the drill include sample acquisition, drilling holes for emplacing scientific instruments and anchors, and testing foundation quality at proposed facility sites.

Slinger

The primary purpose of the slinger implement is to cover a lunar habitat module with loose regolith. The regolith must be classified into large and small particle sizes to avoid damage

to the skin of the module by large particle impact. The tool at the operating point of the implement is a rotating disc that has intermittently spaced radial tabs attached to both flat surfaces. The implement engages the disc into the surface of the soil and as the disc rotates, the tabs dig and accelerate the smaller particles into a trajectory. This stream of soil is directed toward the module by manipulating the orientation of the disc. Particles much larger than the working edge of the tabs are thrown to the side rather than along the stream of the smaller particles. Thus a single moving part digs, classifies, and ejects the desired particles toward the module. A proof-of-principle device has been shown to be capable of slinging only the sand from a sand-gravel mix.

Both the disc and partial guard are expected to wear, so a rack of replacements is incorporated in the implement. The arm is capable of loading the replacement wheel/guard assembly onto the spindle. Overall, the device is somewhat analogous to a snowblower except that it preclassifies by size of the particles to be thrown.

Robotic Arm

The robotic arm implement may be connected to the upper or lower interface on SKITTER. Its uses include maintenance and repair of other machines, emplacing scientific instruments and handling of small secondary equipment. It includes a rack of interchangeable end-effectors and adaptors. The walker's onsite dexterity can be used to extend and shape the useful work envelope of the arm.

Palletized Cargo

The walker is capable of transporting cargo that is engaged at the lower interface. The pallet or cargo container would be equipped the same as an implement with respect to the mechanical configuration of the interface. The cargo mass, geometry, and rigidity must conform to identified constraints.

Procedurally, the walker would orient itself to engage the pallet interface, actuate the latch mechanism, then raise to walk to the desired site. There, the procedure would be reversed after placing the pallet on the surface or other fixed location.

Bulk Transport Vehicle

This four wheeled vehicle is intended for transportation of a variety of bulk materials and cargo on the lunar surface. It is equipped with a direct-coupled, curvilinear synchronous motor at each wheel. The wheel spindles are rigidly mounted to the chassis. The chassis is comprised of two nearly identical sections, one at the front and one at the rear, providing independent roll and articulated steering motions. A separate body is centered near each of the two axles and can be tilted to dump its contents. In dumping lunar soil, as an example, one body would dump to the rear, and the other would dump as the vehicle moves in the opposite direction.

Interchangeable bodies can be installed to suit specific tasks. The top of each body is configured similarly to an implement. This allows the walker to handle the body exchange task. It is also feasible to use a combination of the dump, steer, and wheel actuators to self-right the vehicle following a rollover accident.

CONCLUSION

During the past year great progress was made in three areas.

Teaching of the Design Process. Nearly 180 students met the challenge of designing equipment for the unique lunar environment with creative and innovative designs. In the process, they learned about system organization, database usage, Computer Aided Design (CAD), finite-element analysis, patent proceedings, product liability, and engineering professionalism which will enhance their design careers.

Expanding the Design Program. Discussions with the top academic administrators at Georgia Tech are currently underway for the development of an interdisciplinary design program. The new program would expose more students from a variety of backgrounds to the challenges of designing for space applications.

Georgia Tech looks forward to the exciting year ahead in continuing their relationship with NASA, USRA, and other universities for developing new concepts for space applications.

THREE SYNERGISTIC STUDIES: A MANNED LUNAR OUTPOST, A MANNED MARS EXPLORER, AND AN ANTARCTIC PLANETARY TESTBED

UNIVERSITY OF HOUSTON

The students at the University of Houston College of Architecture undertook three synergistic studies during the 1987-1988 academic year. These studies included a Manned Lunar Outpost, a Manned Mars Explorer Mission, and an Antarctic Planetary Testbed which would provide the necessary data and facilities for testing proposed missions to the Moon, Mars and beyond. All research was based on existing or near-term technology.

MANNED LUNAR OUTPOST

The Manned Lunar Outpost (MLO) is proposed as an initial permanent base for manned activities on the Moon. The study concentrated on identifying the equipment, support systems, and initial base configuration necessary to accomplish the various science, industrial, and exploration activities envisioned. The mission planning included goals of low dependence on Earth-based goods, support of the Space Station, and the eventual self-sufficiency of the MLO by incorporating an agriculture facility.

The primary concepts of the MLO were: using hard modules for habitation areas with inflatable interconnect nodes; creating a flexible, modular transportation system; designing a multifunctional vehicle; and using an overhead radiation protection system.

The transportation system, dubbed the Lunar Mobile Surface Transport System (LMSTS), carries the hard modules to the surface of the Moon and provides a method to move them to the desired location through the use of interchangeable pallets (Fig. 1). The avionics pallets are changed out with wheel and hitch pallets, transforming the LMSTS into a "tractor-trailer" used with the Multi-Functional Vehicle (MFV) (Fig. 2). In addition, the LMSTS aids in the positioning and leveling of the modules as they are docked into the outpost configuration.

The MFV design consists of a pressurized temporary safe haven, a crane, and modular implements. It would be used extensively during the installation of the outpost.

The modules are placed under the Regolith Support Structure (RSS) which provides a stable environment and radiation protection for the entire base (Fig. 3). The overhead structure was selected, as opposed to simply burying the modules, to provide the opportunity to study the advantages and disadvantages of this type of system. The advantages were determined to include easy access to the exterior of the modules, providing a protected area for vehicles and equipment used in EVA, and creating an area of constant temperature. Disadvantages include a need for prefabrication of structural components in low Earth orbit (LEO), and the need to develop a conveyor system to lift the regolith into place. However, once in place, the RSS provides a very flexible system, readily accommodating the future growth of the outpost.

The research considers all components in depth, including the preconstruction and construction phases of the initial MLO. Study team members included Nathan Moore, Thomas Polette, and Larry Toups, with Nilanjan Bhattacharya consulting.

MANNED MARS EXPLORER

The Manned Mars Explorer study had two primary objectives: to develop a mission scenario to deliver a crew of six to the vicinity of Mars; and to design a transportation system to accomplish this mission.

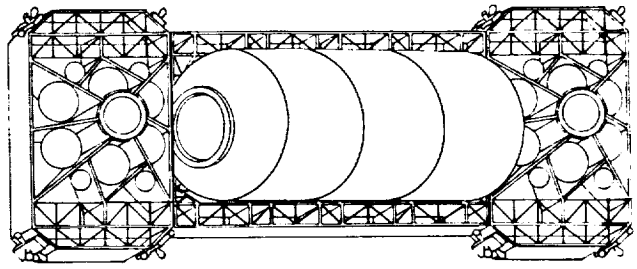

Fig. 1: Lunar Mobile Surface Transport System

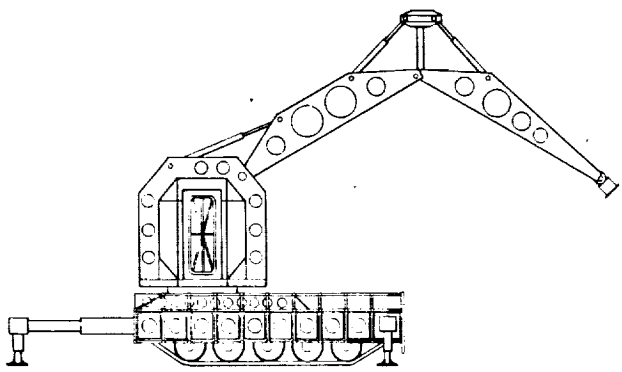

Fig. 2: Multi-Functional Vehicle

Several criteria were established as principal drivers for the mission scenario. These included:

1. Using an opposition class Venus inbound swingby trajectory. This option offers a relatively short overall mission, compared to conjunction class missions, while allowing a Mars vicinity staytime of 60 days for exploration, prospecting, and resource evaluation and utilization.

2. Planning a manned Mars landing for scientific as well as political reasons.

3. Concentrating on studying Phobos and/or Deimos as an initial staging base for Mars vicinity activity. Phobos and Deimos offer incentives for utilization which include natural resources, a negligible gravity environment, and Mars observation capability. Many excursions will be planned for the surface of Phobos and/or Deimos after a manned Mars landing.

4. Depending on highly reliable and reusable vehicles and components for redundant tasks throughout the mission.

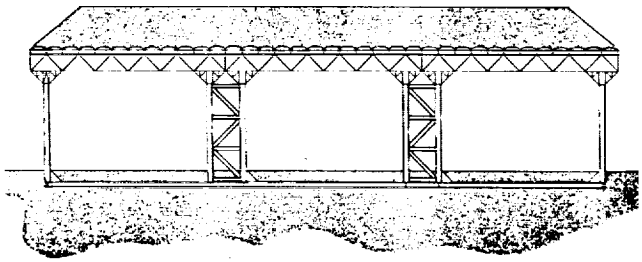

Fig. 3: Regolith Support Structure

Based on these criteria the following mission scenario was developed: A Manned Planetary Vehicle (MPV) would be built in LEO, then outfitted with a crew of six. The MPV would travel to the vicinity of Mars in approximately 300 days, where it would stay for 60 days before the return leg to LEO of approximately 210 days.

The 60-day exploration period to the vicinity of Mars would consist of sending a crew of three to the surface of Mars for one week. The crew would then return to the MPV and spend the remainder of the time ferrying between the MPV and Phobos/Deimos. During this period, they would perform scientific study on resource utilization of Phobos/Deimos, and remote sensing of Mars.

The transportation system design encompassed several considerations including: all chemical propulsion vs. nuclear electric propulsion; the issue of reliability vs. redundancy; the need for artificial gravity vs. zero gravity; and the use of necessary but undeveloped technologies such as large-scale aerobraking and tether systems. The illustrated design proposes the use of mature technologies combined with those just over the horizon to offer alternatives for a cost-efficient mission to Mars.

The primary components of the transportation system included a Manned Planetary Vehicle (Fig. 4) and a Crew Command Vehicle (Fig. 5). As part of an alternative split mission to Mars the design of an Interplanetary Cargo Transport Vehicle and Manned Planetary Vehicle were developed, both using nuclear electric propulsion.

A detailed comparison of chemical vs. nuclear electric propulsion for the MPV was made, and an all chemical mission was chosen as the most realistic. The MPV was designed to create 1 g of artificial gravity for crew health and safety. To

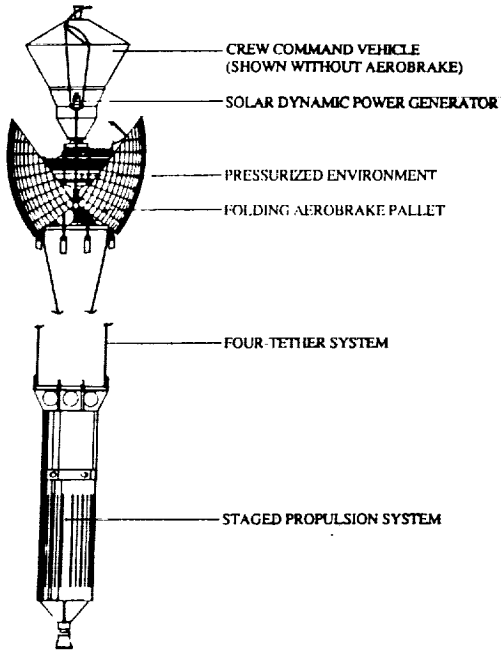

Fig. 4: Manned Planetary Vehicle Components

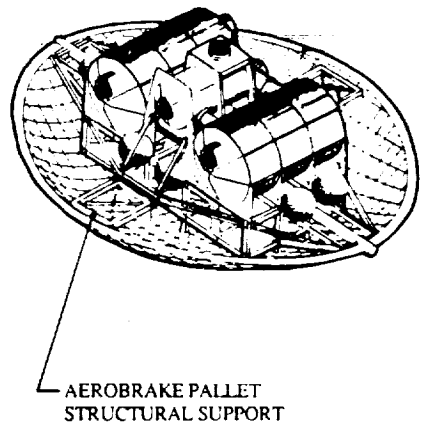

MPV Detail

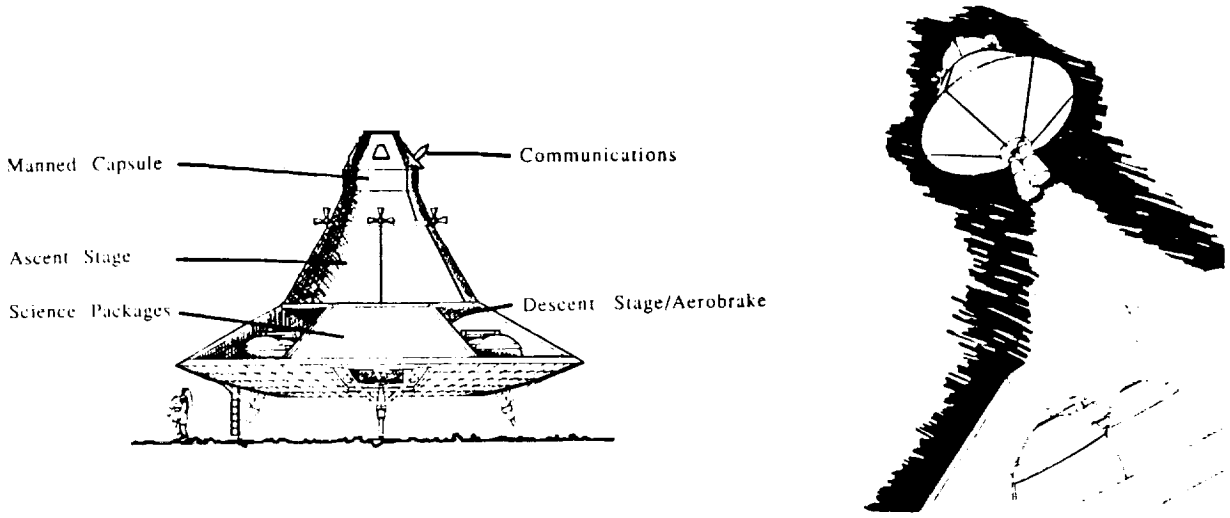

Fig. 5: Crew Command Vehicle

accomplish this task, a tether system was developed which resists twisting through a unique spreader system. The tether would be deployed during trans-Mars coast and trans-Earth coast and reeled in for all propulsive maneuvers.

Due to the long and dangerous nature of this mission, reliability of vehicle components was established as a driving force in design. This was shown through the design of a multifunctional Crew Command Vehicle (CCV) which would house the crew during all propulsive maneuvers and ferry the crew between the MPV, Mars, and Phobos/Deimos.

Study team members included Sean Nolan, Deborah Neubek, and C. J. Baxmann.

ANTARCTIC PLANETARY TESTBED

The Antarctic Planetary Testbed was conceived as a project to complement crew preparation and construction technology development for a lunar base, Mars, and other planetary exploration. The primary focus of the research was the development of a program that defined the needs of a planetary testbed. Through the research of appropriate analogs, these needs were defined as a masterplan, selection of a transportation system, development of a construction system, and design of a module which responds to the program requirements.

The project's proposed Dry Valley site was chosen because of its similarity to the harsh Martian environment as well as the bare lunar landscape. The analogs also include international cooperation, scientific research, supply/resupply logistics and "launch windows" determined by weather conditions that limit or prohibit sea and air access to the continent (Fig. 6).

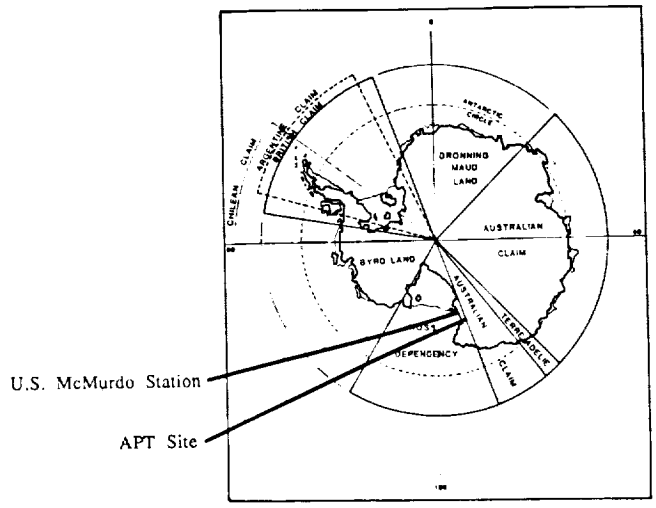

Fig. 6: Map of Antarctica

The masterplan consists of sixteen circulation modules, two habitation and laboratory/work modules, a galley module, a recreation module, an experiment/health maintenance module and a utility/logistics module. An inflatable structure is envisioned to provide a large area for vehicle storage and agricultural facilities. An observation/control tower is also included to be used for construction coordination and scientific use.

The transportation system, construction system, and design of the modules were interrelated in their development. Because of the limitations of delivery vehicles, the Sikorsky "Skycrane" helicopter was chosen as the method of transportation and placement for the modules. A module had to be developed using volume and weight limitations of this delivery vehicle that also adhered to Space Station module dimensions and ratios.

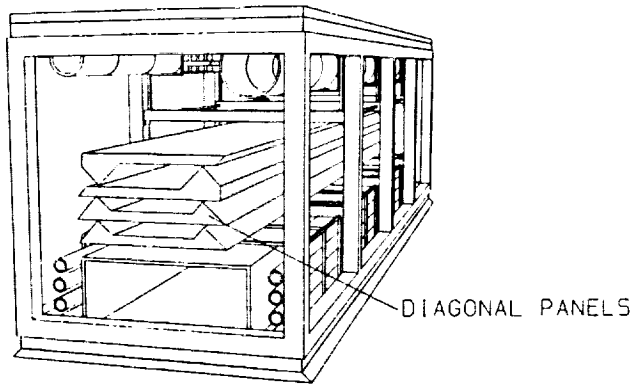

Fig. 7: Packed Module

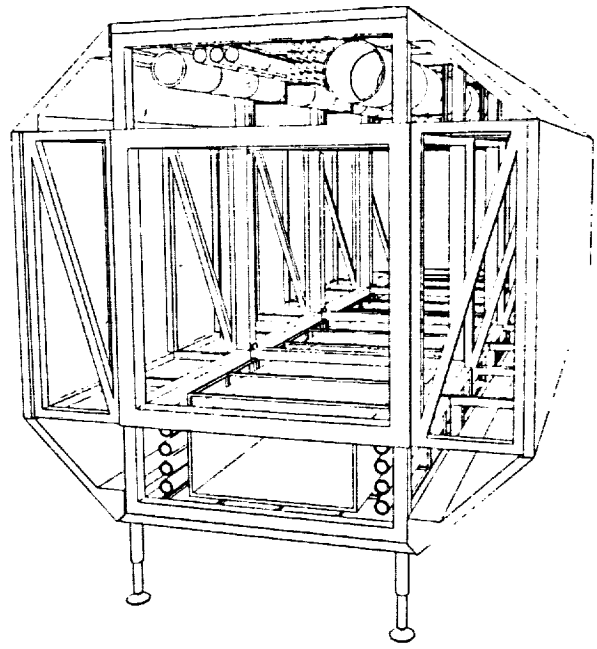

Fig. 8: Fully Deployed Module

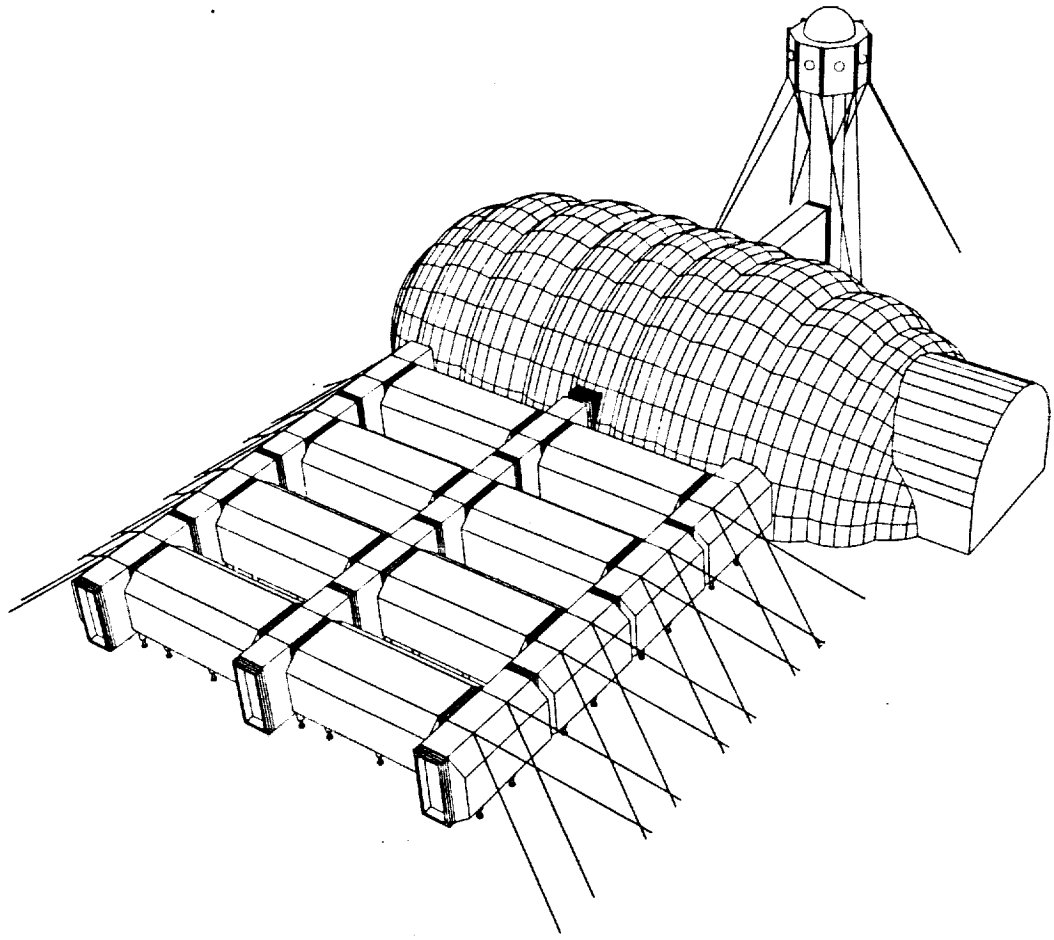

Fig. 9: Perspective of Masterplan

This module became the basic building block of the base. It consists of a compact core with two telescoping utility compartments, one on the top and one at the bottom. Once these utility compartments are deployed, the circulation core is exposed and Space Station-derived racks are attached to the sides. The modules are then leveled by six hydraulic jacks (Figs. 7 and 8).

In addition to the master planning and design of basic module types, a conceptual analysis was done for support facilities such as power generation systems, waste management systems, and space planning for the crew habitation modules (Fig. 9).

As the project evolved, it became increasingly evident that its potential uses go far beyond just the training of space mission crews. If appropriately executed and managed, this facility could offer an ideal testing ground for advanced technologies and systems for immediate benefits on Earth.

Study team members included Mashid (Shi Shi) Ahmadi, Alejandro Bottelli, Fernando Brave, and Muhammad A. Siddiqui.

MARSPLANE

UNIVERSITY OF ILLINOIS AT URBANA-CHAMPAIGN

INTRODUCTION

The concept of utilizing a winged vehicle for the remote exploration of Mars was studied in the 1970's[1,2]. This study, directed by NASA's Jet Propulsion Laboratory, considered an unmanned, instrumented platform to perform the necessary mission requirements to study the Mars environment. Two versions were considered. In one, the Marsplane was deployed during the entry maneuver and flew until its fuel was exhausted. Its mission ended with the subsequent landing. In the second version, the Marsplane could land and take off a limited number of times.

In the past decade, technological advances[3,4,5] in materials, aerodynamics, and propulsion systems have increased the feasibility of a Marsplane. It was the objective of this year's design project to examine the impact of these technological advances and to investigate (1) the feasibility of a manned Marsplane, and (2) the spacecraft system necessary to deliver the Marsplane to the surface of Mars.

MARSPLANE SUMMARY

Mission and Design Specifications

The general specifications for the Marsplane design were:

Payload: 1200 N; two suited astronauts with life support systems sufficient for eight hours,

Airfield Performance: Operations from prepared airstrips no longer than 1.0 km,

Cruise Performance: A unrefueled endurance of 8.0 hrs. at a cruise altitude of 1500 m, and

Crew Rescue: Scenario for the rescue of the crew of a down and disabled Marsplane.

(All Marsplane weights are those that would be experienced on Mars.)

For the purposes of the design, it was assumed that the mission would occur in the 1995 to 2020 timeframe, that facilities on the martian surface would be available for assembling and servicing the Marsplane, and that all necessary operational facilities, materials, and supplies (e.g., fuel) would be available.

The major technical areas of responsibility for the Marsplane design group members were Aerodynamics, Performance, Power and Propulsion, Stability and Control, Structures and Materials, Surface Operations, and Weights and Balance. Because of the special problems of takeoff and landing (and the wide range of possible solutions to these problems), airfield performance and design of the takeoff and landing systems were included as part of surface operations. In addition to the above major technical areas, several areas of less importance (e.g., auxiliary systems, packaging and assembly, and rescue scenarios) were studied by the design groups.

Design Drivers

The principal design drivers were found to be:

Low martian atmospheric density. This led to the need for very low wing loadings (and correspondingly low component weights) and for aerodynamic designs that were efficient at low Reynolds numbers.

Need for a lightweight propulsion system (including fuel weight). This was exacerbated by lack of fuel components in the atmosphere. This led to the need for high propulsion system and aerodynamic efficiencies.

Airfield performance specification and rescue capability. This stimulated several designs to include Vertical Takeoff and Landing (VTOL) capabilities.

Design Considerations and Results

1. Aerodynamics. The low atmospheric density together with the need for high aerodynamic efficiency (i.e., low power required) at cruise required the designs to incorporate large wing areas, large aspect ratios and high cruise lift coefficients. It was also necessary to select wing airfoils with good stall characteristics (maximum C_L>1.0) and low-profile drag at the low cruise Reynolds numbers (i.e., in the neighborhood of 1×10^5). All of the design groups found satisfactory solutions to this problem, although in some designs the stall speed and low cruise speed were uncomfortably close together. The resulting Marsplane configurations included conventional tail aft, canard, joined wing and, in one case, a sail wing.

2. Propulsion Systems. The need for high overall propulsion system efficiency drove all the design groups to select propellers for climb and cruise. In most cases, other propulsion systems were proposed for airfield operations. In seven of the eight designs, the propellers were driven by electric motors; in the other design, rocket motors at the blade tips were used. The power sources for the motors were batteries, fuel cells, solar cells (or a combination of these), and, in one case, a Stirling engine. The most promising systems appeared to be based on hydrogen/oxygen fuel cells with the resulting water conserved and recycled at the Marsplane base.

3. Materials, Structures, and Weights. In all cases, composite materials were selected for the aircraft structure. Due to the lack of algorithms for estimating the weight of an advanced aircraft concept such as the Marsplane, the estimated mass results for conventional structures were reduced by 15 to 25% to account for the use of composites. In addition, the estimated weight of joined-wing designs was further reduced on the basis of results reported. The structural designs were

essentially conventional except for the sail wing. In that case, the wing was formed by a leading-edge spar, a trailing-edge cable, and a fabric envelope.

The weight breakdowns for the Marsplane are presented in Table 1. Note the major importance of the propulsion system (including fuel) weight.

A serious question that was not addressed was whether durable structures can be made at the weights used in these studies. In particular, the design of wings with the large aspect ratios needs further study.

4. Climb and Cruise Performance. The climb performance was modest because low installed power (corresponding to low propulsion system weight) was a resultant design parameter. Surface level maximum climb rates ranged from 0.34 m/s (67 fpm) to 7.91 m/s (1557 fpm) with an average value of 2.7 m/s (531 fpm), corresponding to an average time to climb to cruise altitude of about 10 min.

Cruise speeds ranged from 60 to 100 m/s with an average of 78 m/s. At cruise altitude, the stalling speeds ranged from 41 to 87 m/s with an average of 57 m/s. The average ratio of cruise to stalling speed was 1.37.

The average total range for all designs was 2140 km with results from 1812 to 2761 km. Two of the designs failed to meet the endurance requirement.

5. Surface Operations. Takeoff and landing performance proved to be the most difficult design specification to satisfy. Because of the very low power-to-weight ratios dictated by the cruise performance specifications, none of the designs could meet the 1.0-km takeoff field length requirement without additional propulsion assistance. All of the designs used some form of rocket-based assistance. The solutions were grouped as follows.

Take-off Method	Number of Designs
Towed by a cart	1
Carried by a cart	3
Auxiliary rocket package; jettisoned	1
Vertical take-off	3

All designs had conventional landing capabilities; however, two of the designs did not satisfy the 1.0-km field length specification. In addition to conventional landing capability, three of the designs had rocket-powered vertical landing options.

The above airfield performance characteristics resulted in only three designs that could carry out the required rescue mission. This was accomplished by carrying extra fuel for a vertical takeoff and landing sequence at the rescue site. The remaining five designs were limited to dropping emergency supplies to downed crew.

Table 1. Marsplane Weight Data

Group No.	Airframe		Propulsion System (including fuel)		Payload		Misc.		Total
	(N)	(%)	(N)	(%)	(N)	(%)	(N)	(%)	(N)
1	2435	48.7	1210	24.2	1200	24.0	155	3.1	5000
2	2437	52.5	806	17.4	1200	25.9	199	4.3	4642
3	2747	36.6	3246	43.3	1200	16.0	309	4.1	7502
4	2977	48.7	1707	27.9	1174	19.2	260	4.2	6118
5	2216	36.9	2524	42.1	1200	20.0	60	1.0	6000
6	1429	29.8	2075	43.2	1200	25.0	95	2.0	4799
7	2688	54.5	932	18.9	1214	24.6	99	2.0	4933
8	2532	42.5	1839	30.9	1200	20.1	386	6.5	5957

SPACECRAFT SUMMARY

Mission and Design Specifications

The spacecraft mission was characterized by two primary infrastructure components; a payload re-entry system carrying the Marsplane and an instrument bus carrying scientific instruments for remote sensing of the planet's surface. The instrument bus was to remain in orbit after separation from the re-entry system.

Enclosed in a sealed capsule and decelerated into a parking orbit by an advanced aerobrake, the re-entry spacecraft will await an opportune window for descent to the surface. Remote-sensing instruments will determine if the predesignated landing site is suitable before committing the re-entry system for descent to the surface. After the spacecraft's descent from orbit, the instrument bus remaining on-orbit will act as a relay satellite supporting the plane in its operations.

Packaging requirements specifying volume and mass were dictated by the Marsplane design groups. Several additional mission requirements were also specified for the interplanetary transport system in a Request for Proposal (RFP) given to the students at the start of the semester. A partial list is given here:

1. Subsystems identified for the purposes of system integration were: Aerobrake (including orbit capture, reentry, and detachment), Structure (including materials, design layout, thermal control), Power and Propulsion, Command and Data Control, Science and Radio Relay Instrumentation, and Mission Management, Planning, and Costing.

2. The spacecraft's components and payload will be delivered to orbit in the cargo bay of the space shuttle and be assembled on-orbit at the space station spacecraft assembly and repair facility. The extent of shuttle support should be identified and minimized.

3. The spacecraft will be able to be retrieved by a remote manipulation device on the space station or space shuttle.

4. Nothing in the delivery system's design shall preclude it from performing several possible missions, carrying vastly different payloads to different destinations.

5. The spacecraft will have a design lifetime of four years, but nothing in its design shall preclude it from exceeding this lifetime.

6. The vehicle will use technology available before 1998 and use the latest advances in artificial intelligence where applicable to enhance mission reliability and reduce mission costs.

7. The design will stress simplicity, reliability, and low cost.

8. For cost estimating and overall planning, it will be assumed that four spacecraft/delivery systems will be built. Three will be flight ready while the fourth will be retained for use in an integrated ground test system.

9. Mission science requirements were based on the NASA Solar System Exploration Committee's recommendations and included: (a) determining the elemental and mineralogical composition of the martian surface; (b) determining the distribution, abundance, sources, and concentration of volatile materials and dust; (c) defining the global gravitational magnetic fields; (d) measuring the global surface topography; and (e) examining the structure and circulation of the martian atmosphere.

Configuration Descriptions

Seven different configurations resulted from the spacecraft design groups. Inertia configurations were obtained for each spacecraft and delivery system[8]. Analysis showed that a thermal stagnation point exists approximately two aerobrake shield diameters behind the aerobrake. Accordingly, the aircraft payloads were packaged to fit within the resulting protected conical volume behind the aerobrake. In most instances the aerobrake was reused for re-entry protection.

Propulsion Systems Design and Integration

One of the mission requirements specified the use of an aerobrake for the delivery system to reduce the total mission fuel requirements. The use of an aerobrake at the Mars terminal end of the trajectory reduced total ΔV requirements to approximately 4.5 km/s. A one-year time of flight was typical for these trajectories.

Conventional liquid oxygen-liquid hydrogen propulsion systems were typically used to accelerate the delivery system from low Earth orbit on its way to Mars. For the initial orbit capture and subsequent terminal orbit maneuvers, space-storable propellants were used. Typically, these were nitrogen tetroxide/50% UDMH-hydrazine based systems, with an I_{sp} of 293 s. Thus, it was demonstrated that it is possible, using today's technology, to deliver the plane/spacecraft payload to Mars.

A program called AEROB[9] allowed the optimization of shield size vs. injected mass vs. initial semi-major axis of the Mars capture orbit to be performed. Shield sizes of 120 m^2 were typical for injected masses of 4800 kg with an initial semi-major axis of 150,000 km and maximum allowable shield temperatures of 600°C. Three-dimensional terrain plots produced with the data obtained from AEROB were then constructed to identify the optimal operating parameters. Compared to conventional orbit capture propulsion systems, one group concluded that a 30% upmass savings resulted from the use of the aerobrake.

Performance

Several different trajectory options were explored for the mission using the MULIMP trajectory generation program[10]. While Venus flybys were examined, requirements for a minimum ΔV were best made by a direct ascent for the optimistic launch window between 2005 and 2010.

Total upmass (wet delivery vehicle, spacecraft, and payload) varied from 15,800 kg to 28,000 kg.

With an assumed base in place at Mars, one group found it to be advantageous to transfer vehicle control from the Earth to the Mars base at an appropriate time during the mission. This decreased roundtrip communications times from the spacecraft to the base of control from 36.94 minutes (control always at Earth) to 6.65 minutes (switched from Earth to Mars at Launch + 76 days).

Terminal orbit selection varied among the design groups. While some groups sought to provide maximum global coverage of the planet's surface, others sought to maximize contact time with the Marsplane when it was in flight. Taking advantage of the fact that three delivery systems would carry their respective payloads (Marsplane and spacecraft) to Mars and then be available for operations, one group selected a sun-synchronous orbit for two of their spacecraft. This arrangement guaranteed global coverage of the planet by the remote-sensing instruments as well as continuous contact with the Marsplane.

A strawman science instrument package was defined by each of the design groups. A representative package included a gamma-ray spectrometer, a near-infrared mapping spectrometer, a UV photometer, a dust detector, an atmospheric sounder, a UV spectrometer, and a magnetometer.

Downmass to the surface was on the order of two Viking landers. Parachutes and landing rockets were sized to provide a soft touchdown on the surface. Two 6.2 m disk-gap-band parachutes typically were used to decelerate the landing payload from Mach 2.1 to 100 m/s. At an appropriate point above the surface, Viking-type retro rockets provided the terminal thrust profile, and hydraulically operated shock absorbers provided the final landing load support.

Economic Analysis

Two types of cost analysis were undertaken by the seven groups. Most relied on a spreadsheet program obtained from the NASA Marshall Space Flight Center[11]. Input to the spreadsheet consisted of subsystem mass totals which were directly proportional to the estimated cost of the spacecraft systems. Two groups used equations developed by Science Applications International Corporation (SAIC)[12] for generating cost estimates. Most of the cost estimates were on the order of $1.5 billion.

CONCLUSIONS

The Marsplane and Delivery System Project demonstrated the technical feasibility of transporting an atmospheric flight system to Mars, assembling it there, and using it to carry out manned aerial reconnaissance of the martian surface. Given certain enabling technologies now under development (e.g., low mass propulsion and structural systems, in situ fuels, etc.), a manned Marsplane appears to be a viable tool for use in future exploration of Mars.

REFERENCES

1. Clarke V.C., Kerem A, and Lewis R. A Mars Airplane, *Astronautics and Aeronautics*, pp. 42-53, January, 1979.
2. Kerem A. A Concept Study of a Remotely Piloted Vehicle for Mars Exploration, Developmental Sciences Inc., August, 1978.
3. Boucher R.J. Sunrise, The World's First Solar-Powered Airplane, AIAA J. Aircraft 22, No. 10, pp. 840-846, October, 1985.
4. Burke J.D. The Gossamer Condor and Albatross: A Case Study in Aircraft Design, AIAA Professional Study Series, June, 1980.
5. Hall D.W, et al. A Preliminary Study of Solar-Powered Aircraft and Associated Power Trains, NASA Contractor Report 3699, 1983.
6. Wolkovitch J. Principles of the Joined Wing, Eagle Engineering Co. Report No. 80-1, December, 1980.
7. Wolkovitch J. The Joined Wing: An Overview, AIAA J. Aircraft 23, No. 3, pp. 161-178, March, 1986.
8. INERT program developed for USRA program at the University of Illinois by AAE 241 teaching assistants.
9. AEROB program made available by Dr. Steve Hoffman, Science Applications International Corporation, Schaumburg, IL
10. MULIMP trajectory generation program made available by Science Applications International Corporation, Schaumburg, IL
11. MSFC cost model made available by Dr. Joe Haymaker, Huntsville, AL.
12. Science Applications International Corporation Cost Estimation Techniques for Planetary Missions, 1987.

A DUAL-ARMED FREE FLYER

UNIVERSITY OF MARYLAND

INTRODUCTION

In this summary, we present the main conclusions and results of a design study conducted by a group of 25 students at the University of Maryland. The students, all participants in the spring 1988 courses ENEE488Q and ENEE418 in the Electrical Engineering Department, considered the problem of designing a free-flying space robot for applications in satellite servicing. In addition to the paper study, a subgroup of eight students undertook the ambitious task of designing and building a laboratory testbed for the concept of a free flyer. This subgroup has already completed the main fabrication of the mechanical hardware and most of the onboard electronics. When completed by the end of the summer, the test bed will consist of a seven-degrees-of-freedom dual-armed planar robot that will float on an air table and carry out various commanded tasks. All the fabrication and testing is being conducted in the Intelligent Servosystems Laboratory at the University of Maryland.

The project team split up into subgroups as follows: (a) articulation concepts 1 and 2, to study competing ideas for the overall systems architecture and manipulator design; (b) real time control systems group; (c) a computer graphics group to provide animations of a planar design; (d) a mechanical hardware design group for the laboratory testbed; and (e) a control systems hardware design group for the same.

In this summary report, we discuss the results in functional terms rather than in terms of the breakdown into groups.

A principal source of specifications for the design study was the Request for Proposals (RFP) issued by NASA Goddard Space Flight Center for the Flight Telerobotic Servicer Project (FTS). (Phase-B FTS Design Study was awarded to Martin Marietta Aerospace and Grumman Space Systems.)

1. System Architecture for the Free Flyer

The design of our Free Flyer is based on the existing Multimission Modular Spacecraft (MMS) system architecture since this design has already been built and tested extensively. The MMS consists of four removable modules and an adapter ring to carry the payload (the free flyer). The four modules are (1) Communication and Data Handling, (2) Attitude Control System (ACS), (3) Power, and (4) Propulsion.

The Communication and Data Handling module contains a computer which controls the Propulsion and Attitude Control modules, the antennae of the free flyer, and all housekeeping tasks related to the MMS. It does not control the manipulator arms of the free flyer. A separate computer on the free flyer will control the arms. Our design uses this module with no alterations.

The Attitude Control System (ACS) is used to orient and stabilize the spacecraft. The ACS, as we have adapted it to our design, uses momentum wheels for attitude stabilization and a propulsion system for orbit control in addition to the following hardware components to achieve fully autonomous orbit determination: one earth sensor, four sun sensors, one polaris sensor, and one onboard clock.

The requirements for the power system are from 1500-3000 W nominal load power for a maximum time without recharge of 8 hrs. For the power system, we had the choice of two types of storage cells, either nickel-hydrogen ($Ni-H_2$), or nickel-cadmium (Ni-Cd). The $Ni-H_2$ weighs less and is less expensive when used above 1500 W. The Ni-Cd is superior in cell volume but the volumes approach each other as the power approaches 3000 W. Also under consideration was a retractable solar array which would be used as a source for recharging as well as backup power. The retraction capability is necessary because of free-flyer robotic operations and maneuvers which would be encumbered if the solar array was permanently fixed. Both gallium-arsenide (Ga-As) and silicon solar cells were compared and the Ga-As cell was found to have better performance. Two designs for mechanical retraction and a third design using an umbilical cord instead of the solar arrays were worked out and their performance analyzed.

The propulsion will consist of 12 low-level thrusters and 4 high level thrusters. Functions include correction of orbit error, normal mode attitude control, station keeping, and repositioning. Of the three types of propellant (solid, liquid, and electrical), a liquid propellant was chosen due to various adverse effects from the others that preclude their use.

There are three modes of operation for the free flyer. In independent mode, the free flyer will be mounted onto the MMS system and will operate away from the space station for applications on free-flying platforms. In this mode the MMS system will provide the attitude control and limited-range (1000 km) translational motion and local orientation motion. If orbit transfer is required, the MMS propulsion module will be connected to the Orbital Maneuvering Vehicle (OMV). Power will be provided by the MMS power module and the internal battery module of the free flyer. Communication will be provided through the high-gain antennae via the MMS system communications module.

The other two modes of operation call for the free flyer to be disconnected from the MMS system and mounted on either the space station manipulator or the space shuttle manipulator arm. In these modes, the manipulator arm will provide the attitude control and necessary translational and orientational motion. Power will be provided by the space station or shuttle

power systems through an umbilical connection as well as from the internal batteries, and communication will also be provided through the umbilical.

2. Arm Design

Each of two groups designed an arm. One group worked on a novel "elephant trunk" design, whereas the other group chose a more conventional multi-link arm with both translational and rotational degrees of freedom.

Initially the first group wanted to design a flexible arm that behaved like an elephant trunk because the flexible nature of the arm would allow it to work well in constrained spaces. The arm was to be composed of a number of flattened spheres or "Go stones," all in contact with each other. The stones would have holes in the sides where control wires could be fed through to form an appendage. The shape of the arm would depend on the position of the control wires. The design group favored this but it also noted some serious drawbacks if this design were to be used in space. The group modified this design to use hollow cones stacked on one another instead of the "Go stones," and added a ball joint at the top of each cone to support bearing forces. Structurally this was a stronger design but it still employed wires that could become brittle in a space environment. To solve this problem, the wires were replaced by four linear actuators connected between each cone at the outer portion of the cone. This design is similar to the remote manipulator design developed by L. Leifer and V. Scheinman at Stanford University. Once they had the basic design, they then chose the materials, bearings, linear actuators, cone parameters, and general sizing of the hardware. For the cone material, the group considered metals, plastics, composites, Aramid, and finally settled on a fiber-reinforced graphite/epoxy with a silicone coating to shield it from radiation. This material has been used previously by General Electric for the Air Force Defense Satellite Communications Systems III as well as by General Dynamics for NASA's Remote Manipulator System. The approximate weight of each cone would be 0.56 lbs. For the outer coating, Dupont has developed a teflon fluorinated ethylene propylene which rejects up to 100,000 BTU/hr and has excellent UV resistance.

The workspace of the cone arm depends on parameters determining the cone geometry; the optimal design had 10 cones with an angle between any two cones of ± 20°.

3. Tactile Sensing

The Free Flyer must be able to determine when contact is made with an object at the end effector and how much force is being exerted upon the object. Tactile sensors can decompose the applied force into its three components whereas a pressure sensor can only measure normal force. Tactile sensing involves both transduction, or the conversion of the force into an electrical signal and data processing, or the conversion of the signal into useful information. The ideal tactile sensor should have capabilities similar to those of the human sense of touch. It should have high sensitivity and high dynamic range (1-1000 g). The spatial resolution should be approximately 0.1 mm. The sensor's response should be stable, repeatable, and fast (a response time of 1-10 msec). Nonlinearities are tolerable but they require more processing, and hysteresis should be eliminated. The sensor should be durable and should survive in the space environment. To satisfy these goals, we considered piezoelectric, electro-optical, and piezoresistive sensors.

Piezoelectric sensors are very durable and flexible but they measure only dynamic forces and are highly temperature sensitive. Electro-optical sensors rely on the modulation of a light source by mechanical deformation of a flexible material. Their main advantages are their high sensitivity and immunity to outside effects such as electromagnetic interference. Problems with these devices are short fatigue life, slow reaction time (1/30 sec), restricted dynamic range of 18:1, and highly nonlinear response. The third and probably most useful design is the silicon piezoresistive tactile sensor. It works on the principle that forces on a piezoresistive material can be measured by changes in the internal resistance of the material. The piezoresistive sensor measures static as well as dynamic forces and is not nearly as temperature dependent as the piezoelectric sensor. Finally the sensor can be fabricated in silicon and is very cost effective. Therefore, the group chose the piezoresistive tactile sensor and designs incorporating it have been done by a student in the course.

4. Laboratory Testbed Design

The design and assembly of a small-scale, two-dimensional, dual-armed free flyer (DAFF) robot for simulations and other experimental procedures in zero gravity (0-g) was the goal of the hardware simulation group. In designing the DAFF robot, the foremost goal was to provide an accurate simulation of 0-g in two dimensions. For this reason, the DAFF contains gas jet propulsion and two manipulator arms, each with two segments and a simple, pinching end effector. Permanent magnet DC (PMDC) servo motors are used to power the manipulators and parallel, gripping end effectors. The arms, in the present configuration are limited to two degrees of freedom each, but allowances were made to add another degree of freedom easily.

For the DAFF control system, a hierarchical computer control structure similar to that proposed for the actual free flyer has been implemented. The placement of levels of the hierarchy has been distributed both on and off the DAFF, linked by radio control to provide the greatest flexibility and accessibility for software programming. All the control parameters for the DAFF motors and propulsion are implemented in software. The onboard computer, a VME-bus-based 68000 system was chosen for its high power, its expendability via the standard bus, and the availability of an operating system which can support the hierarchical control structure likely to be used on an actual free flyer. It also allows for very easy software development and testing.

4.1 Propulsion System for the DAFF. The jet propulsion system will consist of four fixed-position jet nozzles, two firing forward and two firing backward, located at the four corners of the DAFF platform. The jets will function primarily for translational motion by firing either the forward or the reverse

jets. The system will also be capable of rotational control by firing alternate-corner jets for either clockwise or counterclockwise rotation. The jets will be controlled by four two-way, normally-closed valves coupled with a common propellant canister through a four-output manifold. The pneumatic valves will operate on a 5-volt trigger level, and will require two bits of control for forward, backward, clockwise, and counterclockwise rotation. The propellent will be transferred to the jets by flexible pneumatic tubing. The jets will be affixed to the DAFF platform by a rigid bracket which will allow for easy replacement of the jets for experimental purposes. Care will be taken in placement of the jets so that exhaust gases do not impinge on the DAFF platform or the experimental target object.

4.2 DAFF Architecture. The architecture of the DAFF control system is based on two design goals. We want to closely simulate the actual Dual-Armed Free Flyer, and to make the system as versatile and expandable as possible. The DAFF control system consists of a onboard computer and an offboard personal computer (PC). The onboard computer, a VME-bus-based 68000 microprocessor, is responsible for running the control loops for the motors and actuators and for some housekeeping tasks. The 68000 is given control command over the radio link from the PC and the radio link is also used for return information from the 68000 to the PC. The PC is used for high-level algorithms which can range from simple direct control of the DAFF in an open-loop configuration to complex analysis of motion under computer control. The PC serves as a user interface, and is capable of both human interaction or connection to another computer running decision algorithms.

The architecture of the onboard computer consists of a single microprocessor card, the MIZAR 8115, a disc controller for the MIZAR, a card containing the components of the cordless-telephone radio link, and one or more computer interface cards for control, containing electronics that link to various cards containing amplifiers and drivers for the motors and gas jets. This architecture is designed to provide expandability through use of the VME bus and from the modularity of the various systems. It is also intended to allow for easy development of software, because the MIZAR is a full-featured computer that can be hooked up to a terminal, and has an operating system that allows programs to be developed and tested interactively and saved to disk. In the DAFF system, the computer can operate in development or remote modes. In development mode, the DAFF is hooked up to its two external connectors which provide external power and link the MIZAR to a disk drive and to the PC, which will be used as an RS232 terminal to connect to the operating system. In remote operation mode, the DAFF is run from batteries, and once programs have been booted, the terminal and disk drive are disconnected and the computer takes command through the radio link to its other port.

Interfacing with the DC motors and the propulsion system is accomplished by the addition of interface cards to the bus. These cards contain the custom digital-to-analog converters and data latches. The power circuitry of the necessary amplifiers and drivers is positioned on cards that are not connected to the backplane, although they are held in the subrack.

5. Graphics and Real Time Systems

A significant proportion of the semester's work was devoted to the design of a real-time control system as an operating system and also the design of good graphical animation environment for the study of sophisticated motion-planning algorithms. The details are discussed in the main body of the Final Report. A current version of the operating system runs on a Sun 3/260 and the animation runs on Silicon Graphics Workstations.

CAMELOT II: PERSONNEL TRANSPORT BETWEEN EARTH AND MARS

UNIVERSITY OF MICHIGAN

A summary of the second phase of a design study of a cycling spacecraft for regular and frequent personnel transport between Earth and a Mars base is presented. The first-phase study, called project CAMELOT, was a mission analysis and configuration design and was completed by the Space Systems Design class at the University of Michigan in the winter term, 1987. In the second phase, the configuration and component design has been developed by the Space Systems Design class in the winter term, 1988, beyond the initial configuration study. Analysis has led to numerous design modifications and improvements, as well as providing more detailed system definition. Major components of the second-phase study include innovative detailed designs such as an interface between the rotating and non-rotating portions of the spacecraft, an elevator system that changes orientation to eliminate Coriolis forces, an electromagnetic radiation shield that significantly reduces the mass of the spacecraft, and a detailed assembly sequence and cost analysis. In addition, modifications to the propulsion and the power generation subsystems, taxi-docking facilities, and internal layout design have led to a more efficient, more reliable, and more comfortable vehicle. Finite-element stress and dynamic analysis has verified much of the system and indicates the validity of the design. Computer simulation of many moving components, including torus rotation, elevator and interface operations, and attitude control mechanisms further validate and support the various systems.

INTRODUCTION: DESIGN REQUIREMENTS

The initial study examined the mission objectives, functions, and requirements for the spacecraft. The mission of the spacecraft is to provide frequent and regular transportation of personnel between Earth and a Mars base. One of the assumptions for this study is that 17 engineers and scientists are required every few years to replace existing crew of the Mars base. The primary objective of Project CAMELOT is to transport these seventeen people to Mars in the shortest possible time that will allow for regularity and frequency of such transfer. The Mars base is assumed to be well developed with a large support infrastructure consisting of supply tankers, fueling stations, a Phobos mining station, and adequate communications facilities.

Consideration of the trajectories required and the functions that the transportation system would perform led to an initial configuration whose main features were a large rotating torus, a non-rotating boom, two docking ports, a microgravity research facility, and three solar dynamic collection clusters. As a result of the requirements and subsequent design to meet these requirements, the initial design team coined the acronym CAMELOT-Circulating Autonomous Mars-Earth Luxury Orbital Transport. In the current study no changes were made in the mission objectives or trajectory requirements, but several key changes have been made in the spacecraft systems and layout. Figure 1 shows the resulting design of the spacecraft from the second phase study.

NOMINAL TRAJECTORY

The nominal trajectory was calculated using several standard simplifications, namely:

1. Earth and Mars are in concentric, co-planar, circular orbits around the sun.
2. Gravity effects of Mars are ignored.
3. The synodic period of Earth and Mars is 2.135 yrs.

These assumptions result in an up-escalator orbit that has a period of 2.135 yrs, exactly equal to the synodic period, with a short-leg transfer time between Earth and Mars of only 4.5 months and a long-leg transfer time between Mars and Earth of 21 months. By equating the period of the escalator orbit with the synodic period of the two planets, the spacecraft should encounter Earth and Mars in the same relative positions each orbit. The issue is complicated, however, by the fact that the Earth-Mars alignment, while repeating every synodic period relative to each other, does not repeat itself in an inertial reference frame. The Earth-Mars alignment occurs 48.7° beyond the initial encounter relative to heliocentric coordinates. This advance in the positions of the planets requires that the semi-major axis of the escalator orbit also be rotated by 48.7° in order for the encounters to occur on a regular basis. With a flyby altitude of 1000 km from the Earth's surface, a rotation of 43.7° is achieved using a gravitation assist at Earth. This is almost the entire rotation required and a small impulsive burn (ΔV) near aphelion of the spacecraft's orbit provides the remaining 5° of rotation.

MISSION OVERVIEW

After the spacecraft has been assembled in low Earth orbit (LEO) and inserted into the escalator trajectory, two taxis (orbital transfer vehicles) will depart from a LEO space station with seventeen passengers (the three spacecraft crew members will already be on board) and rendezvous with the spacecraft. The two taxis will berth and remain attached until five days prior to flyby of Mars. The seventeen passengers will then disembark via the taxis to replace seventeen people currently serving their tour of duty on the Mars base. The three spacecraft crew members will remain on board for station-keeping and maintenance purposes until the next encounter with Earth.

At approximately the same time of taxi departure for the spacecraft, two taxis will depart the Phobos spaceport with the

replaced Mars-base personnel for eventual rendezvous with the spacecraft. The taxis will be required to complete impulsive burns that will allow each taxi to escape planetary gravity along hyperbolic trajectories that will intercept the spacecraft escalator trajectory. These two taxis will remain with the spacecraft until the next planetary encounter. Earth encounter and taxi transfer will occur in a similar manner. The Earth taxi base will most likely be stationed in a low Earth orbit, possibly as a space station.

PROPULSION

In order for the orbital maneuvers to be correctly performed, various propulsion and attitude control systems were designed. These include thrusters to spin up and maintain the spin rate of the torus, engines for initial spacecraft orbital insertion, engines for the propulsive ΔV to rotate the orbit, and attitude control thrusters for solar alignment.

To provide torus spin four pairs of thrusters are placed on the torus with the required amount of fuel. The actual spin-up takes about four hours. Orbital insertion from LEO is accomplished with nine liquid hydrogen/liquid oxygen (LH_2/LOX) rocket engines which generate about 70,000 N of thrust each. The burn time for insertion is approximately eight hours. The insertion burn is made with the end of the spacecraft boom and solar collectors facing almost 90° in relation to the sun. Immediately after insertion a moment is applied to rotate the vessel. This is accomplished by placing three engines near the end of the boom. Each generates 2500-4400 N of thrust. The entire maneuver takes approximately one hour. During this time electrical power must be provided by fuel cells, as the solar collectors will not be in their optimum operating position.

Once the solar collectors are oriented towards the sun, a continuous force of approximately 55 N is provided by nine hydrogen resistojets, each producing about 0.1 N of thrust, mounted at the end of the boom near the main engines in order to keep the collectors pointed at the sun.

The torus must maintain a relatively constant rotation for artificial gravity. As it spins, there will be some frictional forces in the interface which will induce boom rotation. To prevent boom rotation small thrusters will be mounted along the length of the boom and on the trusses which support the solar collectors.

Due to the nature of the up-escalator orbit and its interaction with the orbits of the Earth and Moon, no corrective orbital burn will be required until the third, fourth and fifth orbits. The corrective orbital burns require no additional rotation, as they are to be perpendicular to the plane of the spacecraft's motion, a ΔV away from the sun. The ΔV required can be provided by five main engines firing at full power, over a period of approximately one hour at aphelion of the orbit.

Other considerations are engine lifetime and fuel storage. Because the initial insertion uses 80% of the effective lifetime of the nine main engines, and they are not needed again until the third aphelion, they will be removed when the spacecraft encounters the Earth for the first time. At that time a pod with only five engines of the same type will be attached, to be used for the orbital corrections. Additional fuel tanks for LH_2 and LOX will be included in this pod. As the total time required for orbital corrections is less than four hours, the maintenance required for these five engines should be minimal.

During the course of the mission the LH_2 and LOX will suffer a certain amount of boil-off due to solar radiation. To minimize boil-off the main engines are shielded from their fuel tanks by a thermal insulator. The shape, insulation, and paint of the tanks are also designed to minimize boil-off. A small amount of extra fuel will be carried in each tank as a safety factor. Because the temperature of LOX is higher than that of LH_2 it is less vulnerable to radiation-induced boil-off, thus the LOX tanks will be placed sunward of the LH_2 tanks to provide further shielding.

DOCKING

A two-module docking facility has been designed incorporating significant changes since the earlier study. The two modules are the Docking and Operations Capsule (DOC), and the Cargo Acquisition Bay (CAB). The DOC contains all the operations and control for (1) berthing of aeroassisted manned transfer vehicles (Taxis), (2) Mobile Remote Manipulator System (MRMS), (3) Cargo Acquisition Bay (CAB), and (4) Extra Vehicular Activity (EVA).

The DOC contains the two berthing ports where the taxis mate with the spacecraft. The berthing is done using a system of two arms for each port that attach to the taxis after they have achieved rendezvous and berth them to the spacecraft. The DOC also contains an airlock chamber that is used for transfer of large cargo between the CAB and the rest of the spacecraft. This airlock is the interface to the unpressurized CAB and serves as an EVA staging area. In addition, the airlock has a contingency exit leading directly to the outside and can be used as a hyperbaric chamber in case of an emergency.

The Cargo Acquisition Bay (CAB) was designed to be a multipurpose port for transfer of all nonmanned cargo and also to serve as a multipurpose space platform for a number of established and unforeseen uses. The CAB uses two MRMS to transfer the cargo that is brought up on the supply spacecraft. These MRMS are mounted on tracks, allowing them to traverse the entire nonrotating structure of the spacecraft. In addition, the CAB is also used for (1) a platform for repair and maintenance of the CASTLE, (2) taxi maintenance, (3) space-based manufacturing, and (4) long-duration exposure experiments.

POWER SYSTEMS

Three important power levels-minimum life support, normal operations, minimum power available-have been detailed in the original CAMELOT report. The revised figures for power allotment are (1) minimum life support = 200 kW, (2) normal operations = 350 kW, and (3) minimum power available = 400 kW.

Based on these power allotments, as well as other considerations, it was determined that a solar dynamic power

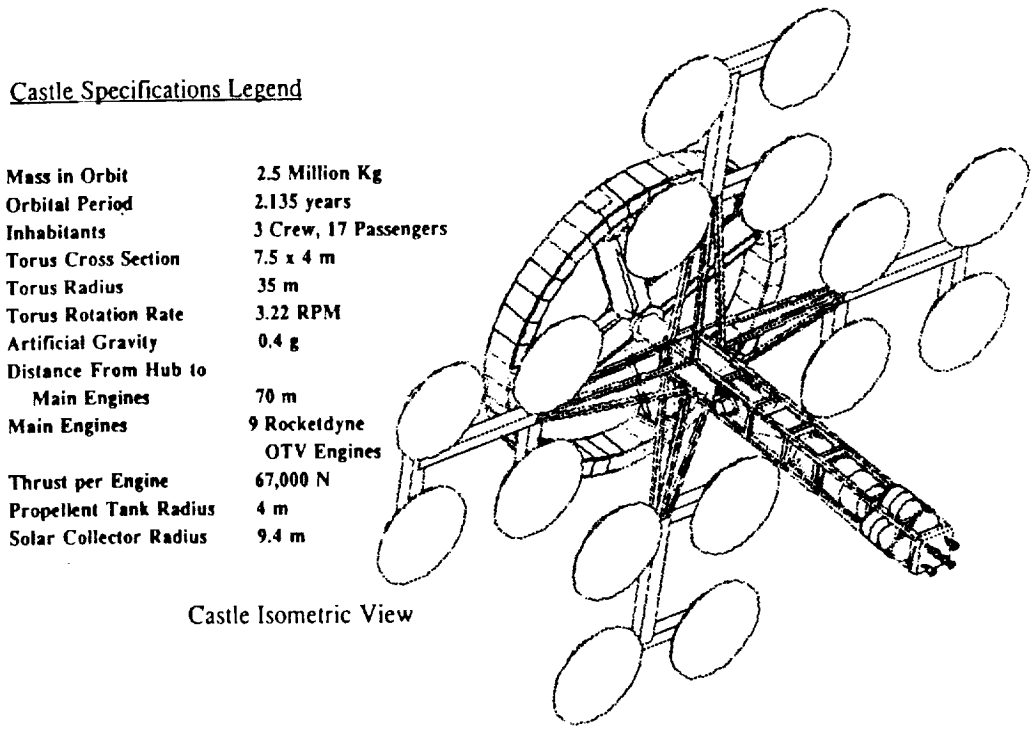

Fig. 1. Design Specifications

system would be used as the primary power system. A solar dynamic power system consists of an energy source subsystem, a power conversion subsystem, and a radiator subsystem. The energy source subsystem is made up of a solar concentrator that focuses energy from the sun into a receiver. The power conversion subsystem consists of a heat engine that converts thermal energy into electricity by using an alternator. The radiator subsystem rejects the waste heat from the heat engine.

The solar dynamic system has sixteen solar dynamic units. At the ends of each of the four booms, which are spaced evenly and extend out from the main truss, are four solar dynamic units. Each of the sixteen concentrators will be of the Newtonian parabolic type. The sixteen heat engines are free-piston Stirling engines with linear alternators and the radiators are of the Curie point radiator design. The reverse power system consists of hydrogen-oxygen regenerative fuel cells. Conditioning and regulation of all power generated is done by a power management and distribution system of 20 kHz, 440 V, AC power relying upon expert systems.

INTERFACE

The nonrotating section of the spacecraft houses the solar dynamic power units, orbital insertion burn engines, and communications systems, all of which require careful control and precise orientation throughout the mission. Other important operations undertaken in the nonrotating section are the docking of taxis and microgravity research.

An interface system has been devised to maintain a zero relative rotation between the torus and the boom. Sections of the interface are arranged as concentric cylinders. The outer cylinder is the rotating portion of the interface and is connected to the truss structure of the boom and the microgravity lab. Bridging the cylinders are two sets of bearing races. The angular contact bearings which are contained in these races allow the torus to rotate while the boom remains stationary. The major problem that arises is friction in the bearings. This will cause the boom to "bleed" energy from the torus, thus decreasing the rotation rate of the torus and increasing rotation of the boom. While the system is made as friction free as possible, a torque compensation system (TCS), which is a combination of a drive gear around the circumference of the interface with four electric drive motors, is required.

The TCS uses thrusters on the solar array booms, four 1/4-hp (137.5-W) feedback-controlled AC induction motors, and a gearing system in the hub. When the torus slows down due to friction (i.e., the nonrotating boom begins to rotate), thrusters on the solar arrays will be fired to counteract the angular momentum of the non-rotating boom. Simultaneously, the AC motors will be activated to bring the angular velocity of the torus back up to 3.2 rpm.

Load Transfer

The interface also serves as the means of transferring thrust loads from the boom to the torus. These forces will be greatest during insertion and other correction burns. The boom truss structure carries the loads to the interface through the load transfer cone, which connects the end of the boom to the

inner cylinder of the interface. The angular contact ball-bearing system then transfers the forces to the outer cylinder of the interface which is connected to the hub of the torus.

Personnel and Crew Transfer

A third concentric cylinder located within the inner, nonrotating portion of the interface, called the egress tube, serves as a hallway through which personnel and equipment are transferred in a shirtsleeve environment. The egress tube is pressurized from the micro-gravity lab section of the boom, and at the hub end of the egress tube there is a hydraulically extendable connection which then mates with the elevator to form a pressurized hallway.

Power and Data Transfer

Since electricity is generated in the solar arrays positioned on the nonrotating boom, the majority of the power generated will have to cross the interface to get to the torus. Power transfer is completed by utilization of up to six electrical conducting rollers located between the two surfaces. This method has a 99% efficiency and offers very small frictional contribution. Continuous communications flow through the interface is also essential. Data transfer and communication is accomplished through two sets of six laser transmitters, one on either side of the gap, paired with two sets of optical collectors found directly opposite.

ELEVATOR

In order to reach the torus, which is the main living and working area, personnel and supplies must travel through the interface. At the interface, astronauts enter an elevator car and travel out to the torus outer ring. Conversely, to disembark at Earth and Mars, to work in the microgravity module, or to perform EVA or repairs in the CAB, personnel are required to travel to the interface. In order to facilitate this movement, an elevator has been designed that not only moves "up" and "down" the shafts, but also rotates to compensate for and eliminate disorienting and uncomfortable effects due to coupling of the various velocities of the spacecraft, the elevator, and the rotating torus. The elevator subsystem consists of an elevator cabin that rides in a cradle inside the shaft. The cradle consists of two circular tracks separated from the outside of the cabin by two rings of ball bearings which allow the cabin to rotate within the tracks to compensate for the Coriolis force. Four rails attach to the circular tracks and orient the cabin within the shaft. An electric motor uses a pulley system to drive the cabin's motion from the torus to the hub, and gains potential energy in doing so. This potential energy is then used to power motion in the opposite direction, thus minimizing power requirements.

The shaft is unpressurized and therefore the pressurized cabin must mate perfectly with the interface entrance and with the torus entrance in order to avoid pressure losses. This is accomplished by use of telescoping airlocks at the interface and torus that move toward the cabin. The cabin is stationary at the hub and spinning with velocity equal to that of the torus. The telescoping airlocks lock onto the doorway creating a pressurized passage.

Only two of the four shafts have been designed to house elevator cabins. These two are 180° opposed so as to minimize walking distances within the torus. The cabins move with a two m/s radial velocity thus covering the 35-m spoke in 17.5 s. Actual travel time, including acceleration and deceleration as well as interface and habitat matching is 50-70 s per trip.

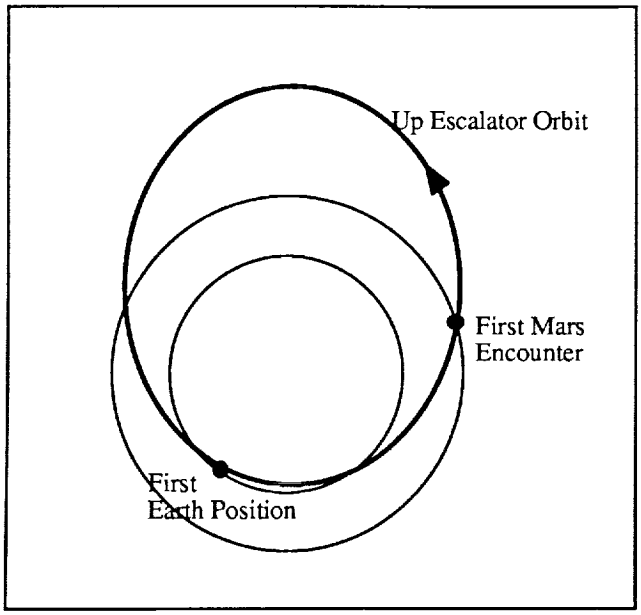

Fig. 2. Up Escalator Orbit

RADIATION PROTECTION AND TORUS STRUCTURAL ANALYSIS

Radiation Protection

Radiation shielding is a problem inherent in long term space travel away from the protective atmosphere and magnetic field of Earth. During an Earth-Mars mission several intense solar flares are likely to be encountered and any craft expected to deliver a healthy crew must provide protection in case of solar events. Adding material to the spacecraft is a design alternative but the extra weight leads to fuel requirements and mission constraints that become excessive. For that reason the use of superconducting cables to generate a magnetic field about the torus and thereby deflect virtually all of the impinging radiation away from the habitat area was investigated. It is estimated that the magnetic field scheme of protection requires about half as much mass as does the passive method described in the earlier study.

In its simplest form a superconducting magnet consists of a spool of superconducting wire, an insulated container with provisions for maintaining the operating temperature below the critical limit, and a power source for starting ("charging") the magnet. The superconducting material (which consists of

brittle ceramic fibers embedded in a metallic, often copper, medium for ductility) has the unique property of exhibiting zero resistance to the flow of direct current when operating below its critical temperature and critical current density. The material that appears to have the greatest potential for development as a high-critical-temperature superconductor is yttrium-barium-copper oxide ($YBa_2Cu_3O_{7+d}$).

To protect the interior of the torus it was determined that a magnetic field of 0.43 Tesla is required. Four superconducting cables, each of 2.4 inches outer diameter, are required to obtain the necessary field. Two cables are positioned along the inner radius of the torus while the other two cables are positioned along the outer radius. The cables are placed between the inner wall, which acts as a pressure vessel to maintain suitable air pressure within the habitat, and the outer hull of the ship, which acts to protect the ship from damaging collisions with particles drifting in space. By positioning them in this way, the cables are protected from colliding with space particles, and the hull serves as additional insulation to eliminate the need for four redundant cables as a safety feature. If any cable happens to fail, the other cables serve as adequate backup while repairs are made.

The operating principal is relatively simple. A low-voltage (70 V), high-current power supply is needed. Once the magnet is energized the power supply is removed. The current within the cables will continue to circulate and maintain the field as long as the cable is kept below the critical temperature. Methods were devised to minimize losses in power as well as to maintain the temperature of the coils below the critical temperature and to control temperature gradients between the "light" and "dark" sides of the torus.

Structural Requirements

The four superconducting cables will exert very large forces on one another when they are fully charged. The force is expected to be on the order of 2 MN/m. In addition, forces due to propulsive burns, torus rotation, thermal stresses, and intense pressure all contribute to the overall structural loads. Finite-element methods were used to ensure that the structure will withstand these loads.

INTERNAL HABITAT DESIGN

In order to optimize the benefits of the low gravity field and minimize discomfort due to the rapid rotation rate required to produce artificial gravity, a detailed study of all the rooms and their functions was performed. In addition, launch vehicle constraints require that the torus be manifested into eleven modules of varying sizes, each separated by airlock-type doors. Each of these modules is integrated into the overall ventilation, water supply, waste disposal, and electrical systems. In addition, an innovative mass balancing system has been designed that employs water tanks beneath the torus floor to compensate for movement of people and objects within the torus.

Detailed floor plans were developed indicating location, function, utilities, lighting, floor space and other variables required to optimally design and locate a room. Crew comfort and safety are the primary goals of the design.

TRUSS DESIGN

Most of the components of the spacecraft are very sensitive to vibration and shocks and thus require adequate protection from loads that would cause these effects. The propulsive burns for orbital insertion and axis rotation are sources of such loads. Other sources include attitude control thrusters and taxi-docking maneuvers. In order to protect the spacecraft, a truss structure was designed that carries most of the loads away from the various modules housed within the truss. The main component of the truss structure is the main boom which houses the propulsion system, the taxi-docking ports and cargo acquisition bay, the solar dynamic trusses, the microgravity facility, and the interface. The solar dynamic trusses make up the remainder of the truss work.

The main boom is a single-bay, single-laced four-element design, with a one-meter-square cross-section per corner element. A single bay thus has an eight-meter cross-section that allows for containment of all modules within the boom. The modules are connected to the corners of the truss with viscous dampers that dampen any loads travelling along the boom.

The solar booms are made up of the same truss elements arranged in a slightly different pattern. Use of the same design allows for redundancy and interchangeability of elements and connecting nodes. The solar booms are 35 m long and hold the solar collectors beyond the range of the docked taxis.

All elements of the trusses are made of graphite-epoxy composite clad with aluminum, which is considerably stronger and lighter than traditional aluminum and withstands radiation and temperatures encountered in space.

Finite-element analysis of the entire spacecraft held together by the trusses verified that the maximum stresses in the truss did not exceed yield. In addition, deflections are seen to be very small and optimization should lead to considerable weight savings. Natural modes and rigid body dynamics were also studied using finite element methods and yield similar positive results.

ASSEMBLY

As indicated in earlier chapters, the spacecraft will be assembled in a low Earth orbit. The orbit chosen has an altitude of 1113 km and is inclined to the equator at an angle of 28.5°. This orbit was selected to minimize cost of launching the components, final insertion into cycling trajectory, and radiation hazards to the assembly crew.

In order for the assembly sequence to proceed as outlined, it is assumed that a heavy lift launch vehicle (HLLV) capable of transporting a maximum load of 210 metric tons to the construction site will have been developed. Such an HLLV would be similar to the one described in NASA TM 86520 with a few minor modifications. In addition, development of several key technologies is assumed, including robotics and artificial

intelligence, telerobotics, and remote manipulator technologies. In addition, it is assumed that the LEO space station will be in place, along with a manned lunar base.

Several techniques and tools have been designed to allow for a small crew, inhabiting two modules, to easily and efficiently complete the assembly. Specially designed devices allow for the orientation and mating of the eleven torus modules, the four radial elevator spokes, the hub and interface assemblies, the numerous trusses, and the solar boom and main boom assemblies. Some of these devices are modifications of current designs, other are original and very innovative.

A detailed HLLV launch and assembly sequence has been devised that calls for assembly to take from four to twelve months, with a further six-month period devoted to system verification and startup. Contents of each HLLV or Shuttle II launch are described and crew activities are mapped out for the entire sequence.

A cost analysis including all development, terrestrial manufacture, and orbital assembly costs (but excluding development of the global infrastructure such as space station, Shuttle II, HLLV, lunar base and various technologies) was performed and indicates that the total cost from initiation of development to insertion into cycling trajectory will be on the order of 150 billion 1988 dollars.

CONCLUSION

A cycling spacecraft for regular, frequent transit between Earth and a Mars base has been analyzed and developed beyond the initial configuration study. Analysis has led to numerous design modifications and improvements, as well as providing more detailed system definition.

Major components of the second-phase study include innovative detailed designs of an interface between a rotating portion of a spacecraft to a non-rotating portion, an elevator system that changes orientation to eliminate Coriolis forces, an electromagnetic radiation shield that significantly reduces the mass of the spacecraft and a detailed assembly sequence and cost analysis. In addition, modifications to the propulsion and the power generation subsystems, taxi docking facilities, and internal layout design have led to a more efficient, significantly more reliable, and more comfortable vehicle. Finite elements stress and overall dynamic analysis has verified much of the system and indicates the validity of the design. Computer simulation of many moving components, including torus rotation, elevator and interface operation, and attitude control mechanisms further validate and support the design.

REFERENCES

1. Project CAMELOT: A Cycling Transportation System in Support of a Manned Mars Base, University of Michigan Space Systems Design Class 1986-87.
2. Friedlander A., Niehoff J., Byrnes D. and Longuski J. Circulating Transportation Orbits Between Earth and Mars, AIAA Paper 86-2009. AIAA/AAS Astrodynamic Conference, Williamsburg, Virginia. August 18-20, 1986.

VARIABLE-GRAVITY RESEARCH FACILITY CONCEPTUALIZATION AND DESIGN STUDY SUMMARY

UNIVERSITY OF NORTH DAKOTA

BACKGROUND

The Variable Gravity Research Facility (VGRF) is a conceptual design of a manned orbiting station that will be used to study the effects of different levels of gravity on human physiology. The VGRF is a simple design which makes use of existing equipment as much as possible to keep costs low (Fig. 1). This approach is intended to make the project affordable under congressional budget constraints.

The United States and the Soviet Union have a modest amount of data on human physiology in zero-gravity (0-*g*) conditions as compared to the large amount of data in Earth-gravity (1-*g*) conditions. It is clear that the physiological changes that occur after adaptation to 0 *g* are prohibitive to peak performance on return to 1 *g*. In order to be physiologically fit to return to 1 *g* from 0 *g*, one must spend hours every day in exercise. Furthermore, it is not clear that all physiological systems do readapt in reasonable time periods after extended time in 0 *g*. The VGRF will provide a small amount of data on the physiological adaptation to gravity levels between 0 and 1 *g*.

PROPOSAL

It is proposed that three six-month missions be performed at different gravity levels (0.255, 0.39, and 0.64 *g*) with crews of three individuals to obtain the first approximation of the curves for physiological responses to different levels of gravity. The resulting data will permit preliminary evaluation of the appropriateness of artificial gravity as a countermeasure for the deconditioning that occurs in 0 *g*.

CONCEPTUAL DESIGN

The basic design of the VGRF is a habitation module (HM) attached by flexible Kevlar tethers to a counterweight. This structure can be spun while in orbit to provide artificial gravity. The cheapest counterweight is an external tank (ET) from the Space Transportation System (Fig. 2). The HM will be slightly modified from the Space Station Common Module (SSCM). After the three six-month missions are completed it can be reconfigured and used as the SSCM. The HM by itself lacks some of the equipment needed to make the system habitable, so one node (node 2 of the Space Station) will need to be included as part of the VGRF. In addition, as with the SS, a crew emergency return vehicle (CERV) will be needed for safety purposes. The VGRF cost can be substantially reduced by using the HM, node, and CERV from the SS, then incorporating them back into the SS infrastructure after the VGRF experiments are completed.

Several minor modifications to the SSCM are required to make it suitable for use in a gravity environment.

Sleeping compartments must be rearranged to permit sleeping horizontally under gravity.

Racks to support equipment modules of the HM will have to be taken to orbit since the system will now be under gravity.

Due to the rotation, the power requirements must be handled differently than the SS; photovoltaic arrays which can provide power during the rotation of the VGRF will need to be developed. A 15-kW fuel cell system using residual fuel from the ET seems to be most appropriate.

Radiators will need to be mounted on the side of the HM instead of at a remote location as on the SS truss.

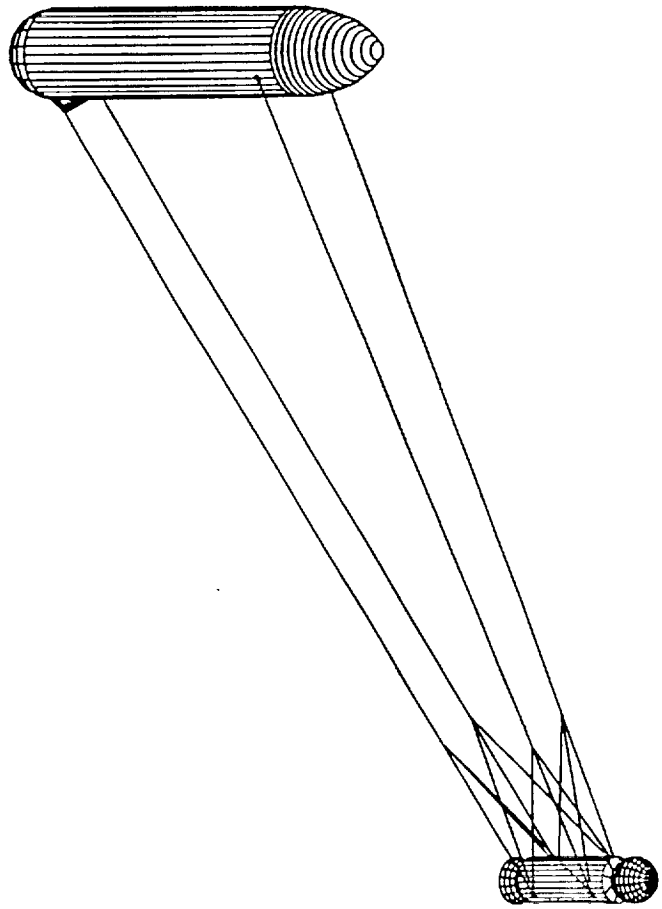

Fig. 1. University of North Dakota Variable Gravity Research Facility

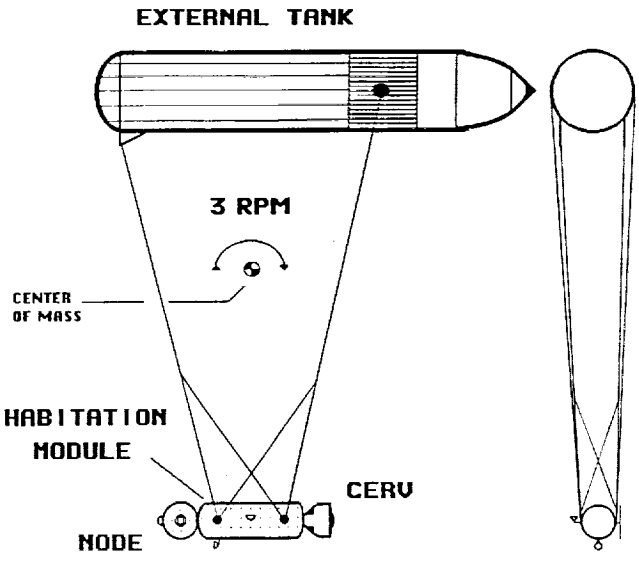

Fig. 2. VGRF

Antennae must be mounted to compensate for the VGRF's rotation while tracking communication satellites.

Kevlar tethers will be the connecting element between the HM and ET. These can be attached to the HM and ET at the handling points used to move these structures in 1 *g* on Earth.

Small rocket motors for spin-up will be installed on the HM and ET.

Despinning will be accomplished by detaching the tethers from the HM. Successive missions will use new tethers and ETs.

MISSION SEQUENCE

The HM will be carried to orbit on the first shuttle flight (SF1). This must occur during normal SS deployment, but the flight would need to be advanced by two years to permit the SSCM to be adapted for the VGRF.

Shuttle flight 2 (SF2) will carry the node, CERV, ET, and first crew to orbit. The VGRF will then be assembled, the crew will enter the VGRF, and the system will be spun up for the first mission.

After eight months the ET and HM components of the VGRF will separate to despin the HM portion of the VGRF assembly.

Shuttle flight 3 (SF3) will carry an additional ET and tether along with the second crew. During SF3, the first crew will be recovered, the ET and tether attached to the HM, the experimental samples unloaded, and the consumable supplies loaded. The second crew will then enter the VGRF, and it will be spun up for the second mission. After eight months the ET and HM ends of the VGRF will separate to despin the HM.

Shuttle flight 4 (SF4) will carry the third-mission ET, tether, and the crew. The second crew will be recovered, the ET and tether attached to the HM, the experimental samples unloaded, and the consumable supplies loaded. The third crew will then enter the VGRF, and it will be spun up for the third mission. After eight months the ET and HM ends of the VGRF will separate to despin the HM.

Shuttle flight 5 (SF5) will recover the third crew and the experimental samples. The HM will be picked up and transported to the SS to be incorporated into that infrastructure.

COSTS

The funding sequence for the HM, node, and CERV will need to be modified to permit them to be utilized two years before they are scheduled to be incorporated into the SS.

Modifications to the HM, node, CERV	$10 million
Tethers and other flight specific hardware	$100 million
Equipment subtotal	$110 million
Two shuttle flights*	$220 million
Total Program Costs less than	$400 million

*Only two of five Shuttle flights are charged to the VGRF program for the following reasons.

	VGRF	SS	Other
SF1 required for SS		all	
SF2 can carry other experiments and node, CERV for SS	1/2	1/2	
SF3 can carry other experiments	1/2		1/2
SF4 can carry other experiments	1/2		1/2
SF5 can carry other experiments and HM, node, CERV movement to SS	1/2	1/2	
Total	2	2	1

TETHER STABILITY TEST EQUIPMENT

At a more practical level, test equipment has been built to evaluate stability of the tether system. A rotation arm has been designed and constructed that will release a model HM-ET tethered system and photograph it while it is in free fall. Disturbances can be introduced into the HM model to permit examination of their propagation in the tethers. To complement the experimental analyses, a substantial effort has been made on the development of a computer model addressing tether vibrations. The combination of a physical model and computer model will be ideal for evaluating various tether designs.

MARS OXYGEN PRODUCTION SYSTEM DESIGN

OLD DOMINION UNIVERSITY

This report summarizes the design and construction phase of the Mars oxygen demonstration project. The basic hardware required to produce oxygen from simulated Mars atmosphere has been assembled and tested. Some design problems still remain with the sample collection and storage system. In addition, design and development of computer compatible data acquisition and control instrumentation is continuing.

INTRODUCTION

The combination of a stronger gravitational field and greater distance from the Earth makes round-trip missions to the surface of Mars more difficult than to the lunar surface. Using conventional propulsion approaches, the ascent vehicle required for Mars liftoff and Earth return is a large part of the payload at Earth launch. Furthermore, propellant mass accounts for as much as 90% of the Mars ascent vehicle mass. When liquid propellants are used, liquid oxygen accounts typically for 80% of the propellant mass; however, oxygen can be produced at Mars[1]. While oxygen production from Mars atmosphere is straightforward, acceptance of oxygen production as an option for early round-trip missions to Mars is lacking. The research goal of Old Dominion University's Mars oxygen demonstration (MOD) project is to build and operate an oxygen production system to establish its viability for near-term Mars missions.

Mars oxygen production is an ideal candidate for extraterrestrial resource utilization because (1) the carbon dioxide feedstock is certain; (2) the feedstock is not landing site dependent; (3) collection of a gaseous feedstock is simple and requires little equipment; (4) electrochemical extraction of oxygen from the feedstock is simple, requiring no moving parts; and (5) oxygen is a vital resource for human survival and an enabling resource for a variety of propulsive applications. The ability to produce oxygen on the martian surface reliably and autonomously for long periods of time and in large quantities is an important goal for future space missions.

The martian atmosphere is 95.32% carbon dioxide[2]. A variety of devices can be used to collect martian atmosphere, and since dissociation of carbon dioxide is not affected by pressure, it is only necessary to pressurize the atmosphere mildly to move it through the system and keep the volume of the oxygen separation system small. Oxygen separation is accomplished by heating martian atmosphere to temperatures on the order of 1000 K where measurable dissociation of carbon dioxide into carbon monoxide and oxygen occurs. Stabilized zirconia can conduct oxygen ions (O^{--}) at elevated temperatures. (Ionized oxygen is produced at the cathode of the electrolyte and pumped across the membrane to the anode where it is converted to O_2). Hence, oxygen can be removed and separated from a heated martian atmosphere stream by applying a voltage across a sealed zirconia membrane. The oxygen thus collected can be pressurized and liquified for storage using a variety of machines[3].

The MOD system has been designed to operate a zirconia cell at temperatures and pressures similar to those that would be used on Mars. The design assumes that martian atmosphere is provided at pressures between 50 and 100 mbar and at temperatures on the order of 300 K. The supply temperature will be at least 300 K if a compressor is used to pump the feed gas and will exceed 300 K if thermal absorption devices are used for compression[3]. The zirconia cell environment is controlled by the oven temperature, and the supply and collection pressures. Both the supply and oxygen collection pressures will be varied as part of this study. In addition, the oven temperature will be varied. The MOD system terminates at the point where oxygen is supplied for liquefaction and storage. The spent exhaust gas is returned to the surroundings.

OVERALL SYSTEM DESIGN

The Mars oxygen processor is shown schematically in Fig. 1. Simulated martian atmosphere is provided from pressurized bottles of custom-mixed specialty gas. The compositions of the simulant and of martian atmosphere are compared in Table 1. Trace elements and water vapor (which is variable) are omitted for economic reasons. In addition, rather than increase the carbon dioxide content to achieve a proportional approximation of martian atmosphere, the argon content was increased. Additional argon was used since it is inert and will act as a buffer gas, degrading dissociation of carbon dioxide, rather than increasing performance artificially.

A two-bottle, manifold system (Union Carbide System SG 9150) is used to provide a continuous supply of feed gas for endurance testing. The bottles are switched automatically and can be replaced when they are empty. The feed gas, which

Table 1. Nominal and Simulated Martian Atmosphere Compositions

Component	Percent by Volume	
	Nominal* (Mars Gas)	Simulated
CO_2	95.32	95.32
N_2	2.7	2.7
Ar	1.6	1.78
O_2	0.13	0.13
CO	0.07	0.07
Trace†	Balance	—

*Reference 2

†H_2O, 0.03%; Ne, 2.5 ppm; Kr, 0.3 ppm; Xe, 0.08 ppm; O_3, 0.03 ppm.

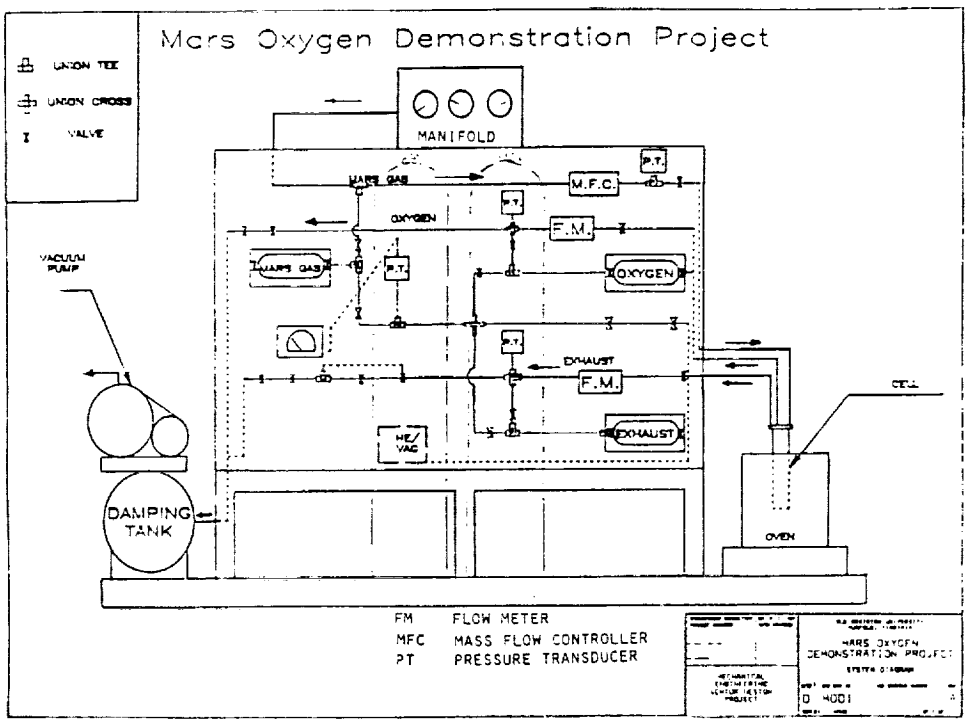

Fig. 1. Schematic diagram of Mars oxygen production system.

is supplied at a pressure of 55 atm (800 psi), is throttled to a pressure of ~4 atm before it is introduced into the flow network. The supply line upstream from the flow controller is of sufficient length to resublimate any dry ice that might form through the throttling process.

A mass flow controller (Omega Engineering, Model FMA-766-V) is used to control the flow of simulated martian atmosphere. Flow rates between 0 and 370 standard cubic centimeters per minute (SCCM) can be maintained. The feed gas pressure is monitored using a Datametrics Barocell Type 600 pressure transducer which has a useful range of 0-100 torr absolute. The controlled feed-gas stream is then introduced into the zirconia cell and oven where it is heated to temperatures on the order of 1000 K. The yttria-stabilized zirconia cell was manufactured by Ceramatec Corporation and a schematic of the cell assembly is shown in Fig. 2. The cell assembly consists of an outer ceramic-alumina housing, a thermocouple well, a tubular zirconia cell and seal, stainless steel electrical leads and connections, and an endplate with plumbing for the carbon dioxide, oxygen, and exhaust gas flows. The zirconia tube is open only at the oxygen outlet end (at the top of the assembly). Both sides of the zirconia tube are coated with a porous platinum paste which form the anode and cathode. Voltage and current are controlled and supplied through a DC high-current power supply. The oven used presently was also manufactured by Ceramatec Corporation and has a useful upper temperature limit of approximately 1500 K. It is capable of maintaining constant temperatures to within ± 2°C of its setpoint.

The oven exhaust-gas flow is monitored using an Omega Engineering Model FMA-866-V, mass flow meter which measures a maximum flow rate of 500 SCCM. The oxygen production rate is monitored using an Omega Engineering Model FMA-863-V mass flow meter with a full scale range of 50 SCCM. Line pressures are measured with silicon-diaphragm, peizo-resistive differential pressure transducers (Omega Engineering, Model 241PC15G).

System pressure is maintained through a 45.3-liter ballast tank which is connected to a Gast, Model 5BA-1 vacuum pump. The vacuum pump is capable of removing 0.1 l/sec at 0.01 torr and its volume flow characteristics are shown in Fig. 3 over the pressure range of interest. Both the oxygen and exhaust gas lines are connected to the ballast tank, where the two streams are combined and pumped back to the atmosphere. Hence the vacuum pump controls the system throughput.

Because of the low flow rates, additional heat exchangers are not required. Rather, using thermal analyses, the tube runs have been made long enough between the oven and the pressure and flow transducers to ensure that the fluid temperatures are approximately at ambient conditions.

Temperatures will be measured throughout the system using thermocouples. The thermal instrumentation has not been installed fully at this time due to problems with the computer interface. Copper-constantan, iron-constantan, chromel-alumel and nicrosil-nisil (type N) thermocouples are being evaluated for various measurements throughout the system. A source of concern in thermocouple selection has been the reported degradation of chromel-alumel thermocouples during prolonged, cyclic use at 1000°C[4]. Presently, type N thermocouples are being considered because they have been shown to be more stable[4].

A Keithley 500 data acquisition and control system (DAC) has been used during the year for data acquisition and control

studies. The DAC was connected to an IBM PC-AT Computer which served as the data acquisition host as well as the control system manager. The DAC employed Soft 500 operating software which was compatible with BASIC to facilitate data acquisition and control programming. Different circuit boards are installed in the data acquisition and control box for thermocouple measurements, voltage measurements and analog outputs. However, a major system or software failure occurred during the semester, requiring the DAC and one circuit board to be shipped back to the manufacturer. Presently, a Keithley 570 system is being used which has similar features to the original system but which is not capable of supporting the number of data channels and output channels that will be required for the autonomous system. The data acquisition and control aspects of this project are still in the development phase.

Computer-based data acquisition and control system design has become the primary focus of the project at this time. In order for autonomous oxygen production to be demonstrated, a network of sensors must be integrated into the system that provides sufficient digital information to enable a computer to monitor the health of the oxygen production system. The initial focus has been to identify and install sensors that measure temperature, pressure, mass flow rate, voltage and current, and which provide signals to the data acquisition system. Presently, the following measurements have been identified as necessary for autonomous operation: (1) cell voltage, current, and temperature; (2) supply gas bottle pressures; (3) supply mass flow rate; (4) supply gas temperature and pressure; (5) oven temperature distribution and power consumption; (6) oxygen temperature, pressure, and mass flow rate; (7) exhaust gas temperature, pressure, and mass flow rate; (8) ballast tank pressure; (9) power consumed by the vacuum pump; and (10) availability of external electrical power. These measurements represent approximately 20 channels of data that must be monitored and evaluated by the computer.

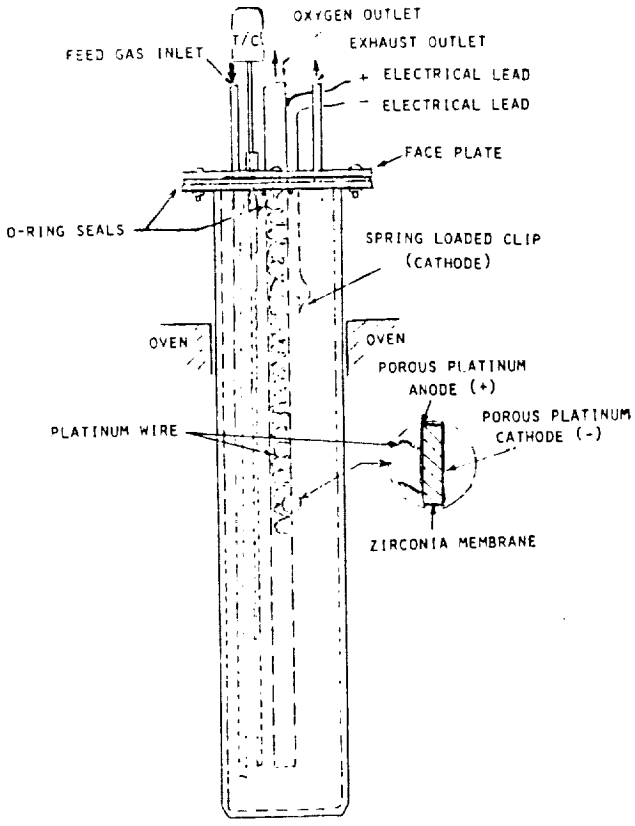

Fig. 2. Ceramatec oxygen separation cell assembly showing zirconia cell on central axis.

At this time, the only quantities that will be controlled actively by the computer are: (1) the supply gas mass flow rate; (2) power to the zirconia cell; and (3) power to the oven. The mass flow is controlled via the computer because its design facilitates computer control. Cell voltage and power must be controlled actively to avoid cell destruction during a system upset. In addition, even though the oven has its own very primitive (but reliable) "bang-bang" temperature control, it is necessary only to cut off the oven power in the event that certain types of system failures or upsets occur. Tests have shown that the oven cools down gradually when power is removed, thereby protecting the cell from destruction due to thermal stresses.

The long range plans for the system are to implement more computer-based control elements and ultimately employ a symbolic logic expert-system controller which can identify and avoid certain types of system failures as well as enable extended, autonomous operation. That activity will require significant graduate student involvement[5].

The present, Ceramatec cell design does not address two key Mars design questions-long-life, high temperature, seal designs and the relative ratio of thermal to electrical energy requirements. The Ceramatec cell has been designed so that all of the seals and virtually all of the electrical connectors are in a thermal environment near ambient conditions. While Fig. 2 does not show the oven, it does indicate that the upper assembly extends outside of the oven. This part of the system is air cooled with a small electric fan, mounted on the oven controller. The thermal aspects of the seal design problem are thus avoided, but the heat losses for a Mars system would be excessive using this approach. Furthermore, since Mars lacks an electric power generation facility, the magnitude of any extra electric power requirement translates directly into additional system mass[1]. Hence, the actual Mars oxygen production system should be designed to utilize either solar or radioisotope thermal energy supplies wherever possible, since electric power translates into a fourfold or larger corresponding thermal energy requirement (than do direct thermal needs). The present design wastes a good deal of electrical energy for unnecessary heat generation.

A Mars design requires that the cell system, which may employ a network of more than 1000 cells[6], minimize heat losses to the Mars environment. That energy can be managed properly only if the majority of the cells and their seals are maintained within the same 1000-K thermal environment. Hence, the seals and connections must be designed differently than the present design. Furthermore, Richter[7] has shown that the energy required for dissociation of the carbon dioxide can

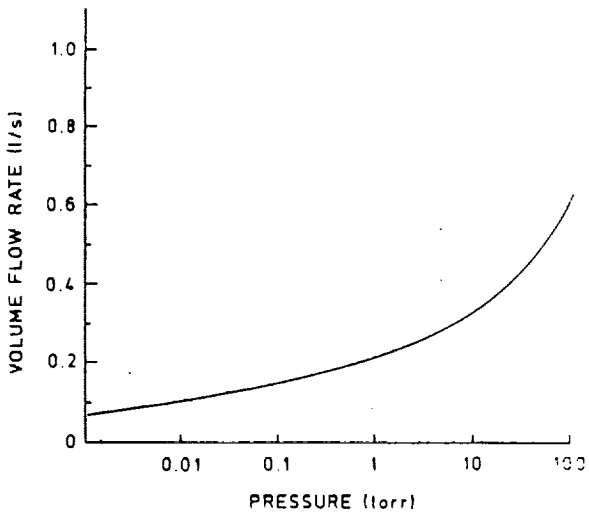

Fig. 3. Combined oxygen and exhaust gas flow rate as a function of ballast tank pressure.

be supplied at least partially by thermal means. It is anticipated that the work at Clemson University, which is part of the USRA program, as well as research at Stanford University, Jet Propulsion Laboratory, and Ceramatec Corporation will address cell optimization in terms of seal design, geometry and energy management.

Single-cell tests using the Ceramatec design will demonstrate the stability of the electrochemical process for Mars applications. The tests will not address seal and geometry issues which require more sophisticated (and expensive) design talent than a team of undergraduate students can realistically produce. The endurance tests, which still represent the ultimate goal of this program, will occur intermittently to accommodate a variety of other tests which have been delineated during this study. The following tests have been identified: (1) nominal cell performance tests; (2) MOD system certification and failure tests; and (3) cell deterioration and repair tests. Each of these test programs are described briefly in the following paragraphs.

(1) Nominal Cell Performance Tests

Starting with pure carbon dioxide, or during Phase-A tests, the cell(s) will be evaluated over a range of cell voltages, operating temperatures, pressures, and mass flow rates. Those tests will establish conversion efficiency and cell power requirements as a function of the control parameters. In addition, the system will be monitored carefully to make sure that the various flows obey the known physical laws (i.e., no leaks or other system anomalies).

Subsequently, in Phase B, the simulated martian atmosphere will be used over a somewhat narrower parametric range to establish the overall performance of the cell when the feed gas is no longer a single species. Those measurements should be the first tests which measure oxygen yield under Mars-like conditions.

(2) MOD Certification and Failure Tests

During the carbon dioxide tests, where the yields and cell performance are predictable, the system will be monitored as closely as the cell performance. The goal of the system evaluation will be to certify that all of the instrumentation and gas streams are consistent. Those tests will be carried out in parallel with the Phase A cell study. Both studies require the ability to take accurate samples from the various system lines. The sampling system has been given special attention and will be described at the end of this section.

Some types of system failures (such as deliberate leaks and instrument malfunctions) will be introduced during this study in order to verify that the instrumentation will record the upset and permit its identification. Those studies will be especially helpful to the graduate students assisting in this study.

(3) Cell Deterioration and Repair Tests

Depending on the operating conditions, the stability of zirconia in conducting oxygen ions becomes critical. Since oxygen is already contained in the zirconia cell lattice, albeit stabilized with yttria, some migration or oxygen depletion may occur over time. That depletion will be observable through changes in cell resistance and electrical current for fixed-voltage operation. Tests will be conducted to determine deterioration rate as a function of operating conditions. Interestingly, Gur and Huggins[8] have observed that depletion of oxygen near the cathode surface of a zirconia membrane enhances or catalyzes the production of oxygen from a nitric oxide supply and this may also be true for carbon dioxide. However, regardless of deliberate or accidental oxygen depletion, cell life must be studied under those conditions.

Simple cell repair may also be possible by briefly reversing the cell polarity and conducting oxygen back into the feed-gas stream. That process is known to clear or even open new oxygen paths through the porous platinum electrodes. In addition, it may be possible to replace depleted oxygen atoms in the cell matrix under the proper set of applied voltage and controlled thermal conditions. Those tests will be conducted as part of this study.

SAMPLING SYSTEM

Because most of the MOD system is operated at pressures < 1 atm, sample collection and prevention of sample contamination during handling are major concerns. As shown in Fig. 1, a sample collection flow network (including sample bottles for martian gas, oxygen, and exhaust) has been designed into the MOD system. The system can be evacuated below operating conditions using an independent vacuum pump. The sampling system, including sample bottles, can be pumped down to pressures as low as 0.1 torr to minimize residual gas contamination.

By properly operating the valve system on the MOD network, a sample can be taken of the feed gas, exhaust gas, or oxygen. The feed gas can be collected at a pressure > 4 atm, and therefore sample leaks reduce only the sample size.

However, the oxygen and exhaust gases must be collected at pressures between 50 and 100 mbar and can be contaminated by leaks. In order to preserve subatmospheric samples, the exhaust and oxygen sample bottles will be pressurized above 1 atm using helium gas before they are removed from the MOD system. Since helium is used as the carrier gas for gas chromatograph analytical systems, it will not influence gas chromatograph analyses. That part of the sample collection system has not been added to the MOD system at this time.

SUMMARY AND CONCLUSIONS

To date, the MOD system has been operated with a carbon dioxide feed gas to produce oxygen. Tests will be started during the summer which will begin to define the optimal operating regime. A significant amount of instrumentation and control work will be needed before autonomous-operation endurance tests can be demonstrated.

ACKNOWLEDGMENTS

The hardware required for this project was purchased with a grant from the Planetary Society. The students also gratefully acknowledge the involvement of Dr. J.-K. Huang and Mr. M.-T. Ho, who are supported by a grant from NASA, Johnson Space Center, for their assistance.

REFERENCES

1. Ash R.L., Richter R., Dowler W.L., Hanson J.A., and Uphoff C.W. Autonomous Oxygen Production for a Mars Return Vehicle, XXXIII Congress of the International Astronautical Federation Paper No. IAF-82-210, Paris, September 1982.
2. Owen T., Biemann K., Rushneck D.R., Biller J.E., Howarth D.W. and Lafleur A.L. The Composition of the Atmosphere at the Surface of Mars, *J. Geophys. Res., 82,* pp. 4634-4639, 1977.
3. Lawton E.A. and Frisbee R.H. A New Look at Oxygen Production on Mars: ISPP, Jet Propulsion Laboratory Report, JPL-0-2661, 1985.
4. Burley N.A., Powell R.L., Burns G.W. and Scroger M.G. The Nicrosil versus Nisil Thermocouple: Properties and Thermoelectric Reference Data, *National Bureau of Standards Monograph 161,* Washington, D.C., April, 1978.
5. Huang J.-K., Wei Y.-H., Ash R.L. and Ho M.-T. An Expert Systems Approach to Automated Maintenance for a Mars Oxygen Production System, 18th Intersociety Conference on Environmental Systems SAE Paper No. 88-1056, San Francisco, July 11-13, 1988.
6. Ash R.L., Huang J.-K., Johnson P.B. and Sivertson W.E., Jr. Elements of Oxygen Production Systems Using Martian Atmosphere, AIAA/ASME/SAE/ASEE 22nd Joint Propulsion Conference AIAA Paper No. 86-1586, Huntsville, Alabama, June 1986.
7. Richter R. Basic Investigation into the Production of Oxygen in a Solid Electrolyte Process, AIAA 16th Thermophysics Conference AIAA Paper No. 81-1175, Palo Alto, CA, June 1981.
8. Gur T.M. and Huggins R.A. Decomposition of Nitric Oxide on Zirconia in a Solid-State Electrochemical Cell, *J. Electrochem. Soc., 126, No. 6,* pp. 1067-1075, 1979.

CONCEPTUAL DESIGN OF A WATER TREATMENT SYSTEM TO SUPPORT A MANNED MARS COLONY

PRAIRIE VIEW A&M UNIVERSITY

SUMMARY

The initial tasks addressed by the Prairie View A&M University team were the conceptual design of a breathable-air manufacturing system, a means of drilling for underground water, and a method for storing water for future use. Subsequently, the design objective of the team for the 1987-1988 academic year was the conceptual design of an integrated system for the supply of quality water for biological consumption, farming, residential and industrial use. The source of water for these applications is assumed to be artesian or subsurface.

The first step of the project was to establish design criteria and major assumptions. The following list includes some of the ground rules used in this study.

1. Water is scarce, therefore efficient water management through maximum recovery and reuse is critical.

2. Pollution problems will be minimized by exercising strict control on water discharge.

3. An effective hierarchical monitoring and control system will provide for quality control and prompt attention to faulty equipment and leaks.

4. Since the pressure of the martian atmosphere is a small fraction of the Earth atmosphere, all vessels and equipment must be sealed to prevent evaporation.

5. Four classes of water are defined: (a) water for farming must have a maximum mineral content so that plant life will flourish; (b) water for drinking must be free of pathogenic organisms and have a maximum salt content of less than 200 ppm; (c) water for manufacturing must be sufficiently free of ions so that it will not interfere with manufacturing processes or damage the quality of products; and (d) ion-free water will be provided for use in boilers in order to avoid corrosion of construction materials.

6. The various impurities in water that are reduced or removed at successive stages of treatment are turbidity, color, hardness, alkalinity, free-mineral acid, carbon dioxide, pH, silica, oil, oxygen, hydrogen sulfide, ammonia, dissolved solids, suspended solids, organic solids, micro-organisms, and sulfate, chloride, nitrate, fluoride, iron, and manganese ions.

7. It has been assumed that the potential underground raw water supply on Mars resembles, in quality, representative sources of underground water in Texas.

The assumed water impurities are:

	meq/l	ppm
Sodium chloride [NaCl]	7.80	456.3
Magnesium chloride [$MgCl_2$]	0.60	28.6
Magnesium bicarbonate [$Mg(HCO_3)_2$]	0.36	43.9
Calcium bicarbonate [$Ca(HCO_3)_2$]	0.57	46.2
Calcium sulfate [$CaSO_4$]	3.07	208.0

8. Advanced technologies, which are not widely applied on Earth, rather than traditional biological treatment, softening, and clarification techniques were sought.

The second step of the effort was to generate a block diagram of the expected treatment system and assign tasks to individual students. Among the treatment steps considered were sedimentation, softening, sand filtration, disinfection, ultrafiltration, reverse osmosis, demineralization, electrodialysis, vapor-compression evaporation, domestic waste treatment, and industrial waste handling.

During the conceptual phase of study, no specific industries were selected, and hence no specific waste facilities were designed. It appears appropriate at this point to assume that evaporation by depressurization is a feasible means of recovering a major portion of the industrial waste water.

The list of processes for water purification and wastewater treatment given above suggests that there will be a need for on-site chemicals manufacturing for ion-exchange regeneration and disinfection.

The third step of the project was to establish a basis for the design capacity of the system. A total need of 10,000 gal/day was assumed to be required. It was also assumed that 30,000 gallon raw-water intake volume is needed to produce the desired effluent volume. The following is a summary of the potential users and the level of treatment required.

Farming. Municipal (domestic) wastewater treatment effluent. All waste produced by quarters and biological waste is directed to the wastewater treatment facility. Additional water needed can be supplied by proper blending of reverse osmosis (stage 1) unit effluent and raw water to arrive at the desirable salinity level.

Fig. 1. Effective Ranges of Some Separation Techniques

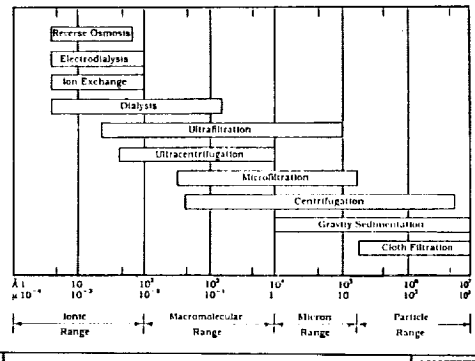

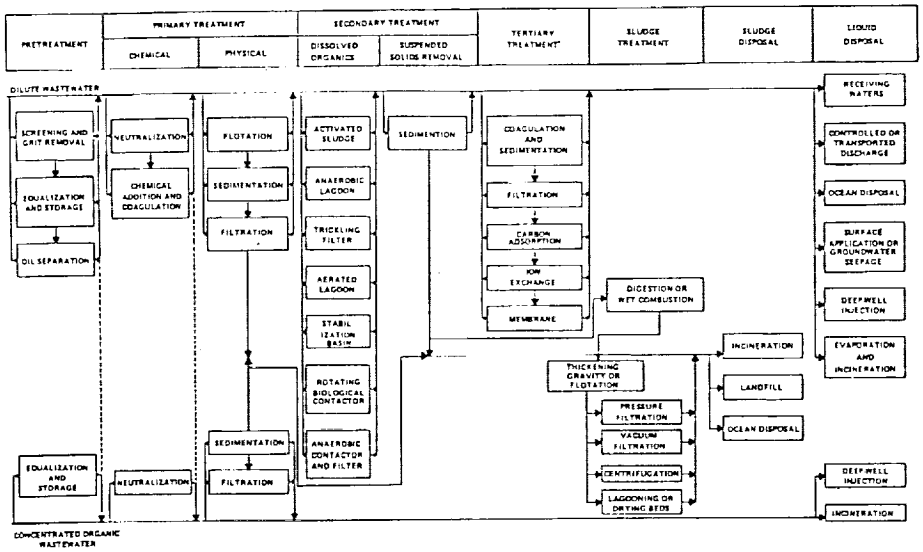

Fig. 2. Wastewater Treatment Sequence — Processes Substitution Diagram

PVAM	**NASA / USRA** **INTEGRATED WATER SYSTEM FOR SPACE COLONY PHASE II - TASK 1B**	DEPARTMENT OF CHEMICAL ENGINEERING ADVANCED DESIGN PROJECT APPROVED BY: K. FOTOUH PAGE:

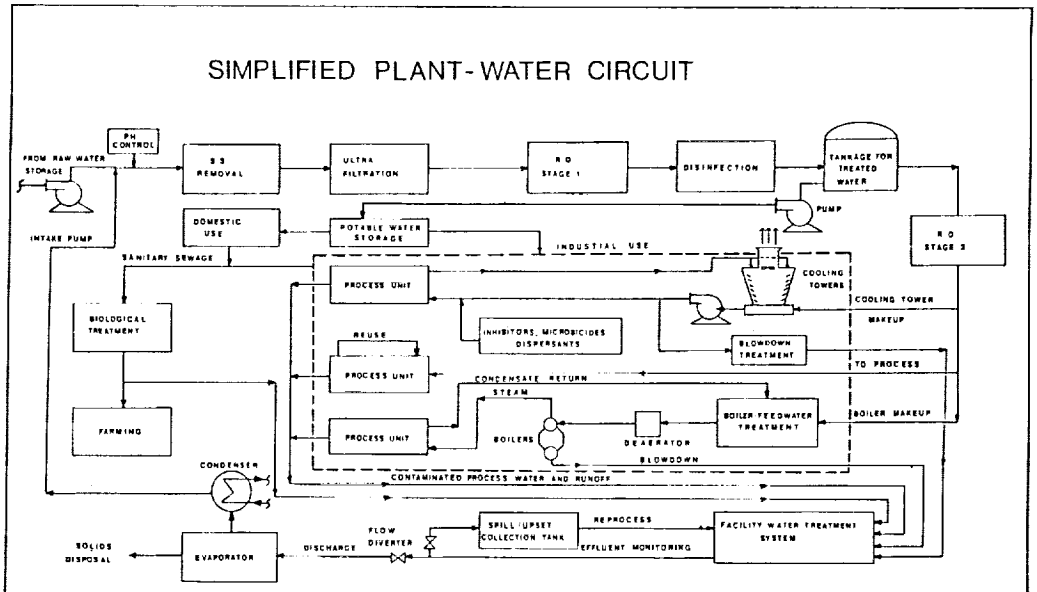

Fig. 3. Simplified Plant-Water Circuit

PVAM	NASA/USRA INTEGRATED WATER SYSTEM FOR SPACE COLONY PHASE II-TASK 1B	DEPARTMENT OF CHEMICAL ENGINEERING K. FOTOUH ADVANCED DESIGN PROJECT

Domestic (Washing/Cooking). The effluent from the reverse osmosis (stage 1) is disinfected and stored for use in the quarters.

Drinking. Part of the effluent from the reverse osmosis (stage 2) is disinfected and stored.

Processing (Manufacturing). The major part of the reverse osmosis (stage 2) effluent is directed for this application.

Steam and Special Users. Ion-free de-aerated water is produced for applications that require high purity water.

The fourth step of the project was for each student to screen the technology available and select the most suitable process(es) for the specific treatment phase. Detailed assumptions and criteria were established for each individual unit. As a result of these screening studies, the following sequence of treatment steps were selected for the system.

Sand Filtration. The purpose is to remove suspended solids with particle sizes > 10 m. The process selected is a sand-on-gravel bed constructed on site. This has been chosen over cloth filtration and rotary vacuum filtration. The former is excluded because of the semi-manual nature of operation; the latter was excluded because it employs moving parts and requires frequent maintenance. Fig. 1 shows the solid removal process.

Ultrafiltration. The process was selected as an additional cleaning step for the removal of fine suspended solids (other candidates were microfiltration, centrifugation, and ultracentrifugation). Ultrafiltration was selected because it has a high removal efficiency for a wide range of particle sizes and has fewer moving parts. Size range of particles removed is 0.01-10 m.

Reverse Osmosis. The process operation is based on increasing the pressure above the osmotic pressure of the brine solution to force clear water molecules across a permeable membrane. Two stages of reverse osmosis, with each membrane having a different permeability, were preferred over one stage. The first stage effluent can be used, in part, for domestic and farming applications. The remaining part of the first stage effluent is directed to the second stage osmosis process to produce extra clean water for industrial processing. This process was selected over electrodialysis because of lower power requirements, and over the ion exchange process for size and weight considerations.

Demineralization. This is an ion exchange process, and is selected as an additional cleaning step to produce an ultra ion-free water for speciality manufacturing and steam-making.

Domestic Wastewater Treatment. The technology available is divided into two types based exclusively on cost. The diversity of processes to select from is shown in Fig. 2. Industrial wastewater facilities were not addressed at this point due to lack of information regarding the nature and concentrations of contaminants produced.

A general arrangement of the designed system is shown in Fig. 3. The industrial portion is hypothetically drawn for future analysis. The names of investigators are also written on the corresponding unit of the system.

1987-88 ADVANCED SPACE DESIGN PROJECTS: RESULTS FROM THE FALL SEMESTER OF 1987 AND THE SPRING SEMESTER OF 1988

UNIVERSITY OF TEXAS AT AUSTIN

1987-88 DESIGN PROJECTS

Students in Aerospace Engineering (ASE) and Mechanical Engineering (ME) at the University of Texas at Austin completed eight separate design projects under the sponsorship of the NASA/USRA Advanced Space Design Program. During the Fall semester of 1987, ASE and ME students worked on various aspects of a "bootstrap" lunar base. ASE students concentrated on the overall definition of the base while the ME team designed a convertible lunar lander lower stage. Six design projects were executed during the spring semester of 1988. Aerospace engineering students designed a fast Mars mission crew transfer vehicle, an Earth-orbiting transportation node to support the lunar base, a lunar base construction shack/initial habitat vehicle, and carried out a systems assessment aimed at arresting ozone depletion in the Earth's atmosphere. The ME students designed a lunar surface personnel navigation system and investigated radiation shielding structures for a lunar base.

The design objectives, a summary of the results, and selected comments are given concerning each of the projects. Due to the number of projects completed, the reader should refer to the text of the final project reports for additional and detailed information. (Final project reports can be obtained from Universities Space Research Association, 17225 El Camino Real, Suite 450, Houston, Texas 77058.)

BOOTSTRAP LUNAR BASE

A design for a bootstrap lunar base was specified that required minimal total payload to be delivered to the Moon in the process of establishing a preliminary base. The specifications required that there be maximum utility of every item delivered to the lunar surface and that every item be reusable or "transformable" (capable of being used for another purpose). The ASE design team divided its efforts into three areas: lander fleet requirements definition, lander design development, and lunar surface operations definition. The lander fleet group defined the trajectory, navigation, and communications requirements for the fleet. The lander design group defined preliminary specifications and design for candidate lander vehicles, concentrating on transformable lower-stage designs that would provide resources for establishing the bootstrap base. The surface operations group defined a base development scenario in which the bootstrap base becomes the cornerstone for development of a permanent lunar base.

CONVERTIBLE LANDER LOWER STAGE

A team of ME students designed a lower stage for a lunar lander vehicle that can be converted into a shaft head and elevator for vertical access to a buried lunar base facility. The design specifications were the same as those given to the ASE group designing candidate lower stages for lunar landers, namely that no items transported to the lunar surface could be of the single-use variety. The elevator provides compression and decompression operations that are required during astronaut transfer to and from the lunar surface and the habitat.

ASE and ME design specifications required that all items transported to the Moon have secondary uses after completing their primary task/mission. In particular, the requirement stated that the often-depicted scene of a lunar landscape littered with spent descent stages should not occur, and that all lower stages should be transformable into items useful in the on-going development of a lunar base. Conceptual designs were presented for lower stages that convert into a crane, a storage shelter, a nuclear power plant support structure, and a vertical access shaft/elevator. In addition, a generic truss lander (nicknamed the "tinker toy lander") was presented. This lander is constructed of generic structural elements which can be used as needed elsewhere in the lunar base. Diagrams of these landers are shown in Fig. 1.

FAST MARS-MISSION CREW TRANSFER VEHICLE

This design consists of trajectories and vehicle specifications for the crew transfer vehicle required in the piloted, split mission to Mars. The purpose of the fast crew transfer is to reduce the trip mission, trip time, and thus minimize the total radiation dosage and the effects of microgravity on the crew. After the interplanetary transfer from low Earth orbit to a predetermined Mars orbit, the crew vehicle is serviced at the cargo transfer vehicle already in orbit about Mars and remains in Mars orbit for 40 days. The crew vehicle then flies a 150-day trajectory back to Earth. The crew spends approximately 40 days in the vicinity of Mars. In case of a mission abort prior to entering Mars orbit (and being refueled), the crew transfer vehicle would be capable of a low energy (slow) return to Earth. An abort after Mars orbit would require refueling prior to return to Earth. In the proposed scenario, all propulsive velocity changes are made using LH_2/LOX propellants.

The vehicle itself does not employ artificial gravity and the life support system is designed for a nominal mission duration of one year with reserves for a slow-return abort. The vehicle

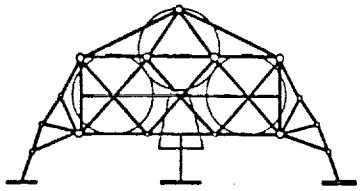

GENERIC TRUSS ELEMENT
LANDER

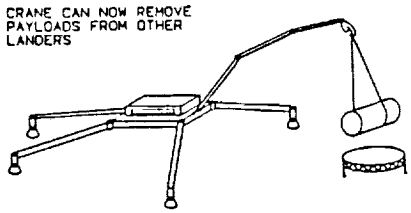

CRANE LANDER

THE PORTAL / ELEVATOR DESIGN

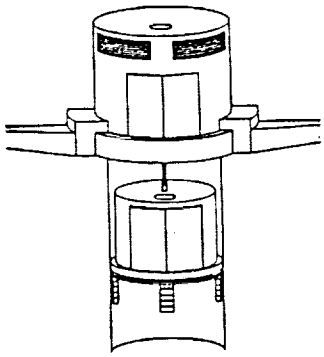

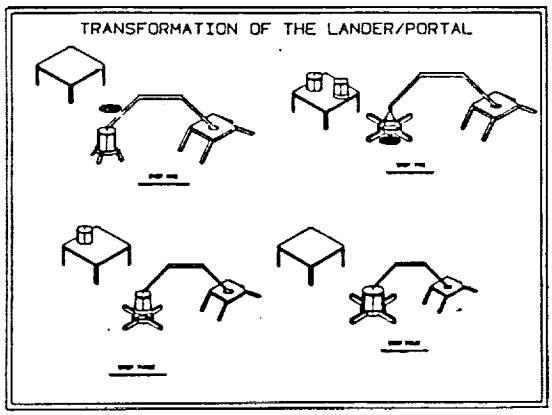

Fig. 1. Transformable Lower Stages

employs four crew modules similar to the proposed Space Station Common Modules plus a heavily shielded command module. The shielding is designed to protect the crew in case of a major solar radiation event. Figure 2 shows the trajectories for a typical mission along with a sketch of the fast crew transfer vehicle itself.

EARTH ORBITING TRANSPORTATION NODE

This design specifies the components of an Earth-orbiting transportation node which supports the establishment and maintenance of a permanent lunar base during its first decade. The study includes a comparison of two lunar base traffic models and assumes the existence of orbital transfer vehicles (OTVs), orbital maneuvering vehicles (OMVs) and heavy lift launch vehicles (HLLVs). It is assumed that the transportation node, called GATEWAY, is distinct from the space station, and is designed to be a high-activity "noisy" environment unsuitable for microgravity experiments.

GATEWAY is characterized by a delta truss design and has facilities for a dedicated crew of four plus temporary accommodations for transient personnel. Propellant storage sufficient to meet the fuel and oxidizer requirements of the OTVs is provided. Provision is made for assembly of OTV payload stacks at a hangar area within the facility. Remote

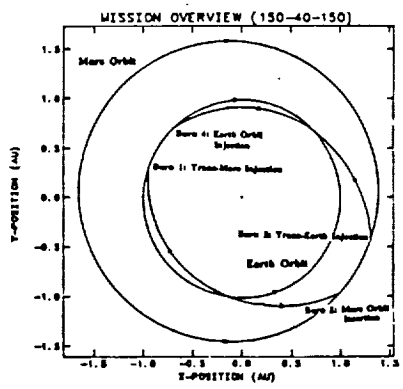

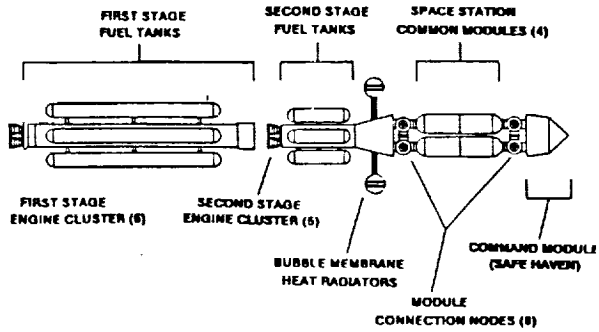

SIDE VIEW

MARS FAST CREW TRANSFER VEHICLE

Fig. 2. Fast Crew Transfer Trajectories and Crew Transfer Vehicle

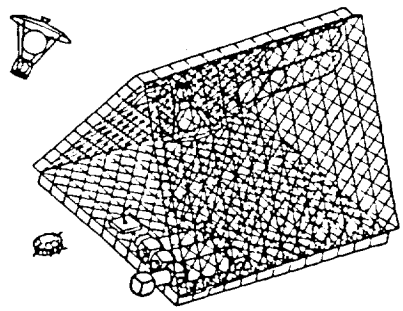

Fig. 3. GATEWAY Transportation Node

manipulators and other facilities necessary for OTV and OMV maintenance are included in the design. A sketch of the GATEWAY design is given in Fig. 3.

Several candidate launch sites and orbital inclinations were studied for use by GATEWAY and its associated vehicle fleet. A circular orbit at an altitude of 240 to 260 nautical miles and an inclination of 28.5°, supported by launches out of Kennedy Space Center (KSC) was chosen. Analyses of the number of launch windows available per year between GATEWAY and various lunar orbits and lunar orbiting facilities are included. It is concluded that unless a lunar orbiting facility (MOON-PORT) is in a lunar equatorial orbit, it will only be occasionally accessible from GATEWAY and might as well not exist. It seems much easier to reach most points on the lunar surface directly from GATEWAY than to go through a seldom accessible lunar orbiting transportation node.

LUNAR CONSTRUCTION SHACK VEHICLE

The lunar shack vehicle is a lunar lander which provides an initial construction crew of eight with a habitat and radiation protection during the initial phases of lunar base construction.

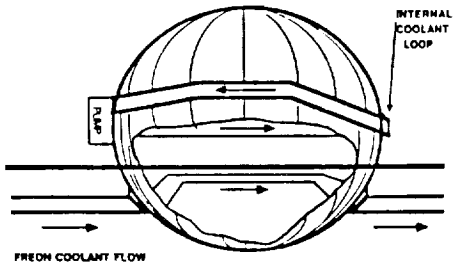

Fig. 4. Water Reservoir Heat Exchanger

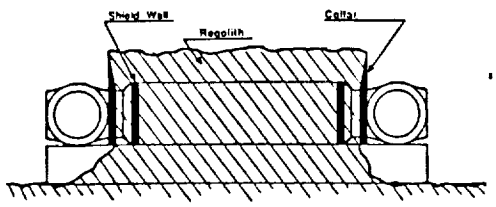

Fig. 5. Lunar Shack Vehicle

The lunar shack vehicle carries supplies for an initial construction period of three weeks and can be resupplied. The crew and additional supplies are brought to the surface via a manned lunar module. It is assumed that a nuclear power plant has been landed prior to the arrival of the lunar shack and that it takes approximately one week to activate the nuclear power plant. During the first week, power is obtained from fuel cells in the lunar shack. The fuel cells also serve as a backup power supply for the shack vehicle. The descent engines and the fuel cells share a LOX/LH_2 fuel system.

Several design features deserve comment. First, the thermal control system of the vehicle features a water reservoir heat exchanger consisting of an insulated water reservoir that acts as a heat sink during the lunar day and as a heat source during the lunar night. Provision is made to radiate heat from the reservoir during the lunar night if and when necessary. Second, crew radiation protection is provided by partially burying the shack vehicle. The center of the cylindrical vehicle is buried with the ends, which contain airlocks, remaining uncovered. Slumping of the regolith over the airlocks is prevented by collars at the ends of the buried segments. Finally, interior layouts for the chosen design and an alternate design are provided. Figure 4 depicts the functions of the water reservoir heat exchanger. Figure 5 depicts the lunar shack as it lands, after it is lowered to the ground, and after it is covered with regolith for radiation protection.

OZONE DEPLETION ARRESTING SYSTEMS ASSESSMENT

This study is an initial inquiry into (1) the nature of the mechanism(s) which is causing the depletion of ozone at high altitudes over the south pole (and to a smaller extent over the remainder of the Earth), (2) the possibility of slowing or stopping the ozone depletion process either by accelerating the formation of ozone or by removing substances responsible for ozone depletion from the atmosphere, and (3) the preliminary characterization of vehicles and/or mechanical systems which might be useful in combatting the ozone depletion problem. The study resulted in more questions than answers, but this was expected. The primary motivation of this study was to focus the immediate attention of engineers on this problem because of its possible extreme consequences. It was felt that early thought on possible solution mechanisms, even with a lack of complete understanding of the underlying causes, would be beneficial.

Important questions identified during the study are: (1) What are the effects of the decrease in atmospheric ozone and at what stage does the problem become critical? (2) How can we accelerate the natural processes that "wash" out of the atmosphere substances that attack ozone? (3) Can we shift the reaction equilibrium away from ozone destruction by introducing additional substances without causing other harmful effects? (4) Can we filter ozone-destroying substances from the atmosphere, either near the surface or at altitude? and (5) What facilities and/or vehicles will be necessary to implement a solution?

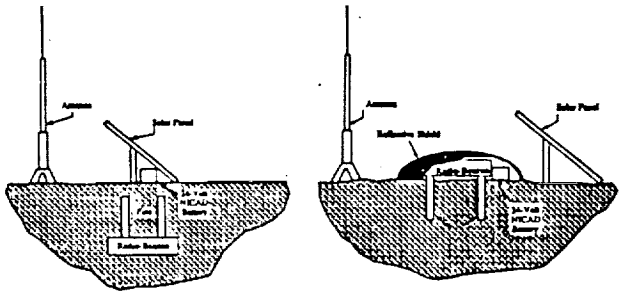

Fig. 6. Radio Beacon Installation for Lunar Surface Navigation

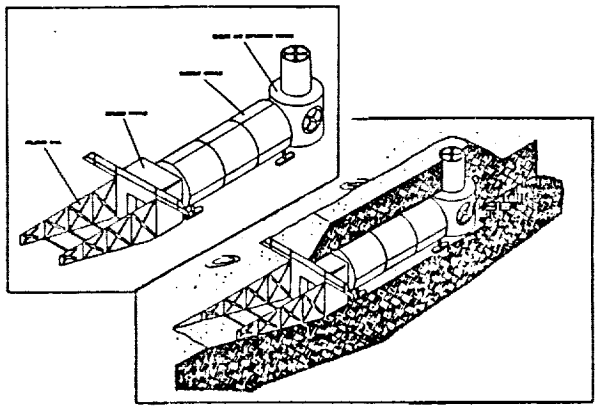

Fig. 7. Candidate Radiation Shielding Concepts for the Lunar Base

LUNAR SURFACE NAVIGATION SYSTEM

This study investigates a navigation system to be used on the lunar surface by astronauts to locate their positions when beyond the line of sight of the base facility. The navigation system is to be deployed for use in the early development of lunar surface operations. The navigation system must be usable by an astronaut while in full pressure suit. The study provides an analysis of four navigational methods for adaptation to the lunar surface: celestial, satellite, inertial, and radio-beacon. The study revealed that a spread-spectrum, radio-beacon navigation system is best suited for the design needs. The report develops the scenario necessary for initial operations of a lunar base, and provides alternatives which will allow the original system to be expanded as lunar surface activities expand. A celestial navigation system is suggested as a back-up in case of power failure of the spread-spectrum, radio-beacon navigational system. Figure 6 shows a buried radio-beacon installation with a Ni-Cd battery recharged by solar energy.

LUNAR BASE RADIATION PROTECTIVE STRUCTURES - ME

This study analyzes alternatives and proposes a design that will provide astronauts protection from lunar radiation and micrometeorite hazards. The protective structure is designed for use on a manned lunar research outpost. As in other studies performed by the University of Texas at Austin this year, emphasis was placed on increased use of *in-situ* materials. Any material delivered to the lunar surface is designed for continuous use or is to be transformable. The study investigated both surface and below-surface alternatives. The most promising solution was the use of existing lunar lava tubes to provide radiation protection. However, the design team concluded that current information is insufficient to design the necessary structures using the lava tubes. As a result, the team designed a structure consisting of a cylindrical module buried in lunar regolith. Figure 7 depicts the shielding alternatives considered.

CLOSING REMARKS AND A CHALLENGE

One of the key conclusions from this year's design experiences was the importance of transformable elements in space mission design. One of the constraints that will be placed on all future projects at the University of Texas at Austin will be that each design results in a "zero junk heap." This means that any piece of equipment, or tool, or component that has been designed for a specific purpose (one-time use) must also be transformable to perform additional tasks. The faculty found that as students become more adept at transformable concepts, they easily can implement the multiple-use philosophy. The potential savings from the implementation of this concept are tremendous.

The University of Texas *challenges* all participants in the Advanced Design Program to incorporate the transformable philosophy in future design efforts.

SUMMARY OF AEROSPACE AND NUCLEAR ENGINEERING ACTIVITIES

TEXAS A&M UNIVERSITY

INTRODUCTION

The Texas A&M Nuclear and Aerospace engineering departments have worked on five different projects for the NASA/USRA Advanced Design Program during the 1987/88 year. The aerospace department worked on two types of lunar tunnelers that would create habitable space. The first design used a heated cone to melt the lunar regolith, and the second used a conventional drill to bore its way through the crust. Both used a dump truck to get rid of waste heat from the reactor as well as excess regolith from the tunneling operation. The nuclear engineering department worked on three separate projects. The NEPTUNE system is a manned, outer-planetary explorer designed with Jupiter exploration as the baseline mission. The lifetime requirement for both reactor and power-conversion systems was twenty years. The second project undertaken for the power supply was a Mars Sample Return Mission power supply. This was designed to produce 2 kW of electrical power for seven years. The design consisted of a General Purpose Heat Source (GPHS) utilizing a Stirling engine as the power conversion unit. A mass optimization was performed to aid in overall design. The last design was a reactor to provide power for propulsion to Mars and power on the surface. The requirements of 300 kW of electrical power output and a mass of < 10,000 Rg were set. This allowed the reactor and power conversion unit to fit within the Space Shuttle cargo bay.

NEPTUNE

At the present time there are no definitive plans for a manned, outer-planetary mission. The goal of the NEPTUNE design is to fill this void. To satisfactorily explore the outer planets, a long mission time is required. The mass of chemical-thruster propellant required for such a mission is prohibitive. Currently, the only system capable of providing a reasonable mission time with an acceptable propellant mass is nuclear electric propulsion. The power requirements for nuclear electric propulsion are very high for the amount of thrust necessary to achieve a reasonable mission time. In addition, the outer planets are too far from the sun to use current photovoltaic technology. The only system capable of supplying large amounts of power reliably for long periods under these conditions is a nuclear reactor.

The specific requirements for the NEPTUNE system were determined by an acceptable mission time and the required power level for propulsion. As a reference mission, a 10-year, manned-return voyage to Jupiter was examined. Based on the necessary thrust to meet this goal, the power level required is ~6 MW. Since the mission is manned, additional power is required for life support and scientific equipment. For exploration beyond Jupiter, a system lifetime of 20 years was specified.

The propulsion system selected to meet the reference mission thrust requirements is a mercury bombardment ion drive. This system was chosen on the basis of its high specific impulse and demonstrated feasibility.

The high power level required by the propulsion system necessitates the use of dynamic energy conversion. The Rankine cycle provides the potential for relatively high thermal-to-electric conversion efficiency and was selected for this reason. Additionally, the high temperatures needed for efficient waste-heat rejection led to the selection of a liquid-metal working fluid. Figure 1 shows the reactor system diagram.

A liquid-metal coolant is boiled directly in the reactor core, and a wet mixture is sent to a pair of Ljungstrom turbines for electric power conversion. Turbine exhaust is condensed in a shell-and-tube heat exchanger to the reactor inlet temperature. Primary-loop potassium is condensed in the heat exchanger tubes with a sodium-potassium (NaK) secondary fluid on the shell side. The NaK fluid rejects waste heat to space in a tube-and-fin radiator. Parallel centrifugal pumps are employed in both loops.

The reactor fuel is uranium nitride for high thermal conductivity and high uranium density. High uranium density provides a high power density and thus, a compact core. Since the reactor operates at high temperatures for long periods of time, the primary concern in selecting cladding is creep strength. The molybdenum-1.25% titanium-.025% zirconium-0.1% carbon alloy (Mo-TZC) was selected on this basis as the clad.

Due to material limitations in the high temperature/high burnup environment of the reactor, two cores are needed to fulfill the mission lifetime requirements. The initial core is burned for ten years, while a standby core located within the same reactor vessel is held in a shutdown mode. After ten years, the standby core is activated, and the initial core is shut down while still immersed in flowing liquid potassium. The reactor is controlled by movable absorbing blades within the core.

The potassium from the turbine exhaust is condensed within tubes in a shell-and-tube heat exchanger by the NaK on the shell side. The volume of the secondary loop is much greater than that of the primary loop. By using NaK as the secondary fluid, good heat transfer characteristics are maintained while providing a lower mass than if potassium alone was used. The

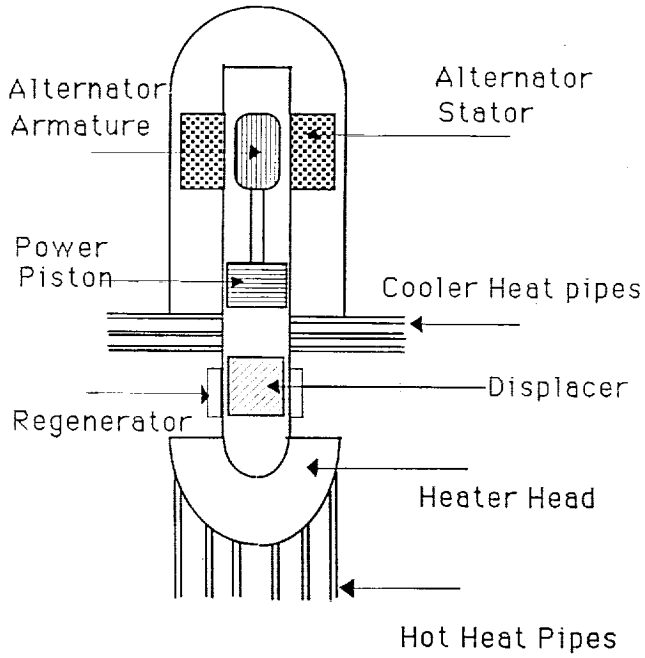

Fig. 1. Reactor System Diagram

radiator consists of rows of parallel tubes with connecting fins in a cruciform arrangement. Titanium-6% aluminium-4% vanadium was chosen as the radiator material on the basis of low material density and high strength at operating temperatures. The radiator surface is coated with calcium titanate to improve emissivity.

MARS SAMPLE RETURN POWER SUPPLY

For centuries scientists have studied Mars by means of telescopes, satellites, and deep space probes. Valuable geological, chemical, and other information could be gathered by sample and data collection on the Martian surface. The object of this design is to conceptually develop a vehicle to be used for the Mars Sample Return Mission. The vehicle must be lightweight, reliable, and if possible, have redundant parts in case of a component failure.

This study is restricted to the power supply of the vehicle; equipment necessary for the actual collecting of the soil samples is not included. The design will be divided into four categories consisting of the power supply, power converter, heat transfer devices, and a radiator. A mass optimization will then be performed on the entire system and the system efficiency calculated.

The power supply design is illustrated in Fig. 2. The hot-side heat pipes run vertically out of the GPHS assemblies and are attached to the Stirling engine/linear alternator configuration. The cold-side heat pipes radiate horizontally from the engine, passing through the vehicle body. The radiator is attached to both heat pipes and the vehicle body.

MPR-300 FOR MARTIAN APPLICATIONS

This design project was to provide power for a 2-6 month, unmanned geosynchronous Earth orbit GEO-to-Mars mission and to provide 6 years of terrestrial power on Mars. Research sources were the German HTR reactor, current U.S.-government journal articles on particle-bed space reactors, and the British MAGNOX carbon dioxide reactor of the 1960's. From this research it was determined that a carbon dioxide, gas-cooled, pebble-fueled reactor would be feasible to meet our requirements. The main reasons for this choice were availability of carbon dioxide on the martian surface and the high power densities achievable in a small reactor with particulate-type fuel.

The design objective was an electrical power level of 300 kW to provide power for the GEO-to-Mars journey and a high cycle efficiency to keep the reactor thermal power output around 1 MW. The system mass was required to be < 10,000 kg to ensure that it be transported as a single shuttle payload. This led to the choice of heat pipe radiators for waste heat rejection, as the total mass of the heat rejection system was of utmost concern. Reliability, provided by a redundant system, was another design objective in order to meet mission goals.

The report outline consists of seven different sections which are contained in the body of the report. (A copy of the final project report can be obtained from Universities Space Research Association, 17225 El Camino Real, Suite 450, Houston, Texas 77058.) The first section consists of neutronics which calculates flux distributions and fuel requirements. The second section is made up of thermal-hydraulics considerations for calculating reactor core temperature and pressure characteristics. Section three consists of the thermodynamic cycle calculations which defines states and arrives at an overall cycle efficiency. The turbomachinery selections can be seen in section four. The heat pipe radiators for waste heat rejection are explained in section five. The sixth section contains the shadow shield configuration necessary to protect electronic components from radioactivity. Section seven is comprised of propulsion and space logistics in order to successfully complete the GEO to Mars mission.

The thermodynamic cycle is a Brayton cycle consisting of CO_2 gas coolant and the reactor, heat pipe radiator, and compressor loop.

LUNAR TUNNEL-BORING MACHINE

A need exists for obtaining a safe and habitable Lunar Base that is free from the hazards of radiation, temperature gradient, and micrometeorites. A device for excavating lunar material and simultaneously generating living space in the subselenean environment has been researched and developed at the conceptual level. Preliminary investigations indicate that a device using a mechanical head to shear its way through the lunar material while creating a rigid ceramic-like lining meets design constraints using existing technology. The Lunar Tunneler is totally automated and guided by a laser communication system. Potentially, the excavated lunar material could

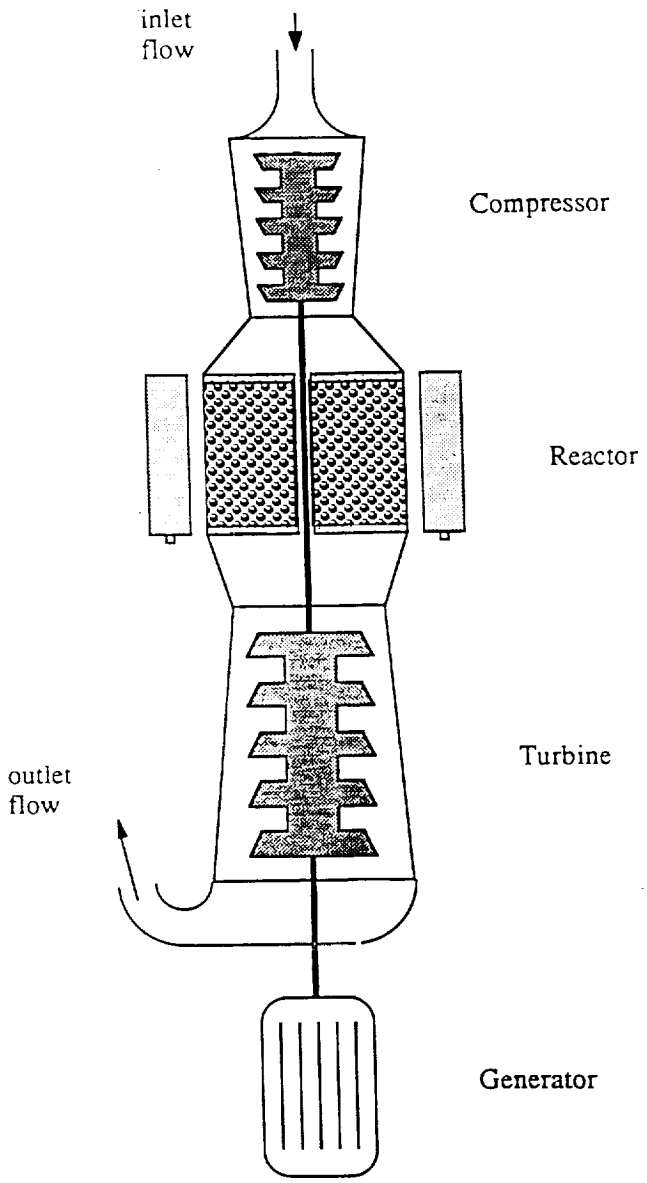

Fig. 2. Power Supply Design

be used in conjunction with surface mining for extraction of oxygen and other elements. Experiments in lunar material excavation and further research on the concept of a mechanical Lunar Tunneler are suggested.

From the findings presented in the final project report, it is concluded that a mechanical Lunar Tunneler is a viable and efficient technique for creating large amounts of underground living space. An SP-100 high-speed atomic reactor is the best choice for supplying the power requirements because of its compactness, longevity under adverse conditions, and ability to provide ample power for lunar tunneling. The completely mechanical cutterhead, with 26 disc cutters, would be able to shear through the lunar material without using the large amounts of power required by a melting tunneler. The mechanical head is based on a proven design and should be very reliable with minimal downtime. In addition, using a mechanical head would eliminate the problem of transporting molten lunar material through the interior of the tunnel-boring machine. Using the existing lunar materials to form a rigid ceramic structure was found to be totally viable and more efficient than transporting structural lining materials from Earth. Propulsion of the Lunar Tunneler would be performed by a proven existing design built by Lovat and other companies. Features of the propulsion system include low power requirements, a hydraulically-activated gripper system, and the ability to maneuver in all directions. The Lunar Tunneler can be guided with a computer operating in conjunction with the laser guidance system. Removal of the unheated lunar material to the rear of the Tunneler would be accomplished by an existing conveyor system developed by Flexowall. The conveyor system is very reliable, has adjustable speed control, and has the advantage of a large capacity for transporting excavated material. The conveyor system would move the excavated lunar material into a holding tank, where excess heat would be transferred to the material. Once the holding tank is filled, it transfers its load to the Dump Truck for removal from the tunnel. This would eliminate the accumulation of heat within the tunnel without requiring additional cooling elements. In this conception, the Lunar Tunneler should prove to be a straightforward and reliable design.

SUBSELENEAN TUNNELER MELTING HEAD DESIGN

The placement of base facilities in subsurface tunnels created as a result of subsurface mining is described as an alternative to the establishment of a base on the lunar surface. Placement of the base facilities and operations in subselenean tunnels will allow personnel to live and work shielded from the problems of radiation and temperature variations. A conceptual design for a tunneling device was executed, and its feasibility was assessed. A tunneler was designed to melt through the lunar material at a rate of 25 m/day (81 ft/day), leaving behind glass-lined tunnels for later development. The tunneler uses a 20 MWt nuclear generator to supply the heat flux necessary to melt the regolith about its cone-shaped head. Melted regolith is excavated through intakes in the head and transferred to a truck that hauls it to the surface. The tunnel walls are solidified to provide support lining by using an active cooling system about the mid-section of the tunneler. Results of the conceptual design analysis indicate that the concept is viable given further research and development in a few key areas, namely nuclear power production and high-temperature-tolerant materials. The benefits resulting from locating a lunar base in subselenean tunnels should encourage further investigation of tunneling technology.

PROJECT LONGSHOT

UNITED STATES NAVAL ACADEMY

Project Longshot presents a preliminary design for an unmanned probe to Alpha Centauri with a planned launch early in the 21st century. A 100-year estimated travel time was baselined for the mission. The work was based upon the requirement stated in the National Commission on Space Report, *Pioneering the Space Frontier*. One of the elements of the Commission's solar and space physics plan is "a long-life, high-velocity spacecraft to be sent out of the Solar System on a trajectory to the nearest star." Adequate lead time is included in the scenario to allow the development of several enabling technologies and to ensure that the required space operations infrastructure will be in place.

Using current technologies, such a mission would be impossible. The main technology areas requiring advancement are propulsion, power, communications, control, and data processing. The solutions envisioned in this report are: pulsed-fusion microexplosion propulsion with 10^6 sec specific impulse, a space-rated, 300-kW fission reactor with a 10-year active-power life once in the target system (as well as for starting the fusion drive), an advanced high-power (hundreds-of-kilowatts) laser communications system, and advanced, artificially-intelligent, high-speed computers to provide adequate internal command and control functions.

Due to the 100-year transit time required and the enormous distance involved, present propulsion systems are inadequate. A pulsed-fusion interstellar drive derived from the *Daedalus Report* produced by the British Interplanetary Society in the late 1970's was chosen as the best possible system to satisfy the mission requirements.

In order to provide sustained power for spacecraft operations and for propulsion system ignition and reignition, a long-life, high-power electrical source is required. No power systems exist today that can meet this demand. It is reasonable to expect that such a system can be extrapolated from the current SP-100 and Multi-Megawatt Reactor programs. The power system for the Longshot probe must deliver a sustained power level of 300 kW after operating at a reduced power level for 100 years. The system must be highly survivable and fault-tolerant, in addition to providing the necessary shielding to protect the instrument and processing packages.

The interstellar probe must operate autonomously with no outside input or control for a period in excess of 100 years. All probe systems must be highly reliable, multiply-redundant, and self-repairing if possible. Moving parts should be kept to a minimum; new long-life lubricants will be necessary for critical moving parts. This autonomy demands highly sophisticated, artificially-intelligent control and data processing systems. The Longshot control system must be able to control all probe operations, compensate for equipment failures, and handle emergency situations. Also, the processing system must control the propulsion and instrumentation of the probe and should be able to select interesting targets for investigation and analysis.

The spacecraft will be boosted in modular components to the U.S. Space Station in low Earth orbit. There it will undergo systems checks as it is assembled and prepared for launch. Longshot will then be nudged a safe distance away from the station and will ignite its first-stage rockets to make a plane-change into an orbit inclined 61° to the ecliptic. Once this maneuver is accomplished, second-stage rockets will fire to escape Earth-orbit into a 61° heliocentric orbit. Finally, the last stage will propel the probe out of the solar system where the interstellar drive will be started for constant acceleration to the target system. At the 70-year point in the mission, the probe will shut down the drive, rotate 180°, and reignite the drive to decelerate into the target orbit about Alpha Centauri B.

During transit from the solar system to the Alpha Centauri system, information concerning systems operation and scientific data will be returned to the Earth-orbital receiving station utilizing laser communications power levels commensurate with the distance from Earth. The communications lasers operate at a wavelength at which the target stars' emission spectra have a deep "hole." Once in the target system, data from the various instruments will be analyzed by a processing subsystem and transmitted back to the Earth at maximum power and data rate. Instruments will include packages for studying the stars in the system and any planets that might be encountered. Scientific data on the interstellar medium and astrometry can be gathered during transit. The astrometric data will be particularly useful since it will extend the distance to which accurate parallax measurements can be made to more than 1.2 million parsecs and thus allow the accurate determination of distances to hundreds of trillions of stars.

The probe will consist of a large, truss-like structure that will support four main components: the instrument package, the fission reactor, the fusion drive system, and the fuel tanks. The fusion drive and fission reactor will be placed at the rear of the truss, separated from the remainder of the spacecraft by thermal and radiation shielding. The tanks will be cylindrical, five meters in diameter and 35 meters long, and will be attached to the sides of the truss (forward of the nuclear systems) in a hexagonal arrangement. Instrumentation will be positioned forward of the fuel tanks. Particle shields will be installed at both ends of the probe for protection from collisions with dust particles at the high velocities the probe will be expected to reach. To conserve fuel, tanks will be

jettisoned as emptied, and the fusion drive will be discarded at the target system. The forward particle shield will be jettisoned when the spacecraft rotates 180°; the rear particle shield will be discarded with the fusion drive.

Excess power produced by the fusion drive will be used by spacecraft systems so that the fission reactor will operate at minimum power levels during the interstellar transit. The fission reactor will be the sole source of power for the probe as it orbits Alpha Centauri B.

THE LUNAR ORBITAL PROSPECTOR

UTAH STATE UNIVERSITY

INTRODUCTION

The Apollo program's scientific output greatly increased our understanding of the Moon's geophysical and geochemical nature. Vast amounts of data were obtained through surface sampling and orbital-based remote sensing measurements. Although a large amount of data was collected, overall surface coverage remains woefully incomplete. The low latitude orbits of the Apollo Command Modules, combined with the relatively small amount of time spent there, provided limited remote sensing of the surface and offered only a tantalizing glimpse of the Moon.

One of the primary rationales for establishing a manned lunar presence is the possibility of utilizing the Moon's resources. The Moon is abundant in oxygen and various metals all of which can find ample application in cislunar space. Additionally, undiscovered resources and large deposits of known resources may exist on the Moon. Water ice has been theorized to exist in permanently shadowed polar craters,[1] and early lunar volcanic activity may have provided a mechanism for forming large ore and mineral deposits near the lunar surface[2]. Given the known resource potential of only a few explored lunar sites, the existence of large deposits of these resources and other undiscovered resources elsewhere on the Moon seems highly likely. As such, a continued search and exploration for lunar resources on a global scale in conjunction with a manned lunar base will aid in the utilization of these resources.

A remote sensing orbital mission, such as the planned Lunar Geoscience Orbiter (LGO), is a necessary precursor to the development of a manned lunar base. The need for a mission of this nature, however, does not end with the establishment of the base. Long-term observation of the Moon, continued search for lunar resources with new techniques, and continued lunar science studies are paramount to understanding the Moon and fully benefitting from its total resource potential.

Accompanying humankind's return to the Moon will be a renewed interest in lunar science studies. A manned lunar base provides an invaluable opportunity to study the Moon via surface sampling and monitoring. However, lunar science at a base site cannot properly address the full spectrum of science questions and objectives. Several of the most fundamental geophysical and geochemical issues, such as the composition, structure, and thermal state of the interior, can only be adequately addressed by long-term observation and electromagnetic sounding of the lunar surface[3]. A long-term remote-sensing mission in conjunction with a lunar base can expand on LGO's geochemical and geophysical data base and serve as the "eyes and ears" of a manned base by searching for lunar transient events and by monitoring man's impact on the lunar environment.

The limited lifetime of the LGO and its inherently limited ability to respond to changes in science and exploration needs are its main deficiencies. The LGO's two-year projected lifetime is adequate for its mission objectives but it fails to provide substantial long-term observation of the Moon. LGO is, by its very nature, inflexible to changes in science needs. New methods for locating resources, unforeseen science questions, long-term observation, orbits tailored to specific needs, and new instrument technologies cannot be adequately accommodated by LGO.

THE LUNAR ORBITING PROSPECTOR

The Lunar Orbiting Prospector (LOP) is a lunar-based orbiting platform whose primary mission is to prospect the Moon in support of early lunar colonization and utilization efforts. Using the LGO mission as a baseline, the LOP mission is designed to direct the next generation of lunar exploration in conjunction with a manned base.

The LOP design concept is divided into two distinct parts; an orbiting platform carrying remote-sensing instruments and a servicing vehicle that is lunar launched and landed. The orbiting platform contains its own propulsion system for orbital maneuvering and remains in lunar orbit indefinitely. The platform mounts modular remote-sensing instrument packages, communications modules, and power systems. The servicing vehicle, called the Generic Transfer Vehicle (GTV), launches from a base site, accomplishes rendezvous with the platform for servicing, and returns to the base site. The GTV serves as a "lunar truck" to deliver replacement instrument modules, refueled propulsion modules, etc., and provides servicing of the platform in the event of failure. The orbiting platform is the focus of this paper.

The primary purpose of the orbiting platform is to map the chemical and mineralogical composition of the Moon. Remote-sensing instruments mounted on the platform probe the lunar surface and subsurface with electromagnetic energy. The data returned from the instruments will give an indication of the mineral and chemical species present and an indication of the subsurface geological structure of the Moon. Through careful processing and examination of this data, lunar resource distribution on a global scale can be determined.

The ability to replace, repair, and upgrade remote sensing instruments is a critical attribute. The modular concept permits the orbiting platform to be upgraded and modified as needed. The spacecraft can be repaired, refueled, and its instrument packages upgraded to perform nearly any required remote-sensing task. Highly specialized lunar remote-sensing missions can be performed and/or small lunar experiments flown without tailoring and deploying an entire spacecraft for each application. The value of this concept has been proven

in Earth applications by shuttle-based experiments and the second generation Mariner spacecraft.

MISSION DESCRIPTION

The LOP mission is divided into three primary phases: transport from Earth to low lunar orbit (LLO), operation in lunar orbit, and platform servicing in lunar orbit. Transport of the platform from Earth can be accomplished by a vehicle with a 1000-kg translunar payload capability. This is within the capabilities of the Titan 34D with an upper stage or a Space Shuttle/upper stage combination. An upper stage, such as the inertial upper stage (IUS) with a reduced propellant mass, provides the initial translunar insertion burn, and the platform's on-board propulsion system provides midcourse corrections and lunar orbit insertion burns.

After delivery to low lunar orbit, normal orbital operation commences. The initial orbit is baselined to be a 100-km-altitude near-polar orbit. Here the platform can alter its orbit to obtain the desired surface viewing, and the orbit can be changed periodically as needed. The initial remote-sensing package is baselined to be an updated version of LGO instruments. The initial mission can thus serve as a means for calibrating instruments, gaining experience with the spacecraft, and obtaining an overall remote sensing picture of the Moon.

Since the platform can mount various remote-sensing instruments, many types of orbital missions can be performed. After completion of the first remote-sensing mission, more ambitious and/or complicated prospecting and exploration missions can be contemplated. When such missions are desired, the servicing vehicle provides a means for changing instrument systems and spacecraft subsystems. The propulsion module can also be replaced at this time by a refueled version renewing the platform's orbit change ability. Since other remote-sensing mission objectives will require differing orbits, the coincidence of instrument changeouts and platform refueling is necessary. The concept of servicing the platform in lunar orbit gives a great deal of flexibility to mission planning, allows the spacecraft to meet new exploration and science needs, and is vital to the utility and usability of the LOP.

SYSTEM DESCRIPTION

The general configuration of the LOP is driven by three major requirements: overall system modularity and expandability, on-board propulsion, and a preferential-nadir-pointing instrument platform. Figure 1 shows the system configuration.

The overall goal of the configuration is to allow the system to grow and adapt to new and different science and exploration needs. The base structure of the spacecraft serves to house the propulsion module and mount the required power, control, and communication subsystems. The sides of the spacecraft provide 24 instrument drawers for mounting required subsystems and sensor payloads. The instruments and all other subsystems communicate through an optical spacecraft data bus. The instrument drawers provide the

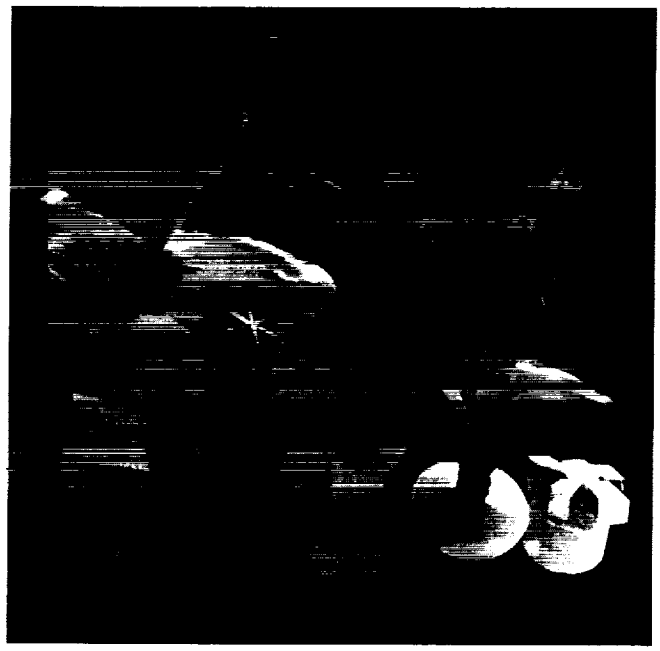

Fig. 1. The Lunar Orbiting Platform Configuration

opportunity for replacing, adding, and upgrading any compatible instrument system. The primary remote-sensing instrument module is mounted opposite the propulsion module in the nadir-pointing direction. This position gives the instruments the required nadir and anti-nadir viewing while providing for unrestricted expansion away from undesired spacecraft thermal and magnetic interference.

The spacecraft is expected to continuously pitch to maintain nadir pointing and yaw as required to maintain solar panels normal to incident sunlight. The attitude control system consists of four bias momentum wheels, hydrazine control thrusters, and pitch and roll attitude sensors. Present estimates indicate average pitch-pointing accuracy to be approximately $\pm$ 2 mrad, and in the event of attitude control failure, the satellite is gravity-gradient stabilized[4].

Communications is provided by four phased-array medium-gain antennae mounted on the sides of the spacecraft. These antennae are electronically steered to track relay satellites located at LaGrange points L1 and L2. The relay satellites and their locations allow constant data transmission to either the lunar base or Earth. Present estimates indicate the 1 Gbps will be attainable, and if this rate is achieved, real time transmission of a 1024 $\times$ 1024 $\times$ 8-pixel system can be performed without data compression or storage techniques[5].

REMOTE SENSING CONCEPTS

Many variations of remote sensing instruments can be flown on the LOP as a result of its modularity. Examination of these instruments reveals the remote-sensing methods possible and illustrates the LOP's versatility.

REFLECTANCE SPECTROSCOPY

Sunlight reflected from the lunar surface contains absorption lines that are characteristic of minerals present. Earth-based observations of the Moon's reflectance spectra, coupled with Apollo-based groundtruth data, has validated this technique for several lunar regions. Mineralogical mapping by this method, combined with data from other instruments, can lead to a much improved understanding of the Moon's surface properties and lunar crust history[6]. Spectrometers such as LGO's visual and infrared mapping spectrometer (VIMS) use this technique. Typically the experiment utilizes an optical system to focus the reflected infrared light on a spectrally sensitive detector array whose output is sent to the spacecraft data system. Data collected by infrared spectroscopy can provide complementary information with other instrumentation systems.

GAMMA RAY SPECTROSCOPY

Measuring the Moon's natural gamma-ray emissions is recognized as a powerful means for measuring surface elemental abundances. Gamma-ray spectrometers were flown on Ranger 3, 4, and 5 missions and on Apollo 15, 16, and 17 command modules[7]. A gamma-ray spectrometer records the Moon's natural gamma-ray emissions caused by the decay of radioactive elements such as U, Th, and K. Other elements can be detected by sensing the emitted gamma rays due to high-energy cosmic-ray interactions with lunar surface materials. This method can be used to detect hydrogen, indicative of trapped water ice in permanently shadowed polar craters[1]. Historically, these instruments utilize a Germanium crystal cooled to a temperature of 125 K to detect incoming gamma-ray emissions[7]. Due to its intrinsic sensitivity, the gamma-ray spectrometer needs to be boom mounted away from the spacecraft to reduce mass interactions. Elemental sensitivity and ground resolution of the spectrometer vary depending on the total counting time available. Thus, the resolution of the spectrometer is best over regions overflown frequently.

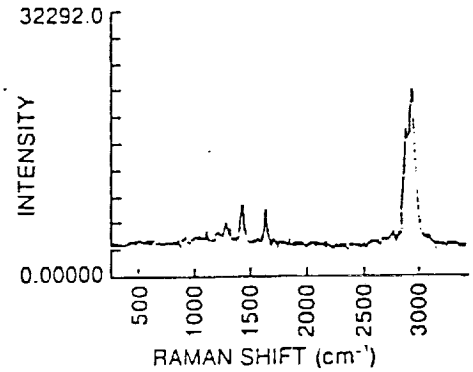

Fig. 2. Raman Spectrum of Nylon

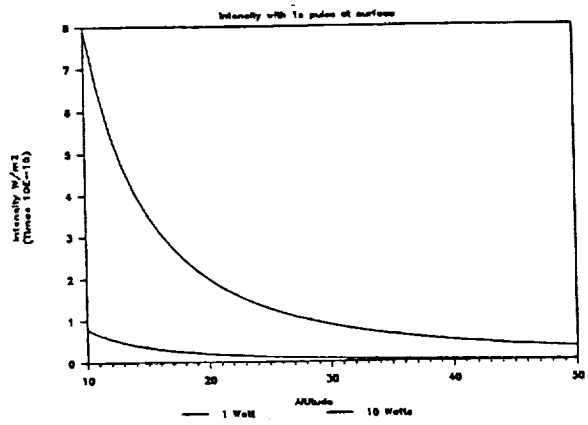

Fig. 3. Returned Raman Energy

RAMAN SPECTROSCOPY

Incident light can interact with a molecule by either absorption or scattering. If a photon interacts elastically with the molecule, Rayleigh scattering occurs. If a photon interacts inelastically with the molecule, Raman scattering occurs. The distinguishing characteristic of the Raman effect is the shift in frequency that occurs between the exciting energy and the scattered energy. This frequency difference, called the Raman shift, is directly characteristic of the molecule and is generally independent of the excitation frequency. Figure 2 illustrates the Raman spectrum of nylon. The characteristic frequency shift is denoted by a high-intensity spike at 2900 cm^{-1}. The Raman effect occurs as a consequence of molecular electron-state transitions which can give rise to an increase in frequency, called the Anti-Stokes line, or a decrease in frequency, called the Stokes line. Figure 2 illustrates a Stokes line that is generally more intense than the Anti-Stokes line. The Raman spectrum covers wavelengths of 2.5 to 1000 μm. The advent of tunable lasers has led to great success with this technique in laboratory applications and, to a lesser degree, in remote-sensing applications[8].

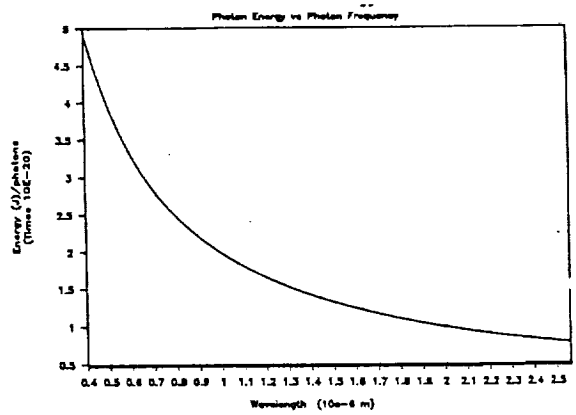

Fig. 4. Photon Energy vs. Frequency

The Raman sensing technique typically utilizes a tunable laser for excitation and a spectrally sensitive detector with a mask filter to remove the laser signal. The main drawback of the Raman spectrum method for remote sensing is the extremely small returned signal, around six orders of magnitude smaller than the incident energy. Figure 3 plots the returned Raman energy for different laser powers and differing spacecraft altitudes. In general, the intensities are very small, but present estimates indicate that sensor technologies are capable of detecting these small signals[9].

If one chooses the proper exciting frequency, the problems of instrument sensitivity can be compensated for. Figure 4 shows photon energy vs. wavelength. The lower wavelengths give higher photon energies, but these wavelengths limit laser power and can cause problems with mineral fluorescence. Higher wavelengths, in the infrared, represent low photon energies and stiff cooling requirements due to thermal interference. This region should be avoided.

The resonance Raman effect can occur as a result of both electronic and vibrational transitions. The resonance occurs when the exciting frequency falls within the interior of the observable vibrational structure of the electronic absorption band responsible for Raman scattering[8]. The intensities of some resonance Raman effects may be up to six orders of magnitude larger than Raman effects observed with the exciting frequency removed from the resonant frequency.

Sensor sensitivity and available laser power appear to be the primary limitations of remote Raman spectroscopy. If the proper laser frequency is not utilized, the required sensor sensitivity, cooling, and laser power are highly restrictive. The sensor requirements can be reduced by using visible and near-ultraviolet spectra where instrument cooling requirements are not significant and photon energies are higher. The baseline Raman spectrometer configuration is shown in Fig. 5. A krypton laser excites the surface sample, and the returned Raman spectrum is focused by a Cassegrain optics system on a spectrally sensitive detector. The operating wavelength of the laser is in the visible range, and the spectrometer operation is thus limited to lunar darkside sensing.

RADIO SUBSURFACE MAPPING

In order to fully understand the subsurface characteristics and engineering qualities of the Moon, an orbital-based instrument capable of examining the subsurface is needed. The absence of moisture on the lunar surface indicates that radio frequency electromagnetic energy penetration will be substantially greater than that on Earth. The use of VHF frequencies pulsed at the lunar surface can explore the lunar subsurface at depths of at least tens of meters[10]. Radar sounders carried by Apollo 17 penetrated as much as 1.5 km below the lunar surface. This simple technique detects, stores, and analyzes the return signal from a pulsed VHF transmission that penetrates the surface before reflection. The system baselined for the orbiting platform is based on Apollo systems and Shuttle-based SIR-A and SIR-B systems. This technique can be used to detect subsurface structures and formations, giving geologists a three-dimensional picture of the Moon. Subsurface

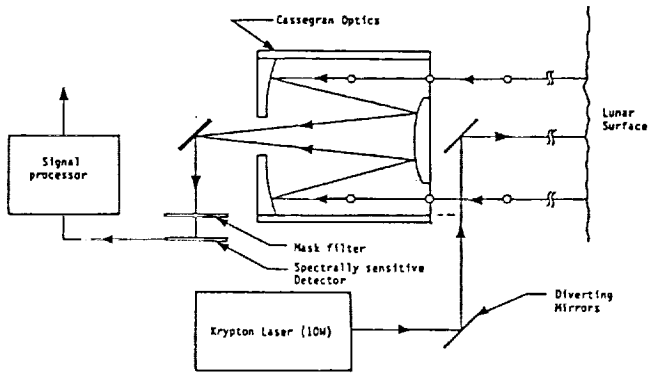

Fig. 5. Raman Spectrometer Configuration

mapping can lead to the location of subsurface mineral and ore deposits formed by early lunar volcanic and geologic activity[2].

By correlating subsurface maps with data from other remote-sensing instruments, a greater understanding of the local geology and geochemistry can be obtained[2].

ORBITS

The Moon's low mass and lack of an atmosphere make it a very attractive body for remote-sensing orbiters. The Moon's mass is small, about 1/80 that of Earth, hence, most orbits about the Moon are generally low in energy relative to equivalent orbits about the Earth. This property substantially reduces propellant requirements for lunar orbiting satellites. The range of possible orbital altitudes about the Moon is also attractive. Since the Moon does not possess an atmosphere, orbital altitudes and lifetimes are limited only by topography and lunar gravitational perturbations.

ORBITAL COVERAGE

The platforms's ability to change orbital parameters is important to achieving the desired mission versatility. To optimize the relationship between surface coverage and mission requirements, a variety of orbits is required. These orbits may vary in altitude, eccentricity, and inclination. Each

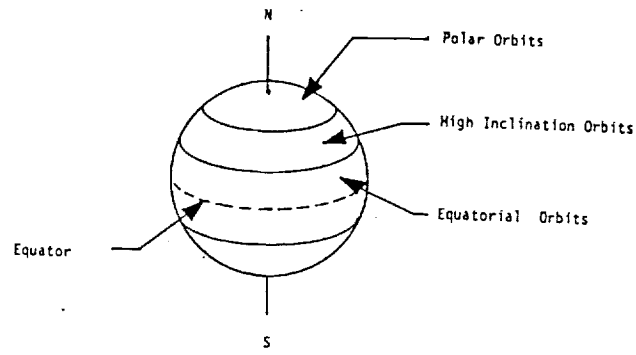

Fig. 6. Regional Coverage vs. Orbit Inclination

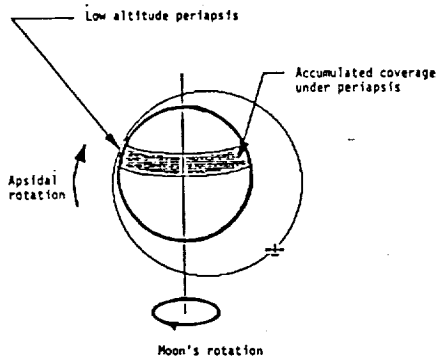

Fig. 7. High Resolution Coverage Via Periapsis Rotation

instrument package will require an orbit tailored to its specific need and the platform must be capable of a wide variety of orbits. Several classes of orbital coverage are considered: optimal global surface coverage at moderate to low resolution, regional coverage at moderate to high resolution, and very high-resolution, site-specific coverage. Orbital parameters dictate the type of surface coverage obtained, and by varying orbital inclination, eccentricity, and periapsis, various remote-sensing mission objectives can be realized.

Orbit inclination strongly influences the quality of regional surface coverage. Figure 6 illustrates the effect of various orbit inclinations on local coverage. In general, viewing is most complete at the lunar latitudes corresponding to the orbit inclination angle. Viewing of the entire lunar surface is offered only by polar orbits but this advantage is offset by sparse coverage at low latitude regions where successive orbit tracks are far apart. Reducing orbit inclination from 90° improves the coverage at low latitudes and equatorial regions but this completely eliminates polar coverage. Low inclination orbits are consequently best suited to high-resolution, site-specific coverage at low-latitude regions and polar orbits are best suited to lower-resolution, global coverage and high-resolution coverage of the polar regions.

Orbital altitude exerts a strong influence on instrument resolution. High altitudes decrease optical resolution and increase instrument dwelltime while low-altitude orbits increase resolution and decrease dwelltime. Higher orbital velocities, which are directly coupled to low altitudes, decrease the amount of time available for instruments to sense the surface. For reasonably small altitude differences, dwelltime is not a significant factor as lunar orbits exhibit small changes in orbital velocity with changes in orbital altitude. Orbit altitude selection is therefore a primary function of instrument optical resolution, viewing needs, and orbital stability considerations.

ORBITAL STABILITY

Mission objectives require orbits stable enough to permit orbital maintenance with a reasonable amount of maneuvering but low enough for good instrument resolution. Due to the Moon's anomalous gravity field, the stability of lunar orbits appears to be a direct function of altitude and inclination. Experience from earlier lunar flights and known lunar gravitational harmonics indicates that polar orbital inclinations and low-altitude orbits are unstable. Exactly polar orbits exhibit a rapid rise in eccentricity, lowering periapsis, and leading to impact into the lunar surface. Large lunar gravitational anomalies are known to exist but the overall gravity field and its effect on low-altitude orbit stability is poorly known. Numerical simulations of lunar orbits, based on low-order spherical harmonics, suggest a pattern of rising eccentricity on polar orbits[11] and of oscillating eccentricity on equatorial orbits[12]. Present estimates of a 100-km polar-orbit lifetime before periapsis crash are 9 months.

The net effect of orbital instabilities is to increase propellant use for orbital sustenance. General avoidance of very low altitudes and certain inclinations can partially negate stability problems. Estimates of lunar gravity harmonics indicates stable, near-polar orbits may be available. These are the so-called "frozen" orbits[7]. This family of slightly eccentric orbits has the periapsis fixed near the Moon's south pole and may remain stable for up to two years[13].

STRATEGIES

Several surface-coverage strategies are made possible by simply varying the orbital altitude (e.g., large regions at low resolution, small regions at high resolution, and global coverage at moderate to high resolution). Global coverage at moderate resolution can be achieved through the use of a 100-km polar orbit such as that planned with the LGO mission. Higher altitudes reduce the resolution obtained but increase the instruments' field of view thus allowing the equatorial regions to be more adequately viewed. Complete surface coverage from a polar orbit can be obtained in 27 days.

A highly elliptical orbit with a low periapsis over the region of interest gives a high-resolution sensing opportunity without the stability problems caused by strong lunar gravity anomalies that are associated with low, circular orbits. Since a small fraction of the orbit is spent at low altitudes, the net effect is to provide a low-altitude sensing opportunity while maintaining a higher average orbital altitude. The drawback to this method is the small region of coverage that accumulates under the periapsis. The highly eccentric orbit is also capable

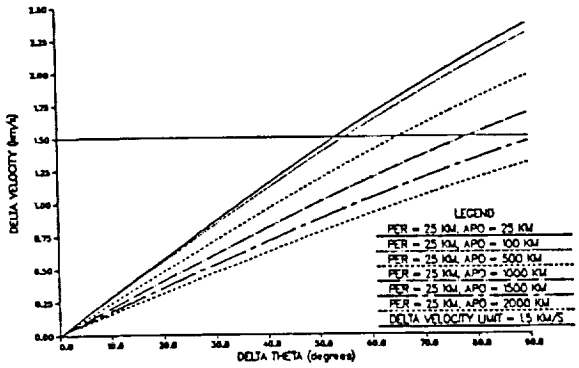

Fig. 8. ΔV Requirements for Orbit Plane Changes

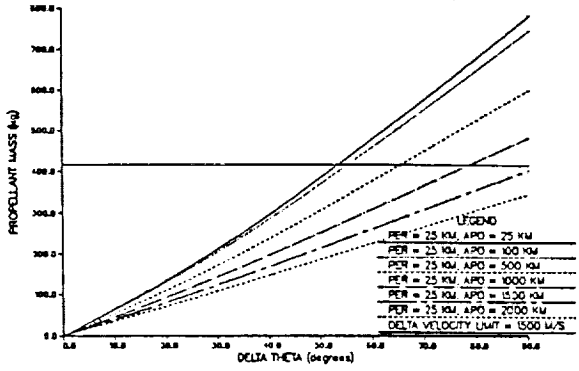

Fig. 9. Propellant Requirements for Plane Changes

of giving low-resolution, large-regional coverage on the apoapsis side with a smaller ΔV requirement than is associated with an equivalent transfer to a high circular orbit. The elliptical orbit offers a variety of surface-coverage opportunities, and by properly choosing periapsis latitude and orbit eccentricity, a significant variation in surface coverage can be obtained in one orbit.

A possibility exists for high-resolution global coverage by using a highly eccentric orbit and periodically shifting the latitude of periapsis. Figure 7 illustrates this concept. Since the orbit precession is small, the orbit can be considered to be fixed in space while the Moon rotates under it. By rotating the orbit line of apsides at appropriate intervals, enough to allow high-resolution coverage under the periapsis to accumulate, the entire lunar surface can be viewed from a low altitude without severe orbital stability problems.

ΔV REQUIREMENTS

Figure 8 displays velocity requirements for plane changes of various lunar orbits[14]. Figure 9 displays propellant requirements for the plane changes shown in Figure 8. The ΔV requirements are based on velocity change occurring at the high altitude aposelene where the maneuver is most efficient. With the platform ΔV capacity of 1.5 km/s, plane changes greater than 50° are possible with most lunar orbits and an orbital plane rotation of 90° is possible with highly elliptical or high-altitude orbits.

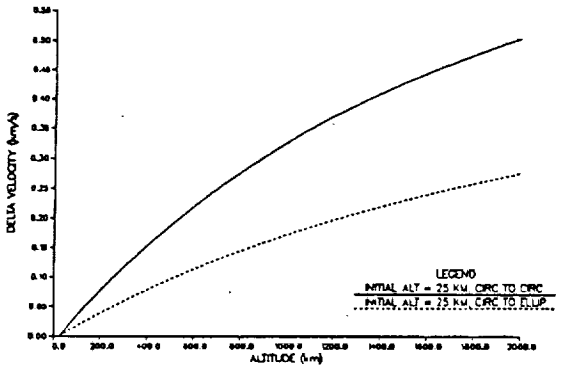

Fig. 10. ΔV Requirements for Coplanar Orbit Changes

Figure 10 plots ΔV requirements for coplanar orbit changes. An initial 25-km circular orbit is used to compute ΔV requirements to both circular orbits and elliptical orbits with a 25-km periapsis, since a 25-km circular orbit is the assumed servicing location. Transfer from a 25-km circular orbit to a 2000-km circular orbit requires a modest 500 m/s ΔV, and an eccentric orbit with a 2000-km apoapsis requires only 300 m/s ΔV. Computing propulsion requirements with a specific impulse of 300 s translates into propellant burns of 100 kg and 40 kg, respectively. With such small maneuvering requirements, many platform orbital changes and adjustments are possible in one mission.

Rotation of the line of apsides can be accomplished in two ways: successive Hohmann transfers or a direct periapsis velocity direction change followed by an orbital eccentricity correction maneuver. The successive Hohmann transfer method involves a maneuver to circularize the eccentric orbit to a low circular orbit and another maneuver to locate the new periapsis and correct orbital energy. It is believed that this method is the most efficient, particularly for large apsidal rotations. The ΔV requirements can be deduced from Fig. 10.

PROPELLANT CONSIDERATIONS

The LOP mission strategy is centered around three goals: low operating cost, minimum Earth support, and provision of a versatile orbiting platform for lunar science, exploration, and prospecting missions. Since a primary operating expense of the LOP is likely to be propellant cost, this can be substantially reduced through the use of lunar-derived fuels that do not require costly transport out of Earth's gravity well. Use of lunar-derived fuels also helps to minimize Earth support requirements.

MINERAL AND ELEMENT CONCENTRATIONS

Lunar minerals that show the most promise for lunar propellant production are olivine $[(Mg,Fe)_2SiO_4]$, pyroxene $[(Ca,Mg,Fe)SiO_3]$, and ilmenite $(FeTiO_3)$. Olivine and pyroxene occur in concentrations of up to 60% and ilmenite in concentrations of up to 20%[15]. These minerals are particularly promising for oxygen production.

Since the Moon is primarily composed of oxygen, it becomes an obvious choice for a bipropellant oxidizer. Oxygen can be easily extracted from lunar minerals by many chemical and thermal processes. The critical element of a lunar-derived propellant is thus the fuel. Hydrogen is an excellent fuel when used with oxygen but its lunar concentrations are sorely lacking. Other lunar-derived propellant possibilities include, but are not limited to, silane (SiH_4/O_2), $AlCa/O_2$, Al/O_2, $AlCaMg/O_2$, Ca/O_2, and lunar soil/O_2.

In theory, silane should perform well but has never been used in practice. Silane's primary advantages are its lunar-derived silicon, its high specific impulse (360 s), its thermal stability for regenerative cooling, and its high boiling temperature. Silane production from lunar materials, however, is quite slow due to its reliance on MgO in the production process[16].

Liquid hydrogen/liquid oxygen (LH_2/LOX) gives the best performance of the propellants but production of hydrogen from lunar soils is time intensive. Silane performs well but is also time intensive. Aluminum and oxygen thus show the most promise for lunar-derived fuels[17]. Powdered aluminum, when used in combination with an Earth-imported binder and lunar-derived oxygen, can provide upwards of a 300-s specific impulse[19].

Performance levels of Al/O^2 are approximately 80-90% that of current solid-grain propellants and LOX/RP-1. Peak performance of 290 s with Al/HPTB/O_2 is obtained with a mixture ratio of 0.5, i.e., with large amounts of excess oxygen. This appears to be due to the predominance of metallic oxides (in liquid form) and gaseous oxygen in the combustion species[18].

THRUSTER PARAMETERS

The thruster is a hybrid design. A refuelable oxygen tank is mounted in the center of the spacecraft where it is insulated and shaded to minimize cryogenic boil-off. The solid fuel portion of the thruster mounts on the end of the orbiter and is fully replaceable. The solid fuel, casing, injector, and nozzle are replaced with a refueled version on orbit. The nozzle and combustion chamber is regeneratively cooled for reusability.

CONCLUSIONS

The Moon is a body rich in natural resources and full of intriguing scientific questions, and it will most certainly play a central role in the growth of near-Earth and deep space ventures of the twenty-first century. The LOP mission is an example of one way to catalog the Moon's natural resources and to answer lunar science questions in parallel. In a realistic planetary exploration program, this mission must compete with other interesting planetary missions and therefore the LOP must be as low cost and adaptable as possible. This flexibility is reflected in the LOP's heavy design emphasis on modularity. The LOP mission can easily be expanded to include new technologies, and additional orbiters could be launched into lunar orbit to provide a constellation of remote-sensing platforms. This design thus projects a broad range of possibilities for continued lunar exploration in the next century.

ACKNOWLEDGMENTS

The USU design team wish to acknowledge funding support from NASA/USRA, design support from the Utah State University systems design team, and technical support from James D. Burke of the Jet Propulsion Laboratory.

REFERENCES

1. Watson K., Murray B.C., and Brown H. (1961), The Behavior of Volatiles on the Lunar Surface. *J. Geopys. Res., 66(9),* 3033-3045.
2. Barnum L. (1988), Lunar Orbiting Prospector. Final Report for USRA/NASA Advanced Design Program, 17225 El Camino Real, Suite 450, Houston, TX 77058.
3. Hood L.L., Sonnet C.P., and Russell C.T. (1986) The next generation geophysical investigation of the Moon, *Lunar Bases and Space Activities of the 21st Century*, (W.W. Mendell, ed.), pp. 253-270, Lunar and Planetary Institute, Houston.
4. Siapush, A. (1988), Lunar Orbiting Prospector. Final Report for USRA/NASA Advanced Design Program, 17225 El Camino Real, Suite 450, Houston, TX 77058.
5. Meline R. (1988), Lunar Orbiting Prospector. Final Report for USRA/NASA Advanced Design Program, 17225 El Camino Real, Suite 450, Houston, TX 77058.
6. Burke J.D. (1986) Merits of a lunar polar base location, *Lunar Bases and Space Activities of the 21st Century*, (W.W. Mendell ed.), Lunar and Planetary Institute, Houston, pp. 77-84.
7. Burke J.D. (1976) Lunar polar orbiter: a global survey of the Moon, *Acta Astronautica, 4,* pp. 907-920.
8. Freeman S.K. *Applications of Laser Raman Spectroscopy,* Wiley and Sons, New York, 1974.
9. McCurdy G. (1988), Lunar Orbiting Prospector. Final Report for USRA/NASA Advanced Design Program, 17225 El Camino Real, Suite 450, Houston, TX 77058.
10. Barrington A.R. Radio frequency reflectivity experiments for AES lunar orbital flights, *Advances in the Astronautical Sciences, vol. 20,* pp. 418-433, 1986.
11. Chesley B., Korsmeyer D., and Monroe D. (1988) Mixed vehicle transportation fleet for missions to lunar polar orbit, (abstract). In *Papers Presented to the Symposium on Lunar Bases and Space Activities of the 21st Century,* p. 50, Lunar and Planetary Institute, Houston.
12. Bond V., Mulichy D. Computation of seleocentric orbits using total energy (abstract). In *Papers Presented to the Symposium on Lunar Bases and Space Activities of the 21st Century*, p.29, Lunar and Planetary Institute, Houston. Lunar bases conference paper 88-172.
13. Uphoff, C. (1976), Stabilizing Influence of Earth Pertrubations on Polar Lunar Orbiters, *AIAA Paper No. 76-843,* AIAA/AAS Astrodynamics Conference.
14. Cristensen C. (1988), Lunar Orbiting Prospector. Final Report for USRA/NASA Advanced Design Program, 17225 El Camino Real, Suite 450, Houston, TX 77058.
15. LGO Science Workshop (1986). Contributions of a Lunar Geoscience Observer, Dept. of Geological Sciences and the Anthro-Graphics lab, Southern Methodist University.
16. Rosenberg S.D. (1986) A lunar based propulsion system, *Lunar Bases and Space Activities of the 21st Century*, (W.W. Mendell, ed.), pp. 169-175, Lunar and Planetary Institute, Houston.
17. Voyer P., (1988), Lunar Orbiting Prospector. Final Report for USRA/NASA Advanced Design Program, 17225 El Camino Real, Suite 450, Houston, TX 77058.
18. Streetman J.W. (1978) Investigation of the feasibility of chemical rockets using lunar derived fuels, Proceedings of 14th Joint Propulsion Conference.

A COMPARISON OF TWO OTVS

UNIVERSITY OF VIRGINIA

KEY ABBREVIATIONS

CCM	Crew Command Module
ECLSS	Environmental Control and Life Support System
EPS	Electrical Power System
EVA	Extravehicular Activity
EVAM	EVA Module
GEO	Geosynchronous Orbit
GNC	Guidance, Navigation, and Control
LEO	Low Earth Orbit
LH	Liquid Hydrogen
LO_2	Liquid Oxygen
MMU	Manned Manuevering Unit
OTV	Orbit Transfer Vehicle
RCS	Reaction Control System

INTRODUCTION

For a low Earth orbit (LEO) to geosynchronous orbit (GEO) mission scenario, it can be shown that both a chemically-propelled, aerobraked orbital transfer vehicle (OTV), and a high-thrust, nuclear OTV use approximately 50% less propellant than a comparable, chemical OTV. At the University of Virginia, two teams worked on designs for these types of OTVs. One group formed WWSR Inc. and worked on the aerobraked OTV, which was named Project Orion. The other group, named MOVERS, collaborated on the design for the nuclear engine OTV. This report will briefly review the nature and specifics of their work. This introduction will summarize each of these propellant systems and their corresponding cost savings. It will also highlight the strengths and weaknesses of each OTV concept.

The cost savings made possible with either the Project Orion OTV or the MOVERS OTV are significant as compared to a traditional chemical engine OTV without aerobraking. For the 15,000-pound payload, roundtrip mission, the Project Orion OTV required 132,000 pounds of propellant, and the MOVERS OTV 121,000 pounds. An OTV which employed only a chemical engine would require approximately 250,000 pounds of propellant. If a launch cost of $2500/pound is assumed, the propellant savings made possible by using an aerobrake and a chemical engine result in cost savings of $236 million. The use of a high-thrust nuclear engine results in slightly greater savings of $250 million.

An assessment of potential savings is incomplete without addressing the associated development costs. Both aerobrake and high-thrust nuclear engine technologies are in approximately the same stage of development and it is anticipated that development costs would be approximately equal.

Although both OTV concepts result in significant dollar savings, there are nonetheless a number of important distinctions between the two concepts.

The first distinction is a subtle one, and becomes apparent by looking at the weight summaries of the two craft and the propellant requirements for the LEO-GEO mission. In short, the MOVERS high-thrust nuclear OTV is designed to deliver more dry mass to GEO at a smaller cost than the WWSR's aerobraked, chemical OTV. Indeed, the MOVERS vehicle delivers an extra 21,100 pounds (or 9,510 pounds after accounting for the fact that the nuclear propulsion system weighs 11,590 pounds more than the aerobraked, chemical system) of dry mass to GEO and back to LEO using 4.9% less propellant than WWSR's craft. Note that, in this case, "dry mass" refers to the weight of the cargo as well as the entire structure of the unfueled system.

The weight difference between the two propulsion systems is the crucial detail. As the dry mass of the spacecraft increases, the relative significance of the weight difference decreases, making the nuclear OTV increasingly more efficient in its use of propellant than the chemical OTV. For smaller spacecraft, the weight difference in the propulsion systems become increasingly important. However, when light cargo or unloaded missions are considered, the chemical OTV becomes more efficient in its use of propellant than the nuclear OTV.

Implicit in the preceeding discussion is the assumption that both types of OTV's can handle heavier payloads. The MOVERS OTV, for example, could easily handle an Earth-Moon mission with a requirement to deliver and return an 80,000-pound payload by simply adding extra tankage along its boom. The addition of tankage to the Project Orion OTV is problematic. Aerodynamic passes require that the vehicle be compact, and that the center of gravity be accurately known. This does not mean that the Project Orion OTV could not handle the larger payloads. It would just be much more difficult for such a mission to be accomplished.

Although it may be more complicated to reconfigure the Project Orion OTV to handle the heavier lunar payloads, the demanding requirements of aerobraking do give the craft the structural integrity to possibly handle a lunar landing. In lunar orbit, the Project Orion OTV might simply replace its aerobraking shield with orbiting lunar legs. This exciting possibility requires further research. In any case, this is simply not an option available to the MOVERS OTV.

Another important distinction between the two OTV concepts has to do with the environmental impacts. The Project Orion OTV is perfectly safe to use in LEO and can easily be docked at a space station. There are, however, a number of environmental concerns associated with the MOVERS OTV.

The worst case scenario would be a misfired thrust vector which puts the craft on a trajectory into the Earth's atmosphere. Such a scenario would require the destruction of the reactor at high altitude, and the incorporation of some sort of escape module for the crew into the design of the OTV. The destruction of the reactor in LEO has been shown to be safe for the human population on Earth. However, more research is required to assess these risks better.

The MOVERS OTV also has difficulty in docking with the space station. The approaches to the station have to be handled carefully due to the residual gamma radiation being produced in the reactor. A preferred technique would be to dock the OTV at a docking station and then ferry the crew to the space station. It is important to note that such a docking station is currently being considered for even the chemical spacecraft that are intended to dock with the space station. However, even if the problem of residual radiation could be managed somehow, the size of MOVERS OTV might pose a threat to the orbital stability of the Space Station if it were to hard dock. Because of the radiation and stability problems that the MOVERS OTV could cause for the Space Station, Project Orion's OTV would perhaps be more suited for missions where hard docking to the Space Station would be required.

Before a nuclear-powered OTV could be used, yet another environmental issue must be dealt with: the storage and disposal of spent reactor assemblies. These simply cannot be allowed to accumulate in low Earth orbit. It may be possible to reprocess the fuel, store in an orbit closer to the sun, or to bury it on the Moon. In any case, this issue must be addressed.

Finally, the last point of comparison between the MOVERS OTV and the Project Orion has to do with stresses to which the craft is exposed. The Project Orion OTV must endure the high temperatures and the aerodynamic forces associated with an aerobraking pass at very high Mach numbers, and this may limit the design life of the spacecraft.

Clearly, each type of craft has both strengths and weaknesses. Both offer potential for enormous cost savings. It should also be emphasized that neither technology is mutually exclusive. Indeed, for more ambitious, manned missions into the solar system, both technologies could be used together to achieve enormous propellant savings. In fact, those savings could make such exciting missions possible.

In the following two sections of this report, there are summaries of the designs for WWSR's and MOVERS' OTVs. These summaries contain design specifications for each vehicle that were completed as of June 11, 1988. A more detailed analysis of these systems can be found in the final reports submitted by WWSR and MOVERS. (A copy of the final project report can be obtained from Universities Space Research Association, 17225 El Camino Real, Suite 450, Houston, Texas 77058.)

PROJECT ORION

The goal of the Project Orion team was to submit a proposal for a chemically propelled, manned, orbital transfer vehicle (OTV) that would meet the criteria set forth by the National Commission on Space in *Pioneering the Space Frontier* (1986). The OTV will consist of modular components and be capable of transporting a crew of three and a 12-ton payload between the Space Station and geosynchronous orbit (Fig. 1).

Mission Requirements

Mission Objectives. The OTV will leave the Space Station carrying components for an experiment assembly (payload, 15,000 lbm). Such an assembly may be used for space defense initiative (SDI) testing, but of course any payload is possible. The OTV will also carry provisions for a full crew of 3 for a 7-day mission. Five days on station will be anticipated for carrying out the experiments. Upon completion of the experiments, the OTV will return with the assembly to the Space Station.

Mission Profile. Following separation from the Space Station and subsequent systems checkout, the OTV performs a phasing-orbit injection burn (PIB). The phasing orbit is designed to bring the OTV to the transfer-orbit injection point at the proper time so it will arrive at the correct location in GEO. The transfer injection burn places the OTV in an approximate Hohmann elliptical transfer to GEO, which lasts approximately five hours. Following circularization and a plane-change burn at GEO, the OTV can remain on station for five days to complete the required experiments.

After the experiments are completed, an injection burn places the OTV in a GEO-LEO transfer orbit that will take it through the Earth's atmosphere. The first aerobraking pass, dipping the OTV to a height of 85 km above the Earth, lasts only five minutes and leaves the vehicle in an intermediate orbit. Based on the results of the first pass, correction burns take the OTV through the atmosphere a second time. This time the maneuver lasts about 11 minutes and places the OTV in an orbit that can be circularized at LEO by a small propulsive burn.

Configuration. This mission will require the use of 6 sets of propellant tanks containing LO_2, and LH_2, EVAM, and CCM.

Weight Estimates

System		Weight (lbm)
Dry Weight:		
ECLSS		2,500
Fuel Tanks and Supporting Structure		3,660
Engine System		1,050
CCM, EVAM, and Components		13,260
Aerobrake		2,800
Electronics		980
EPS		1,730
RCS		3,250
MMU		1,280
Crew		510
	Total	31,125
Wet Weight (15,000 pound payload, LEO-GEO Option):		
Propellant		132,000
		(127474 lbm used
		4526 lbm reserve)
Payload		15,000
	Total	178,125

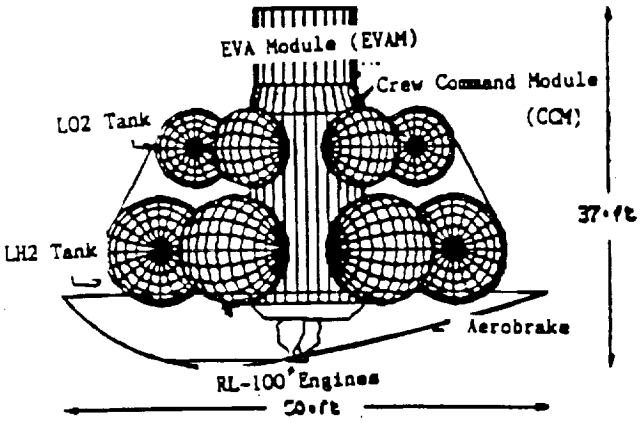

Fig. 1. Orion OTV Configuration

Design

To complete the above mission, as well as our "worst case scenario" (see Project Orion's final report), several systems needed to be integrated. Each posed unique problems. The aerobrake required that the OTV be compact and symmetrical. The chemical propulsion system required that the OTV be lightweight. Being able to support manned-missions required redundant failsafe systems. Major trade-offs were demanded between redundancy and weight in order to maximize performance. What follows is a brief description of some of the primary systems of the OTV.

Aerobrake. The design of the OTV is based on a raked sphere cone configuration (Fig. 2). This design has a blunt nose configuration, similar to but not the same as the Apollo space capsule. Several factors led to the selection of the configuration. The most important is its low ballistic coefficient (10 lb/ft^2) which makes it ideal for high-altitude maneuvering where heating effects are small.

The aerobrake is 50 ft in diameter. This provides a cone of protection from atmospheric heating large enough to envelope the OTV and payload fully. The structure consists of aircraft-type-aluminum skin, stringer, rib, and frame construction. The skin is covered with high-temperature, reusable, surface insulation similar to that used on the Space Shuttle. This material consists of sintered silica fibers reinforced with silicon fibers, bonded to the skin with a thin layer of RTV-560 adhesive and NOMEX felt pad.

Control during the aerobraking maneuver is assured by the asymmetrical design of the airbrake, thus rotation of the OTV by firing the RCS system results in a time-averaged lift to drag ratio. Also, propellants are pumped between tanks to achieve a predetermined position for the center of gravity before entering the atmosphere. Calculations by the design team have shown that two passes through the atmosphere will be necessary to minimize heating effects and to ensure safety by allowing intermediate correction maneuvers.

Engine System. The propulsion system selected by the Project Orion team was the RL-100 engine currently being designed by Pratt & Whitney. Two engines were deemed necessary to provide redundancy. Using two engines ensures a reliability of 99.6% over an expected lifespan of 25 missions. The RL-100 was selected over other engines because of its high reliability, high thrust, and low weight. The RL-100 uses LH_2 for its fuel and LOX for its oxidizer. Suspending metallic aluminum in the hydrogen will boost the specific impulse of the system to 502 seconds and thus lower propellant requirements. The total expected thrust of the system is 15,000 lbs. Even if one engine should fail during the mission, the other engine will have ample thrust to return the OTV to the Space Station. The engines nozzles will be extended through the aerobrake during firing. During aerobraking the nozzles will be retracted so that they are flush with the aerobrake.

The fuel system consists of six pairs of spherical 2029 aluminum alloy tanks containing LOX and LH_2. The LOX tanks are 8.4 ft in diameter and hold 18856 lbs LOX; LH_2 tanks are 11.6 ft in diameter and hold 3144 lbs LH_2. The tanks are pressurized to 7 psi in order to reduce structural loading. Pairs of tanks can easily be disconnected from the structure so that extra weight can be eliminated for missions that do not require maximum propellant. Two main pumps feed propellant to the engines. Six auxiliary pumps are used to control the c.g. of the OTV. Bleedoff from the tanks is used for tank pressurization, EPS, and ECLSS.

CCM and EVAM. The modules are semimonocoque 2090-aluminum structures stiffened with ring frames and skin stringers. The CCM, which is 22 ft long and 12 ft wide, contains various control, power, and life-support systems, as well as crew quarters for three people. The cabin will be pressurized to 14.7 psia with a mixture of nitrogen and oxygen similar to Earth's atmosphere. The EVAM, which is 8 ft long and 10 ft wide, will house two MMUs and tools needed for various missions. It will be evacuated at all times but contains an airlock which allows access to the CCM and to space. A robot arm similar to the one used on the Space Shuttle and a satellite berthing ring are externally mounted to the EVAM for satellite servicing.

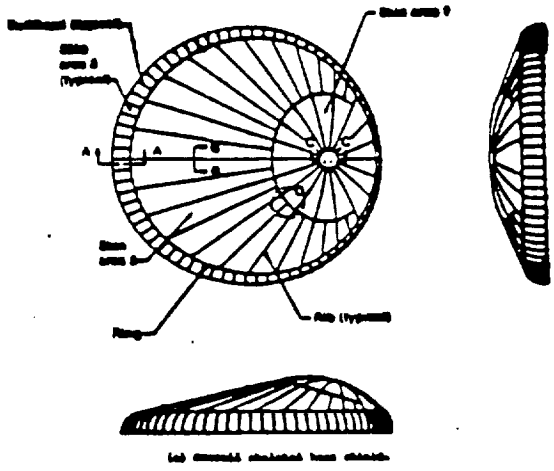

Fig. 2. The Rake Sphere-Cone Aerobrake

Power, Control and Life-Support Systems. Most of these systems will be similar to those used on the Space Shuttle. The EPS will consist of two hydrogen-oxygen fuel cells and one bipolar nickel-hydrogen battery for backup. ECLSS consists of an atmospheric revitalization system, freon/water-cooled thermal control system, and appropriate systems for food preparation and hygiene. GNC will utilize the planned Global Positioning System as well as onboard systems. RCS consists of 36 hydrazine-fueled jets placed in 8 stations. Data management will be controlled by three IBM 1750A avionic system computers.

Cost Estimates

The estimated cost to construct and deploy the first OTV is $1.09 billion. For construction and subsystem components $800 million will be needed. Research and development will require $250 million. Most of this amount will be needed for developing the aerobrake and software for the computer system. Transporting the OTV on the Space Shuttle and deploying it at the Space Station will require $40 million.

Conclusions and Recommendations

There is still a considerable amount of research that needs to be completed before the Project Orion team will be fully content with its design. The current design consists of modular components—propellant tanks, CCM, EVAM, and engines—and can easily be adapted for many missions other than the one illustrated in this summary. The Project Orion team feels confident that with a few minor changes the OTV could be used for lunar missions. Possible missions include retrieving a payload in orbit or landing on the Moon. The possibility of Project Orion's OTV being capable of completing such ambitious missions truly makes it a transfer vehicle for the 21st century.

THE MOVERS ORBITAL TRANSFER VEHICLE

The objective of the MOVERS design team was to explore the potential of a high-thrust, nuclear, orbital transfer vehicle.

The following criteria were used in the design of the OTV. The OTV must be capable of delivering a 15,000-pound payload to GEO from LEO. The craft must be able to sustain a crew of three for seven days, and support extra-vehicular activities (EVA). The basic spacecraft, moreover, should be adaptable to Earth-Moon missions with payloads as large as 80,000 pounds.

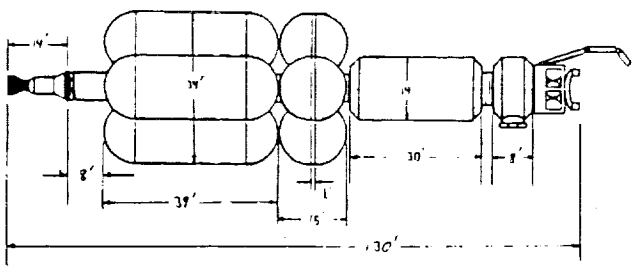

Fig. 3. MOVERS OTV Design Configuration

Basic OTV Configuration

Figure 3 is a diagram of the configuration for the MOVERS OTV. Looking from right to left, the configuration includes the satellite-servicing system, the command module, the living-quarters module, the eight propellant tanks, the reactor shield, the high-thrust nuclear engine, and the exhaust nozzle.

Weight Estimates for MOVERS OTV

Subsystem		Weight (lbm)
Dry Weight		
Habitation Module Interior (bulkheads, galley, etc.)		3,000
Command Module Interior (panels, chairs, etc.)		800
Power Systems and ECLSS		4,000
Reaction Control System		1,041
Avionics and Rendezvous Equipment		1,039
Satelllite Serving (propellant and Hardware)		7,900
Nuclear Reactor and Engine		4,000
Reactor Shielding		8,500
Radiation Shielding and Skin		19,875
Tankage		6,600
	Total	56,775
Wet Weight (no payload, LEO-GEO option):		
Propellant		93,293
	Total	150,068
Wet Weight (15,000 pound payload, LEO-GEO option):		
Propellant		121,184
Payload		15,000
	Total	192,959

Description of OTV Subsystems

In designing the OTV, the MOVERS design team studied the following subsystems extensively: avionics, crew systems, electrical power systems, environmental-control and life-support systems, navigation and orbital maneuvers, propulsion systems, reaction-control systems, servicing systems, and structures. Considerable trade-offs were encountered in preparing the design. This section briefly outlines the various systems that were ultimately chosen for the MOVERS OTV.

Avionics. State-of-the-art equipment, both hardware and software, was chosen for the OTV. New features of the computer system include bubble memory and electroluminescent screens, while all software will make use of the Ada programming language.

Crew Systems. The crew compartment was designed to maximize privacy and minimize crowding and sensory deprivation. The command module will house all of the command and control modules, as well as the spacesuits and other equipment needed for EVA operations.

Electrical Power and Environmental Control and Life Support. A chemical power-production system was chosen to provide power for the OTV. It uses two hydrogen-oxygen fuel cells to produce the electrical power needed by the spacecraft. The environmental control and life support system

is integrated with OTV's power production system. The craft will operate with a partially closed system. The system receives water, which is produced in the operation of the fuel cells, and regenerates waste carbon dioxide into elements which can be used again in the OTV's atmosphere.

Navigation. The OTV employs a combination of reliable instruments from the Space Shuttle such as IMU's and star trackers, and recently developed state-of-the-art equipment such as a Global Positioning System (GPS) processor/receiver, and a laser docking system. In addition, a maneuver, termed the PIB maneuver, was devised to make it much easier to rendezvous with satellites in GEO.

Propulsion. The MOVERS elected to employ nuclear power on the OTV in order to study the potential of this exciting new propulsion technology. A high-thrust, Nuclear Engine for Rocket Vehicle Application (NERVA) derivative engine was chosen. The engine, including the neutron/gamma shield, weighs 12,500 pounds, has a specific impulse of 880 seconds, and can deliver 30,000 pounds of thrust. For the LEO to GEO mission, these engines result in significant propellant savings over traditional chemical engines, and were also found to be very competitive with proposed, aerobraked, chemical systems. Environmental analysis indicated that the problems of catastrophic failures and of diffusion of radioactive particles though the fuel rods in low Earth orbits do not pose significant health hazards to the human population on Earth.

Reaction Control System (RCS). A supercritical hydrogen/oxygen RCS was chosen for the OTV. This system has a specific impulse of 410 seconds, which gave it the lowest wet mass of all the RCS systems considered for the OTV. This was an important design criterion given that the OTV's large moments of inertia mean that considerable RCS thrusting is necessary to obtain desired rotations and translations. The system was also chosen because the propellants are the same gases which are used in the fuel cells, thus minimizing the number of fluids that must be stored at the space station and on the OTV.

Tankage. The optimum configuration of propellant tanks for the OTV was four cylindrical and four spherical aluminum tanks. The tanks were made out of aluminum because alternative composite materials would tend to delaminate when exposed to the reactor's radiation and the ambient background radiation of space. The cylindrical shape was chosen because it maximizes the amount of propellant that can be transported to the space station within the Shuttle's cargo bay. Additionally, all tanks are shielded by the radiation shield. This is important because it minimizes cryogenic heating, and thus cryogenic boiloff.

Satellite Servicing. Three types of satellite-servicing missions were identified: resupply of expendables such as attitude-control system propellants and water; replacement of failed elements; and the upgrading of spacecraft systems to incorporate advances in technology. To capture satellites, a remote manipulating system (RMS) has been incorporated into the OTV design. A manned maneuvering unit is also included onboard the OTV. The satellite-servicing station includes a berthing system to facilitate the changeout of defective or obsolete satellite parts, and to provide for fluid resupply.

Structures. The exterior skin of the OTV is an aluminum alloy. A thickness of 5 g/cm^2 provides sufficient protection against background radiation. In the event of a sudden solar flare, the OTV will be oriented so that the radiation shield will protect the crew from the flare.

Sample Mission: April 24, 1996, Telstar Satellite Repair

The OTV and crew are called upon to service a failing Telstar satellite. After preparing the OTV for departure, the crew performs a phasing-orbit injection burn (PIB). This is used to position the OTV so that when it returns to its initial position it is correctly aligned to rendezvous with the target satellite in GEO. The dry mass of the OTV at the time of the first burn is 50,300 pounds, and 84,926 pounds of propellant are onboard to complete the roundtrip. Up to 2 hours and 11 minutes are required to complete the alignment orbit. When the OTV returns to the initial departure point, a second transfer burn is performed to place the OTV into an approximate Hohmann transfer for rendezvous. The time of flight for this Hohmann transfer orbit is 5 hours and 16 minutes. Once the OTV reaches its destination, a third circularization and plane-change burn is performed to put it into the same orbit as the Telstar satellite. At this point, 4.5 days of servicing begins.

To return to the Space Station the above sequence is essentially repeated in reverse. A deceleration and plane-change burn is initiated to put the spacecraft into an approximate Hohmann transfer orbit. Time of flight is again 5 hours and 16 minutes. Once the OTV reaches perigee, another burn is performed to put the craft into an alignment orbit. The time of flight for the alignment orbit is 1 hour and 43 minutes and the OTV returns to the point where the second burn was performed, just as the Space Station gets there. A third deceleration burn is then performed to put the OTV into the Space Station's orbit. The total mission time is 5 days, 2 hours and 29 minutes.

Cost of an OTV

To develop and build the first nuclear OTV, $5.09 billion will be necessary. In addition, it will cost $101 million to deliver the craft to the space station assuming a launch cost of $2000/pound.

Conclusions

This report has outlined the basic components of the MOVERS design team's orbital transfer vehicle. A significant aspect of this research is that it indicated that high-thrust, nuclear propulsion may be appropriate for OTV applications, and that further research is warranted.

SPACE-BASED LASER-POWERED ORBITAL TRANSFER VEHICLE (PROJECT SLICK)

VIRGINIA POLYTECHNIC INSTITUTE

The project SLICK (Space Laser Interorbital Cargo Kite) involves conceptual designs of reusable space-based laser-powered orbital transfer vehicles (LOTV) for ferrying 16,000 kg cargo primarily between low Earth orbit (LEO) and geosynchronous earth orbit (GEO). The power to LOTV is beamed by a single 32-MW solar-pumped iodide laser orbiting the Earth at an altitude of one Earth radius. The laser engine selected for the LOTV is based on a continuous-wave, steady-state propulsion scheme and uses an array of seven discrete plasmas in a flow of hydrogen propellant. Both all-propulsive and aerobraked LOTV configurations were analyzed and developed. The all-propulsive vehicle uses a rigid 11.5-m aperture primary mirror and its engine produces a thrust of 2000 N at a specific impulse of 1500 sec. For the LEO-to-GEO trip, the payload ratio, $m_{payload}/(m_{propellant} + m_{dry\ vehicle}) = 1.19$ and the trip time is about 6 days. The aerobraked version uses a lightweight, retractable wrapped-rib primary mirror which is folded for aerobraking, and a 20-m-diameter inflatable-ballute aeroshield which is jettisoned after aeromaneuver. Lifecycle cost analysis shows that the aerobraked configuration may have an economic advantage over the all-propulsive configuration as long as the cost of launching the propellant to LEO is higher than about $500/kg in current dollars.

MISSION SPECIFICATIONS/REQUIREMENTS

The concept of the space-based LOTV is based on placing the propulsion-power source in an orbit independent of the vehicle. For the SLICK project, the power source is a direct solar-pumped iodide laser (1.315 μm) orbiting at an altitude of one Earth radius and zero inclination. The 32-MW laser beam is transmitted by a 30-m aperture and is captured by the LOTV onboard optics and focused inside a thrust chamber. Within the chamber, the laser energy is converted into thermal energy of the flowing propellant to produce thrust.

Two basic mission scenarios concerned with cargo transportation have been adopted for the project. In the first scenario, an all-propulsive LOTV transfers payloads between the 28.5° LEO and an equatorial geostationary orbit. For the second scenario, the LOTV shuttling between LEO and GEO uses aerobraking on the downleg to LEO to reduce ΔV and propellant mass. Both scenarios assume that the Laser Power Station (LPS) consists of either (a) a single 32-MW laser, or (b) one laser and two laser transmitter relays to eliminate constraints due to line-of-sight between the laser and LOTV, or (c) one laser, one laser transmitter relay, and one relay equipped with both laser transmitter mirror and solar collector-transmitter. System (c) ensures that the LOTVs are always illuminated, even when the laser is in Earth shadow. The LOTVs are designed to function with any of the three LPS systems.

Mission models assume a 16,000 kg payload transfer from LEO to GEO and either 16,000 kg (all-return option), 5000 kg (standard option), or 1,600 kg (minimum-return option) payload transfer from GEO to LEO. Also, it has been established that a one-way trip duration should be no longer than two or three weeks. While the project has focused on the LEO/GEO transportation, an additional scenario concerned with cargo transportation between LEO and low lunar orbit (LLO) at 100-km altitude has also been considered. This scenario assumes a second nuclear-pumped laser placed on the lunar surface. The lunar LOTV uses aerobraking on its return to LEO and has an option of supplementing the laser engine with low-thrust chemical (LH_2/LOX) rockets for the trans-lunar and/or trans-earth injection.

The basic laser engine to be used for all scenarios has the following key characteristics: the propellant is hydrogen; thrust = 2000 N; specific impulse = 1500 sec; and thermal conversion efficiency = 50%. These values have been established from the continuous-wave thruster relation:

$P_{laser} = TI_{sp}\, g_o/2\eta$ where P_{laser} = laser power and g_o = acceleration of Earth gravity, and from assessment of results and recommendations found in recent studies of laser propulsion.

Throughout the design process, a technology level projected for 2000-2010 has been generally assumed and the following criteria have been given high priority: (a) maximize the payload-to-propellant mass ratio; (b) provide maximum reusability of the LOTV; and (c) provide flexibility in terms of payload and propellant capacities.

ORBITAL DYNAMICS

The orbital dynamics of the LOTV has been calculated from Lagrange's planetary equations, modified by changing the independent variable from time to true anomaly. Time is calculated as a function of the eccentric anomaly. For the low thrust-to-weight ratio of the LOTV, a multiple impulse trajectory is required and the ΔV required depends on the thrusting duration. For transfers between LEO and GEO, the most advantageous trajectory of the LOTV features a sequence of near-elliptic orbits with multiple firings first near perigee points and then near apogee points (Fig. 1). Tradeoffs between ΔV, transfer duration, and number of spirals have been analyzed, and the optimal arc angles from start-to-stop firing have been determined to be approximately 120° for perigee thrusting, 90° for apogee thrusting, and 50° for plane change at the nodes.

For the range of thrust-to-weight ratios pertinent to our LOTVs (5×10^{-3} to 6×10^{-3}), the ΔV required for LEO-to-GEO transfer is about 4.5 km/s.

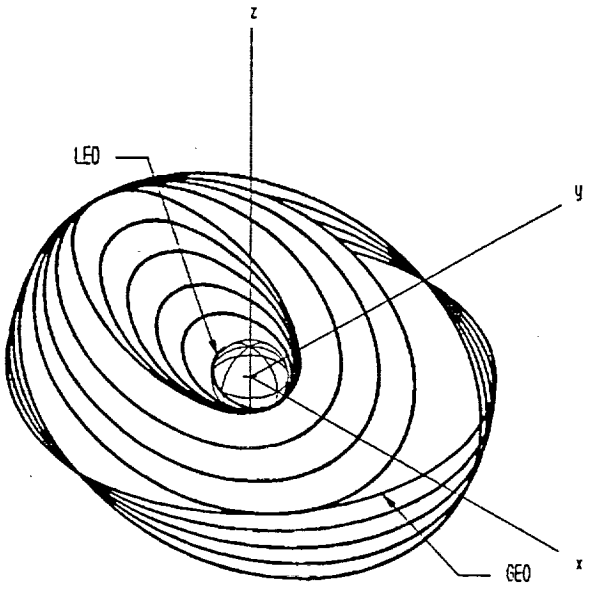

Fig. 1. LEO-GEO Transfer

The return to LEO of the all-propulsive LOTV involves a reversed sequence of near-elliptical orbits. The return of the aerobraked version, however, differs. Thrusting reduces perigee of the orbit until it lies within the fringes of the Earth's atmosphere. Friction forces due to atmospheric drag reduce the speed of the vehicle, thereby lowering apogee. At this point, only a reduced ΔV circularizing maneuver is required. The aerobraking will also complete the necessary plane change to return to the orbital inclination of 28.5°.

Only initial, approximate calculations have been performed for the lunar mission. The LEO-to-LLO transfer consists of spiral-elliptical maneuvering into a high apogee (at 192,000 km from Earth) elliptical orbit, a translunar injection (at the median point between apogee and perigee) performed by two low-thrust chemical thrusters, a 22.5° plane change, an LLO injection and circularization. On the return trip, the LOTV, powered by the lunar laser, spirals out and is aided by two chemical thrusters in trans-Earth injection followed by aerobraking maneuver and circularization. It is expected that most of the 15,000 kg payload returned from LLO will contain lunar-derived liquid oxygen.

CONFIGURATION

All-Propulsive LOTV

The all-propulsive configuration which emerged from initial studies and a final selection process is shown schematically in Fig. 2. Its major components are a hexagonal main truss structure, the optical train and propulsion system, pointing and tracking system, dynamics control system, and communication system.

The main truss of the vehicle is an open structure made of a boron/aluminum composite and titanium fittings. It houses two liquid hydrogen tanks, a single liquid oxygen tank, the fuel management/pump system, the control moment gyroscopes (CMGs) electrical power system, instrumentation, and the variable optics mirror. The LOTV utilizes a detachable payload system. A payload mounting/docking apparatus is located on the front face of the main hull. This apparatus is used to attach the payload to the vehicle as well as for docking with space stations or refueling/service platforms. To allow for fuel tank removal for major servicing, repair and/or replacement, as well as for providing optional docking or payload attachment mechanisms, the truss members on the front face of the hull can be unlocked and removed.

The LOTV optics consist of the 11.5-m-aperture primary mirror and three secondary mirrors. The primary and two secondary mirrors are placed on a 14-m optical truss structure which is mounted on a turntable allowing the system to rotate thru 360° independently of vehicle orientation. The third secondary mirror (employing adaptive optics) is mounted on the main vehicle truss in a fixed position with respect to the laser engine. Coupled with attitude and roll control of the vehicle, the rotation of the optical truss allows laser beam capture regardless of its incoming direction. The attitude and rolling control of the vehicle is done primarily by the control moment gyroscopes (CMG) located near the vehicle mass center. The Reaction Control System (RCS) is composed of

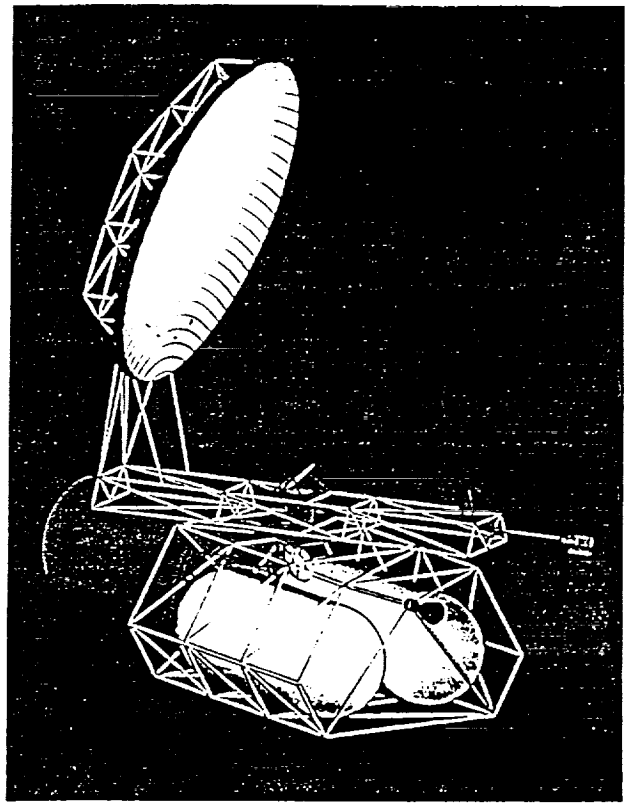

Fig. 2. All-Propulsive LOTV

four arrays of chemical thrusters (primary RCS) and fourteen small magnetoplasma thrusters (secondary RCS), all mounted on the edges of the main truss structure. The system is used to desaturate CMGs, to perform any required trajectory corrections or readjustments throughout the transfer and to perform departing and docking maneuvers.

A continuous-wave laser propulsion scheme adopted for the vehicle uses an array of discrete laser-sustained plasmas in a steady flow of hydrogen propellant[1]. The plasmas are created by an array of thrust chamber window lenses and the variable optics mirror which splits the incoming beam into seven components and directs these components into the thrust chamber. The thruster has a moveable nozzle with an external gimbal ring and a ball-socket bearing to provide thrust vectoring capability within 8° off the engine main axis. This capability enables the vector thrust to line up with the vehicle center of mass.

The pointing and tracking system is located at the end of the optical truss which points toward the incoming laser beam. It includes a low-powered, pulsed YAG laser (0.532 μm) transmitter, a telescope and an optical sensor array. A similar unit is assumed to be located on the LPS laser transmitter. Both units can communicate with each other to control the rotation of the optical truss as well as the pointing of the laser transmitter. When both units are locked onto one another, very fine tracking with an accuracy in the submicroradian range can be performed.

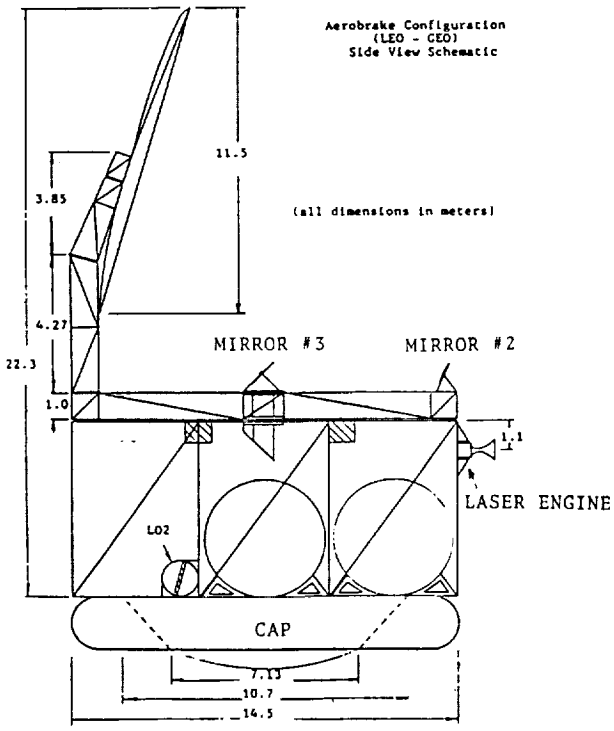

Fig. 3. Aerobraked LOTV

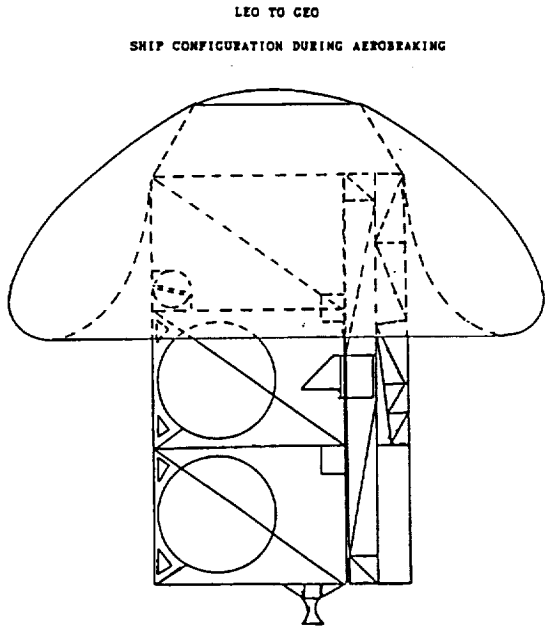

Fig. 4. Aerobraked LOTV

Aerobraked LOTV

The aerobraked configuration is shown in Fig. 3. The main truss structure has an equilateral-triangle cross-section which accommodates the three-bag ballute arrangement. The aerobrake system consists of a rigid cap designed to withstand the stagnation conditions, three Nextel bags which, upon inflation, protect the majority of the vehicle, inflation mechanisms, deployment system and a support truss. The cap and its support structure are designed to hold the ballute in place, carry the forces developed during braking and to provide a rigid heatshield capable of withstanding the stagnation heating rates. The aluminum cap is covered with a rigid surface insulation formed of small hexagonal tiles. Stored within the cap structure are three spherical liquid nitrogen tanks and a system of two-way pumps and valves which carry the nitrogen into the ballute for inflation. Before aerobraking, the cap, with the ballute bags folded around it are moved from their stored position on the base of the vehicle into male-female locks at the front of the vehicle; these locks are used for the detachable payload during the LEO-to-GEO trip. (On a return trip to LEO, a payload having a mass of 6,000 kg or less is stored in an empty space behind the cap.) The aerobrake is moved on tracks with a cable/pulley system and N_2 jacks. After the aerobrake is positioned, the bags are inflated to a 20-m diameter and the vehicle is prepared for reentry (Fig. 4). The 2.5-mm-thick ballute is made of a Nextel-type fabric (inner surface), quartz felt insulation and Nicalon fabric (outer surface). After the aeromaneuver, the ballute is jettisoned along with the outer ring of tiles and the aluminum skirt around the cap.

The 11.5-m-aperture primary mirror is of a wrapped-rib design which allows for the mirror to be folded and retracted for the duration of the aerobraking maneuver. The secondary mirrors including the variable optics mirror are the same as on the all-propulsive LOTV; however, their mounts and supporting truss structure allow for retraction and storability for the aerobraking. The laser engine is very similar to the one used for the all-propulsive LOTV. The main difference is a lower thrust value (1900 N) resulting from somewhat lower optical quality and response of the wrapped-rib mirror as compared to the rigid one.

The fuel tanks of the aerobraked LOTV are smaller which reflects propellant savings due to aerobraking. The electrical power system is somewhat larger than that of the all-propulsive LOTV to account for the power needs of the mechanisms involved in folding, storing, retracting, and re-erecting of several components. The systems of pointing and tracking, Guidance, Navigation and Control (GNC), and Data Management and Communication are similar for both aerobraked and all-propulsive LOTVs.

Lunar LOTV

Only an aerobraked version of the lunar LOTV has been investigated. Its general configuration is similar to the LEO/GEO aerobraked vehicle. It uses a 30-m-diameter wrap-rib primary mirror and a 33-m-diameter inflatable ballute aerobrake. For translunar insertion, the laser propulsion is supplemented by two LH_2/LOX chemical thrusters which are part of the reaction control system.

PROPULSION SYSTEM

The basic concept behind the LOTV is that the power for the propulsion system is supplied by a source separate from the LOTV itself. Since energy generation is remote and independent of the vehicle, its propulsion unit can be very lightweight and the specific impulse can be raised significantly above that of chemical systems. Actually, for cargo orbital transfers, laser propulsion may represent an excellent compromise between high-thrust, short transit-time systems that burn a lot of fuel (chemical OTV) and low-thrust systems that burn little fuel but have very long transit times (electric OTV). For many cargo missions, increased trip-time during transit can be readily accepted as a price for significantly reduced propellant needs.

The propulsion system of the LOTV includes the optical train, laser engine, and fuel storage and delivery system. The proposed optical system is similar to a true Cassegrain and contains an off-center parabolic primary mirror and three secondary mirrors (Fig. 5). From analysis of laser beam transmission in space, small tracking errors, and maximum LOTV-to-LPS distances during LEO/GEO transfers with a single laser in orbit, the maximum beam diameter incident on the primary mirror was set at 11.5 m. Optimization studies performed on a CAD/CAM system led to selection of mirror shapes, dimensions and focal length shown below:

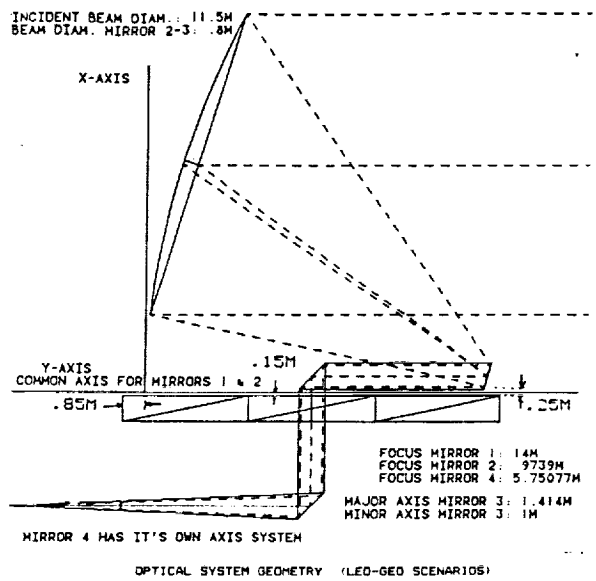

Fig. 5. Optical System Geometry

Mirror #	Reflecting Surface	Shape/ Minor Axis, m	f/value
1	Concave,off-center parabolic	Slightly elliptical/11.5	1.2
2	Convex off-center parabolic	Slightly elliptical/1	1.2
3	Flat	Elliptical/1	
4	Seven slightly concave panels	Elliptical/1	7.2

The primary reflector of the all-propulsive LOTV consists of a lightweight support frame upon which 19 hexagonal panels are fixed. If the mirror is damaged, only a few panels will need to be replaced. Each panel is fixed to a support structure at three points for stability. A honeycomb core is used for support with composite facesheets for rigidity. The mirror surface has reflective coating as well as a protective coating to reduce degradation resulting from the laser beam and environment. The mirror mass per unit area is approximately 2.92 kg/m^2. The secondary mirrors use a reflective surface which consists of a multilayer dielectric coating applied to a substrate of fused silica supported by a 7.62-cm-thick honeycomb backing also of fused silica. Dielectric coatings provide 99.5% reflectivity at a wavelength of 1.315 μm. High mirror reflectivity and limited thrusting duration reduce a need to provide cooling of the mirrors. The variable optics mirror, fixed to the vehicle main truss, transforms the incident parallel beam into seven separate, slightly converging beams entering the engine. This mirror together with the engine window constitute a special feature of the proposed LOTV.

For the primary mirror of the aerobraked LOTV, a wrapped-rib design has been chosen using a basic structure of the reflector similar to an umbrella. It consists of a flexible material

(polyester film-Mylar) stretched taut between graphite-epoxy ribs which define the parabolic shape of the reflector. The ribs can be wrapped around a small central hub making the stored volume small enough to fit within the protection of the aerobrake. Obviously, this system does not have the optical response and the lifespan that the rigid system does. The weight of the mirror is 200 kg. The mirror support arm is foldable and its tip, which attaches to the hub of the mirror, is able to rotate 120° to allow the hub to be slid alongside the vehicle. The secondary mirrors of the aerobraking version are the same in all details except that the mirrors #2 and #3 can be folded inside the optical truss for aerobraking.

The laser engine consists of a laser-beam-to-hydrogen-thermal-energy conversion chamber and a movable nozzle (Fig. 6). The conversion chamber is designed for an array of seven discrete laser-sustained plasmas with peak temperatures of approximately 17,000 K, corresponding to the maximum absorptivity of hydrogen to 1.315 μm radiation. The plasmas are created by seven lenses in the front window of the chamber. A multi-plasmas scheme has a potential of higher fractional absorption of the laser energy by the plasma than a single-plasma scheme[1]. This may be related to the effect of plasmas being in shadow of one another. Also, the performance of individual, lower-power-level plasmas can be easily inferred from current experimental studies. Finally, at high laser fluxes, problems of the structural integrity of window lenses may be lessened by using smaller lenses. The size and shape of the conversion chamber are dictated by the window size allowing sustained operation of lenses at laser flux level of 2.5×10^4 W/cm^2, plasma-front stability requirements, and an internal wall reradiation pattern that would promote energy absorption. In order to withstand the high chamber temperatures encountered, a combination of (a) regenerative cooling, and (b) protection by means of reflective material selection and coatings is utilized. The liquid hydrogen is injected into the chamber through six window injectors which vector the hydrogen directly toward the plasmas. Gaseous hydrogen is injected along the perimeter of the diameter wall just beneath the window. This provides face cooling for the window and a recirculatory mixing pattern for the hydrogen.

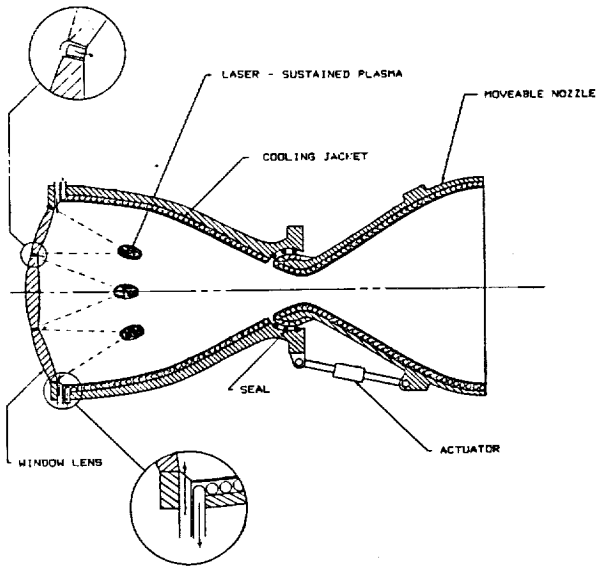

Fig. 6. Laser Engine

Table 1. Characteristics of the All-Propulsive LOTV for LEO/GEO Transportation

Characteristic	Standard Option	All-Return Option
Propulsion:		
Overall efficiency of the optical train	92.5%	92.5%
Thermal conversion efficiency	50%	50%
Specific impulse	1500 sec	1500 sec
Propellant flow rate	0.136 kg/s	0.136 kg/s
Thrust	2000 N	2000 N
Masses:		
Vehicle dry mass, M_s	3,855 kg	4,065 kg
LEO/GEO payload, M_{pll}	16,000 kg	16,000 kg
GEO/LEO payload, M_{pll}	5,000 kg	16,000 kg
Initial propellant at LEO (for round trip, including RCS and reserve)	14,000 kg	20,200 kg
Overall initial mass	33,855 kg	40,265 kg
Performance:		
LEO/GEO trip time	6.4 days	9 days
GEO/LEO trip time	5 days	7 days
LEO/GEO payload mass ratio, $M_{pll} / (M_{pl} + M_s)$	1.19	1.03
GEO/LEO payload mass ratio, $M_{pll} / (M_{pl} + M_s)$	0.69	1.38

The movable nozzle will be equipped with a fully-cooled ball-socket bearing, O-ring seals, and actuators-gimbal rings system. Due to the very high temperatures of the engine, gimballing the nozzle may be quite difficult and will require advances in high temperature materials.

The propellant feed system uses a turbopump system with an electric motor to initiate the rotation of the pump until the operational speed is achieved. The gaseous hydrogen from the regenerative cooling system is used to drive the turbine.

The liquid hydrogen will be stored in two cylindrical tanks with spherical endcaps. A 21-layer insulation scheme consisting of double aluminized Mylar with silk net spacers vented to outer space (to prevent convective heat transfer) is proposed to limit the boiloff to less than 1% during a 12-day trip.

VEHICLE CHARACTERISTICS AND PERFORMANCE

Preliminary design and performance calculations included, among others: (a) orbital mechanics calculations (see Orbital Dynamics section); (b) laser beam spread calculations based on an approach used by Jones et al.[2]; (c) optical system analysis and optimization using ray tracing techniques; (d) thruster chamber estimates based on initial results obtained at the University of Tennessee Space Institute and heat transfer

Table 2. Characteristics of the Aerobraked LOTV for LEO/GEO Transportation

Characteristic	Standard Option	All-Return Option
Propulsion:		
Overall efficiency of the optical train	87.9%	87.9%
Thermal conversion efficiency	50%	50%
Specific Impulse	1500 sec	1500 sec
Propellant mass flow rate	0.129 kg/s	0.129 kg/s
Thrust	1900 N	1900 N
Masses:		
Vehicle dry mass at LEO, $M_{s\ell}$	4843 kg	4971 kg
Vehicle dry mass at GEO, M_{s_g}	4317 kg	4445 kg
LEO/GEO payload, $M_{pl\ell}$	16,000 kg	16,000 kg
GEO/LEO payload, M_{plg}	5,000 kg	16,000 kg
Initial propellant at LEO (for round trip, including RCS and reserve)	12,500 kg	16,400 kg
Overall initial mass (LEO)	33,443 kg	37,371 kg
Performance:		
LEO/GEO trip time	7.5 days	
GEO/LEO trip time	1.5 days	
LEO/GEO payload mass ratio, $M_{pl\ell} / (M_{p\ell} + M_{s\ell})$	1.1	1.0
GEO/LEO payload mass ratio, $M_{plg} / (M_{pg} + M_{sg})$	0.79	1.83

and cooling analyses; (e) approximate nozzle flow calculations obtained from the computer program NOTS (Naval Ordinance Test Station); (f) liquid hydrogen tank insulation and boiloff rate calculations; (g) mass and moments of inertia calculations; (h) structural analyses obtained mostly from modified SASM programs (Structural Analyses Software for Microcomputers) and compiled for our uses; (i) aerobrake aerodynamics and stability calculations based on 3-D Modified Newtonian theory; (j) Aeromaneuver trajectory analysis and aerobrake heat transfer at the stagnation point determined by POST code (at NASA); (k) Heat transfer rate and temperature along the ballute surface calculated from the laminar and turbulent boundary-layer equations coupled to the inviscid flowfield solutions[3]; and (l) estimates of RCS and CMG characteristics derived from the mass/moments of inertia values, roll rates of the vehicle, slew rates of the optical train system and assumptions on CMG desaturization and docking maneuvers.

The main characteristics of the LEO/GEO all-propulsive and aerobraked LOTVs are listed in Tables 1 and 2, respectively.

SPECIAL FEATURES

Mirror #4 of the optical train converts the vertical parallel laser beam into seven horizontal, slightly converging beams that enter the lenses of the engine (Fig. 7). This requires that the mirror be subdivided into seven parabolic facets. Each of the seven beams is required to have intensity distribution within certain limits permitting the corresponding engine lens to produce proper focusing on the plasma and at the same time preventing overheating of the non-transparent lattice joints between the lenses. To ensure proper focusing and to correct beam deviations due to structural deformations and fluctuations, the individual mirror facets have some measure of adaptability. Each facet is controlled by linear actuators which vary the position of the facet by rotating it about a spherical mount. Feedback control is provided by a "template" of filtered and protected x-y error detectors. The template is mounted between the mirror and the engine window. If a beam error is detected by a template, corrective software first identifies the mirror facet(s) in question and then sends a corrective command to readjust the facet's position. The variable-optics mirror, the window lenses, and the error detection and control unit form a system responsible for creation and control of the engine plasmas that play a critical role in laser propulsion.

ECONOMIC ANALYSIS

Life-cycle cost analysis has been performed assuming a 20-year useful operational life of the LOTV, mission frequency of 5 or 10 per year, and major overhauls once every 20 or 30 missions for the aerobraked or all-propulsive configuration, respectively. Cost estimating relationships[4,5] have been used for estimates of unit or material cost and of the design, development, test, and evaluation costs. The analysis shows that the aerobraked configuration may have an economic advantage over the all-propulsive one as long as the cost of delivering propellant to LEO is higher than about $500/kg in current dollars.

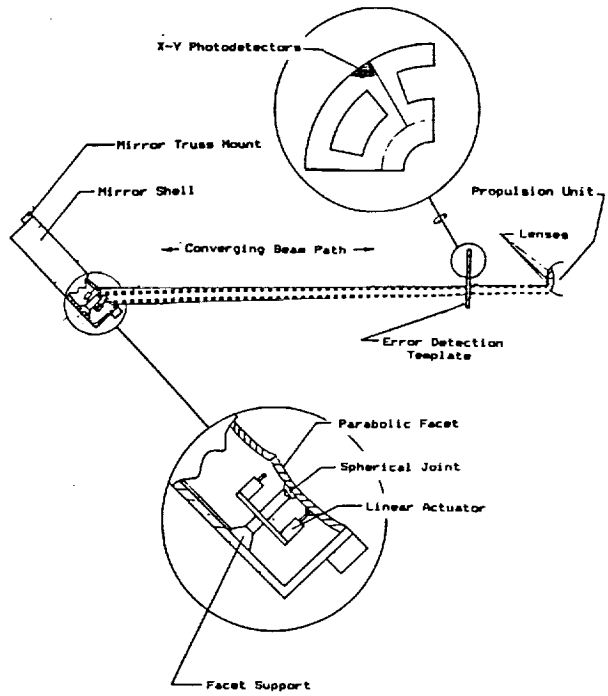

Fig. 7. Adaptive Optics System

CONCLUSIONS AND RECOMMENDATIONS

Our preliminary design studies have outlined two workable designs of laser-propelled orbital transfer vehicles. Results of the studies indicate that the LOTV is a very attractive candidate for cargo transportation around the Earth and in an Earth-Moon system. With laser propulsion, the payload mass ratio values are twice (or more) as high as with the baseline chemical propulsion system. It is expected that the technical problems associated with laser propulsion will be fully overcome by the next decade. Therefore, a further, continuous design/research effort directed at various design aspects and applications of laser propulsion is fully justified.

REFERENCES

1. Myrabo L. The "Mercury Lightcraft" Concept, *Proceedings SDIO/ DARP Workshop on Laser Propulsion,* Lawrence Livermore National Laboratory, July 1986.
2. Jones W.S., Forsyth J.B. and Skratt J.P. Laser Rocket System Analysis, *NASA CR-159521,* 1978.
3. Deshpande S.M. Approximate Heat-Transfer and Wall-Temperature Calculations for Aeroassisted Orbital Transfer Vehicles, M.S. Thesis, Virginia Polytechnic Institute and State University, 1988.
4. Cathcart J.A., et al. Advanced Orbit Transfer Vehicle Propulsion System Study, Martin Marietta Aerospace, Denver, February 1985.
5. DeYoung R.H.,et al. Preliminary Design and Cost of a 1-Megawatt Solar-Pumped Iodide Laser Space-to-Space Transmission Station, *NASA TM 4002,* 1987.

DESIGN OF A RAM ACCELERATOR MASS LAUNCH SYSTEM

UNIVERSITY OF WASHINGTON

The Ram Accelerator, a chemically propelled, impulsive mass launch system, is presented as a viable concept for directly launching acceleration-insensitive payloads into low Earth orbit. The principles of propulsion are based on those of an airbreathing supersonic ramjet. The payload vehicle acts as the ramjet centerbody and travels through a fixed launch tube that acts as the ramjet outer cowling. The launch tube is filled with premixed gaseous fuel and oxidizer mixtures that combust at the base of the vehicle and produce thrust. Two modes of in-tube propulsion involving ramjet cycles are used in sequence to accelerate the vehicle from 0.7 km/sec to 9 km/sec. Requirements for placing a 2000 kg vehicle into a 500-km circular orbit, with a minimum amount of onboard rocket propellant for orbital maneuvers, are examined. It is shown that in-tube propulsion requirements dictate a launch tube length of 5.1 km to achieve an exit velocity of 9 km/sec, with peak accelerations not to exceed 1000 g's. Aerodynamic heating due to atmospheric transit requires minimal ablative protection and the vehicle retains a large percentage of its exit velocity. An indirect orbital insertion maneuver with aerobraking and two apogee burns is examined to minimize the required onboard propellant mass. An appropriate onboard propulsion system design to perform the required orbital maneuvers with minimum mass requirements is also determined. The structural designs of both the launch tube and the payload vehicle are examined using simple structural models and finite element analysis for various materials.

INTRODUCTION

The viability of any large-scale, permanent space structure relies on the capability of launching mass easily and efficiently into orbit. The Ram Accelerator mass launch system has recently been proposed to greatly reduce the costs of placing acceleration-insensitive payloads into low Earth orbit.

The Ram Accelerator, conceived and experimentally demonstrated at the University of Washington[1,2], is a chemically propelled, impulsive mass launch system capable of efficiently accelerating relatively large masses from velocities of 0.7 km/sec to greater than 9.0 km/sec. The principles of propulsion are based upon those of a conventional supersonic airbreathing ramjet; however the device operates in a somewhat different manner (Fig. 1). The payload-carrying vehicle resembles the centerbody of the ramjet and accelerates through a stationary tube which acts as the outer cowling. The tube is filled with premixed gaseous fuel and oxidizer mixtures that burn in the vicinity of the vehicle's base, producing a thrust which accelerates the vehicle through the tube. The requirements for placing a 2000-kg vehicle into a 500-km circular orbit with a minimum amount of onboard rocket propellant for orbital maneuvers are examined. The goal is to achieve a 50% payload mass fraction.

The proposed design requirements have several self-imposed parameters that define the vehicle and tube configurations. As a result of structural considerations the launch tube inner diameter was fixed at 1.0 m. In-tube propulsive requirements and vehicle structural constraints resulted in a vehicle diameter of 0.76 m, a total length of 7.5 m and a nosecone half angle of 7°. An acceleration of 1000 g's was chosen as the upper limit due to structural considerations on the vehicle and tube wall. An ablating nosecone constructed from carbon-carbon composite was chosen as the thermal protection mechanism for atmospheric transit. The remainder of the vehicle is constructed from titanium alloys and/or composites.

IN-TUBE PROPULSION

To achieve the desired launch velocity, two modes of in-tube propulsion involving ramjet cycles are required[2]. The two modes that have been investigated are a thermally choked subsonic combustion mode (Fig. 1a) and a mode which utilizes a stabilized, oblique detonation wave for combustion (Fig. 1b). As with a ramjet, an initial velocity is required to start the propulsive process. Thus, an initial accelerator system is needed to accelerate the 2000-kg vehicle from rest to a starting velocity of 700 m/sec. This initial velocity is provided by firing the vehicle into the launch tube using a combustion-driven gas gun.

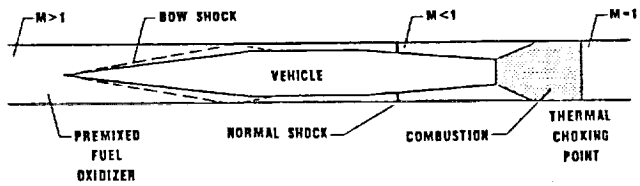

Fig. 1a. Modes of Ram Accelerator Propulsion: Subsonic Combustion Mode

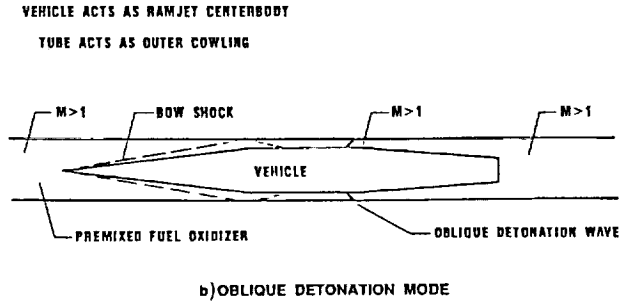

Fig. 1b. Modes of Ram Accelerator Propulsion: Oblique Detonation Mode

Initial Accelerator

The gas gun utilizes a stoichiometric methane-air mixture at a fill pressure of 47 atm and temperature of 300 K. To maintain rapid-fire launch sequencing, the methane and air are premixed in a feed pipe and injected into the combustion chamber transverse to flowing air. A muzzle-blast relief section surrounded by a dump tank open to the atmosphere is needed to provide for gas exhaust and recoil control. The vehicle then enters the ram accelerator launch tube.

The combustion chamber is 0.76 m in diameter and 42 m in length. A peak combustion pressure of 428 atm drives the vehicle at a maximum initial acceleration of 1000 g's causing it to reach a velocity of 700 m/sec in a barrel length of 48 m. The combustion chamber and barrel are constructed from AISI 4340 steel with a yield point of 138 kN/cm^2 (200,000 psi). Using the maximum detonation pressure of 834 atm with a factor of safety of 3, structural computations indicate a uniform wall thickness of 7.8 cm.

Ram Accelerator

The thermally choked subsonic combustion mode (Fig. 1a) accelerates the vehicle from 0.7 km/sec to 2.5 km/sec. The composition of the pressurized gas mixture is chosen such that the vehicle Mach number is sufficient to ensure that the flow remains supersonic through the throat of the diffuser. A normal shock is located downstream of the diffuser throat and is stabilized by the heat release which chokes the flow downstream of the vehicle. The flow behind the normal shock then expands subsonically aft of the vehicle where combustion begins and proceeds to thermal choking. At a velocity of 2.5 km/sec, a transition is made to the oblique detonation mode.

The oblique detonation combustion mode, which accelerates the vehicle from 2.5 km/sec to 9 km/sec, requires a strong oblique shock wave to raise the propellant temperature high enough for combustion to occur (Fig. 1b). This is accomplished by means of a small azimuthal protuberance located on the vehicle profile to initiate an oblique detonation wave. Both modes require that the nosecone half-angle be small enough to ensure that the bow and reflected bow oblique shock waves in the diffuser do not ignite the propellant.

The analyses for both modes of propulsion were performed using one- and two-dimensional gas dynamics to model the flow around the body[2,3]. The performance parameters of the ram accelerator can be described by the ballistic efficiency (ratio of the rate of change of vehicle kinetic energy to the rate of chemical energy expenditure) and thrust pressure ratio (ratio of effective thrust pressure to peak cycle pressure). These parameters were kept near optimum levels by varying the propellant mixture along the length of the launch tube. Nine different propellant mixtures were utilized in achieving the desired velocity range, each at a fill pressure of 33 atm and a fill temperature of 300 K. In this manner the acceleration of the projectile can be kept near the design limit of 1000 g's at an average ballistic efficiency of 24% and an average thrust pressure ratio of 14%. Based on the analysis, the required total length of the stationary launch tube is 5.1 km, 93% of which is required for the oblique detonation propulsion mode.

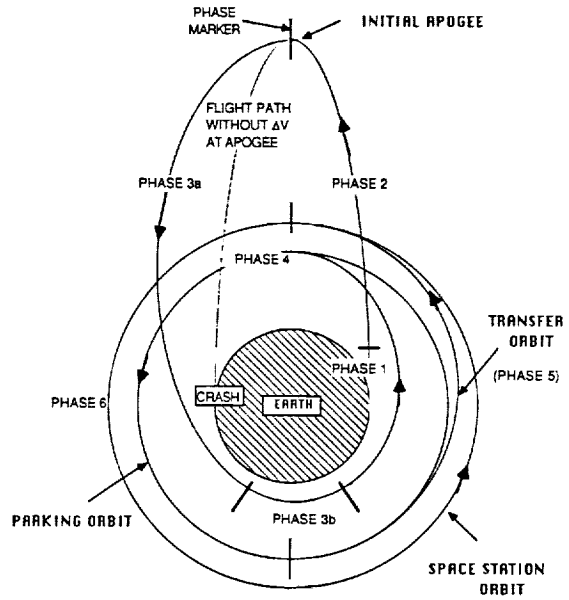

Fig. 2. Proposed Trajectory of the Ram Accelerator Vehicle

The analysis of the propulsive modes indicates that the vehicle experiences peak pressures of 1000 atm and 1940 atm in the thermally choked and oblique detonation modes, respectively. Peak pressures on the launch tube wall were likewise calculated to be 1000 atm and 1870 atm for the respective propulsive modes.

Using thick-walled tube theory, the wall thickness for the launch tube wall was determined for AISI 4340 steel (assuming a conservative yield stress of 138 kN/cm^2) with a safety factor of 3. The wall thickness required for the thermally choked portion of the barrel (1.0 m ID) is 12.7 cm while the wall thickness of the oblique detonation portion is 27.6 cm for the first 2.3 km and 24.8 cm for the remaining 2.5 km.

ATMOSPHERIC TRANSIT

Once the necessary launch velocity of 9 km/sec is obtained, the vehicle must traverse the atmosphere. At such high hypersonic exit velocities, the vehicle will experience severe aerodynamic heating and forces that will require adequate thermal protection and stability augmentation for a controlled ascent. Convective heating dominates the heat input to the nosecone, which experiences severe stagnation temperatures, on the order of 9,000 K-13,000 K, even after considering the effects of equilibrium dissociation across the bow shock wave and in the boundary layer. Radiative heating, even at the high velocities considered, can be shown to be negligible in comparison to convective heating.

A carbon-carbon ablating nosecone was chosen to protect the vehicle from the atmospheric heating. If an ablative

nosecone with low thermal conductivity is used, a large amount of heat can be absorbed through the chemical charring and sublimation of the ablator. Ablation will result in blunting of body shape during ascent. Since the drag of the vehicle, being primarily pressure drag, is affected almost exclusively by body shape, the blunting nosecone shape due to ablation increases the drag, thereby increasing the velocity loss.

The analysis of atmospheric heating on the nosecone was divided into two separate areas, non-stagnation and stagnation regions. It was found that the non-stagnation (i.e., sidewall) heating was very small in comparison to stagnation region (i.e., nose tip) heating. Thus, only the stagnation-region convective heat input rate needs to be considered in detail, using relations for high speed dissociated flow[4]. A mass loss due to the heat input is calculated and the resulting shape change is modeled as a cone with a spherical cap whose radius increases with mass loss (assuming the ablation process is axisymmetric).

The transit of the vehicle through the atmosphere is broken down into altitude increments of 100 m so that variable parameters such as C_D, density, deceleration and velocity, can be assumed constant for each increment. For each of these increments, the shape change and mass loss of the vehicle nose is determined and the resulting C_D of the vehicle is calculated using a tangent-cone method and modified Newtonian flow. All incremental mass and velocity losses are summed to result in a total ablated mass loss and velocity loss.

All analyses have been performed between altitudes of 4 km (launch altitude determined by geographical considerations) and 40 km, with launch angles ranging from 16° to 30°. An altitude of 40 km was assumed to be the edge of the sensible atmosphere. The 16° to 30° launch angle constraint is the consequence of parameters specified by orbital mechanics considerations. Preliminary results indicate that a launch angle of 20° is optimum. At this angle, the vehicle retains 85% of its original launch velocity and suffers an ablative mass loss of only 1.3%. The drag coefficient increases from .058 at launch to .11 during the atmospheric transit.

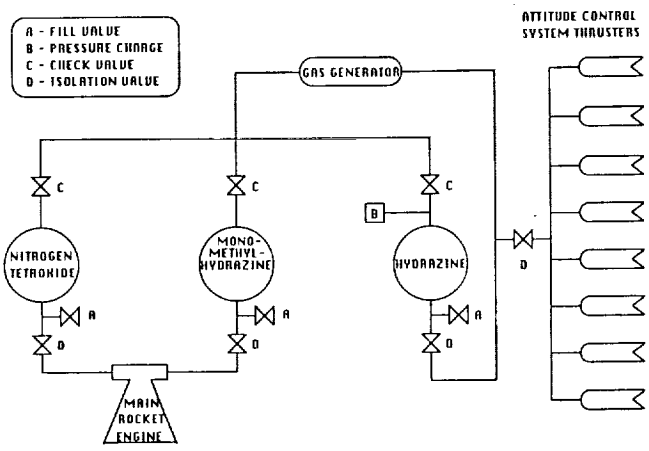

Fig. 3. Schematic of Gas Generator Pressure Fed Propulsion System

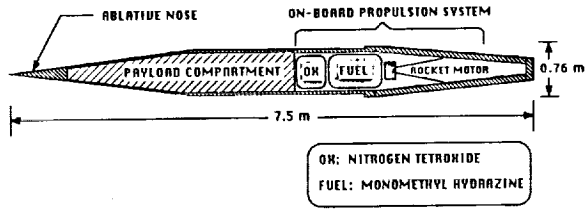

Fig. 4. Configuration For a Graphite/Epoxy Ram Accelerator Vehicle

Vehicle instability was investigated by using small perturbation theory. Since the center of pressure (c.p.) is located in front of the center of gravity (c.g.), the vehicle is inherently unstable. The effect of changing atmospheric density on the magnitude of instability is also of primary concern. The vehicle appears to be highly unstable at launch for any atmospheric disturbance. Angular accelerations on the order of 164 rad/sec^2 at a 4-km launch altitude and .16 rad/sec^2 at a 40-km altitude were estimated. Stability augmentation devices, such as control surfaces, will clearly be required.

ORBITAL MECHANICS

Before the vehicle's orbital path can be studied, a launch site must be chosen. The primary factors to be considered are maximizing the velocity imparted by the earth's rotation by launching as close to the equator as possible and minimizing the amount of atmosphere to be traversed by choosing a site with a high altitude. In addition, an equatorial launch site is desirable so that a frequent launch schedule will place all projectiles into the same orbit. A launch site matching these and other criteria is proposed at Mt. Kenya in Kenya. This site offers a launch altitude of about 4000 m and lies very near the equator.

Following atmospheric transit, the projectile follows a ballistic trajectory which, if left undisturbed, would intersect the earth. Therefore, to place the projectile into the desired low Earth orbit (LEO) an appropriate circularization maneuver or series of maneuvers must be carried out. This requires the projectile to carry an onboard propulsion system. By minimizing the mass of the onboard propulsion system it is possible to maximize the payload-carrying capacity of the vehicle.

A number of possible orbital insertion scenarios have been proposed[1]. Of the various scenarios the multi-step maneuver involving aerobraking (Fig. 2) appears to offer the potential for lowest onboard propulsion system mass. Therefore, this scenario was studied in detail for the Ram Accelerator mass launch concept. The proposed set of maneuvers increases the velocity at the initial ballistic apogee so that the vehicle is placed into an elliptical orbit whose perigee is within the upper atmosphere (phase 3a in Fig. 2). As the vehicle traverses the atmosphere, aerodynamic drag (i.e., aerobraking) slows it down (phase 3b). This places the projectile into a new orbit with a lower apogee which is tangent to the desired orbit. A propellant burn is then made to circularize the orbit.

To increase the flexibility of this launch concept the use of a parking orbit below the desired final orbit, e.g., a space station orbit, has been proposed. The parking orbit would be used to "store" the vehicles until needed in the final orbit at which time an orbital transfer would be performed. This allows the continuous launching of vehicles without having to synchronize the vehicle launch with the orbital position of the permanent structure in the final orbit.

Analyses have been made based on a parking orbit altitude of 450 km and a final orbit of 500 km. The total velocity change needed from the onboard propellant at the optimum launch angle of 20° from an equatorial launch site is approximately 770 m/sec. At this angle, the multi-step orbital maneuver with aerobraking allows a 40% savings in the orbital velocity change required from onboard propellant in comparison to a similar orbital maneuver without aerobraking, thus considerably decreasing the amount of onboard propellant needed.

ON-BOARD PROPULSION SYSTEM

The orbital requirements of the payload vehicle dictate the necessary velocity change and thrust performance for the onboard propulsion system. The optimization of the mass fraction of payload limits the size and mass specifications of the propellant system. Furthermore, feasibility considerations set cost and safety limitations on the system. The optimal system to meet these requirements using current technology has been narrowed down to a chemical-propellant rocket which employs the liquid propellants monomethylhydrazine and nitrogen tetroxide (Fig. 3). This propulsion system provides an I_{sp} of 297 sec with a velocity change capability of up to 1300 m/sec. Solid propellant rockets were also investigated and subsequently discarded as not meeting the necessary mass limitations and performance requirements.

The onboard propulsion system operates most effectively using a pressurized propellant delivery configuration, which employs a gas generator and diaphragm-equipped tanks. This setup can be easily expanded to incorporate the necessary attitude control thrusters, operating from the same propellant system. A nozzle designed to fit within the tail of the vehicle employs an exit diameter of approximately half the vehicle diameter. This nozzle configuration provides the necessary thrust levels and gives an acceptable specific impulse value for the propellants used. The entire onboard propulsion system, including propellants, constitutes approximately 630 kg of the proposed mass of the vehicle, and a volume fraction of slightly more than one quarter. The cost of such a system at current industry prices is in excess of a million dollars. To be cost effective using this type of onboard propulsion, the launch system must employ a recovery method to ultimately return the rocket motors to the launch site.

STRUCTURAL DESIGN OF VEHICLE

Preliminary analyses on the structural design of the Ram Accelerator payload vehicle (Fig. 4) were performed using simplified models to determine stress components and required shell thicknesses. Various structural configurations and their corresponding masses for the vehicle were first examined using aluminum alloys, titanium alloys, and composite materials. These results served as starting points for a more detailed finite-element analysis. The pressure distributions on the vehicle used in the structural analysis were obtained from computer simulations of the two in-tube launch modes of the Ram Accelerator. The payload vehicle must structurally withstand a maximum pressure of 1000 atm in the subsonic combustion mode and 1940 atm in the oblique detonation mode, and temperatures on the order of 3000-4000 K for brief periods (approximately 1 sec).

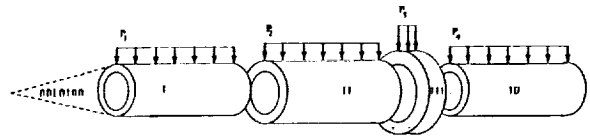

Fig. 5. Structural Model of the Ram Accelerator Vehicle With Axisymmetric Pressure

To perform the structural analysis, the vehicle was approximated as four sections (Fig. 5), and each section was further approximated as a cylinder. To obtain a conservative stress estimate, the average radii of the leading and trailing cones (sections I and IV) were used as the effective radii of the simple cylindrical models. The ablative material on the nosecone was not considered as part of the structure. The vehicle midsection (II and III) consisted of two sections that were in fact cylinders. (Note that section III provides the necessary frustum for the oblique detonation mode). Thus, all sections of the vehicle were analyzed using cylindrical pressure vessel models.

Section II experiences relatively favorable radial pressures which allowed for a thin-walled cylindrical analysis. However, due to severe radial pressures, thick-walled cylindrical analysis was necessary for sections III and IV. For the latter two sections, the hoop stress was determined to be larger than the longitudinal, radial, and shear stresses. Thus, using a factor of safety of 1.4, sections III and IV were designed using the hoop stress criterion, while it was necessary to design section II for longitudinal buckling considerations. The buckling stress criterion for section II actually requires a larger thickness than needed for hoop stress considerations.

A vehicle configuration incorporating T300/5208 graphite/epoxy[5] resulted in minimum structural mass when approximating the composite material properties as isotropic. The analysis produced a structural mass of approximately 600 kg for a vehicle length of 7.5 m.

The effect of placement of the internal components, such as payload, onboard propulsion system, guidance and controls, on such factors as center of gravity and moments of inertia was analyzed. Estimates of the vehicle center of gravity place it 3.8 m behind the nose tip with a moment of inertia of 6,200 kg/m^2 about an axis perpendicular to the axis of the vehicle.

CONCLUSIONS

The Ram Accelerator mass launch system was conceived as a means of economically launching acceleration-insensitive payloads into low Earth orbit. Its study was divided into five areas. Each area was analyzed for feasibility using current technology to launch a 2000-kg-payload vehicle with as high a payload fraction as possible (the goal being 50%).

Following initial acceleration to 0.7 km/sec by a combustion-driven gas gun, two ram accelerator propulsive modes are needed to accelerate the vehicle to its 9.0 km/sec launch velocity. These modes are a thermally choked subsonic combustion mode which propels the vehicle to 2.5 km/sec and an oblique detonation mode which accelerates the vehicle to 9.0 km/sec. The total length of the stationary launch tube is 5.1 km.

A carbon-carbon ablating nosecone was chosen to protect the vehicle during atmospheric transit. At an optimum launch angle of 20°, the vehicle retains 85% of its original launch velocity and suffers an ablative mass loss of only 26 kg. It was found that the vehicle will require stability augmentation devices such as control surfaces to maintain dynamic stability during flight.

The orbital mechanics scheme which minimizes onboard propellant requirements is a multi-step method with aerobraking. At the optimal launch angle of 20°, the total velocity change provided by the onboard propulsion system to obtain the desired orbit is approximately 770 m/sec. Using an MMH-N_2O_4 bi-propellant rocket with an I_{sp} of 297 s, the onboard propulsion system, including propellant, has a mass of approximately 630 kg.

Various structural configurations and their corresponding masses for the vehicle were examined for their capabilities to withstand the high pressures and acceleration in the launch tube. A vehicle incorporating T300/5208 graphite-epoxy was chosen. The mass of this configuration is approximately 600 kg.

At the present stage of the design, the payload fraction of the vehicle is approximately 40%. Further refinements of the in-tube propulsion modes and of the structural design are needed to increase the payload fraction to the desired level of 50% or more. Optimization of parking orbit altitudes and/or eccentricity may also provide an increase in the payload fraction. Methods for recycling vehicle components or for returning them to Earth should be investigated. The work done thus far, however, has proven the potential of the Ram Accelerator concept.

REFERENCES

1. Bruckner A.P. and Hertzberg A. Ram Accelerator Direct Launch System for Space Cargo. *IAF Paper 87-211,* 38th Congress of the International Astronautical Federation, 1987.
2. Knowlen C., Bruckner A.P., Bogdanoff D.W. and Hertzberg A. Performance Capabilities of the Ram Accelerator, *AIAA Paper 87-2152,* AIAA/SAE/ASME/ASEE 23rd Joint Propulsion Conference, 1987.
3. Bogdanoff D.W. and Brackett D. A Computational Fluid Dynamics Code for the Investigation of Ramjet-in-Tube Concepts, *AIAA Paper 87-1978,* AIAA/SAE/ASME/ASEE, 23rd Joint Propulsion Conference, 1987.
4. Schreier S. *Compressible Flow*, John Wiley and Sons, New York, 1982, pp. 406-455.
5. *Advanced Composites Design Guide*, Department of Defense, National Aeronautics and Space Administration, Wright Patterson Air Force Base, OH, 1983.

MARS ROVER VEHICLE

UNIVERSITY OF WISCONSIN, MADISON

INTRODUCTION

This year the University of Wisconsin-Madison design team studied surface operations for a Mars base. Specifically, research was conducted concerning the possibilities for a Mars Rover Sample Return mission. This year's focus was on the development of a system that would accomplish the primary tasks of the rover, to gather and return samples. All the aspects of this complex and challenging task were investigated.

In order to achieve a complete system devices were designed for every stage from sample acquisition to processing and final storage.

The first part of the overall design was to develop a framework in which the sample handling task could be carried out. This was assigned to the rover mobility team, because without an understanding of how a sample handling system fits within the rover concept, the ability to make realistic decisions based on the limitations of a feasible system is lost. It was also necessary to design the rover to be consistent with the overall concept of a complete sample handling system since transportation is needed to get to the samples.

The second facet of the design investigated was the core drilling device. In discussions with NASA representatives, it became evident that the core drill might be the primary sample acquisition device on board the rover. With this in mind, the design team conceived of a device that would meet the requirements set down by NASA. NASA recommended that attention be focused on several key objectives for the designs. First, the design should be durable and reliable. These characteristics are very critical for a mission of this magnitude — and very challenging, since the rover would spend up to 10 years on Mars without scheduled maintenance. Second, NASA suggested that point failures and backup systems be considered. For any NASA mission, critical design aspects are satisfied by overdesign and redundancy. The final aspect cited by NASA was to minimize mass, power requirements, and volume. To accommodate these suggestions, a thorough investigation and analysis of the designs were necessary.

The core drill itself met these requirements very well. The scope of the design was limited to developing a system that would drill at least a meter into any surface substance likely to be found on Mars. The drill also needed to interface with the rest of the rover systems. What the core drill team accomplished is summarized in a later section.

To allow for maximum scientific investigation of the core brought up by the core drill, the Core Handling Device was designed. On the front end of this device is the interface with the core drilling device. Inside the device the core is prepared and analyzed. The device also interfaces with the Sample Return Canister. The summary of this device is contained in a later section.

The final project was a Sample Return Canister, a system to contain and maintain the samples on the rover. The team also developed a system to transfer the samples to the waiting ascent vehicle for return to Earth. The summary of these devices is found in the final section.

SUMMARY FOR THE MARS ROVER MOBILITY STUDY

A Mars Rover Sample Return (MRSR) mission is tentatively scheduled for the late 1990's. The primary goal of the mission is to return samples of martian soil. To accomplish this mission a three-cab rover that uses Grumman's convoluted conical wheel was designed.

The rover was divided into three cabs to lower the center of mass and to provide a smaller turning radius. The convoluted conical wheels developed by Grumman have several advantages. These wheels are non-pneumatic shells made of a reinforced composite material. The flexible nature of the wheels provides for improved stability when traveling over loose soil and sand. Mounted inside each of the wheels is a motor system linked through a harmonic drive to the shaft. Each of the wheels is independently powered, therefore the rover could lose as many as three of its eight wheels and still remain mobile.

Three articulating, three-degree-of-freedom joints connect the cabs of the rover which allow its trailing wheels to move along the same path as the front wheels. These joints are also designed to improve the rover's climbing capabilities. The joints are attached to the true-swing suspension arm. The suspension provides the rover with the capability of moving over one-meter-high obstacles and remaining stable on a 60% slope. The suspension arms also fold back for storage for the trip to Mars inside the aeroshell.

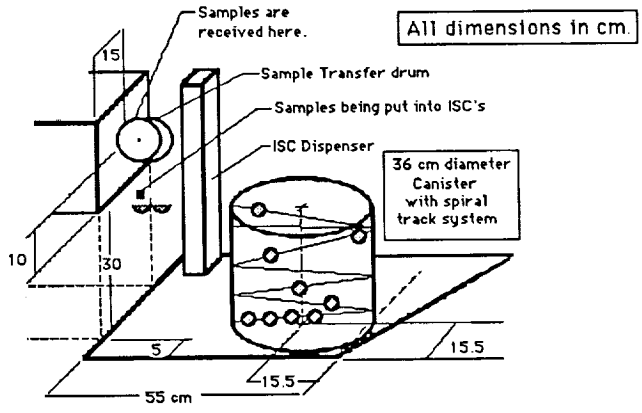

Fig. 1: Sample Return Canister Design - layout on front cab of the Rover

In addition to designing the components of the rover a study was conducted on the problems of heat transfer. The radioisotope thermal generators (RTGs) used to power the rover build up considerable heat. It was determined that by using an aluminum-titanium-alloy tubing for the chassis substructure there would be no significant problems associated with heat buildup from the power systems.

The final thrust of the project was coordinating the layout of the front cab. The other two cabs housed computer equipment and RTG's which were basically black-box designs. There were significant problems with integrating the four design projects onto the front cab. The interface between each of the projects was rather weak but an attempt was made to create a uniform logical capability to deal with the sample acquisition, processing and storage.

SUMMARY OF THE CORE DRILL STUDY

The core drill mechanism is designed to remove a 2.0 cm x 1.0 m core sample from the surface of Mars without the use of water or lubricants. The various components and their descriptions are described in the following sections.

The frame or derrick of the system is designed to provide maximum torsional stability and longitudinal strength while minimizing mass. This is accomplished by a closed box beam constructed with side flanges. The box beam provides torsional stability while the flanges provide for a secure surface to mount the drill mechanism. The drill motor is mounted to the derrick by means of a slide mechanism which is wrapped around the flanges. This method is extremely simple and has no parts to wear out. The derrick will be constructed of a titanium alloy with a protective cover of titanium nitride to prevent corrosion.

The positioning system of the derrick is powered by two permanent magnet stepping motors. One motor provides 90° of motion from the horizontal to the vertical position, while a smaller motor within the derrick provides fine control in the vertical direction.

Downward force is provided to the drilling mechanism by means of another stepping motor connected to the derrick which drives a pair of chains and sprockets. The chains are connected to the motor by a set of spring mechanisms. Each mechanism consists of two springs, one which provides variable tension to convert the motion of the stepping motor into a continuous force, the other to provide tension to remove any slack in the chain. The materials used will be alloys of titanium or aluminum.

The drill motor itself is a permanent magnet, toothless DC motor. The maximum power allowed for the drilling operation is 1000 W. The output power of the motor is 1 hp, with a torque of 19.22 Nm at the point of maximum efficiency, which is about 90%. The output velocity must be geared down to about 350 for maximum drilling efficiency. This is accomplished by the use of a harmonic drive system which is discussed in the final report. (A copy of the final project report can be obtained from Universities Space Research Association, 17225 El Camino Real, Suite 450, Houston, Texas 77058.)

The drill and motor are connected by means of a flexible joint and chuck unit. The flexible joint provides shock absorption and corrects misalignment problems of the shaft. The chuck is designed to provide an easy and sure connection that provides a means for dirt to be removed from the threads. Again, the materials used will be titanium alloys.

The actual drills will be tubes constructed of titanium alloy attached to an integrally designed diamond bit. The bits and auger flights are constructed for dry drilling techniques. There are to be separate bits designed for drilling hard rock as well as loose regolith.

Finally, a device was developed to remove the core from the drill shaft. The device is a 1-M-long plunger rod driven by a linear actuator and mounted to the rover. This will also be constructed of titanium.

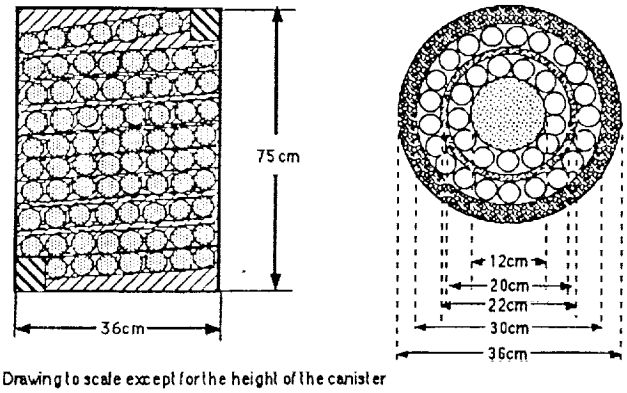

Fig. 2: Canister for Rover (with spherical containers) Capacity - 500 Samples

SUMMARY FOR CORE HANDLING DEVICE STUDY

The core handling device is designed to remove the altered outer skin of a core sample obtained from the core drill on board the Mars rover. This needs to be done because the outer skin (~10% diameter) has been thermally and mechanically altered during the drilling process, thus rendering it useless for scientific investigation. Once this outer portion has been removed, scientific investigation of the pristine inner core will take place. The device was designed to meet the following specifications.

Mass < 5 kg
Power < 100 Watts
Size ~26 x 30 x 28 cm
Withstand temperature range of -50°C to +30°C
Withstand 10 *g*'s during transportation to Mars
Core samples at a rate of 1 per 6-hour period
Expected lifetime of 10 years

The primary design considerations were mass, complexity, ruggedness, reliability, contamination, power, volume, integration, and point failures. Integration proved to be one of the more difficult tasks. This semester the entire rover project was integrated to form a coherent logical system. Integration of the

Core Handling Device was especially difficult since it proved to be the centerpiece of the sample handling process on board the rover.

In order to accomplish its task, the Core Handling Device must complete the following processes.

1. It must break the meter long core down into 10 cm sections.
2. It must use a three-dimension, x-ray scanner to determine density of the section.
3. While holding the core sample lengthwise, it removes the outer 10% of the core. This exposes the inner core to scientific investigation.
4. An optical scanner moves along the core for an initial look.
5. Samples are cut out of the core and sent to a battery of science instruments.
6. Sections to be investigated are removed and sent to the Sample Return Canister.
7. The system is reinitialized and the remaining core material is dumped.

All of the mechanical components of this device have been designed. At this point, scientific instruments are conceptual black boxes.

SUMMARY FOR THE MARS SAMPLE RETURN CANISTER STUDY

The function of the Mars Rover Sample Return Canister is to house the martian samples collected during the mission. The duration of the surface mission on Mars will be approximately one year. This project includes the containment and storage of samples and their transfer to an ascent vehicle for return to Earth.

The driving force of this design is mission planning. The Return Canisters have been specifically designed to support the proposed mission scenario. Options which pertain to other mission scenarios have also been included in this report. The main scenario which this design accommodates is the following (in abbreviated form):

1. Deploy Rover
2. Drill at location (confirmation of all systems on the Rover)
3. Initial loop ~100 meter radius
4. Subsequent loops
5. Sample Selection
6. Transfer samples from Rover Canister to Final Canister
7. Seal Final Canister
8. Secure Final Canister inside ascent vehicle

With this scenario in mind, the design for the Sample Return Canister was developed. The divisions within the project are broken down as follows:

1. Transfer samples from core handling area to individual storage containers
2. Individual storage containers
3. Transfer individual storage containers to Rover Canister
4. Rover Canister
5. Transfer individual storage containers to the ascent vehicle
6. Sample selection mechanism
7. Options

The first part of the process involves interfacing with the core handling device to receive samples. The samples that are received from the core handling device are cut from 2-cm-diameter cores. The cores are received from the Core Drill on board the Rover. The samples are cut into 2-cm increments and pushed out of the core handling area. At this the point, the Sample Return Canister begins its process. Receiving and transferring samples is accomplished by way of a hollow cylindrical drum. The drum has a cavity large enough to receive a sample, but not wide enough for the sample to lose its orientation. For scientific analysis, it will be important to know which side of the sample was deepest in the ground. The hollow drum receives the samples and is then rotated 90° to a position where the samples can be pushed into the individual storage containers. During this process, the orientation of the sample is maintained for future analysis.

The 2 x 2 cm samples are stored inside spherical containers — Individual Sample Containers (ISCs). The ISCs prevent cross-contamination between the samples and protect each sample from internal forces and vibrations generated from the Rover's movements. The spherical shape provides a moment of inertia that aids in the rolling of the spheres. The ISCs are constructed of two hemispheres connected by a hinge. The ISCs have a 1-mm-thick outer shell of titanium aluminum. Inside the ISCs is a cushioning material molded to hold the cylindrical samples. The cushioning is composed of low-density polyethylene foam. The foam was chosen for its flexibility, light weight and because it allows the passage of gases. The ISCs will be stored in the open position inside the ISC dispenser and pushed out one at a time. The ISCs will be sealed using a mechanical clamping system after the samples are dropped in. The seal on the ISCs allows for the samples to breathe, but at the same time it limits the dust that is allowed to get into the ISCs.

The device used for the transfer of ISCs into the Rover Canister is simply a tube made up of four tracks. The tube has a pivot point that allows it to interface between the Rover Canister and the position where the ISCs are sealed. A servo motor rotates the tube allowing the ISCs to roll to the inlet of the Rover Canister. The inlet to the Rover Canister is designed with two doors, in order to isolate the inside of the canister from dust. There are photo sensors on both doors so that the first door is opened and the ISC rolls in. As soon as the ISC is inside, the first door closes and the second door opens. This two-door design protects the inside of the canister from dust storms that occur on the surface of Mars.

The Rover Canister is made up of a spiral tracking system. The tracks are made up of three rails in order to contain the ISCs and allow them to roll. There are actually three separate tracks inside the Canister to best utilize the volume. This storage arrangement has no moving parts within the Rover Canister, utilizing gravity as the only driving force. The helical system provides for a linear arrangement of the samples, thus reducing the structural degrees of freedom and enhancing the labeling scheme for each sample. The Rover Canister can store approximately 500 ISCs and is passively cooled. From this pool of samples, 300 will be returned to Earth for further analysis.

The function of the Container Selection Mechanisms is to select the best 300 samples out of the 500 contained in the Rover Canister. The mechanism is located at the end of the track system of the Rover Canister. The ISCs will be bar coded before they are sent to Mars. The computer will keep track of the order of the samples. A photo sensor will read the bar code and then the computer will decide if that sample is to be kept. The Container Selection Mechanism uses a servo motor to rotate an ISC Pod ± 45° to the discard track or the ascent vehicle track. The total time needed to select and transfer 500 ISCs is approximately 58 minutes, making it a very efficient design.

The last interface requires a device to transfer ISCs from the Rover Canister to the ascent vehicle. An interface device was developed by Rockwell to make and break electrical connections from the Space Shuttle Orbiter to a payload. This device was modified to enable it to transfer the ISCs. The design was chosen over the other ideas because of its adjustment capabilities on all three axes. Since the ascent vehicle may not be on a flat area, the alignment capabilities of this design will be needed to insure an accurate transfer.

"Odd-shaped" samples (samples which do not conform to the 2 x 2 cm size) and gas samples (five 200-ml samples) can also be handled by the standard ISC. The 12-cm-diameter void inside the center of the Rover Canister is the proposed location for these two options. This reservoir serves as a third canister which permits an even larger pool of samples for final selection. The Temporary Storage Reservoir supports another mission, but within the initial weight restriction of 20 kg, this scenario is not feasible.

C-3

FIRESAFETY DESIGN CONSIDERATIONS FOR ADVANCED SPACE VEHICLES

WORCESTER POLYTECHNIC INSTITUTE

Firesafety is a major concern in the design of vehicles and habitats for space. Ignition and spread of fires as well as their prevention, control, and extinguishment are all of significant importance. One element in the minimization of these hazards is an understanding of ignition in a 1-*g* vs. a microgravity environment. Ignition characteristics are significantly different depending on whether buoyant forces are present or absent. Buoyancy tends to disperse pyrolysis products formed from the fuel when energy is added, as from radiant flux. Without buoyancy these products are not circulated and the amount of energy necessary for ignition changes.

By measuring incident energy flux as a function of time in both microgravity and 1-*g* environments, it may be possible to develop a systematic method for characterizing spacecraft materials as to their degree of flammability.

INTRODUCTION

The desire to understand and explore space has driven man to overcome the confines of the Earth's atmosphere and accept the challenge of spaceflight. With our increasing ability to travel, work, and explore in space comes a need for a better understanding of the hazards in this relatively new endeavor. One of the most important and immediate needs is to be able to predict the ignition, spread, and growth of fire on board spacecraft.

Firesafety aboard spacecraft has always been a concern; however, with the increasing number and duration of proposed missions, it is imperative that the spacecraft be designed with a solid understanding of fire hazards, insuring that all risks have been minimized and extinguishment systems are available.

In order to understand microgravity combustion, the process on Earth must first be understood. In the presence of gravity, the major driving force in a fire is buoyancy, or the difference in densities between the surrounding air and the pyrolysis vapors. It supplies the fire with a constant source of oxygen. General predictions can be made regarding the ignition and growth of fire in microgravity using data obtained from groundbased experiments. It is important to conduct experiments both on Earth and later in space under exactly the same conditions.

BACKGROUND

Facilities that are capable of providing a short-term microgravity environment are available and have been used for ignition and combustion experiments. One such facility is the drop tower. In order to produce a microgravity environment, a test is conducted while the experiment package is allowed to freefall from the top of the tower. Small towers provide approximately 2 seconds of testing time, while larger towers provide approximately 5 seconds at about 10^{-5} *g*'s. Low gravity can also be achieved on board an aircraft flown on a Keplerian trajectory which provides about 30 seconds of microgravity conditions time at (about 10^{-2} *g*'s).

In addition to Earth-based testing, Skylab experiment M-479 was designed to observe the ignition and spread of fire for a variety of test samples[1]. In all cases, the crew monitored the extent of surface flame propagation and flashover to adjacent materials, rates of surface and bulk flame propagation, self extinguishment, and extinguishment by both water spray and vacuum.

Drop tower and aircraft tests include premixed flame ignition, propagation, and extinction, flame propagation across solids, laminar gas-jet diffuse flames, premixed particle-oxidizer flames, and droplet combustion.

Results from Skylab experiments and Earth-based microgravity testing provide a general idea of what to expect prior to and during microgravity combustion. In most instances, there is a general reduction in the dangers of combustion in microgravity. The rate of combustion in reduced gravity experiments have been shown to be much slower as compared with 1-*g* combustion. In addition, combustion in microgravity is much sootier and cooler because of the lack of buoyancy to carry the byproducts away from the combustion area. In some cases, flames disappear altogether during the tests, only to reignite as gravity increases. This indicates that the flame is not intense enough for the camera to record.

In all cases, flames in reduced gravity tend to be more globular than their higher gravity counterparts. This includes laminar gas-jet flame and flame spreading over solids. Flames are also shown to be enhanced when the combusted material bubbles. This is theorized to be a result of the burst of fuel vapors in the combustion field. Finally, microgravity flames, although cooler, may radiate more heat as a result of the increased soot particles present. This may result in an increase risk of flashover to adjacent materials.

Recent work[2] at 1-*g* provides a theory for the ignition of vaporizing fuel in microgravity as a result of radiant heat absorption. They disregarded the common assumption that the surface of the solid is hot enough to initiate ignition. Instead they considered heating of vapor emitted from the solid fuel surface to be the process which initiates ignition. By absorbing enough of the radiant heat, the vapor is ignited rather than the surface of the solid. Assuming that radiation absorption is proportional to fuel concentration, that transport and chemical processes are one-dimensional, and that there is no convection, as would be true in zero gravity, (except by the vaporization of fuel), the analysis can be said to be true for zero gravity.

DEVELOPMENT OF IGNITION EXPERIMENT

At WPI an effort is underway to study one of the more important aspects of microgravity combustion and ignition. Understanding how a material ignites is a major step in discovering how to prevent a fire in space applications. To explain the microgravity ignition process, an experiment was designed using specific materials. The microgravity ignition experiment, along with several other WPI experiments, will be flown on board the Space Shuttle as part of a WPI payload in NASA's Get Away Special Program. (This unique program provides universities, industry, and foreign countries the opportunity to place small, self-contained payloads in the cargo bay of the space shuttle at a small cost.) Once ground-based testing of the prototype microgravity ignition experiment has been completed, the actual flight hardware will be assembled. After satisfying all NASA safety requirements for self-contained payloads, the WPI experiment package will await a flight opportunity on an upcoming Space Shuttle flight. By conducting identical experiments on the ground and comparing results with data generated by the flight experiment, a better understanding of the ignition process in microgravity is possible, eventually leading to safer spacecraft designs.

To investigate the ignition process in space, an experiment was designed and built as shown in Fig. 1. Batteries supply power to a high-intensity, infrared lamp which is used to ignite a fuel sample. A radiometer located flush with the sample measures energy flux as a function of time. The experiment is terminated when ignition is detected by a flame ionization sensor or in 30 seconds if ignition is not detected.

Ignition and combustion in microgravity are significantly different than on earth because flow due to buoyancy is not present. It has been proposed that during the ignition process, the absence of buoyancy characteristic of a microgravity environment will result in the accumulation of a layer of pyrolysis products (fuel vapors) at the fuel surface. Further, the absence of gravity will reduce or eliminate normal air circulation patterns seen in Earth gravity. It is this circulation that permits the mixing of air with pyrolysis products to form the correct fuel to air ratio necessary for ignition. This circulation also cools pyrolysis products by entrainment and affects ignition time. Confinement of the fuel vapor and the lack of circulation may result in less energy required for ignition, while the reduced availability of air may have the opposite effect.

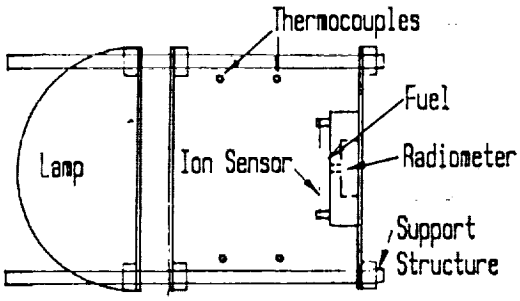

Figure 1. Experiment Schematic

A high-intensity, infrared lamp with a rating of 8 amperes at 30 volts (240 W) was determined to be the most acceptable means of meeting requirements for auto-ignition. The fuel sample chosen for this experiment was alpha cellulose, a pure form of paper, supplied by the National Bureau of Standards. Alpha cellulose was selected due to its uniformity and the repeatability attained during ignition testing. The sample (alpha cellulose) was mounted on a small disk of Torlon (chosen for its resistance to high temperature) which also included the flame ionization detector. When a material combusts, the neighboring gases ionize. The flame ionization detector consists of an open circuit with voltage applied across it. When ignition occurs, the ionized particles close the circuit by conducting a small current, thus detecting the flame. Protruding through a hole at the center of the sample and positioned in the center of the Torlon disk is the radiometer. This device measures the incident heat flux reaching the sample material. The radiometer has a 1/16-inch-diameter probe which is small enough so that it does not absorb a significant amount of the energy transmitted to the sample. Thermocouples were placed at selected locations to provide a temperature distribution during the ignition process.

A microprocessor controls the sequence of the experiment and simultaneously records necessary data. Following the signal to initiate the experiment, power is supplied to the lamp. Feedback signals from the thermocouples, radiometer, and flame ionization detector are channeled to the microprocessor and pertinent information is stored. Once the flame ionization sensor has indicated that the sample has ignited, power to the lamp is removed, ending the experiment. If no flame is detected within 30 seconds, the microprocessor automatically stops the experiment.

The inner structure (lamp, sample holder, radiometer, and supports) is housed in a cylindrical container. Fabricated from aluminum stock, the container has a height of 9.5 inches and a diameter of 6 inches. The purpose of the housing is twofold. First, it prevents combustion products from contaminating the remainder of the Get Away Special package or the remaining ignition experiments, and secondly, it provides a pressure barrier in the event of a large pressure increase.

There will be four, virtually identical, microgravity ignition experiments in the Get Away Special flight package in order to insure that repeatable data has been obtained. Voltage to two of the lamps will be different than the others in order to get different flux rates. As soon as the microprocessor ends one experiment, a signal to initiate the next experiment will be sent.

Data collected during the experiment include temperature as a function of time, energy flux as a function of time, as well as time to ignition. By integrating the time vs. energy flux curve over time from t_0 (lamp on) to t_i (ignition) the incident energy necessary for ignition can be determined Fig. 2. From the results of the four experiments, it may be possible to draw some conclusions about characteristics of the ignition process in space.

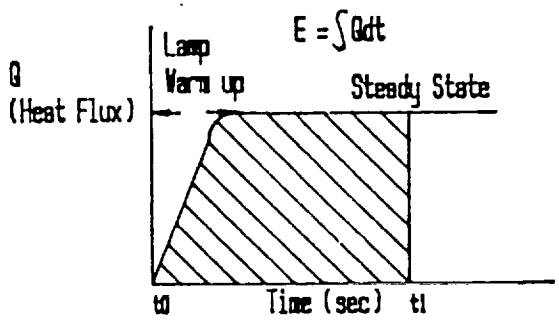

Figure 2. Flux Versus Time During Experiment

GROUND BASED EXPERIMENTAL PROCEDURES

Preliminary groundbased ignition testing using prototype hardware is partially complete. Once the groundbased testing is concluded, a hypothesis regarding the role of gravity in the ignition process will be formulated. Using this hypothesis, predictions with respect to the energy required for microgravity ignition will be made. Following completion of flight hardware assembly, the experiments will be flown on the Space Shuttle when a slot becomes available. Data from the flight experiments will be compared to what was expected as a result of groundbased experiments. This should provide a better understanding of microgravity ignition.

In an attempt to simulate microgravity ignition, groundbased experiments are being performed with the apparatus in various orientations (Fig. 3). Inverting the apparatus (as shown in Fig. 3a) presents the particle cloud created by pyrolysis dispersing readily, because the particle cloud is less dense than the surrounding atmosphere. The particle cloud therefore remains in the vicinity of the fuel sample as would be expected when the experiment is performed in space where gravity is absent.

For comparison, experiments were carried out in the orientation shown in Fig. 3b. In this case, buoyant effects are maximized as pyrolysis products rise from the sample immediately after forming. Results from the testing should provide some indication as to how significant gravitational effects are to the amount of energy necessary for ignition.

SAFETY CONSIDERATIONS

Safety is a major concern when designing and building hardware for spaceflight especially when combustion and resulting high temperatures and pressures are possible. When examining the WPI microgravity ignition experiment, there are many areas where safety must be considered. Using NASA's *Get Away Special Payloads Safety Manual*[3] as a guideline, pertinent safety issues were examined.

The outer structure of each vessel (wall thicknesses, material, and vessel sealing) that contains the individual ignition experiments was designed such that the ASME Boiler and Pressure Vessel Codes[4] are satisfied for pressures and temperatures expected immediately following ignition. The experiment design also took into account Appendix B of *Get Away Special Payloads Safety Manual*, "Payload Pressure Vessel Criteria." This requires that in the event that all pressure vessels fail under worst-case conditions, the resulting pressure of the Get Away Special canister cannot exceed five atmospheres. If the four separate ignition experiments were to fail, the resulting pressure would not exceed this limit.

The case of a "run-away lamp" was considered where the power to the lamp would not be terminated and the lamp would continue to radiate until the batteries were depleted. The result would be a significant amount of radiated energy. Since this process would take place over a long time, most of the heat would be absorbed by the aluminum container of the individual experiments. Therefore, the temperature and pressure rise within any individual experiment would be acceptable. As a precautionary measure, fusible links will be placed in the wires supplying power to the lamps. After an adequate amount of current for ignition has passed through the fuse without the microprocessor terminating power to the lamp, the fuse would burn, interrupting the connection.

Even though some experiments and studies like those discussed earlier have been performed, microgravity combustion research is relatively new. There is still much that needs to be studied if firesafety for space missions is to advance. Other low-gravity combustion processes need to be studied and compared with similar 1-*g* experiments. After more studies have been made, scientists and engineers will be better able

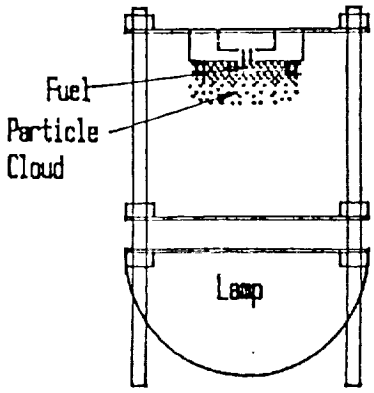

Figure 3a. Orientations to vary effects of gravity for ground based testing: minimum effect

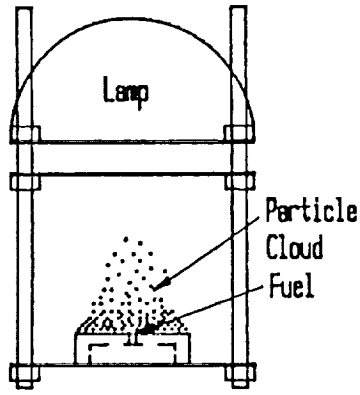

Figure 3b. Orientations to vary effects of gravity for ground based testing: maximum effect

to design a firesafe spacecraft. Selecting materials, providing proper extinguishment, and designing safe life-support systems will be based on firesafety research and sound engineering design practice. When human habitations are built for space and if missions to Mars are undertaken, there should be no question as to how a particular material will behave in the event of a fire.

Although some tests at WPI have already been conducted, the main goal remains to conduct the microgravity ignition experiments aboard the space shuttle. Before that is possible, the final flight hardware will have to satisfy all NASA safety specifications and be assigned by NASA to a future shuttle flight. Once it is known how ignition and combustion behave in space, it will be possible to design safer spacecraft allowing astronauts and scientists to work in space with minimum fire hazards.

REFERENCES

1. Breland A.L., Huggett C., Kaufman F., Markstein G., Palmer H.B., and Yang C.H. Study of Combustion Experiments in Space, *NASA CR-134744,* 1974.
2. Amos B., Kodama H., and Fernandez-Pello A.C. An Analysis of the Ignition by Vapor Radiation Absorption of a Vaporizing Fuel at Zero Gravity, *AIAA 25th Aerospace Sciences Meeting,* Univ. of California, Berkley, 1987.
3. *Get Away Special Payloads Safety Manual,* NASA Goddard Space Flight Center, May 1986.
4. *American Society of Mechanical Engineers Boiler and Pressure Vessel Codes,* Sections VIII, Divisions 1 and 2.